UNIVERSITAT DE BARCELONA

Worker exposure to airborne particles in industrial settings: evaluation of exposure assessment and modelling tool

Carla Ribalta Carrasco

UNIVERSITAT DE BARCELONA

Faculty of Chemistry

Doctoral Program "Analytical Chemistry and the Environment"

Worker exposure to airborne particles in industrial settings: evaluation of exposure assessment and modelling tools

Carla Ribalta Carrasco

PhD Thesis

Barcelona, May 2019

Supervisors:

Dra. Mar Viana Rodríguez
(IDAEA-CSIC)
Full Prof. Dr. Eliseo Monfort Gimeno
(ITC-UJI)

Tutor:

Dr. Alex Tarancón Sanz
(UB-Faculty of Chemistry)

idaea

CSIC
Consejo Superior de Investigaciones Científicas

ABSTRACT

Exposure to particulate matter in work environments has been linked to ischemic heart, cardiovascular and respiratory-related disease risk increase due to inhalation. Increased adverse health effects have been linked to nanoparticles (< 100 nm) due to their ability to reach the deepest sections of the respiratory tract and their longer retention time. Exposure monitoring is widely used method to assess worker exposure to airborne particles. However, other prediction tools have been explored such as the use of the dustiness index, mass-balance models, and health risk assessment tools. Discussions regarding the use and application of the latter tools are ongoing due to their relatively novelty for worker exposure assessment, the need to test their performance under real-world scenarios, and the need to understand the uncertainties related to critical parameters and limitations.

The main objectives of this PhD Thesis are to 1) assess worker exposure to particles (4 nm - 35 μm) in ceramic industry real-world workplace scenarios; 2) evaluate currently used exposure assessment metrics and decision-making approaches; 3) understand the relationship between material dustiness and worker exposure; 4) evaluate the performance of mass-balance models, and 5) compare health risk assessment tools.

Worker exposure was assessed during mechanical handling of powders in 6 different scenarios and for 15 materials as well as thermal spraying of ceramic coatings. Exposure monitoring was conducted using online and offline instruments which allowed for the characterization of particle mass and number concentrations, particle size and size distribution, particle morphology and chemical composition. In addition, some of these scenarios were also selected to assess relationship between the dustiness index and exposure concentrations as well as the ability of different particle metrics to represent worker exposure. Finally, decision making approaches, and the performance of mass-balance models and risk assessment tools were tested. Results evidenced clear impacts of industrial activities on workplace exposure to coarse, fine and nanoparticles.

Significant increases of inhalable and respirable particle mass concentrations (inhalable mass concentration 80-4000 μg m^{-3}) were observed during mechanical handling of raw materials (d_{50} 2.7-40 μm), when compared to background concentrations. The highest mean inhalable mass concentration (3700 μg m^{-3}) was monitored during packing of ceramic materials, when mitigation strategies were inefficiently implemented.

Conversely, particle number concentrations were not influenced by mechanical handling of powders, but by driving of diesel-powdered forklifts, leading to concentrations up to 70000 cm^{-3}. Thermal spraying, on the other hand, increased particle number concentration up to 10^5 cm^{-3} in the worker area. After the application of the ICRP respiratory tract deposition model, airborne particles in the workplaces studied were seen to deposit mainly in the alveolar region (51-64%) during packing of powder materials and (54-70%) during thermal spraying by means of surface area. Source enclosure and modification of the energy settings were pointed out as useful strategies to minimize worker exposure.

The validity, performance and comparability of tools for exposure assessment were evaluated. Several decision-making approaches were tested to determine statistically significant impacts on exposure. Among them, the ARIMA models were seen to be the least conservative while the nanoGEM approach confirmed its usefulness for particle number but slightly underestimated exposure for particle mass concentrations when compared to traditional statistical tests. High degree of correlation was found between dustiness and measured exposure concentrations during mechanical handling of powders in a pilot plant (R^2 up to 0.97) and at industrial scale (R^2 up to 0.80). This correlation was stronger when material characteristics dominated over process characteristics, and an adequate methodology is applied, using the dustiness method which best mimics the activity under study.

Finally, one- and two-box models were used to model particles under high and low concentrations in terms of mass and particle number concentrations. Ratios between modelled and measured concentrations were 0.82-1.22 when modelling inhalable particle mass in the mechanical handling scenario, whereas ratios of 0.2-0.7 were obtained when modelling thermal spraying particles. Thus, model performance was poorer for the high nanoparticle concentration scenario. The addition of background and outdoor concentrations as input improved model performance. Risk assessment and control banding tools (ART, Stoffenmanager and NanoSafer) were tested for the scenarios under study, and it was concluded that the mechanical processes were estimated with higher accuracy and lower variability by Stoffenmanager (64% of the cases). Conversely, ART and NanoSafer showed higher flexibility for introducing more case-specific input data. A clear need for harmonization between risk assessment tools was evidenced.

RESUM

L'exposició per inhalació de material particulat en ambients de treball ha estat relacionat amb l'augment del risc de patir malalties cardiovasculars y respiratòries. En el cas específic de les nanopartícules (< 100 nm), els efectes adversos han estat relacionats amb la seva capacitat per arribar a les regions més profundes del aparell respiratori i al seu major temps de retenció. Per tal de determinar els nivells d'exposició a material particulat, un mètode experimental àmpliament utilitzat és l'ús d'equips de mesura en continu de les concentracions. No obstant això, altres eines estan sent actualment explorades com per exemple l'ús del poder d'emissió de pols dels materials, models basats en balanços de masses per a la predicció de l'exposició, així com eines per a l'avaluació del risc per a la salut degut a l'exposició d'agent químics. No obstant això, degut a la seva relativa novetat, existeix la necessitat d'avaluar la validesa de totes aquestes eines en escenaris reals, així com de comprendre les incerteses relacionades amb els paràmetres i les seves limitacions. Per tant, el seu us i aplicació es troben actualment en debat.

Els principals objectius d'aquesta tesi doctoral són: 1) avaluar els nivells d'exposició laboral a material particulat d'entre 4 nm i 35 μm en escenaris de treball reals, 2) avaluar les diferents mètriques existents per a l'avaluació dels nivells d'exposició i els mètodes de presa de decisions utilitzats en la actualitat; 3) comprendre la relació existent entre el poder d'emissió de pols dels materials i els nivells d'exposició dels treballadors durant la seva manipulació; 4) avaluar la validesa del models basats en balanços de massa; i 5) comparar diferents eines d'avaluació dels riscos de l'exposició a agents químics.

En aquesta tesi s'han avaluat els nivells d'exposició laborals a material particulat, tant durant manipulació mecànica, concentradament de 15 materials pulverulents en 6 escenaris diferents, com durant projecció tèrmica de recobriments ceràmics, amb l'estudi de 2 escenaris amb tres materials per a l'obtenció de recobriments ceràmics sobre peces metàl·liques. El control experimental dels nivells d'exposició es va realitzar mitjançant l'ús d'equips de mesura de partícules en temps real i de la recol·lecció de mostres gravimètriques del material particulat emes, que va ser posteriorment analitzat per microscòpia electrònica. Tot això va permetre la caracterització de la concentració del material particulat en massa, numero de partícules, mida i distribució de mida de les partícules, la morfologia de les partícules i la seva composició química. Addicionalment, en els processos mecànics es va avaluar la relació entre el poder d'emissió de pols dels

materials i els nivells d'exposició, així com la capacitat de diferents mètriques, generalment utilitzades per a l' anàlisis de l'exposició a partícules (massa i numero), de representar l'exposició dels treballadors. Finalment, es van estudiar diferents mètodes per a la presa de decisions, es va avaluar la aplicabilitat en condicions industrials dels models basats en balanços de massa, així com de tres eines per a l'avaluació dels riscs per exposició a agents químics. Els resultats van evidenciar un clar impacte de les activitats industrial estudiades sobre els nivells d'exposició dels treballadors en els escenaris estudiats a partícules grolleres, fines i nanopartícules.

Durant la manipulació mecànica de matèries primeres (d_{50} 2.7-40 μm) es van observar augments significatius de les fraccions màssiques de pols inhalable i respirable (concentració de massa inhalable 80-4000 μg m^{-3}) en comparació amb les concentracions de fons. La concentració mitjana més elevada per a la fracció màssica inahlable (3700 μg m^{-3}) va ser mesurada durant l'ensacat de materials ceràmics amb una implementació ineficient de mesures de mitigació. Per el contrari, les concentracions en numero de partícules no es van veure influenciades per la manipulació mecànica dels materials pulverulents, però si que es van registrar concentracions de numero de partícules de fins $7x10^4$ cm^{-3} degut a l'ús de carretons elevadors dièsel. Per una altra banda, en els escenaris de projecció tèrmica es va observar un augment de la concentració en numero de partícules de fins a valors del ordre de 10^5 cm^{-3} en l'àrea de treball. Mitjançant l'aplicació del model de deposició de partícules ICRP, es va observar que les partícules en suspensió en els llocs de treball estudiats es depositaven principalment en la regió alveolar tant durant l'ensacat (51-64%), com durant la projecció tèrmica (54-70%). L'aïllament de la font d'emissió així com la modificació de l'energia aplicada durant el procés es van detectar com a estratègies útils per a minimitzar l'exposició dels treballadors.

També es va avaluar la validesa, el rendiment i la comparabilitat de varies eines estadístiques per a avaluar la significança estadística de les dades d'exposició. D'entre els mètodes avaluats, els models ARIMA van ser considerats com als menys conservadors, mentre que la metodologia nanoGEM va confirmar la seva utilitat per a l'anàlisis de les concentracions en numero de partícules, però va subestimar lleugerament la significança estadística de les concentracions en massa en comparació amb les proves estadístiques tradicionals. Es van trobar alts graus de correlació entre el poder d'emissió de pols del materials i les concentracions d'exposició mesurades durant la manipulació mecànica

dels materials en planta pilot (R^2 fins a 0.97) i en escala industrial (R^2 fins a 0.80). Aquesta correlació s'ha vist reforçada quan les característiques dels materials dominen sobre les característiques del procés, i quan una metodologia adequada per a la determinació del poder d'emissió de pols va ser utilitzada, aquella que millor simula el procés d'estudi.

Finalment, es van utilitzar els models basats en balanços de massa de una i dos caixes per a modelar dos escenaris diferents, un de baixa exposició a partícules grolleres (manipulació mecànica, ensacat de materials) y un altre d'altes concentracions de numero de partícules (projecció tèrmica). Les proporcions entre les concentracions modelades/mesurades van ser de 0.82-1.22 per a la modelització de la fracció màssica de pols inahalble en el cas de la manipulació mecànica, mentre que les proporcions van ser de 0.2-0.7 per a la modelització de la concentració en numero de partícules durant la projecció tèrmica. Per tant, la bondat dels models basats en balanços de massa va ser menor en l'escenari d'altes concentracions de numero de partícules. Al considerar les concentracions de fons i de l'aire ambient en els models, la bondat i la precisió dels models va augmentar. De les tres eines per a l'avaluació de riscos per exposició a agents químics (ART, Stoffenmanager i NanoSafer) que van ser provades, les concentracions mesurades durant els processos de manipulació mecànica van ser estimats amb una major precisió i menor variabilitat per Stoffenmanager (64% dels cases). Per el contrari, ART i NanoSafer van mostrar tenir una major flexibilitat per a introduir dades d'entrada especifiques per a cada cas.

RESUMEN

La exposición por inhalación a material particulado en ambientes de trabajo se ha relacionado ampliamente con el aumento del riesgo de enfermedades cardiovasculares y respiratorias. En el caso particular de las nanopartículas (< 100 nm), los efectos adversos sobre la salud se ha postulado que se deben a su capacidad para llegar a las regiones más profundas del tracto respiratorio y a su mayor tiempo de retención. Para la determinación de los niveles de exposición a material particulado, un método experimental ampliamente utilizado es la monitorización en continuo de las concentraciones ambientales. Sin embargo, también se están explorando herramientas de predicción, como por ejemplo el uso del poder de emisión de polvo, modelos basados en la aplicación de balances de materia, así como herramientas de evaluación de riesgos por exposición a agentes químicos. No obstante, debido a su relativa novedad, existe la necesidad de evaluar la validez de todas estas herramientas en escenarios reales, así como de comprender las incertidumbres relacionadas con los parámetros y sus limitaciones. Por tanto, su uso y aplicación se encuentran actualmente en debate.

En este contexto, los principales objetivos de esta tesis doctoral son: 1) evaluar la exposición laboral a partículas de entre 4 nm y 35 µm en escenarios de trabajo reales; 2) evaluar las diferentes métricas de evaluación de la exposición y los métodos de toma de decisiones utilizados en la actualidad; 3) comprender la relación entre el poder de emisión de polvo de los materiales pulverulentos y la exposición de los trabajadores a material particulado durante su procesado; 4) evaluar la validez de los modelos basados en balance de materia para la predicción de la exposición, y 5) comparar diferentes herramientas de evaluación de riesgos de exposición a agentes químicos.

En esta tesis se ha evaluado la exposición laboral a material particulado, tanto en procesos mecánicos, -concretamente en la manipulación y envasado de 15 materiales pulverulentos en 6 escenarios industriales distintos- así como en procesos de proyección térmica, con el estudio de 2 escenarios con 3 materiales para la obtención de recubrimientos cerámicos sobre piezas metálicas. La monitorización experimental de la exposición se llevó a cabo utilizando instrumentos que miden la concentración de partículas en tiempo real, además se tomaron muestras, mediante sistemas de captación específicos, que posteriormente fueron caracterizadas por microscopia electrónica. Todo ello permitió la determinación de la concentración en masa y en número de partículas, el tamaño medio y la distribución del tamaño de las partículas, la morfología de las

partículas y su composición química. De forma adicional, en los procesos mecánicos se evaluó la relación entre el poder de emisión de polvo de los materiales pulverulentos y los niveles de exposición a material particulado, así como la capacidad de diferentes métricas (masa o número) para representar la exposición de los trabajadores. Finalmente, se probaron distintos métodos estadísticos para el tratamiento de datos y toma de decisiones, se evaluó la aplicabilidad en condiciones industriales de modelos basados en balances de materia, así como de tres herramientas reconocidas de evaluación de riesgos por exposición a agentes químicos. Los resultados evidenciaron un claro impacto de las actividades industriales sobre la exposición laboral a partículas gruesas, finas y nanopartículas.

Durante los procesos mecánicos de manipulación de materias primas (d_{50} 2.7-40 μm) se observaron aumentos significativos de las fracciones másicas de polvo inhalable y respirable (concentración de polvo inhalable 80-4000 μg m^{-3}) en comparación con las concentraciones de fondo. La mayor concentración media de polvo inhalable (3700 μg m^{-3}) se midió durante el ensacado de materias primas cerámicas, con un bajo nivel de implantación de medidas correctoras. Por el contrario, las concentraciones en número de partículas no se vieron influenciadas por el procesado mecánico de materiales pulverulentos pero si se registraron concentraciones elevadas del número de partículas, hasta de $7x10^4$ cm^{-3} debido al uso de carretillas elevadoras con motores diésel en interiores. Por otro lado, en los escenarios de proyección térmica se observó un aumento significativo del número de partículas, hasta valores del orden de 10^5 cm^{-3} en el área de trabajo. Mediante la aplicación del modelo de deposición de partículas en el tracto respiratorio ICRP, se observó que las partículas en suspensión en los lugares de trabajo estudiados se depositaban principalmente en la región alveolar, tanto durante el ensacado (51-64%) como durante la proyección térmica (54-70%). Se detectó que el confinamiento de las fuentes y la reducción de la energía aplicada durante el procesado son estrategias útiles para minimizar la exposición de los trabajadores.

También se evaluó la validez, el rendimiento y la comparabilidad de varios métodos estadísticos para evaluar la significancia estadística de los datos de exposición. De los métodos evaluados, los modelos ARIMA se consideraron los menos conservadores, mientras que el método nanoGEM confirmó su utilidad para tratar datos del número de partículas, pero subestimó ligeramente la significancia estadística de las concentraciones en masa en comparación con las pruebas estadísticas tradicionales. Se encontraron altos

grados de correlación entre el poder de emisión de polvo de los materiales y los niveles de exposición medidos durante la manipulación mecánica de dichos materiales pulverulentos en planta piloto (R^2 hasta 0.97) y a escala industrial (R^2 hasta 0.80). Esta correlación se ha visto reforzada cuando las características de los materiales predominan sobre las características del proceso y se aplica el método de caracterización del poder de emisión de polvo que mejor se asemeja al proceso estudiado.

Finalmente, se utilizaron los modelos basados en balances de materia, concretamente los de una y dos cajas, para modelizar dos escenarios distintos, uno de baja exposición a partículas gruesas (manipulación mecánica) y otro de altas concentraciones de número de partículas (proyección térmica). La relación entre las concentraciones estimadas por el modelo y las medidas experimentalmente fueron de 0.82-1.22 cuando se modelizó la concentración másica de polvo inhalable en el escenario de procesado mecánico, mientras que las proporciones fueron de 0.2-0.7 cuando se modelizó la concentración en número de partículas emitidas durante la proyección térmica. Por lo tanto, la bondad de los modelos basados en los balances de materia fue menor en escenarios de alta concentración de nanopartículas. Al considerar que las concentraciones de fondo y del aire ambiente exterior no eran despreciables, se aumentó significativamente la bondad del ajuste entre los datos experimentales y los calculados por los modelos. De las tres herramientas de evaluación del riesgo por exposición a agentes químicos (ART, Stoffenmanager y NanoSafer) probadas, la que con mayor precisión y menor variabilidad estimó la concentración en los procesos mecánicos fue el Stoffenmanager (64% de los casos). Por el contrario, ART y NanoSafer mostraron una mayor flexibilidad para introducir datos de entrada específicos para cada caso.

CONTENTS

ABSTRACT 1

1. INTRODUCTION 15

1.1. Air pollution 16

1.2. Workplace exposure to airborne particles 17

1.2.1. Aerosol formation and exposure 17

1.2.2. Exposure to micro-sized particles 19

1.2.3. Exposure to nanoparticles 21

1.3. Particle-related health risk 23

1.3.1. Micro-sized particles 23

1.3.2. Nanoparticles 24

1.4. Exposure assessment 26

1.4.1. Exposure prediction tools: the dustiness index 30

1.4.2. Exposure modelling: mass-balance models 31

1.5. Risk assessment 35

1.5.1. Inhalation deposition models for health risk assessment 35

1.5.2. Risk assessment tools 38

1.6. Legislation: worker exposure to airborne particles 39

1.6.1. Nanoparticle exposure legislation 40

1.7. Gap analysis 42

1.7.1. Gaps in exposure monitoring 42

1.7.2. Gaps in exposure prediction models 42

1.7.3. Gaps in health risk assessment 43

2. OBJECTIVES AND STRUCTURE 45

2.1. Objectives 46

2.2. Structure 46

3. METHODOLOGY 49

3.1. Exposure scenarios and monitoring sites 50

3.1.1. Mechanical processes 50
3.1.2. Thermal processes 52
3.2. Materials physical characterization 53
3.2.1. Particle size distribution 53
3.2.2. Flowability 53
3.2.3. Specific surface area 53
3.2.4. Aspect ratio 53
3.2.5. Dustiness 54
3.3. Particle monitoring techniques and instrumentation 56
3.3.1. Online instrumentation 56
3.3.2. Offline instrumentation 61
3.4. Measurement strategy 62
3.4.1. Discrimination of background particles 62
3.4.2. Sampling locations 63
3.4.3. Decision making based on statistical significance 63
3.4.4. Regulatory compliance 64
3.4.5. Instrument intercomparison 64
3.5. Mass-balance models 65
3.5.1. One-box model 65
3.5.2. Two-box model 66
3.5.3. Emission rate 66
3.6. Risk assessment 69
3.6.1. ICRP inhalation deposition model 69
3.6.2. Risk assessment tools 70
4. RESULTS 75
4.1. Publication I 77
4.1.1. Additional results publication I 99
4.2. Publication II 103
4.2.1. Additional results publication II 119
4.3. Publication III 121

4.3.1. Additional results publication III..... 137

4.4. Publication IV..... 139

5. DISCUSSION..... 157

5.1. Exposure assessment and particle emissions..... 160

5.2. Metrics and tools for exposure assessment..... 167

5.2.1. Metrics for exposure assessment.....167

5.2.2. Statistical significance of particle impacts on exposure..... 167

5.3. Dustiness as an exposure prediction tool..... 168

5.4. Mass-balance models performance..... 170

5.4.1. Dustiness and measurement-based particle emission rates..... 171

5.4.2. Air flow parametrization..... 172

5.5. Risk assessment tools performance..... 173

5.5.1. ICRP Inhalation deposition model..... 173

5.5.2. Risk assessment and control banding tools..... 175

6. CONCLUSIONS..... 179

7. LIMITATIONS AND FUTURE RESEARCH..... 185

8. REFERENCES..... 189

ANNEX A. Glossary..... 213

ANNEX B. Supplementary materials..... 219

ANNEX C. Additional scientific contributions..... 259

ACKNOWLEDGEMENTS.....263

FUNDING SOURCES..... 265

Introduction

Chapter 1

1. INTRODUCTION

1.1. Air pollution

Air pollution is defined as the presence of substances in ambient air, due to natural or anthropogenic causes, and which are likely to have harmful effects on human health and/or the environment (Mészáros 1999, Directive 2008/50/EC). Atmospheric pollution is currently considered as a major environmental health issue affecting nearly 90% of the global population, including low, middle, and high-income countries (Gakidou *et al.* 2017, WHO 2016, Landrigan *et al.* 2018). Specifically, in Europe, 74-85% of the population is exposed to $PM_{2.5}$ in higher concentration than recommended by the World Health Organization (WHO) (EEA 2018). Air pollution caused by particles and gaseous pollutants is estimated to cause more than 4.2 million premature deaths worldwide, from which 92% occur in low- and middle-income countries (Landrigan *et al.* 2018), and 400000 in the EU-28 (EEA 2018). However, air pollution is not only limited to outdoors but also found indoors and in workplaces, with humans spending nowadays approximately 90% of the time in indoor environments (Monn 2001) and 50% in workplaces (Klepeis *et al.* 2001). Indoor and workplace air quality is determined by their own type of source, which depends on the type of environment (homes, workplaces, transport systems, hospitals, schools...), and outdoor infiltration and influence, affected by outdoor air pollution, air exchange rates, penetration factors, as well as deposition and resuspension mechanisms (Chen and Zhao 2011). Due to the vast variety of indoor and workplaces, and their complexity and heterogeneity these type of environments are in general less studied than outdoor air pollution (Viana *et al.* 2011, Weschler 2011). However, recently, numerous studies have focused on air pollution covering exposure in homes and schools (Morawska *et al.* 2003, 2017, Hussein *et al.* 2005, 2006, Mazaheri *et al.* 2014, Reche *et al.* 2014, Isaxon *et al.* 2015, Rufo *et al.* 2015, Klepeis *et al.* 2017, Zhang *et al.* 2018), in public transport systems and during commuting (Onat and Stakeeva 2014, Martins *et al.* 2016, Yan *et al.* 2015, Minguillón *et al.* 2018, Strasser *et al.* 2018), and in different workplaces such as offices, industries, mining and airports (Koponen *et al.* 2001, Koivisto *et al.* 2010, Møller *et al.* 2014, Morawska *et al.* 2017, Viitanen *et al.* 2017) among others. The present PhD Thesis focuses on the industrial workplace exposure as research topic, specifically focusing on particle pollutants.

1.2. Workplace exposure to airborne particles

1.2.1. Aerosol formation and exposure

Aerosols are a mixture of particles (single continuous unit of solid or liquid, or two or more held together by inter-particle adhesive forces, containing many molecules held together by intermolecular forces) suspended in the air (Steinfeld and Pandis 2006). Ambient air contains particle pollutants originated from natural (organic, e.g., pollen, bacteria or virus, or inorganic, e.g. mineral dust, sea salt or volcanic released aerosols), and anthropogenic sources (result of processes related to human activities). Airborne particles typically range between few nanometres up to approximately 100 μm (Figure 1.1). Therefore, exposure is generally assessed as a function of particle size and described as exposure to coarse (> 2.5 μm), fine (< 2.5 μm) and ultrafine particles (UFP) (< 100 nm) (Figure 1.2). It should be noted that in the aerosol research field particles < 100 nm are referred to as UFP and those < 50 nm as to nanoparticles (NPs), whereas in the nanotechnology field particles < 100 nm are referred to as NPs. In this Thesis we will use the term "nanoparticles, NP" as defined in the nanotechnology field (< 100 nm).

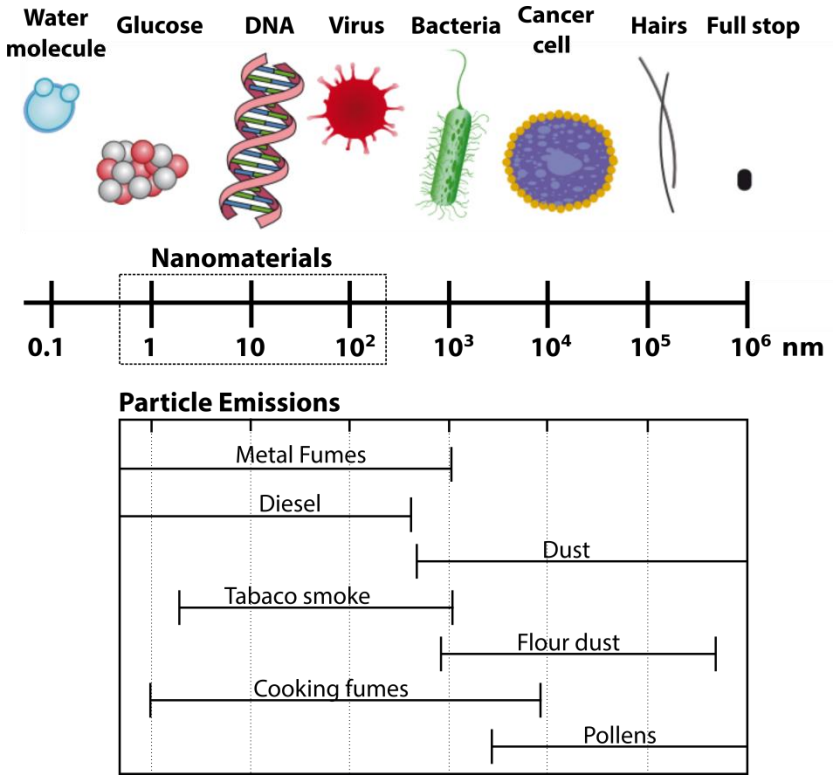

Figure 1.1 Comparative schemes of objects size in a nanometer scale and common atmospheric pollutants sizes. Source: modified from Fonseca (2016), Jensen (2019) unpublished figure by Koivisto, AJ) and Savolainen *et al.* (2013).

Particles behaviour in the air is dominated by formation and transformation processes. Aerosols are commonly divided by their formation mechanisms as follows (Figure 1.2):

- Nucleation mode (< 20/30 nm): new particles formed from gaseous precursors (mainly H_2SO_4, NH_3 and VOCs) in a super-saturated environment without help of condensation nuclei (Kulmala *et al.* 2004, Kumar *et al.* 2010). They quickly tend to coagulate with other particles or grow by condensation (Charron and Harrison 2003, Rodríguez *et al.* 2005, Kumar *et al.* 2010). The nucleation mode also contains primary particles such as a fraction of exhaust vehicle emissions.

- Aitken mode (20-100 nm): includes directly emitted combustion particles and soot, and those which evolve by coagulation and condensation (which implies particle growth) processes on pre-existing particles (Wehner and Wiedensohler 2003, Kulmala *et al.* 2004, Steinfeld and Pandis 2006).

- Accumulation mode (0.1-1 µm): includes combustion, smog particles, marine organic and coagulated nucleation/Aitken mode particles (Hinds 1999, Steinfeld and Pandis 2006, Rodríguez *et al.* 2007). Particles coagulation kinetics is usually slow and they do not reach the coarse mode, hence, they have a relatively long lifetime in the atmosphere (Harrison *et al.* 2000, Kumar *et al.* 2010).

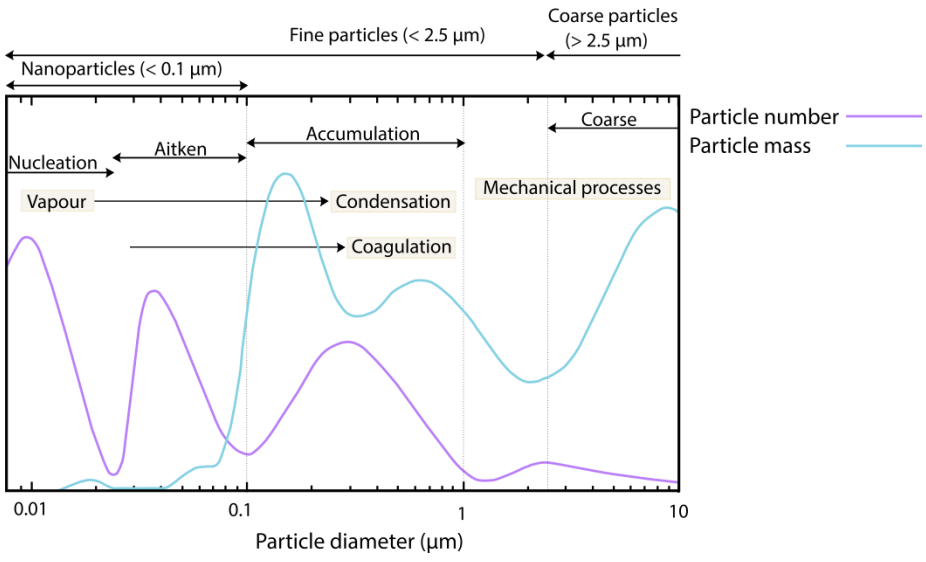

Figure 1.2 Relationship between mass and number distribution of atmospheric aerosols by particle size, and particle formation and transformation processes. Source: modified from Watson and Chow (2007) and Fonseca (2016).

- Coarse mode (> 2.5 µm): this mode is mainly composed by primary particles originated by mechanical processes. It includes windblown dust and mechanically generated

anthropogenic particles (e.g. agriculture or mining), large salt particles from sea spray, and pollen (Harrison *et al.* 2000, Raes *et al.* 2000, Steinfeld and Pandis 2006). Because of their large size, particles readily settle out or impact on surfaces, so their lifetime in the atmosphere is short (generally few hours or days).

Exposure is defined as the state or condition of being unprotected and open to damage, danger or risk. Exposure to particles can occur through dermal or oral inhalation route, the latter being regarded as the main exposure route. Standardization of worker exposure in occupational settings is very complex as workplaces are very diverse and particle sources are highly case-specific. In addition, industrial emissions have the added complexity of being extremely variable over time, shift and location, as they are influenced by a mixture of time changing processes (Ramachandran 2005). Thus, having exactly the same combination of sources in different periods of time is quite unlikely. Whereas the impact of particles on human health is linked to their physicochemical and functional properties (Oberdörster and Kuhlbusch 2018), particle size is one of the most important factors driving the potential adverse health effects of exposure to airborne particles (Aitken *et al.* 2004, Sánchez-Jiménez *et al.* 2011). For airborne particulate matter (PM), the most common metric generally used is mass concentration as occupational exposure limits (OELs) are stablished in terms of mass (NIOSH 2002, Aitken *et al.* 2004). However, particle number concentration and surface area are also used.

1.2.2. Exposure to micro-sized particles

Occupational exposure to PM, as stablished in ISO 7708:1995 and UNE-EN 481 1995, is usually reported in terms of (Figure 1.3):

- Inhalable mass, the mass fraction of total airborne particles which is inhaled through the nose and mouth. The inhalable criterion has 100% penetration for particles < 10 μm, dropping to 50% for 100 μm particles and has no median cut-off aerodynamic diameter.
- Thoracic mass, the mass fraction of inhaled particles penetrating beyond the larynx. The curve has a median diameter of 11.64 μm and geometric standard deviation (GSD) of 1.5.
- Respirable mass, the mass fraction of inhaled particles penetrating to the unciliated airways, with a median aerodynamic diameter of 4.25 μm and 1.5 GSD.

Exposure to micron-sized airborne particles in occupational environments mainly occurs due to mechanical processes such as cutting, breaking and crushing, drilling, abrasive and sand blasting, digging or hammering, and during dry handling due to particle release and/or resuspension (pouring, cleaning, mixing or polishing, among others) (WHO 1999, Finlayson-Pitts and Pitts 2000, NIOSH 2002, Chiu Leung *et al.* 2012). Particle shape and chemical composition in occupational exposure are very diverse and highly dependent on the type of activity, e.g. farming (predominance of PM_{10} particles, fibres and microorganisms with organic composition, feces, skin, and feed) (Cambra-López *et al.* 2010, Viegas *et al.* 2013), agriculture (mainly mineral particles such as silica and aluminium) (Schenker *et al.* 2009, Dewangan and Patil 2014) or mining (metals and inorganic components) (Dubey *et al.* 2012).

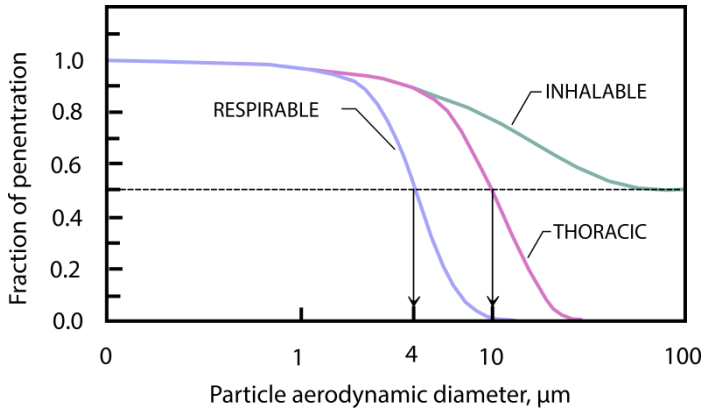

Figure 1.3 Probability of aerosol penetration as a function of aerodynamic diameter, internationally agreed by CEN/ISO/ACGHI. Source: modified from Sánchez Jiménez *et al.* (2011).

In the case of the ceramic industry and related activities, the main type of materials handled are ceramic materials, which are inorganic, non-metallic materials made from metal and a non-metal compounds, and may be crystalline or partly crystalline (Barba *et al.* 2000). Traditional ceramic materials are clay, feldspar, silica (quartz), kaolin, dolomite, talc, calcite, and nepheline with main primary particle morphology being plate-like and prismatic, and d_{50} values ranging from few µm up to hundred µm (Worrall 1982, Barba *et al.* 2000, López-Lilao *et al.* 2015, 2016, 2017). Their chemical composition is mainly SiO_2 and Al_2O_3 although other components can be present in lower amounts. Special attention is given to silica due to its health effects (see more in section 1.3.1) (Fang *et al.* 2010 and references therein, Chiu Leung *et al.* 2012). Activities which can lead to exposure to micron-sized silica dust are abrasive blasting with sand, sawing brick or concrete, sanding or drilling into concrete walls, grinding mortar, manufacturing

brick, concrete blocks, stone countertops, or ceramic products, and cutting or crushing stone (NIOSH 2002, Stefaniak *et al.* 2009, Radnoff and Kutz 2014).

Occupational exposure to airborne particles has been reported during several mechanic and handling processes, e.g.; pouring and packing of paint pigments, fertilizers, ceramic and cement materials (Koponen *et al.* 2015, Notø *et al.* 2018, Ribalta, *et al.* 2019a, Ribalta *et al.* 2019b), cleaning, dry wiping and sweeping (Douwes *et al.* 2017, Notø *et al.* 2018), welding (Notø *et al.* 2018), and repair tasks, floor screed layers, tile setting and mechanical milling (Peters *et al.* 2008, Ribalta *et al.* 2019c). It is interesting to highlight that particle emissions of fine and coarse airborne particles have also been detected during NP handling due to agglomeration, e.g.; packing of carbon black, carbon nanofibers, TiO_2 and Al_2O_3 (Kuhlbusch *et al.* 2004, Evans *et al.* 2010, Koivisto *et al.* 2012a, Kaminski *et al.* 2015), sweeping (Yeganeh *et al.* 2008), storage, weighting and reactor areas (Fujitani *et al.* 2008, Cena and Peters 2011, Kaminski *et al.* 2015).

1.2.3. Exposure to nanoparticles

A nanomaterial is defined as a natural, incidental or manufactured material containing particles, in an unbound state or as an aggregate or agglomerate and where, for 50 % or more of the particles in the number size distribution, one or more external dimensions is in the size range 1 nm-100 nm (Savolainen *et al.* 2013). However, currently there are 14 available definitions for nanomaterial (Boverhof *et al.* 2015).

In recent years, NPs have received special attention from the scientific community because of their larger surface area when compared to their non-nano counterparts, potentially toxic constituents, high alveolar deposition fraction, and therefore higher potential ability to penetrate into the blood vessels. Nanotechnology is currently present in our everyday life (electronics, cosmetics, drugs...) (Aitken *et al.* 2004), but exposure concentrations in work environments are from 60 to 450 times higher compared to non-occupational environments (Viitanen *et al.* 2017). NPs are usually divided in two groups, engineered and non-engineered NPs, both having an impact on worker exposure.

1.2.3.1. Engineered nanoparticles

Engineered or manufactured NPs (ENP/MNs) are intentionally engineered and produced particles with distinct properties and characteristics, affecting their physical, chemical

and biological behaviour (Colvin 2003, Aitken *et al.* 2004, Ibfelt *et al.* 2010, Kaluza *et al.* 2013).

They are usually presented in spherical, regular or irregular shape (nanocrystalls and cubes, quantum dots or dendritic forms), tubes, fibres and wires (ceramic and aluminium) (Aitken *et al.* 2004). In some cases, they can also be found in the form of aggregates (Kuhlbusch *et al.* 2004, Evans *et al.* 2010, Koivisto *et al.* 2012a, Kaminski *et al.* 2015).

Some of the most common chemical composition for engineered NPs are 1) nano-metals or nano-metal oxides such as SiO_2 (amorphous silica), TiO_2, Al_2O_3, Au and Ag, among others; 2) carbon based materials such as carbon black, carbon nanofibers, carbon nanotubes (CNTs), fullerenes or graphene; and 3) organic NPs or nano composites (Aitken *et al.* 2004, Ostiguy *et al.* 2010, Kaluza *et al.* 2013).

The worst scenario of risk of worker exposure to ENPs is during NP manufacture in dry state especially during production (when chambers are opened) capture, drying or packaging (handling) (Fujitani *et al.* 2008). Processes such as pouring and mixing, maintenance and cleaning, dust collection and ventilation, abrasive activities such as sanding and drilling composites, handling under fume hoods or at laboratory level, bagging, cleaning, weighting, spraying, and aerosol generators have been detected as activities with potential risk of worker exposure (Fujitani *et al.* 2008, Demou *et al.* 2009, Tsai *et al.* 2009, O'Shaughnessy 2013, Jensen *et al.* 2015, Mølgaard *et al.* 2015, WHO 2017, Fonseca *et al.* 2018, Jensen *et al.* 2019). Maximum mass levels were seen to range from few micrograms up to few thousand micrograms (O'Shaughnessy 2013). Conversely, maximum particle number concentrations were detected from thousands up to millions (Aitken *et al.* 2004, Brouwer 2010, Nazarenko *et al.* 2011, O'Shaughnessy 2013, Shepard and Brenner 2014).

1.2.3.2. Non-engineered nanoparticles

Non-engineered NPs in indoor workplaces originate from the background and from unintentional release from industrial activities (Brouwer *et al.* 2004, Viitanen *et al.* 2017). Background NPs are those coming from 1) outdoor, typically produced in high energy processes such as combustion (20-30 nm) (Viitanen *et al.* 2017), gas-to-particle conversion (Hämeri *et al.* 2009), nucleation processes or photochemical processes (Kulmala *et al.* 2004); and 2) generation inside the workplace but not related to any

specific activities, such as diesel engines e.g. forklifts, thermal processes or vacuuming among other processes (Maynard *et al.* 2004, Demou *et al.* 2008, Fujitani *et al.* 2008, Elihn and Berg 2009, Huang *et al.* 2010, Koivisto *et al.* 2012a, Ding *et al.* 2017). Thus, chemical composition may be very divers. In some workplaces, background concentrations have been reported to be higher than concentrations in urban environments what is generating current discussions (Viitanen *et al.* 2017).

Unintentionally-released NPs, also referred to as process-generated (PGNP) or incidental NPs, are primary or secondary nano-sized particles from industrial processes with or without relation to nanotechnology. Some examples are particles generated during thermal treatments, 3D printing, laser ablation, melting and combustion, soldering, welding, and metal grinding or abrasion processes among many others (Viitanen *et al.* 2017). Hence, their chemical composition is very variable, and particle morphology is mainly irregular or spherical (Fonseca *et al.* 2015, 2016, Viana *et al.* 2017, Salmatonidis *et al.* 2019). High risk of exposure to unintentional NPs has been observed during thermal spraying in pilot plant and industrial scenarios (Huang *et al.* 2016, Viana *et al.* 2017, Salmatonidis *et al.* 2019), ceramic tile sintering, ceramic firing and laser ablation (Voliotis *et al.* 2014, Fonseca *et al.* 2015, 2016, Salmatonidis *et al.* 2018), welding (Stanislawska *et al.* 2017, Viitanen *et al.* 2017), and ceramic dip coating and electrostatic spray deposition (Koivisto *et al.* 2018a, Koivisto *et al.* 2018b).

1.3. Particle-related health risk

1.3.1. Micro-sized particles

Exposure to PM as a result of air pollution is known as a risk factor for adverse health effects such as respiratory and cardiovascular diseases (WHO 2016, Gakidou *et al.* 2017, Landrigan *et al.* 2018). Specifically, particles are major causes of cardiovascular and respiratory morbidity (Fang *et al.* 2010, Ibfelt *et al.* 2010, Kreatsoulas and Anand 2010). The impact of particles on human health is related to particle size, size distribution, morphology and shape, surface area, agglomeration state, chemical composition and crystallinity (Hinds 1999, Aitken *et al.* 2004, Baron and Willeke 2011, Savolainen *et al.* 2013, Persons *et al.* 2014, Oberdörster and Kuhlbusch 2018) (Figure 1.4).

In occupational environments, exposure to PM differs from ambient air exposure in chemical composition, exposure frequency and duration, and particle concentration (which is usually higher than ambient air concentrations) (Fang *et al.* 2010). These differences require specific worker exposure assessments as they may have different health implications (Fang *et al.* 2010). Ischemic heart and increase on cardiovascular disease risk was observed to increase in, among other examples, mine workers, workers exposed to silica, diesel exhaust and inorganic dust, construction, metal and asphalt workers, and heavy equipment operators (Kuempel *et al.* 2003, Fang *et al.* 2010).

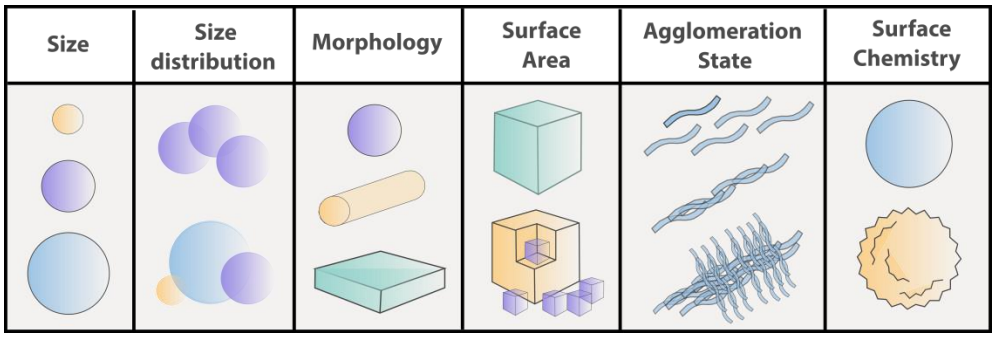

Figure 1.4 Particles characteristics affecting human health. Source: modified from Persons *et al.* (2014) and Fonseca (2016).

In the case of the ceramic industry, no solid link between ceramic workers exposure to PM and cardiovascular diseases has been found (Fang *et al.* 2010); conversely, respiratory-related disease due to inhalable dust have been reported in several studies (Dehghan *et al.* 2009, Neghab *et al.* 2009, Alim *et al.* 2015). For example, inhalation of respirable crystalline silica (RCS) dust can cause silicosis, one of the major causes of morbidity and mortality worldwide, prevalent in low- and middle-income countries (NIOSH 2002, Chiu Leung *et al.* 2012). Moreover, RCS dust generate at workplaces has been recently classified as carcinogenic for humans (Directive 2017/2398/EC). Research is ongoing aiming to minimize RCS hazardous potential, through for example particle coatings using organosilanes (Ziemann *et al.* 2017). Other exposure impacts characteristic of the ceramic industry, driven by particle size and size distribution, are evident in the literature but their specifically health effects are not yet fully understood. This is why this kind of impact is the main focus of this Thesis.

1.3.2. Nanoparticles

Adverse health effects have been linked to particles < 100 nm (Oberdörster 2001) due to their ability to reach the deepest sections of the respiratory tract (alveolus) because of

their small size, the fact that they cannot be removed from the airways by mucociliar clearance and translocation to other organs (Figure 1.5). NPs are removed in the alveolus by macrophage clearance and they can be transferred to other body organs via the gastro-intestinal compartment more easily than non-nano particles (Behrens *et al.* 2002, Aitken *et al.* 2004). In addition, due to high NPs concentration and longer retention time, macrophages disruption occur, which induces inflammation (NIOSH 2002, Fang *et al.* 2010, Saber *et al.* 2014) and NPs penetration through epithelial cells to the blood stream (Gilmour *et al.* 2004). Ultimately, this leads to translocation to other organs as for example the brain (Oberdörster *et al.* 2004, Donaldson *et al.* 2005, Knol *et al.* 2009) (Figure 1.5).

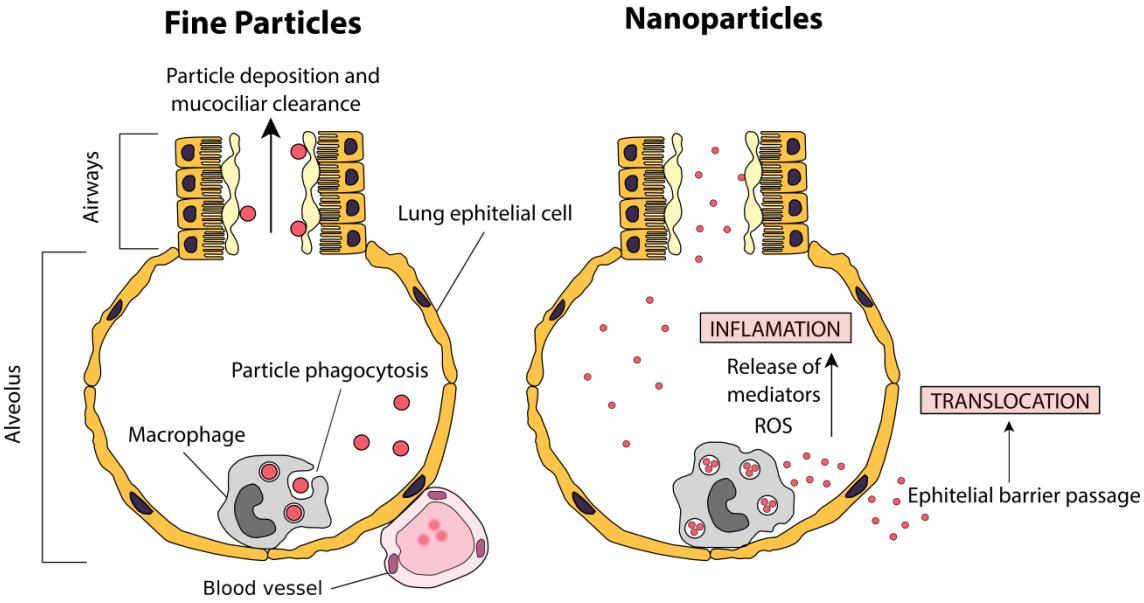

Figure 1.5 Mechanisms of inflammation and translocation. Source: modified from Marianne Dybdahl in Vogel *et al.*(2018).

In vivo studies reveled that NPs can cross the alveolar barrier in much higher numbers than coarser particles and induce inflammation (Dybdahl *et al.* 2004, Hougaard *et al.* 2010, Fröhlich and Salar-Behzadi 2014, Monsé *et al.* 2018) and cause cancer in mice and rats due to CNTs exposure (Kasai *et al.* 2016, Fukushima *et al.* 2018). There is evidence that pulmonary exposure to particles may increase cardiovascular risk by increasing plaque progression in the aorta (Thompson *et al.* 2018, Vogel and Cassee 2018) and lung damage such as fibrosis and plural granuloma (Hedmer *et al.*2014).

Particle surface area has been found to correlate well with pulmonary response regardless of particle size. However, it seems that this may also be a function of the agglomeration state. Primary particles can form aggregates (strongly bonded) when

spherical primary particles stick together by van-der-Waal's forces. These aggregates can then combine to form larger agglomerates (weakly bonded) (O'Shaughnessy 2013 and references tehrein). However, implications of agglomeration state on toxicity are currently under investigation (O'Shaughnessy 2013 and references tehrein) as they may have increased toxicity compared to larger particles (Oberdorster *et al.* 1994, Aitken *et al.* 2004).

1.4. Exposure assessment

Exposure assessment is the process of evaluating the exposures, accumulated doses and the derivate health effects to which a group of individuals is exposed (Ramachandran 2005). In order to assess worker exposure to airborne particles several strategies can be used. The sampling strategy should be effective in capturing the variability of workplace sources, feasible, efficient and should not require a large number of samples (Ramachandran 2005, Dahmann *et al.* 2008). For NP exposure, several authors (e.g., Methner *et al.* 2010, Ramachandran *et al.* 2011, Asbach *et al.* 2012, Brouwer *et al.* 2012, OECD 2015) have identified the need for a tiered approach to facilitate exposure assessment, which is described briefly below (Figure 1.6). This kind of approach is also typically used for exposure other types of workplace air pollutants such as micron-sized particles and chemical agents (UNE-EN-689 2019).

- Tier I - Initial assessment: the identification of potential particle emission mechanisms and worker exposure is qualitatively assessed by gathering as much information as possible regarding the site and the type of particles released. In order to complete this tier, risk assessment and control banding based tools such as ART, Stoffenmanager or NanoSafer may be used in the case of NPs and chemical agents. If particle release or exposure cannot be excluded a second tier level needs to be conducted.

- Tier II - Basic exposure assessment: the main focus of this tier is to conduct a basic release and exposure assessment on-site, by using easy-to-use and portable online and offline instruments (e.g. portable CPC, DiSCmini or OPC, see 3.3). Usually, the use of a combination of instruments is required. One of the main challenges is to quantify background particles in order to differentiate process particles from background particles and to decide whether or not measured concentration increases are statistically significant (Brouwer *et al.* 2009, Ramachandran *et al.* 2011). Background particles can be

assessed by using several sampling strategies (Brouwer *et al.* 2009, Kuhlbusch *et al.* 2011): 1) temporal background (measure in the process location before and/or after the process) (Kuhlbusch *et al.* 2004, Fujitani *et al.* 2008, Yeganeh *et al.* 2008, Bello *et al.* 2009, Asbach *et al.* 2012); and 2) spatial background (measure near the process, but sufficiently far so that process particles do not impact background spatial measurements) (Demou *et al.* 2008, Tsai *et al.* 2008, Asbach *et al.* 2012). In some studies, outdoor concentrations were additionally monitored (Kuhlbusch *et al.* 2004, Demou *et al.* 2008, Fujitani *et al.* 2008).

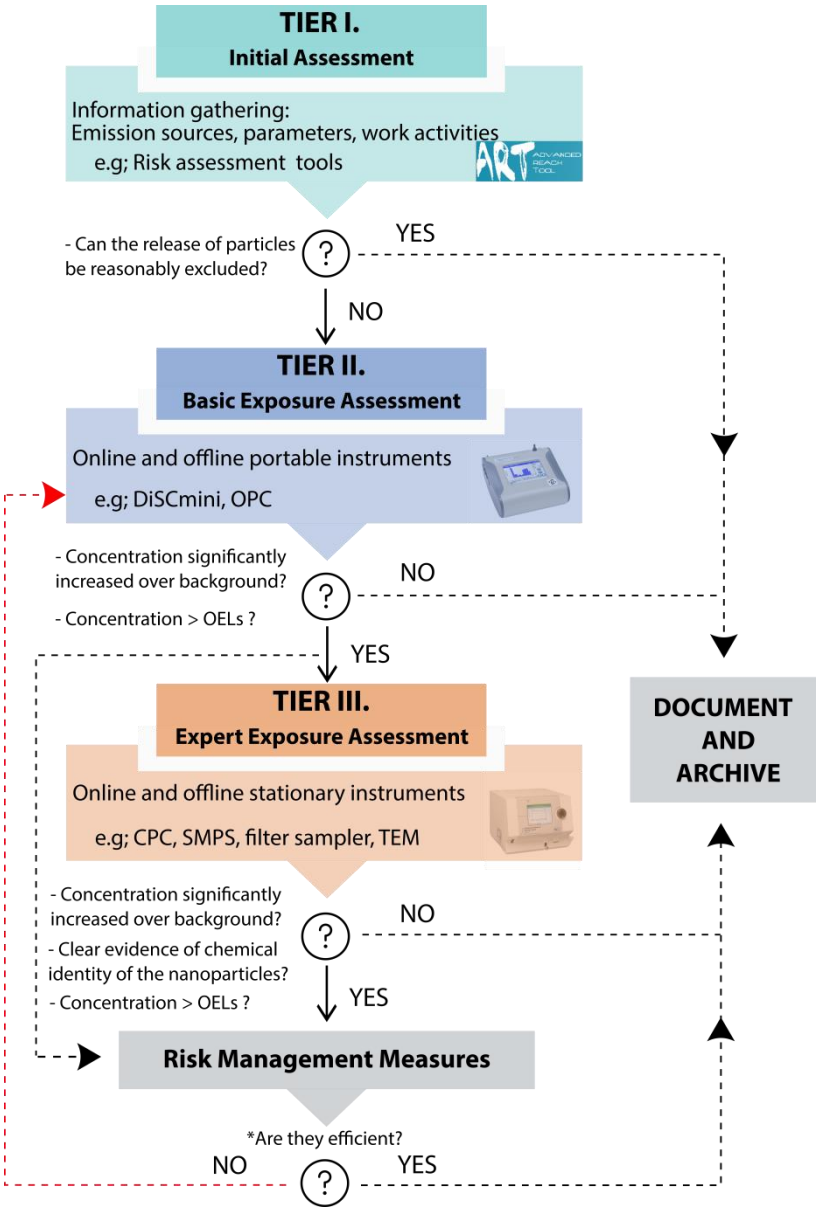

Figure 1.6 Tiered approach flow chart recommended for workplace exposure assessment. Source: modified from OECD (2015) and UNE-EN 689 (2019). * Efficiency of applied measures is assessed going back to tier II and III. DiSCmini, OPC, CPC, SMPS and TEM are online and offline instruments and techniques used in exposure assessment (see section 3.3).

A specific approach using measured background concentrations to assess statistical significant increases of NPs has been designed in Asbach et al. (2012), which is also referred in this Thesis as the nanoGEM approach:

Mean concentration during packing $> BG \pm 3 \cdot (\sigma BG)$, Eq. (1.1)

where BG is the mean temporal background (or pre-activity) concentration and σBG is the standard deviation of the background concentration.

In addition, recently, the ARIMA models, which are the most general type of models used for analyzing time series while considering the autocorrelation between samples, have been proposed in the EN 17058:2018 (standard for workplace exposure- assessment of exposure by inhalation of nano-objects and their aggregates and agglomerates) as the golden standard method for number concentration and other metrics analyses. However, for particle mass there is no specific method to determine statistically significant increases other than conventional statistical tests. This issue is discussed in detail in Chapter 4 (Publication III). In order to evaluate exposure to particle number concentrations, the Tiered approach recommends Eq. 1. Conversely, for particle mass concentration comparison with OEL values is recommended (UNE-EN-689 2019).

When significant particle emissions due to the process under evaluation are detected, tier III must be conducted.

- Tier III - Expert exposure assessment: the aim is to obtain as much information as possible on released NPs in the occupational environment in order to determine whether or not exposure can be excluded or if further risk management steps need to be implemented. In tier III all relevant instruments and techniques available should be used, including personal samplers and high-resolution instruments in order to provide a definitive conclusion regarding worker exposure. If a clear increase on particle exposure due to the process (significant increase over background and higher concentration than reference values) is observed, then risk management measures need to be implemented prioritizing reduction of exposure concentrations over increasing personal protection. Effectiveness of implemented measures needs to be further verified by conducting tier II and III again.

Traditionally, particle mass concentrations (usually expressed as μg m^{-3} or mg m^{-3}) have been the most commonly used metric to report human exposure to airborne particles. However, it is known that mass may not always be the most appropriate metric to report

health effects on humans deriving from particle inhalation (Ramachandran 2005). This is especially true for NP exposure assessment, for which particle number and surface area have been suggested as more appropriate metrics for inhalation exposure assessment and are more widely used (Aitken *et al.* 2004, Brouwer *et al.* 2009, Hämeri *et al.* 2009). This is because contribution to particle mass concentrations of particles between 1 and 100 nm is negligible when compared to coarser particles. Direct links between total surface area of pulmonary deposited particles and cardiovascular risk have been found for example for TiO_2, black carbon NP and CNTs (Donaldson *et al.* 2002, Saber *et al.* 2014, Poulsen *et al.* 2016). Discussions are ongoing regarding the definition of the most appropriate metrics (Park *et al.* 2010, O'Shaughnessy 2013, Viitanen *et al.* 2017), which are in addition complex due to the variability of particle types and diameters in different microenvironments. For instance, studies have revealed that particles emitted during NP handling can be found in aggregate and agglomerate form (Kuhlbusch *et al.* 2004, Fujitani *et al.* 2008, Kuhlbusch *et al.* 2009, Stahlmecke *et al.* 2009), and therefore particle mass concentrations should also be considered a relevant metric when assessing NP exposures (Koivisto *et al.* 2012a).

Worker exposure monitoring can be conducted by using online (real-time) and offline instruments. Online instruments provide size resolved/integrated and time resolved (1 s up to 1 min) information regarding particle size and size distribution, surface area, and/or particle number and mass concentrations. However, they do not allow differentiating particles composition. Online instruments are generally divided in two types according to their portability (stationary and portable). Stationary instruments are those complex in terms of use and transportation, due to their size and weight but provide high-resolution measurements. Portable instruments, on the other hand, are useful for the detection of particle hotspots, personal monitoring, monitoring screening tasks, or testing the effectiveness of preventive measures (as they can be worn by the workers without influencing their work activity).

Offline instruments (size and time integrated), on the other hand, allow not only to gravimetrically determine particle mass concentrations but also physically and chemically characterise the collected particles. Offline techniques cover from simple open-face sampling solutions such as air sampling cassettes, to more complex equipment such as filtration, electrostatic or thermal precipitation instruments, or cascade impactors. The samples collected in the filters can be gravimetrically and chemically analysed. Additionally, morphology, geometry and optical size of particles and

agglomerates can be analysed by using electron microscopy techniques such as high resolution transmission electron microscopy (TEM) or scanning electron microscopy (SEM). Particles and agglomerates chemical composition and surface properties can be additionally identified by using energy dispersive X-ray spectroscopy (EDX) often coupled with SEM or TEM devices.

1.4.1. Exposure prediction tools: the dustiness index

During handling of a powdered material, particle emissions are driven, among other factors, by the material's dustiness index. The dustiness index is a measure of the tendency of a powdered material to release particles in response to a mechanical or aerodynamic stimulus (Plinke *et al.* 1992, Lidén 2006). The amount of emitted material mass (mg) per mass of handled material (kg) is ranked in different levels of emission. Dustiness is not an intrinsic property of powders, it depends on physic characteristics (e.g., humidity, surface coating, primary particle size and aggregate size), as well as on the mechanic or aerodynamic stimulus (e.g. type of method used and energy applied, and environmental conditions) (Plinke *et al.* 1995, Breum 1999, Evans *et al.* 2013).

Several methods are available to determine dustiness in the literature (Hamelmann and Schmidt 2003), such as the Vortex shaker (Dazon *et al.* 2017), the Venturi device (Evans *et al.* 2013) or the Heubach Dustmeter (Type 2000, Heubach GmbH, Germany), but only two are accepted as standard method (EN 15051): the Continuous Drop (C.D) and the Rotating Drum (R.D). The main difference between the two standard tests are that in the C.D fresh material is used continuously (dropped by gravitational forces) whereas in the R.D fresh material is placed inside the device at the beginning of the test and it is repeatedly agitated (drum rotation and drop of the material by gravitational forces). The method selected to quantify the dustiness of a given material should reproduce as closely as possible the type of mechanical stimulus and energy to which material would be subjected (CEN 2013, Evans *et al.* 2013).

Due to its ability to measure material's tendency to generate airborne dust during handling, the use of dustiness has risen as a tool for occupational safety (Hamelmann and Schmidt 2003). The dustiness of a given material is determined under laboratory conditions and following standardized (CEN) methodologies, and is therefore a parameter which is relatively simple to obtain. As a result, dustiness of powders is frequently reported by manufacturers in the technical specifications.

Discussions are ongoing about the use of the dustiness index as a predictor of worker exposure (Brouwer *et al.* 2006, Evans *et al.* 2013, Levin *et al.* 2014, Fonseca *et al.* 2018, Ribalta *et al.* 2019b, 2019c). However, yet no clear direct relationship dustiness-exposure has been established as certain authors found no clear or limited relationship between exposure and dustiness (Brouwer, 2006; Class *et al.* 2001; Fonseca *et al.* 2018; Heitbrink *et al.* 1990), whereas other found statistically significant correlations (Heitbrink *et al.* 1989, Breum *et al.* 2003, Brouwer *et al.* 2006).

When establishing the relationship between dustiness and exposure, certain factors need to be considered: 1) material dustiness depends mainly on material particle size distribution, humidity, density, morphology and specific surface area (SSA) (Hamelmann and Schmidt 2003; Lidén 2006; López-Lilao *et al.* 2016, 2015); 2) dust emissions are known to depend on the amount of material handled, the process, and local controls (Fransman *et al.* 2011); and 3) the dustiness test methodology should mimic as closely as possible the actual process energy applied (CEN 2013, Evans *et al.* 2013), while the different methodologies are often not directly comparable (Hamelmann and Schmidt 2003).

As a result, dustiness is currently used as an input for exposure modelling (Levin *et al.* 2014; Schneider and Jensen 2007) and by material producers to modify products in order to reduce dust generation (Lidén 2006), rather than as a direct exposure predictor. Thus, it is important to continue working on dustiness test performance as well as to understand which the key factors to predict worker exposure are. This issue is addressed in detail in Chapter 4 (Publication I, II and III).

1.4.2. Exposure modelling: mass-balance models

Traditionally, exposure monitoring has been the most common method to evaluate worker exposure. However, due to the need to estimate exposure during a large variety of work micro-environments and materials under REACH regulation (EC 1907/2006), exposure prediction mass-balance models have been proposed as valuable risk assessment tools (Keil 2000, Ramachandran 2005, Spencer and Plisko 2007, Koivisto *et al.* 2019). In this context, models may contribute to understanding critical factors driving exposure and allow for more efficient risk mitigation strategies (Spencer and Plisko 2007, Hussein *et al.* 2015).

Different levels of complexity are available for exposure models, which are mostly based on mass-balance equations (Keil 2000, Ramachandran 2005, Jayjock *et al.* 2011, Ganser and Hewett 2017, Hewett and Ganser 2017). The simpler model is the saturation vapor pressure model, only applicable to gas and vapor exposure, and which provides the most conservative exposure estimates. More complex models are the one-box model (or well-mixed room) which includes ventilation (Hewett and Ganser 2017), and the two-box model (or near-field "NF" far-field "FF" model) (Ganser and Hewett 2017), which has also been expanded to more boxes, e.g. three-box model (Jensen *et al.* 2018). However, higher complexity implies higher input requirement and thus, more complex to parametrize, especially in real-world scenarios (Keil 2000, Jensen *et al.* 2018).

These tools aim to model particle exposure in one-, two- or more boxes in which particle emissions are generated by a source and where particle transport and removal is determined by airflows between the different compartments, structural elements (e.g. doors), the total air exchange through doors, and mitigation strategies (e.g. ventilation extraction systems).

The one- and two-box models (Figure 1.7) are based on a set of mass balance equations including information of the source (contaminant generation), and transport. Usually, and for the sake of simplicity models assume that 1) particles are fully mixed at all times; 2) mass is created by a source inside the limits of the model (NF in the two-box model) and initial concentrations are zero; and 3) particle losses are due to natural and mechanical ventilation (Ramachandran 2005, Ganser and Hewett 2017, Hewett and Ganser 2017, Koivisto *et al.* 2019). However, outdoor or incoming concentrations can be included in the models, as well as other particle removal mechanisms such as deposition or coagulation in order to improve model accuracy (Jensen *et al.* 2019, Ribalta *et al.* 2019a, 2019d).

In the one-box model there is the limitation that the effect of proximity to the source is not considered and, thus, exposure near the source is usually underestimated (Keil 2000, Ramachandran 2005, Arnold *et al.* 2017, Jensen *et al.* 2018). Conversely, in the two- or more box model the effect of source proximity on exposure is included but it comes at the cost of requiring measurements of the interzonal (NF-FF) flow rate (Ramachandran 2005, Jensen *et al.* 2019). The two-box model is a well-accepted exposure assessment tool in the risk assessment field as, even with its simplified assumptions, it is able to adequately simulate actual conditions for various processes

including volatile compounds and PM emissions (Jayjock *et al.* 2011, Arnold *et al.* 2017). The fact of adding extra boxes was seen to increase model performance (Jensen *et al.* 2018). A number of other more complex and resource-intensive models are also available (Ramachandran 2005).

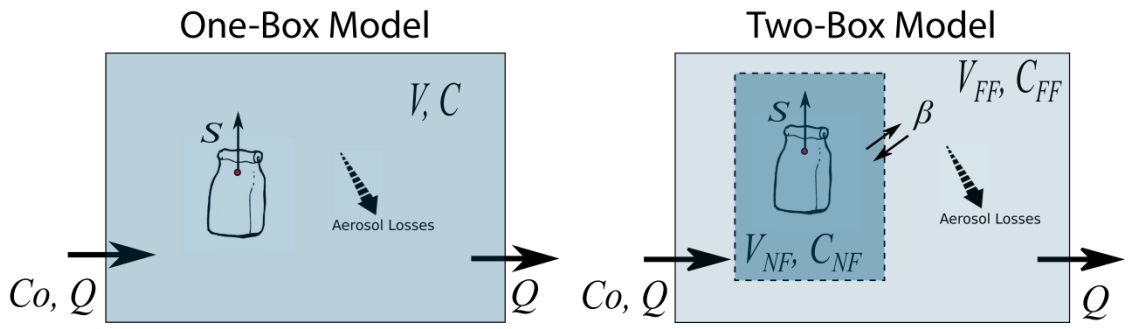

Figure 1.7 Generation and behavior of airborne particles inside a one- and two-box model. C: concentration. C_0: incoming concentration. C_{NF} and C_{FF}: near-field and far-field concentrations. Q: flow. S: emission rate. V: volume. V_{NF} and V_{FF}: near-field and far-field volume. β: near-field (NF)/far-field (FF) interzonal flow rate.

Since the initial application of exposure prediction models, several research papers have been published regarding their theoretical aspects (Nazaroff and Cass 1989, Nazaroff 2004, Hussein *et al.* 2005, Hussein and Kulmala 2008, Ganser and Hewett 2017, Hewett and Ganser 2017) and they have been tested in different environments (Nicas 2016; Sahmel *et al.* 2009 and references therein; Jayjock *et al.* 2011 and references therein; Boelter *et al.* 2009, Johnson *et al.* 2011, Jones *et al.* 2011, Koivisto *et al.* 2015, 2019, Lopez *et al.* 2015, Arnold *et al.* 2017). However, in order to implement exposure prediction models as trustworthy tools in the framework of risk assessment (Spencer and Plisko 2007), additional real-world cases need to be evaluated to test model performance and to understand the uncertainties related to critical parameters (determinants of exposure) (Mølgaard *et al.* 2014, Tielemans *et al.* 2008a) such as source characterization, local controls, and air mixing, which are not yet fully parametrized (Baldwin and Maynard 1998, Sahmel *et al.* 2009, Cherrie *et al.* 2011, Jayjock *et al.* 2011, Keil and Zhao 2017) and are often challenging to estimate (Zhang *et al.* 2009) in real-world scenarios.

Key parameters which drive model performance are (Fig 1.8):

- Particle emission rate: it can be estimated by using two different approaches depending on the type of process and information available: dustiness index and quantification of the emission rates from monitored concentrations. When modelling exposure to airborne particles due to handling of a dusty material, the most common method to

estimate the emission rate is by using the dustiness index. For modelling, dustiness is linked to the actual activity by an energy factor (H), which by definition links the energy applied during the process with the energy applied during the dustiness test (Schneider and Jensen 2007) and can range from 0 to 1 (Lidén 2006, Koivisto *et al.* 2015). The parameter H has been defined for the R.D dustiness test by Van Tongeren *et al.* (2011) for the Advanced REACH tool. However, currently the scaling of the source by using handling energy factor is not yet well understood and works are ongoing in order to parameterize the H factor. For those processes not including handling of dusty materials e.g. emission, or dustiness is unknown, equations to estimate emission rates have been described (Sachse *et al.* 2012, Hewett and Ganser 2017) and used on real scenarios by using mass balance equation and convolution theorem (Koivisto *et al.* 2018a, Koivisto *et al.* 2018b). However, literature regarding emission rates quantification is still relatively scarce (Koivisto *et al.* 2017).

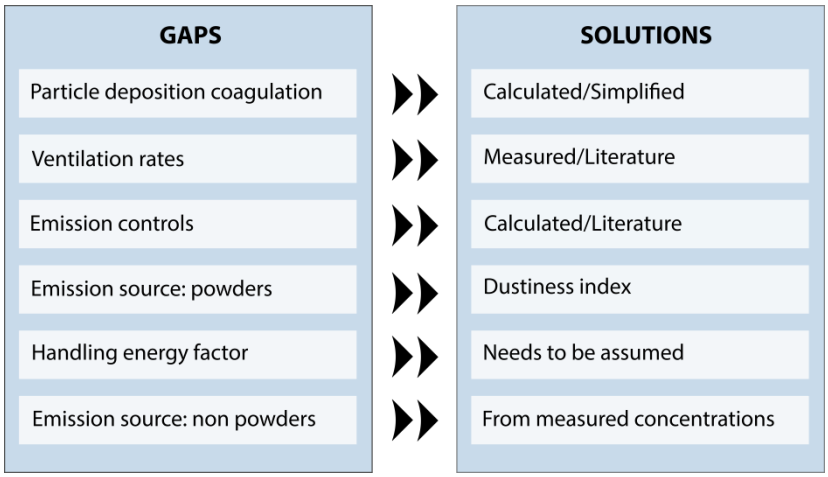

Figure 1.8 Modelling gaps and solutions.

- Local controls or protection factors: all those actions preventing dispersion of the aerosolized particles or removing particles from air, e.g. enclosures or local extraction systems (Fransman *et al.* 2008), need to be included as well in the equations as an estimated or calculated factor of reduction. When having to consider extractions systems, local control values associated can be determined, by using relatively simple equations (Hewett and Ganser 2017), but in some cases key parameters are missing and they are not applicable. Fransman *et al.* (2008), revised by Goede *et al.* (2018), presents an exposure control efficacy library, which contains efficacy values for enclosure, local exhaust ventilation, general ventilation, suppression techniques and enclosure of the

worker, this values can be used when specific data is missing. Additional data are reported by Salmatonidis et al., (under review).

- Air exchange ratios (AER in air changes per hour, ACH) and air flow between near-field and far-field (β): need to be calculated or estimated. This should be a relatively easy to obtain parameter as only speed velocities are needed and box model sizes are required. However, in practice estimating β can be challenging (Vernez *et al.* 2004, Spencer and Plisko 2007) as velocities may be unknown, and thus ventilation needs to be estimated from actual concentrations (Keil 2015, Keil and Zhao 2017) or assumed from literature (Baldwin and Maynard 1998).

1.5. Risk assessment

Risk assessment is a decision-making process to systematically evaluate potential exposures, risks associated to identified hazards and risk factors, and determine appropriate ways to eliminate the hazard or control the risk (CCOHS 2017). Traditionally, risk assessment is a result of a step paradigm including hazard identification and assessment, and exposure assessment (Savolainen *et al.* 2013). Overall risk of adverse health effects due to particle inhalation depends on their hazard (negative action in the organism and cells) and exposure (concentration in the inhaled air and deposition in the respiratory tract).

$$Risk = Hazard\ x\ Exposure \qquad \text{Eq. (1.2)}$$

1.5.1. Inhalation deposition models for health risk assessment

The effects of particles on human health depend mainly on: particle chemical composition, deposition in the human respiratory tract as function of particle size (Heyder *et al.* 1986, Cousins *et al.* 2011) (Figure 1.9), and, especially in the case of NPs, the potential for translocation to other body organs.

While mean particle size can provide a general idea of the likely impact of inhaled particles in respiratory human health, detailed knowledge of particle size distribution can provide additional insights into particle deposition along the regions in the respiratory tract, irrespective of the chemical compositionof the particles.

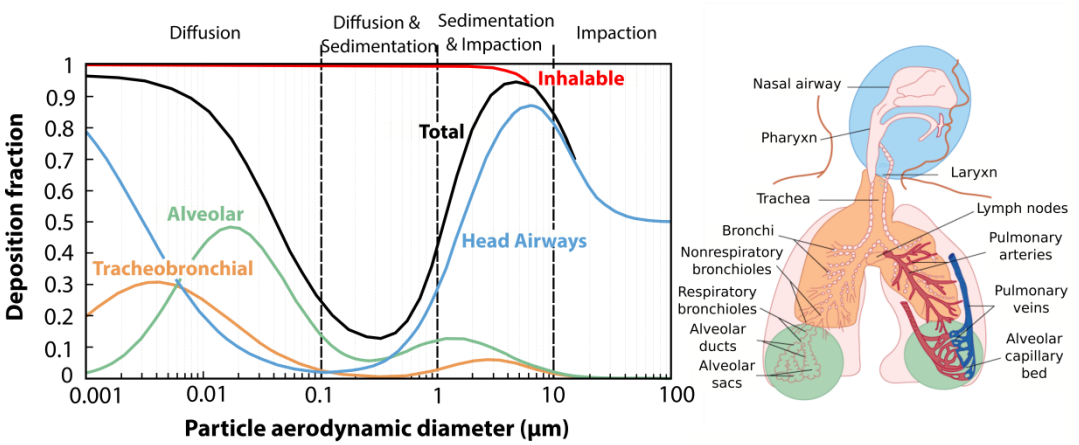

Figure 1.9 ICRP human deposition. Source: modified from Koivisto (2013) and Madanchi *et al.* (2018).

Particle regional deposition in the human respiratory tract is inversely related to particle size and is mainly determined by 4 mechanisms: 1) inertial impaction (particles possess enough momentum to keep their trajectory and not follow the dominant airflow, and thus collide with the respiratory tract walls); 2) sedimentation (time dependent, the more time air is in the respiratory tract, the higher the particle deposition due to gravity); 3) diffusion (particles randomly collide with other objects and are trapped due to van-der-Waals forces); and 4) minor mechanisms such as electrostatic interception (Heyder *et al.* 1986, Carvalho *et al.* 2011, Hussain *et al.* 2011) (Figure 1.10).

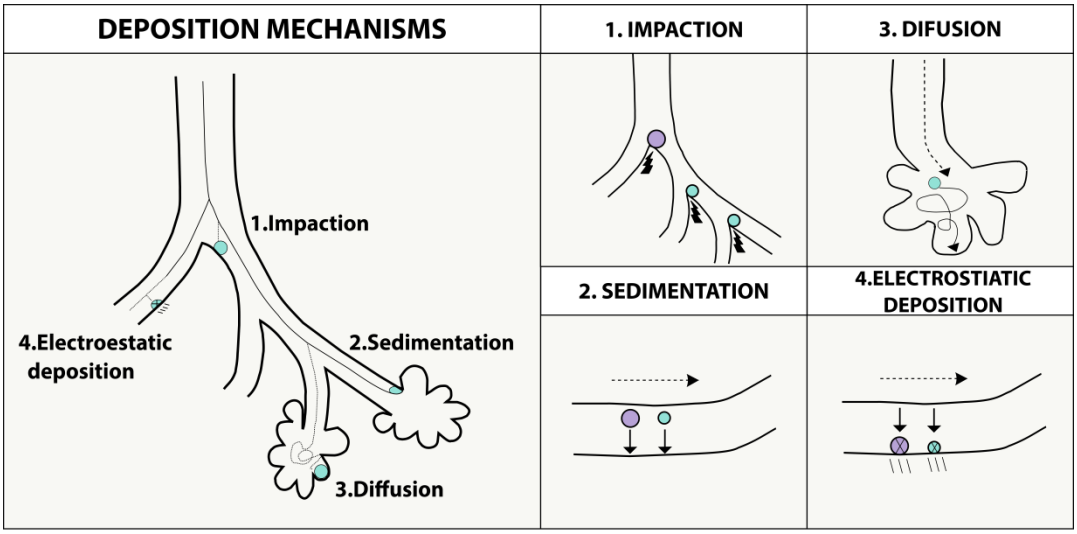

Figure 1.10 Deposition mechanisms. Source: modified from Capstick and Clifton (2014), Dubsky and Fouras (2015) and Keil (2015).

Particles with sizes between 0.01 and 0.1 µm, and 1 and 5 µm mainly deposit in the tracheobronchial and alveolar regions, the deepest areas in the human respiratory system (Heyder *et al.* 1986, Madanchi *et al.* 2018) (Figure 1.9). Conversely, particles > 10

μm rarely penetrate into the respiratory tract, and particles between 0.1 and 1 μm have the lowest deposition rate in the human respiratory system with less than 20% of the inhaled particles depositing in the human respiratory system (Bailey and Roy 1994, Hinds 1999, Cousins *et al.* 2011) (Figure 1.9). Therefore, particles between 0.001 and 0.1 μm, and 1 to 10 μm, are of special concern from a deposition and also translocation perspective. However, regional deposition is not only ruled by the particle size and size distribution, but also affected to a great extent by inhalation flow rates, age and gender (Hussain *et al.* 2011). Other factors such as particle shape, charge, density and hygroscopicity, pulmonary physiology (breathing pattern, inspiration period, nasal or oral breathing and lung geometry) are known to affect particle deposition in the respiratory tract (Heyder *et al.* 1986, Dolovich 2000, Carvalho *et al.* 2011, Hussain *et al.* 2011). Finally, health hazardous consequences due to particle inhalation will also depend on particle chemical composition, uptake (transport to the blood stream), redistribution, storage and removal (clearance and excretion) and translocation (Hussain *et al.* 2011, Fernández Tena and Casan Clarà 2012).

Due to the intrinsic complexity of particle deposition along the human respiratory tract, *in vivo* studies present limitations to understand deposition mechanisms, and thus modelling approaches have been developed (Hussain *et al.* 2011, Koivisto *et al.* 2012b). Currently, the two main types of empirical models used are single and multiple path models (Ramachandran 2005). In single path models the human respiratory tract is considered a series of symmetrical compartments where all pathways are identical and have equal linear dimensions. Conversely, in multiple path models the asymmetry of the lung branching pattern is considered, thus providing more realistic deposition dose fractions. Two of the most widely used empirical deposition models are the International Commission on Radiological Protection (ICRP) single path model, and the multiple path particle dosimetry model (MPPD). Even though empirical models have been widely used and improved, it should be noted that they do not include NP-specific effects (Fröhlich and Salar-Behzadi 2014), particle morphology, chemical composition or translocation, factors which impact human health. The focus of these models is on particle deposition along the human respiratory tract as a driver of respiratory health risk, but not cardiovascular risk (as they do not include translocation to other organs). Particle deposition modelling is discussed and applied in Chapter 4 (Publication II and III).

1.5.2. Risk assessment tools

The Registration, Evaluation, Authorization, and Restriction of Chemicals (REACH) regulation implemented by the European Chemical Agency (ECHA) requires producers and importers of substances (including nanomaterials) to ensure the safety of any product brought to the market (EC 1907/2006) by analyzing their impact on human health and the environment. A large number of empirical models, based on dimensionless exposure modifying factors to calculate an exposure score which is further converted to an exposure value by using calibration factors (e.g. Schinkel *et al.* (2011)), have been developed in order to provide risk assessment of chemical hazards under the REACH regulation (Fransman *et al.* 2011; Kristensen *et al.* 2010; Tielemans *et al.* 2008b; Jensen *et al.* in preparation). ECHA recommended quantitative exposure inhalation tools for risk assessment are the ECETOC TRA (ECETOC targeted risk assessment, 2004, 2009, 2012), MEASE (EBRC, 2010) and EMKG-Expo-Tool (EMKG, BAuA, 2008, 2016) as Tier I, and Stoffenmanager (Marquart *et al.* 2008) and the Advanced REACH tool (ART) (Fransman *et al.* 2011) as higher tier tools (ECHA 2016b). Stoffenmanager (Marquart *et al.* 2008) and ART (Fransman *et al.* 2011) have been tested in different scenarios including dust emissions (Landberg *et al.* 2015, 2017, Riedmann *et al.* 2015, Bekker *et al.* 2016, Savic *et al.* 2018) and were seen to both over and under estimate actual exposure concentrations (Landberg *et al.* 2017, Savic *et al.* 2017, Van Tongeren *et al.* 2017). In addition, the exposure modifying factors are not always clearly described which makes the models challenging to evaluate (Koivisto *et al.* 2018, Koivisto *et al.* 2019). Therefore, there is controversy regarding their use with regulatory purposes and whether or not their results are sufficiently robust (Raul 2003, Koivisto *et al.* 2019). ECHA recommends using measurement data in exposure assessment for substances with high hazardous potential (ECHA 2016a, 2016b).

However, all previously mentioned risk assessment tools present important limitations when it comes to exposure and risk assessment of nanomaterials (Liguori *et al.* 2016). Risk assessment based on control banding represents an alternative approach based on "computational" hazard and exposure for the control of workplace exposure to agents with unknown or uncertain toxicological properties, and lack of quantitative exposure estimations (Liguori *et al.* 2016). Thus, control banding tools, which are frequently user-friendly and have low input requirements, are used to guide the assessment and management of workplace risks due to nanomaterials with the final goal to assess the levels of precaution required to control their risks by grouping them into control

categories or bands (Zalk and Heussen 2011, Hristozov *et al.* 2016). Examples of control banding tools in literature are Stoffenmanager nano-module (TNO, Van Duuren-Stuurman *et al.* (2012)), CB NanoTool (Lawrence Livermore National Institute by Paik *et al.* (2008)), Precautionary matrix (TEMAS, Höck *et al.* (2013)), IVAM guidance (Cornelissen *et al.* 2011), NanoSafer (NRCWE, Kristensen *et al.* (2010) and Jensen *et al.* in preparation), and GUIDEnano tool (LEITAT). However, due to their novelty, control banding tools have not yet been thoroughly tested and compared, and thus they are recommended to be used with care (Sánchez Jiménez *et al.* 2016).

In general it was found that risk assessment and control banding tools comparison and standardization is complex as their input and output data vary considerably (Hristozov *et al.* 2016, Liguori *et al.* 2016, Sánchez Jiménez *et al.* 2016). In addition, many of them still have not been fully validated and/or calibrated (Hristozov *et al.* 2016).

1.6. Legislation: worker exposure to airborne particles

The European Union (EU) has set air quality limit values for ambient air PM and other pollutants (Directive 2008/50/EC). However, there are no direct limit values established for indoor air quality. For occupational exposure, each European member state has to establish its own limits based on the Commission directives of indicative OELs 2000/39/EC (2017/164/EU) and binding OELs 98/24/EC) for chemical agents. In Spain, it is the (Real Decreto 374/2001) which transposes to the Spanish law the directives from the Commission, making reference to the limit values published by the "Spanish National Institute for Health and Safety at Work", Instituto Nacional de Seguridad y Trabajo (INSHT). The INSHT publishes annually a list of daily OELs (value to which workers can be exposed during 40 h a week, 8 h a day, during their entire life without suffering any adverse health effects) and short term OELs (period of 15 minutes or less, depending on the chemical, during the work shift) (Table 1.1).

Table 1.1 INSHT 2018 limits, OEL (occupational exposure values) for inhalable and respirable particles not otherwise specified and respirable crystalline silica.

Description	OEL
Inhalable fraction (particles not otherwise specified)	*10 mg* m^{-3}
Respirable fraction (particles not otherwise specified)	*3 mg* m^{-3}
Respirable crystalline silica: quartz and cristobalite	*50 µg* m^{-3}

Currently, discussions are ongoing regarding OEL limits for low-toxicity dusts, with some authors believing they are too high (Koponen *et al.* 2015; commentary by Cherrie *et al.* 2013 and response letter by Kuempel *et al.* 2014). Additionally, in an analysis of occupational standards in Germany (the maximum workplace concentrations or the MAK values) it was found that these values were also not purely health-based (Ramachandran 2005). Therefore, further studies regarding toxicity and exposure to airborne particles are required to ensure worker health and safety.

1.6.1. Nanoparticle exposure legislation

In October 2011, the European Commission published a recommendation for a definition of a nanomaterial. However, different definitions are available and nanomaterials are not regulated by a separate legislation. Integration of the nanomaterial definition and consequences to specific sectors and regulations has already been implemented for biocides (EU 528/2012), food (EC 2015/2283) and (EU 1169/2011), medical devices (EU 2017/745), cosmetics (EC 1223/2009), and recently for chemical agents (REACH 2006, EC 1907/2006).

Currently, OECD test guidelines for nanometerial characterization are being developed, as well as other measurements for standardization (CEN EN 17058:2018 for occupational nanomaterial exposure assessment and Zhao *et al.* (2018) for indoor/outdoor measurements). However, the lack of 1) systematic and detailed information on the potential hazards; 2) scientific and reliable knowledge on risk assessment; and 3) *in vivo* studies with systematic short- and long-term toxicity tests, which are required for risk assessment (Van Broekhuizen *et al.* 2012, Savolainen *et al.* 2013); are main reasons why regulatory limits are still not available for nanomaterials.

Thus it is essential to gather data regarding toxicity and workplace exposure for risk assessment which can be later used for further development of regulatory decision making, risk management and governance of engineered nanomaterials.

Several guidelines including recommended values for nanomaterials are published by different organizations (Table 2). The REACH (ECHA 2015) proposed a derived no-effect level (DNEL), the National Institute for Occupational Health and Safety (NIOSH 2011, 2013) proposed recommended exposure limit (REL), and the Social and Economic Council of the Netherlands (SER 2012) proposed nano-reference values (NRV), which are background corrected 8h TWA concentrations, based on the German Institute for

Occupational Safety and Health of the German Social Accident Insurance (IFA, 2009) particle number based approach for recommended benchmark limits.

Additionally, permissible exposure limits (PELs) are published by the US Occupational Safety and Health Administration (US-OSHA), and threshold limit values (TLVs) are issued by the American Conference of Governmental Industrial Hygienists (ACGIH), a voluntary organization with members from federal, state, and local bodies as well as industry and academia, since 1946 (Ramachandran 2005).

As a result it becomes evident that a multitude of non-binding targets, thresholds and recommended values is available to benchmark occupational exposures to nanomaterials. However, no common, standardized or legally-binding limit value is currently available for NPs (Table 1.2).

Table 1.2 Recommended occupational exposure limits proposed by different international organizations: [a] SER (2012); [b] NIOSH (2011); [c] NIOSH (2013); [d] ECHA (2015). NRV background-corrected 8h TWA concentrations. REL (recommended exposure limit) 8h TWA concentration during a 40-h workweek. DNEL derived no-effect level. Source: modified from Fonseca (2016).

Description	Recommended limit
[a] Rigid, biopersistent, insoluble, fiber form nanomaterials for which effects similar to those of asbestos are not excluded • SWCNT or MWCNT or metal oxide fibres	*0.01 fibres cm^{-3} (NRV)*
[a] Non-biodegradable granular nanomaterials in the range of 1–100 nm and density > 6 kg/L • Ag, Au, CeO2, CoO, CuO, Fe, FexOy, La, Pb, Sb2O5, SnO2,	*20 000 cm^{-3} (NRV)*
[a] Non-biodegradable granular nanomaterials in the range of 1–100 nm and density < 6 kg/L • Al_2O_3, SiO_2, TiN, TiO_2, ZnO, nanoclay, Carbon Black, C_{60}, dendrimers, polystyrene, nanotubes, nanofibers and nanowires (asbestos-like effects are excluded)	*40 000 cm^{-3} (NRV)*
[a] Biodegradable/soluble granular nanomaterials in the range of 1–100 nm • e.g. NaCl-, fats, flower, siloxane particles	*Applicable OEL (NRV)*
[b] Fine (<2.5 µm) and ultrafine (10-100 nm) TiO_2	*2.4/0.3 mg m^{-3} (REL)*
[c] Carbon nanotubes (CNTs) and nanofibres	*0.001 mg m^{-3} (REL)*
[d] SiO_2 fumes (<100 nm)	*0.3 mg m^{-3} (DNEL)*

1.7. Gap analysis

As a result of the above literature review the following research needs were identified.

1.7.1. Gaps in exposure monitoring

Work environment characteristics are highly variable, and thus particle emission mechanisms and patterns are location and activity specific. Additionally, the study from particle emission patterns of different industrial activities can be useful to test the validity of risk management tools and models. The ultimate goal of these tools is to mitigate exposure by facilitating the implementation of efficient mitigation strategies. Special efforts should be placed in order to understanding unintentional NP emission mechanisms.

As a result, a larger number of real-world exposure assessments in occupational settings would further the current understanding of industrial particle emission sources, mechanisms and impacts on human health. The need to stablish a standardized exposure assessment methodology, which includes metrics improving our understanding of measurement locations and of the definition of statistically significant impacts has been detected.

Further research is necessary to understand the metrics or combination of metrics which better represent particle emissions, taking into account particle diameter, toxicity and agglomeration mechanisms, among others.

Finally, standardised, efficient and quantitative testing of the effectiveness of exposure mitigation strategies from e.g. personal protective equipment (PPE) to general extraction system and local exhaust ventilation systems (LEV) is needed in order to provide users (e.g. industries) with robust and useful information to mitigate and prevent particle exposures.

1.7.2. Gaps in exposure prediction models

Mass-balance models for exposure prediction, e.g. the one- and two- box models, have been tested in different controlled environments. However, model performance in real-world environments, especially in environments where certain parameters are unknown, still needs to be better understood. Specifically, input parameters which are key to enhance model performance and their limitations are:

1) Local controls: reduction of the emission rate due to local controls can be quantified when extensive experimental data are available. When they are not available, literature reviews on rough estimations regarding efficiency should be used, increasing model uncertainty.

2) Emission rate: in the case of handling of powders, emission rate can be relatively easily calculated by means of the material dustiness index. Dustiness is a frequently used tool in occupational exposure; however its direct correlation with exposure concentrations is still not fully understood and works are ongoing in order to understand which the key factors to predict worker exposure are. When used as model emission rate input, the difference between the dustiness test energy and the actual process energy needs to be included as an additional "energy" factor, which is not yet fully parametrized, thus, introducing uncertainty to the modelling. On the other hand, when emission rate cannot be estimated using the dustiness index, several options are available to calculate them based on measured particle concentrations. Furthermore, emission rate libraries are also potentially useful. As a result, the different approaches available for emission rate quantification require testing under real-world conditions. This last point is especially relevant if models are to be used for exposure scenarios impacted by unintentional released NPs (non-engineered).

1.7.3. Gaps in health risk assessment

Worker exposure assessments for several occupational environments have been reported in literature. However, in order to provide a complete human health risk assessment from exposure to airborne particles, not only concentration levels need to be monitored at the workplaces but detailed data are also required on particle deposition along the respiratory tract which can be linked to respiratory disease. The study of particle inhalation and deposition in exposure assessment studies is still often not included, and needs to be further studied and applied.

Risk assessment and control banding tools are promising tools which can help to assess worker exposure risk, especially at industrial level given that they are relatively easy to use. However, in practice, their application is complex, differences between similar processes are difficult to be included in the tools, they do not consider all types of processes (e.g. unintentional NPs are still not included), and there are many different tools available, which are similar in principle but include different parameters and provide different results not only in terms of total concentration but also type of

measure. In addition, their lack of transparency regarding certain functions has been pointed out (Koivisto *et al.* 2019). Two main gaps may be pointed out 1) validation of the different tools in real world scenarios; and 2) standardization of these tools would highly benefit the user communities.

Objectives and Structure

Chapter 2

2. OBJECTIVES AND STRUCTURE

Based on the gaps and research needs identified in the previous chapter, the objectives of this PhD Thesis were defined as follows.

2.1. Objectives

The main objectives of this work are:

1) To assess worker exposure to coarse, fine and NPs in different workplace scenarios at, industrial and pilot-plant scales. Pilot plant studies are easily controllable and therefore allow for the identification of the influence of different process parameters on particle emissions, whereas industrial studies are representative of real-world scenarios.

2) To evaluate, with the aim to contribute to the standardization of worker exposure assessment:

i. decision making approaches for the determination of statistically significant impacts of emitted particles due to a specific process
ii. current available metrics to report worker exposure (mass, particle number concentrations and surface area)

3) To understand the relationship between material dustiness and worker exposure concentrations, with the final goal to contribute to a better understanding of particle emissions patterns, the role of dustiness as an exposure predictor model input, and its standardization for modelling purposes.

4) To evaluate the performance of mass-balance models (one- and two-box models) as worker exposure prediction tools under industrial settings, in order to contribute to model application and parametrization in real-world scenarios.

5) To evaluate some of the existing tools for health risk assessment as users such as the inhalation deposition dose ICRP model, and risk assessment and control banding tools.

2.2. Structure

After the introductory chapter leading to the identification of gaps in the occupational exposure research field and definition of this PhD's objectives, the methodology applied is described. In it details of the measurement sites, instruments, techniques and data processing tools are provided. The results are presented in chapter 4, structured as four

research publications, which are subsequently discussed in chapter 5. In this chapter, the most important findings are integrated into a joint discussion. Finally, in chapter 6 the conclusions of this Thesis are summarized. Additional scientific contributions are listed in Annex C.

The publications which are part of this Thesis are referenced and briefly described below:

- Research Publication I:

Ribalta, C., Viana, M., López-Lilao, A., Estupiñá, S., Minguillón, M.C., Mendoza, J., Díaz, J., Dahmann, D., Monfort, E., 2019. **On the Relationship between Exposure to Particles and Dustiness during Handling of Powders in Industrial Settings.** *Annals of Work Exposures and Health*. 63, 107–123. https://doi.org/10.1093/annweh/wxy092.

In this study, worker exposure during mechanical handling of ceramic powdered materials in a pilot plant was monitored. Seven materials with different compositions, particle shape and characteristics were assessed, as well as different intensities of handling energy. Exposure concentrations were evaluated according to process and materials characteristics. The relationship between materials dustiness and evaluated exposure concentrations was assessed.

- Research Publication II:

Ribalta, C., López-Lilao, A., Estupiñá, S., Fonseca, A.S., Tobías, A., García-Cobos A., Minguillón, M.C., Monfort, E., Viana, M., 2019. **Health risk assessment from exposure to particles during packing in working environments.** *Science of the Total Envi*ronment. 671, 474–487. https://doi.org/10.1016/j.scitotenv.2019.03.347

In this work, worker exposure concentrations were monitored during packing of 5 widely used ceramic materials, under three levels of source containment (low, medium and high mitigation strategies applied). Monitored worker exposure concentrations are discussed as a function of the degree of source containment, and material's dustiness index. Health risk assessment is performed by using the inhalation and deposition ICRP model. This case study was used to evaluate the performance of three risk assessment/control banding tools as well as to test different strategies for decision making with regard to the

identification of statistically significant impacts of particle emissions on particle mass concentrations.

- Research Publication III:

Ribalta, C., Koivisto, A.J., López-Lilao, A., Estupiñá, S., Minguillón, M.C., Monfort, E., Viana, M., 2019. **Testing the performance of one and two box models as tools for risk assessment of particle exposure during packing of inorganic fertilizer.** *Science of the Total Environment*. 650, 2423–2436. https://doi.org/10.1016/j.scitotenv.2018.09.379

Exposure concentrations during packing of a fertilizer in a real-world industrial scenario were monitored in two packing lines (small and big bags). Worker exposure risk assessment was completed with the application of the inhalation and deposition ICRP model, and chemical risk was assessed by using the Stoffenmanager risk assessment tool. This scenario was used to test the performance of the one- and two-box prediction models when challenged with low particle mass concentrations. Emission rates were estimated using the dustiness index, and special attention was given to in model parametrization.

- Research Publication IV:

Ribalta, C., Koivisto, A.J., Salmatonidis, A., López-Lilao, A., Monfort, E., Viana, M., 2019. **Modelling of thermal spraying emissions: testing one box model performance under a high nanoparticle concentration industrial scenario.** *International Journal of Environmental Research and Public Health. 16 (10), 195.* https://doi.org/10.3390/ijerph16101695

Worker exposure concentrations to unintentional NPs were evaluated at an industrial-scale workshop where thermal spraying of ceramic coatings was applied. Occupational exposure evaluation and health risk assessment is presented and thoroughly discussed in Salmatonidis et al., (2019). The data from this study (Salmatonidis et al., 2019) were subsequently processed in the framework of this PhD to test the one-box models when challenged with high concentrations of unintentionally-released NPs. Emission rates were estimated by two different methods, and the results obtained were compared for this real-world setting.

Methodology

Chapter 3

3. METHODOLOGY

3.1. Exposure scenarios and monitoring sites

Worker exposure to airborne particles (micro- and nano-sized) was monitored in this Thesis for two main types of industrial processes; 1) mechanical, assessed at pilot plant and industrial level; and 2) thermal, assessed at industrial level. A total of five different locations were assessed (Table 3.1).

Table 3.1 Description of the studied processes.

Paper Nº	Type of site	Type of process (activity)	Type of material	Sampling locations	Location and date	Objectives	Tools
I	Pilot plant	Mechanical (handling)	5 micron-sized ceramic raw materials (+2 materials in "4.1.1")	Worker area	Castellón (Spain), October 2016	1 and 3	Particle monitoring Dustiness
II	Industrial packing facility 1 and 2	Mechanical (packing)	7 micron-sized ceramic raw materials	Worker area Breathing zone	Onda (Spain), February 2018	1, 2, 3 and 5	Particle monitoring Dustiness Risk assessment tools
III	Industrial packing facility 3	Mechanical (packing)	1 granulated micron-sized inorganic fertilizer	Worker area	Castellón (Spain), January 2017	1, 3, 4 and 5	Particle monitoring Dustiness Mass-balance models Risk assessment tools
IV	Industrial thermal spraying	Thermal (spraying)	Micron-sized materials	Booth Worker area	Blanes (Spain), April 2017	4	Particle monitoring Mass-balance models

3.1.1. Mechanical processes

Mechanical handling of different powdered raw materials was monitored at pilot plant and industrial scales (Figure 3.1).

Pilot plant experiments were conducted at the Institute of Ceramic Technology (ITC) (Castellón, Spain) (**Publication I**) during a process which included feeding of the materials to a dry pendular mill and extracting the powders from it (Figure 3.1 (a) and (b)). Because the primary particle size was not modified by the mill, this activity was considered to be representative of handling of materials (as opposed to milling), at

industrial scale. Seven ceramic materials were studied, at two levels of mechanical energy.

At industrial level, exposure to packing of eight materials was assessed in three different ceramic-related packing facilities (**Publication II and III**). In the three industries different activities were carried out, each of them being conducted in a specific and independent hall. In the packing areas, packing was the main activity.

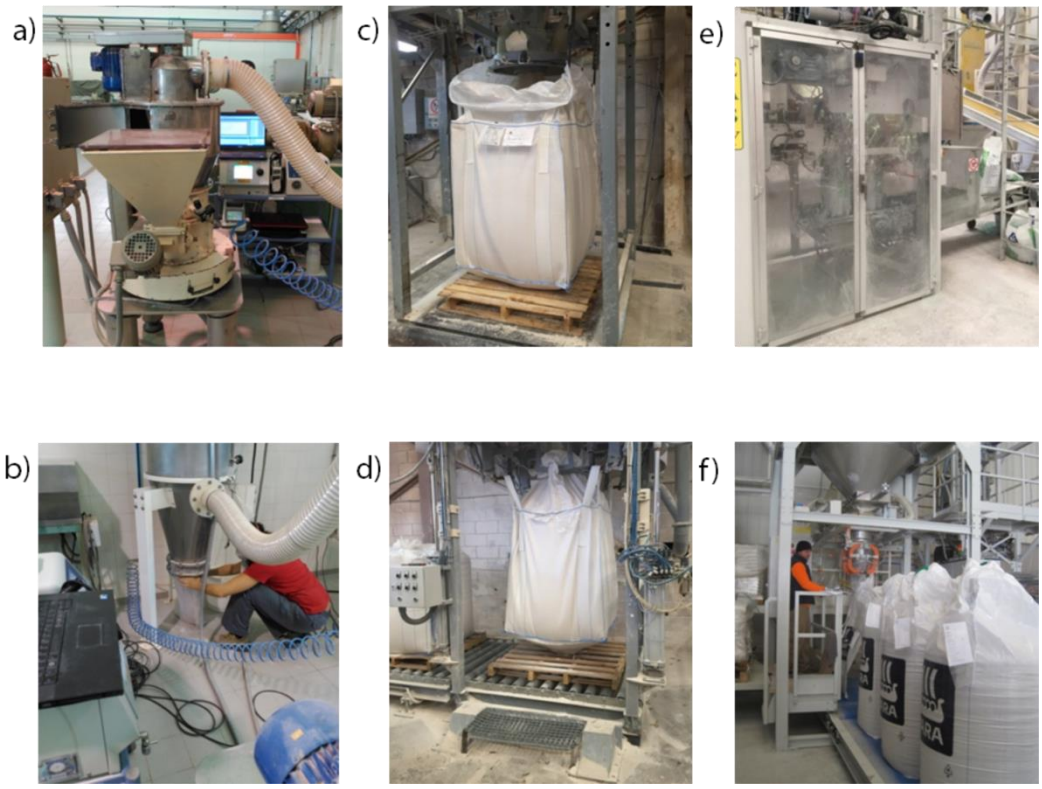

Figure 3.1 Mechanical handling processes studied. (a) and (b) pilot plant mechanical handling, (c) and (d) ceramic materials packing at facility 1, and (e) and (f) inorganic fertilizer packing at facility 3.

In facilities 1 and 2, exposure during packing of seven ceramic materials was monitored (**Publication II**). In facility 1 packing was carried out in two lines of big bags (1200 kg), with low and medium mitigation strategies applied (Figure 3.1 (c) and (d)). The packing line with low mitigation strategies was not enclosed and had no closing system to attach the bag to the feed funnel, and the packing line with medium mitigation strategies was not enclosed but had a partially closing system to attach the bag to the feed funnel. Both packing lines were equipped with a local exhaust ventilation system (LEV), with an operational flow rate of 18000 m^3 h^{-1}, and a subsequent bag filter. Facility 2 contained only one small bags (20-25 kg) packing line with high mitigation strategies. Packing was carried out automatically through a lateral cylindrical opening, and it was not enclosed

but the bag was completely attached to the feed funnel during the filling process. This packing line was equipped with a LEV system (operational flow rate of 2400 m^3 h^{-1}) with a subsequent bag filter.

In facility 3, packing of a fertilizer was monitored (**Publication III**) in two different packing lines, small (25 kg) and big (600 kg) bags. In small bags (Figure 3.1 (e)), packing was carried out through an opening fitting the bag width and subsequently mechanically sealed. The packing process was fully automated and the process area was partially enclosed. In the case of the big bags (Figure 3.1 (f)), packing was carried out through a cylindrical opening, and the bag was manually closed by the worker.

3.1.2. Thermal processes

The thermal process assessed was thermal spraying, a thermal technique used to produce thermally and mechanically-resistant coatings. Monitoring of thermal spraying was carried out at an industrial-scale precision engineering workshop (**Publication IV**), equipped with three thermal spraying rooms (Figure 3.2 (a)).

In the workshop, two types of thermal spraying were carried out: atmospheric plasma spraying (APS), used to project oxides and metals by using high temperatures (5000–20 000°C) and projection velocities of 200–500 m s^{-1}, and high velocity oxy-fuel coating spraying (HVOF) (Figure 3.2 (b)), which is characterized by higher velocities (425–1500 m s^{-1}) and lower temperatures (2900°C). Due to the lower temperatures applied HVOF is frequently used to project carbides and metals. Parallel works such as cooling and sanding of metal pieces were occasionally carried out, but not during spraying process.

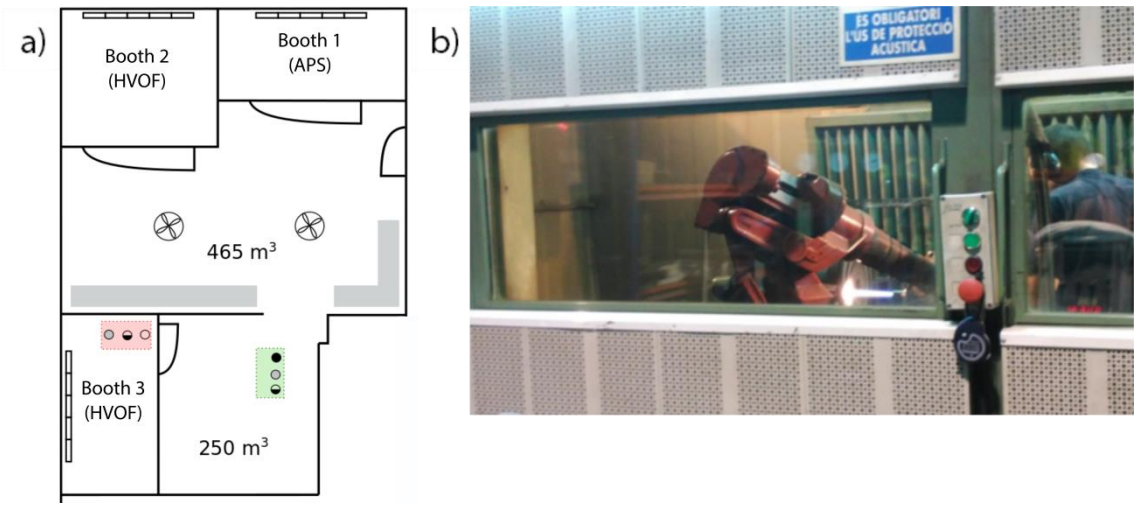

Figure 3.2 (a) Layout of the thermal spraying workshop, and (b) image of the HVOF booth.

3.2. Materials physical characterization

The following measurement and analytical techniques were used in this Thesis to characterize the physical properties of the materials under study.

3.2.1. Particle size distribution

Particle size distribution (PSD) of powdered materials was determined by laser diffraction (dlaser) wet method (ISO 13320-1, 2009) using the Mastersizer 2000 and by X-ray gravitational sedimentation using the Sedigraph method from Micrometrics (dstockes). The Mastersizer 2000 (size resolution of 0.02 - 2000 μm) analyses are based on the theory of Fraunhofer and Mie, using wave lengths 632.8 and 470 nm.

3.2.2. Flowability

Material flowability was assessed using the Hausner ratio (HR). It was calculated as the quotient of the bulk density of the packed particle bed (by tapping) and the aerated bulk density of the particle bed, obtained by dropping powder into a container without stirring or vibration (Amoros 1987). Dry materials with low cohesiveness and with mostly spherical shape show high compaction by gravitational drop, and therefore, the difference between the apparent density by gravitational drop and by tapping is small (HR close to 1). Thus, the lower the flowability, the higher the HR (Mallol *et al.* 2008).

3.2.3. Specific surface area

Specific surface area (SSA) was assessed by measuring the adsorption isotherms according to the BET method by nitrogen absorption (ISO 9277:1995) (Brunauer *et al.* 1928).

3.2.4. Aspect ratio

A particle shape factor defined as the ratio of the particle's major and minor dimension was determined by the Parslow-Jennings method for oblate spheroids (Otterstedt and Brandreth 1998, Jennings and Parslow 2006). This method is based on the fact that dlaser (diameter of a sphere of same diameter as the cross-sectional area of the particle μm) and dstokes (diameter of a sphere of same diameter as the cross-sectional projection area of the particle μm) have different dependence on aspect ratio and, therefore, it can only be obtained the same diameter in the case of spherical particles. This factor is a measure of the irregularity of particle shape, i.e. the deviation from a spherical shape. For

prismatic, platy, and ribbon-like particles the aspect ratios are 1 - 5, 4 - 15, and 5 - 100, respectively (Otterstedt and Brandreth 1998).

3.2.5. Dustiness

Dustiness is a measure of the tendency of a powdered material to release particles in response to a mechanical or aerodynamic stimulus (Plinke *et al.* 1992, Lidén 2006).

The two standard methods, the rotating drum (R.D) and the continuous drop (C.D) EN 15051 (CEN, 2013) (Figure 3.3), were used in order to determine the materials dustiness index.

Method

Rotating drum (R.D)

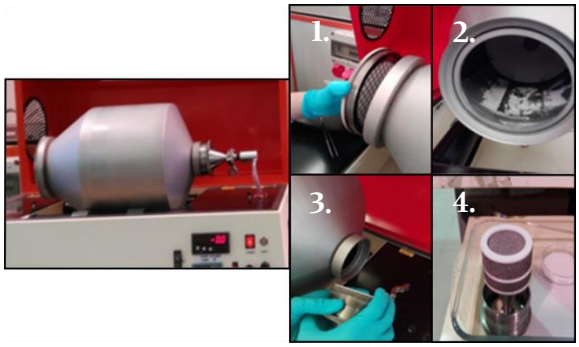

1. Inlet
2. Dust generation section (drum)
3. Dust collection
4. Foams and filter for inhalable, thoracic and respirable fractions

Continuous drop (C.D)

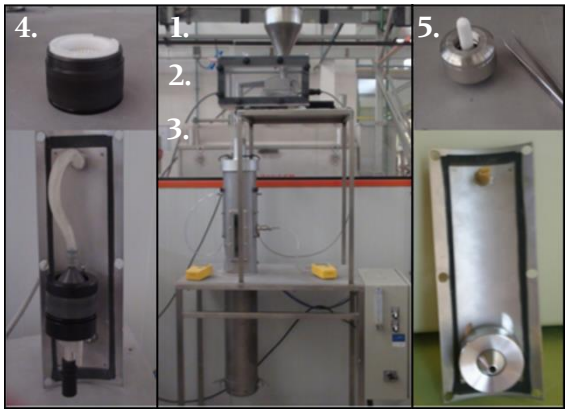

1. Sample tank
2. Metering device
3. Drop pipe
4. Sampling head for the respirable aerosol fraction
5. Sampling head for inhalable aerosol fraction

Figure 3.3 Description of the two methods used for dustiness determination, rotating drum (R.D) and continuous drop (C.D).

The R.D test as described in the standard EN 15051 (part 2), consists of introducing a known volume of material (35 ml) inside a rotating drum which rotates at 4 revolutions per minute. The dust generated inside the drum is collected onto a three-body sampling system, in which the emitted dust cloud is drawn by the air current generated by a vacuum pump at a flow rate of 38 l min^{-1}. The dust sampling system consists of two

sections of selective foam per particle size (one metal coated PE foam of 20 ppi and one metal coated PE foam 80 ppi) followed by a glass fiber filter, to gravimetrically analyze inhalable (W_I), thoracic (W_T) and respirable (W_R) fractions.

The C.D device EN 15051 (part 3), made of stainless steel, consisted of a cylindrical pipe through which air circulated in an upward direction with a volume flow rate of 53 l min^{-1}. Concentric to the cylindrical pipe there was an inner pipe, slightly shorter, through which material was dropped at a flow rate of 6 to 10 g min^{-1}, so that the powdered material was released into a counter-current airflow (López-Lilao *et al.* 2015). The total material drop height during the test was approximately 1.2 m, with a total duration of 10 minutes. Two sampling heads for inhalable (approximately total suspended particles, or TSP; designed by Institut für Gefahrstoff-Forschung-IGF) and respirable (approximately PM_4; FSP-2, BGIA) fractions were located slightly above the discharge position of the material. Samples for gravimetric measurements of inhalable and respirable fractions were collected on cellulose thimbles, single thickness, 10x50 mm 25/pk and PVC filters of 37 mm and 5 μm of porosity, respectively. Each experiment lasted for 10 minutes.

The standard methods establish three repetitions for each sample in order to ensure repeatability of the results for the R.D test, and four for the C.D test. Between repetitions, cleaning the devices is not necessary while at the end of the test the device has to be thoroughly cleaned.

Considering gravimetrically sampled fractions (W_I, W_T and W_R), the EN 15051 establishes 4 categories to classify material's dustiness level (Table 3.2).

Table 3.2 Dustiness level classification according to EN 15051.

Dustiness method	Category, classification	Mass fraction		
		W_I	W_T	W_R
R.D	Very Low	< 300	< 80	< 10
	Low	300-650	80-300	10-60
	Moderate	> 650-3000	> 300-1000	> 60-210
	High	> 3000	> 1000	> 210
C.D	Very Low	< 1000	-	< 20
	Low	1000-4000	-	20-70
	Moderate	> 4000-15000	-	> 70-300
	High	> 15000	-	> 300

3.3. Particle monitoring techniques and instrumentation

3.3.1. Online instrumentation

The online instruments deployed during the experimental campaigns are summarized in Table 3.3.

Table 3.3 Online instrumentation used during the experimental campaigns. N: number concentration (cm^{-3}). M: mass concentration ($\mu g\ m^{-3}$). PSD: particle size distribution. LDSA: lung deposited surface area.

Instrument	Manufacturer	Flow rate ($l\ min^{-1}$)	Metric	Particle size range	Concentration range	Time resolution	Article
Optical Particle Sizer (OPS, TSI Model 3330)	TSI Inc., Shoreview, MN, USA	1	N and PSD	0.3-10 µm (16 channels)	0- $3x10^3$ cm^{-3}	1-min	II, IV
Mini Laser Aerosol Spectrometer (Grimm Mini-LAS)	Grimm Aerosol Technik, Ainring, Germany	1.2	M (occupati-onal and PM)	0.25-32µm	0.1 – 10^4 $\mu g\ m^{-3}$	6-s	I, II, III, IV
Light scattering laser photometer (DustTrak™ DRX aerosol monitor TSI Model 8533)	TSI Inc., Shoreview, MN, USA	3	M (PM)	PM_{10}, PM_4, $PM_{2.5}$ and PM_1	0.001-150 $mg\ m^{-3}$	1-min	I, II, III, IV
Butanol Condensation Particle Counter (CPC TSI Model 3775)	TSI Inc., Shoreview, MN, USA	1.5	N	4-1500nm	$<10^7$ cm^{-3}	1-s	I, II
Electrical Mobility spectrometer (NanoScan SMPS TSI Model 3910)	TSI Inc., Shoreview, MN, USA	0.7	N and PSD	10-420nm (13 channels)	100-10^5 cm^{-3}	1-min	I, III, IV
Diffusion Size Classifier Miniature (DiSCmini Matter Aerosol AG)	Testo, Wohlen, Switzerland	1	N, Size, LDSA	10-700nm	10^3-10^6 cm^{-3}	1-s	I, II, III, IV
Mini Wide Range Aerosol Spectrometer (Mini-WRAS 1371)	Grimm Aerosol Technik, Ainring, Germany	1.2	N,PSD and M (occupati-onal and PM)	10nm-35µm	0.1 – 10^4 $\mu g\ m^{-3}$ $3x10^3$-$5x10^5$ cm^{-3} (electrical) 0-$3x10^6$ l^{-1} (optical)	1-min	I, II, III, IV

Particle mass and number concentration, size and particle size distribution (PSD) were monitored by using portable and stationary instruments, based on different measurement principles:

- Optical detection

Optical particle sizer (OPS), laser aerosol spectrometer (Mini-LAS) and light-scattering laser photometer (DustTrak™ DRX).

Optical techniques are based on the detection of the light scattered by particles after interacting with a light source. They are based on the Mie scattering theory; the light scattered by a particle (0.3-0.6 μm) is proportional to its squared diameter. In optical particle counters, particles in the range between 0.3 up to 32 μm (depending on the instrument) are detected when going through a cell lit up by a lamp or laser beam. The particle size distribution is calculated comparing its scattered light with a calibration curve.

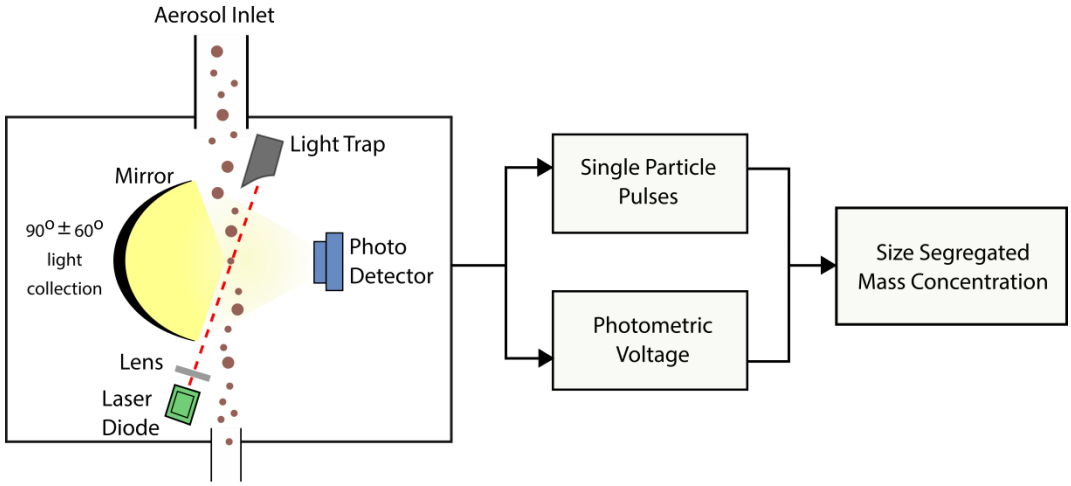

Figure 3.4 Optical detection schematic operational principle. Source: modified from TSI, OPS and DustTrak manual.

In optical instruments, the beam is generated by a laser diode, and passed through a lens to create a thin sheet of light which illuminates the aerosol. The light scattered by the aerosol particles is then captured by a mirror, which focuses the light on a photodetector. Finally, the scattered light pulse of every single particle is counted and the intensity of its signal classified to a certain particle size (single particle side scattering technology) (Figure 3.4). The photodiode signal can be separated into two components 1) the single particle pulses, to size discriminate; and 2) the photometric voltage, to

measure mass concentration (as voltage is proportional to mass concentration) (McMurry 2000).

- Condensation particle counter (CPC)

Condensation particle counters are designed to optically detect small particles (< 300 nm) (Liu 1976, Stolzenburg and McMurry 1991), although they can detect particles up to 3 μm. They are based on liquid (e.g. butanol, water) condensation on to the particles in order to increase their size up to a point where they can be optically detected (Agarwal and Sem 1980). The CPC used in this Thesis was butanol based and provided time-resolved and size-integrated particle concentration data.

The aerosol enters through the sample inlet and reaches a heated, butanol-soaked wick. The wick is dipped into the butanol reservoir and continuously absorbs butanol. Afterwards, when passing into the vertically cooled condenser, the vapour becomes supersaturated and condenses on to the particles, which act as condensation nuclei, forming larger droplets which can be optically detected. The liquid condensed on to the walls runs back down and is removed by the removal system (Figure 3.5).

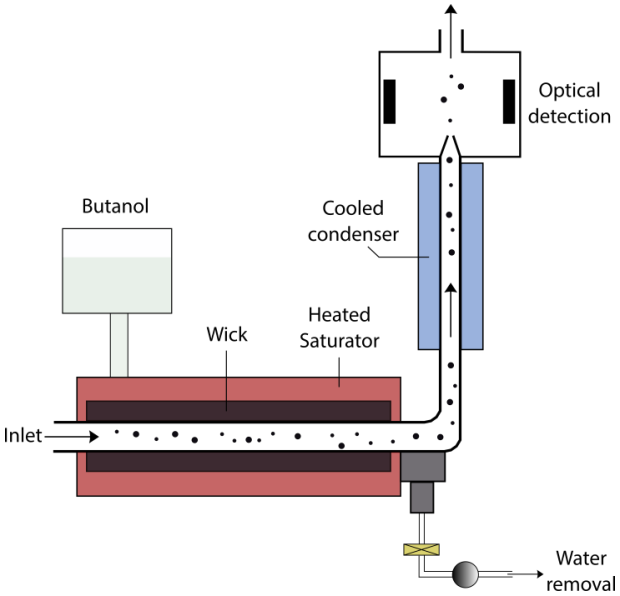

Figure 3.5 Butanol CPC schematic operational principle. Source: modified from TSI, CPC 3775 manual.

- Scanning Mobility Particle Sizer (SMPS)

A SMPS is composed by a differential mobility analyser (DMA) and a CPC. The DMA classifies particles according to their electrical mobility, which is based on the fact that a particle with one charge inside an electric field migrates only according to its size and structure (Knutson and Whitby 1975a). Electrical mobility can be used to obtain particle size distributions of particles < 100 nm with high resolution and it is defined as:

$$Z_p = \frac{neC_C}{3\pi\mu d_p}$$

where n is the number of charges, e is the charge of an electron, C_C Cunningham number, μ air viscosity and d_d the particle diameter. Particles are charged by using two main mechanisms, diffusion or by presence of an electrical field. Particles get in contact with positive and/or negative ions (bipolar/unipolar charger) gaining ions and electrical charge. Ionization sources can be corona or radioactive.

In a stationary SMPS ambient air sampled through the inlet reaches a bipolar charger or neutralizer, which is usually a radioactive source such as Kr85. The aerosol is then classified according to its electrical mobility in the DMA (Knutson and Whitby 1975b, Chen *et al.* 1998), and the number concentration for each specific size range is determined in the CPC (Figure 3.6).

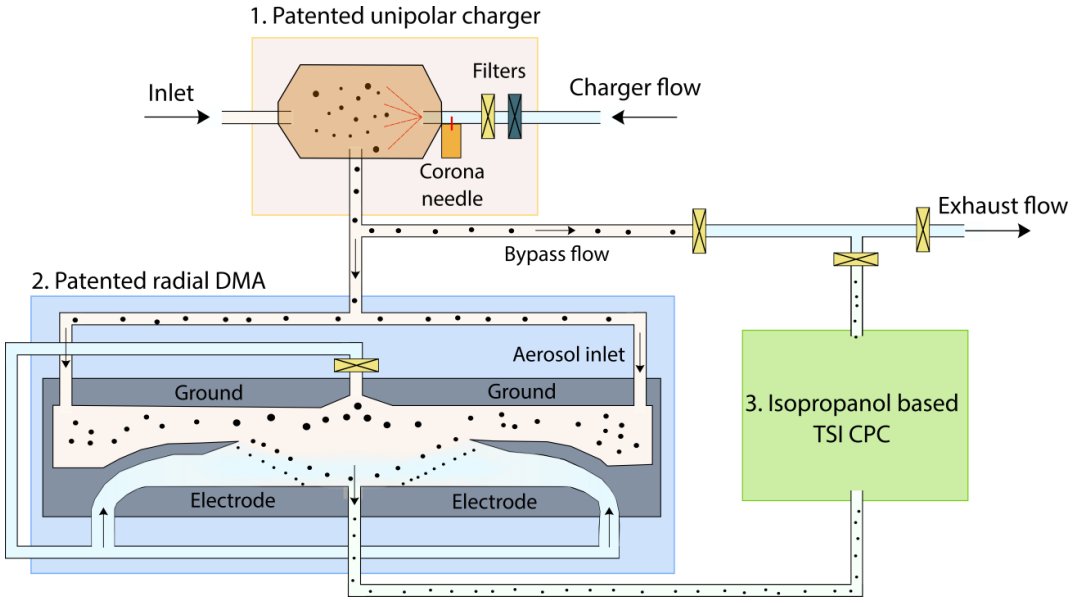

Figure 3.6 NanoScan SMPS simplified schematic operational principle. Source: modified from TSI, NanoScan SMPS manual.

The portable NanoScan SMPS provides time and size-resolved particle number concentration by using a non-radioactive unipolar diffusion charger (corona jet type) (Medved *et al.* 2000), a radial differential mobility analyser (rDMA, Zhang *et al.* 1995) and an isopropanol-based CPC.

- Diffusion Size Classifier Miniature (DiSCmini)

The DiSCmini principle is based on particles positive unipolar charging by using a corona charger. Following particle charge, excess of ions is removed in an ion trap, and particles are detected in two stages by electrometers (diffusion and filter), allowing for particle sizing and counting (Figure 3.7). In the first detector stage small particles are deposited on a pile of steel grids by diffusion and detected as an electrical current. The remaining particles end up in the filer stage, where particles are also detected as an electrical current. The ratio of these two currents is a measure of the average particle size determined during the instrument calibration. Total current is calculated as a function of particle diameter, and together with the flow rate the particle concentration is computed.

DiSCmini has high-time resolution of up to 1 second, but lower precision than the SMPS and CPC, with deviations of up to 30%. DiSCmini calibration is made with monodisperse aerosol, and the instrument's response for polydisperse aerosols with a lognormal size distribution with a geometric standard deviation σ = 1.9 is then calculated (Fierz *et al.* 2010, 2011). When aerosols show a wide size distribution the DiSCmini will overestimate particle diameter and underestimate particle number. In addition, its performance in environments with high coarse particle concentrations was seen to be unreliable (Fonseca 2016).

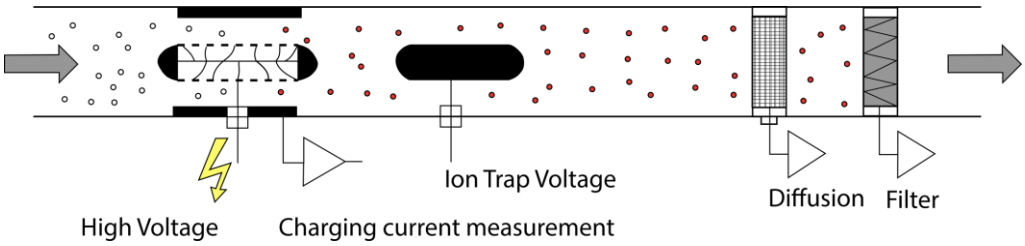

Figure 3.7 DiSCmini schematic operational principle. Source: modified from Testo, DiSCmini manual.

- Mini Wide Range Aerosol Spectrometer (Mini-LAS)

The Mini-LAS instrument combines the optical light scattering (single particle counter) and the electrical mobility principles in order to allow simultaneous measurement of micro- and nano-particles. Mass distribution is then calculated considering spherical particles. The optical particle counter measures the size distribution from 250 nm up to 32 µm and the electrical sensor, measures size distribution from 10 nm up to 250nm. The electrical sensor is composed by a unipolar electrical diffusion charger, a time multiplexed electrode (for particles deposition an extraction from the aerosol) and a

Faraday cup electrometer which measures only particles with an electrical mobility less than a certain limit value.

3.3.2. Offline instrumentation

Additionally to the online instruments, several offline instruments and techniques were used to fully characterize airborne particles and provide personal mass concentration exposures.

Personal exposure to respirable airborne particle mass concentration was gravimetrically determined by pre- and post- weighing of samples collected using a Dorr-Oliver Nylon Cyclone Assembly with Mixed Cellulose Ester Membranes (Figure 3.8 (a) and (b)), 0.80 µm pore size, 25 mm Ø (EDM Millipore™ MF-Millipore™) connected to a pump (Apex, Casella) operating at a 1.7 l min^{-1} flow. Respirable mass concentration was also gravimetrically analyzed using the CIP 10-I (Arelco ARC) sampler operating at a flow rate of 10 l min^{-1} and air filtration by a rotating porous foam filter (Görner *et al.* 2009, Görner *et al.* 2010) (Figure 3.8 (c)).

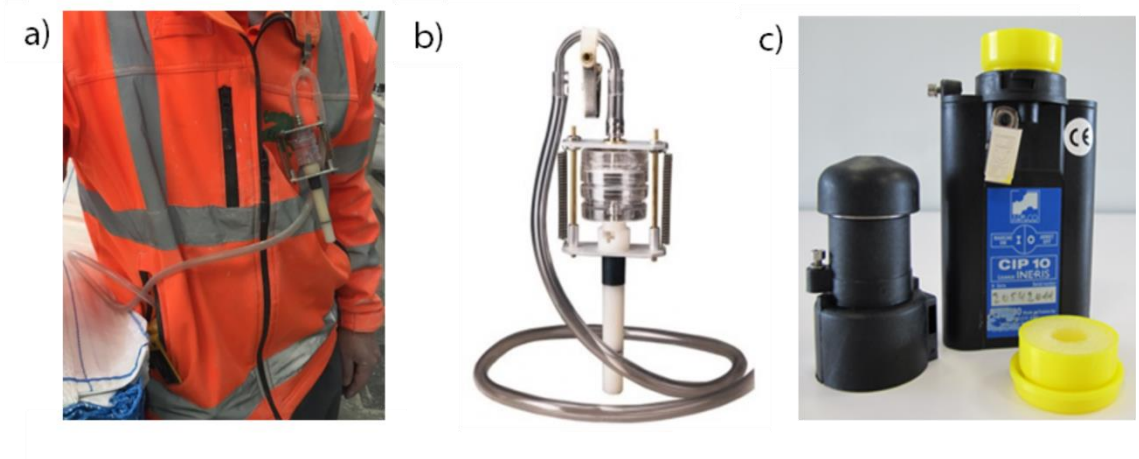

Figure 3.8 (a) and (b) Personal mass exposure samplers, Dorr-Oliver Nylon Cyclone Assembly and (c) CIP 10-I. Source: zefon international, Casella, España (Iván Ruiz, 2016).

From particles collected onto the filters, respirable crystalline silica was quantified by X-ray diffraction, using a BRUKER theta-theta model D8 Advance diffractometer with copper radiation (Kα λ = 1.54183Å) and VÅntec solid-state detector. Data were recorded from 2θ of 26º to 28º, with a step size of 0.07º and acquisition time of 3 s. Certified reference materials were used for quantification and validation (BCR-66, SRM 1878a y SRM 2950-2957). In order to quantify by X-ray diffraction, filters were baked, and then samples were re-suspended, and redeposited onto PVC filters (25 mm Ø) following the

Spanish National Occupational Health and Safety Institute's (INSHT) method based on membrane filter/ X-ray diffraction (MTA/MA -056/A06). Filters were left for at least 2 h in a dryer prior to quantification.

Airborne particles were also collected onto Au grids (Quantifolil ® with 1 μm diameter holes – 4 μm separation of 200 mesh) by using 3-piece conductive polypropylene air sampling cassettes (SKC Inc., USA, 1/8 in. inlet diameter and 25 mm filter Ø). The grids were attached to polycarbonate filters placed in the cassette. The cassette was connected to a Leland pump with an operating flow rate of 3-5 l min^{-1} (Figure 3.9 (a) and (b)).

Particles collected were later chemically and morphologically analyzed by using two techniques, transmission electron microscopy (TEM J2100 coupled with an energy-dispersive X-ray (EDX) spectrometer; Figure 3.9 (c)) and by using a field emission scanning electron microscope (FESEM) FEI CUANTA 200F.

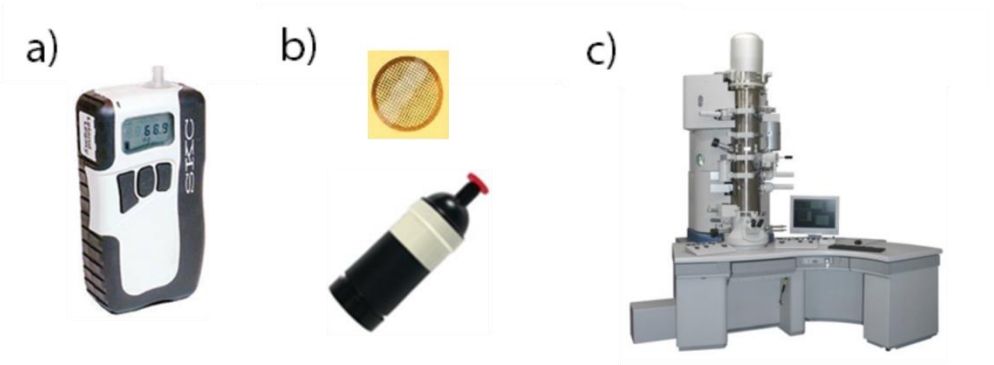

Figure 3.9 (a) Leland pump (b) Particle collection using the 3-piece conductive polypropylene air sampling cassettes SKC Inc., and (c) analysis in the TEM J2100.

3.4. Measurement strategy

3.4.1. Discrimination of background particles

To accurately characterize worker exposure to airborne particles emitted by a given industrial activity it is essential to discriminate them from background particles (see section 1.2.3.2). In order to achieve this, a non-activity time series approach was used (Brouwer *et al.* 2009). This approach is based on the idea that worker exposure during the activity is due to the sum of background particles plus particle concentration and particles generated during the activity. Thus, particle concentration was monitored in the worker area before and/or after each activity under study. The main limitation of

using this approach is that it does not consider temporal and spatial changes of background concentrations. In order to tackle this limitation, indoor measurements were carried out at different locations. Particles were monitored near the activity. In addition, particle were monitored in other indoor locations which were sufficiently far from the studied source, so that particles emitted by the activity would not impact indoor measurements, allowing for monitoring of any potential temporal changes in the background.

3.4.2. Sampling locations

In each workplace assessed, particle concentration and characteristics were monitored simultaneously in at least three locations 1) next to the emission source; 2) in the worker area, where devices were placed at a distance from the emission source similar to where the worker is standing and with instruments inlets being at a similar height as worker mouth (1.5 m height) (the location is representative of the breathing zone, even if it may not be considered strictly as such; Asbach *et al*. (2012); and 3) in indoor air to detect temporal changes. Additionally, when possible, instruments were also deployed to monitor personal breathing zone and outdoor air to detect and characterize outdoor particle influences.

3.4.3. Decision making based on statistical significance

For decision making, the evaluation of the statistical significance of increases in particle concentrations and the comparison of exposure concentrations to legal and/or reference limits is paramount. To determine the statistical significance of particle number and mass concentrations, the approach designed in Asbach *et al*. (2012) for particle number concentrations was used in this work.

$$\text{Mean concentration during activity} > BG \pm 3 \cdot (\sigma BG) \qquad \text{Eq. (3.1)}$$

where BG is the mean temporal background (or pre-activity) concentration and σBG is the standard deviation of the background concentration. This is the most widely used approach in the particle exposure literature (Kaminski *et al.* 2015, Fonseca *et al.* 2016).

Other techniques also used to assess statistical significance of exposure are conventional statistical tests (t-test and Mann-Whitney "U" test, both for independent samples) and the ARIMA (Autoregressive Integrated Moving Average) time series approach.

To apply the conventional tests, log-normality and variance homogeneity were assessed by using the Kolmogorov-Smirnov and Levene's (absolute) tests respectively, and by histogram plotting. When data did not fully fulfil normality assumptions, the non-parametric Mann-Whitney "U" Test (Wilcoxon rank-sum test) was used, whereas when normality assumptions where fulfilled, the two-sample t test was applied (unequal variances).

Finally, the ARIMA approach was used by Klein Entink *et al.* (2011) for particle number concentration, and it was later proposed in EN 17058:2018 (standard for workplace exposure- assessment of exposure by inhalation of nano-objects and their aggregates and agglomerates) as the golden standard method for number concentration and other metrics. To analyze an exposure concentration time series using ARIMA, the time series, the sample autocorrelation function and the sample partial autocorrelation function were plotted, in order to select the ARIMA model which best fit with the data. Afterwards, the selected model was applied using a differentiation factor for background and activity time series. When the statistic factor was > 1.95, concentrations were considered statistically significantly higher during the activity than during the background, whereas when the statistic factor was < 1.95 no statistically significant differences were considered. An example of this model can be found in Publication II, specifically in Supplementary materials (Annex B, section 2).

3.4.4. Regulatory compliance

In order to compare regulatory limits with monitored exposure concentrations, time-standardization is necessary. Usually, exposure limits are given as 8h TWA (time weighted averages) corresponding to a full-shift. To transpose monitored concentrations to 8h TWA the following equation was used:

$$\mathrm{TWA} = \frac{t_1 C_1 + t_2 C_2 + \cdots + t_n C_n}{t_1 + t_2 + \cdots + t_n} \qquad \text{Eq. (3.2)}$$

where C_n is the mean concentration during a specific operation and t_n is the time of the specific activity.

3.4.5. Instrument intercomparison

Because of the need to monitor particle metrics simultaneously at different locations, the comparability of instruments needs to be ensured by means of intercomparison exercises. In this PhD Thesis, instruments were deployed at an air quality monitoring

station in Barcelona where they were challenged with ambient air aerosols. Intercomparison exercises were carried out on several occasions, usually before and/or after the monitoring campaigns. Instruments were placed during 24 to 72h side by side but with sufficient space between them to avoid interferences. Instruments were compared between each other as well as with internal references such as a stationary CPC and SMPS system, and mass concentrations were gravimetrically determined.

3.5. Mass-balance models

The one- and two-box mass-balance models were used and tested for two different industrial scenarios. Both models, are based on a set of mass balance equations including information of the source (contaminant generation), transport and particle losses. Main difference between them is that the two-box model considers that the limits of the model are two boxes one inside the other: near-field "NF" (where the source is) and far-field "FF", and air flows between boxes (Figure 3.10). The performance of mass-balance models depends on their parametrization, as is discusses in Publications III and IV. The main considerations and types of models used in this Thesis are discussed below.

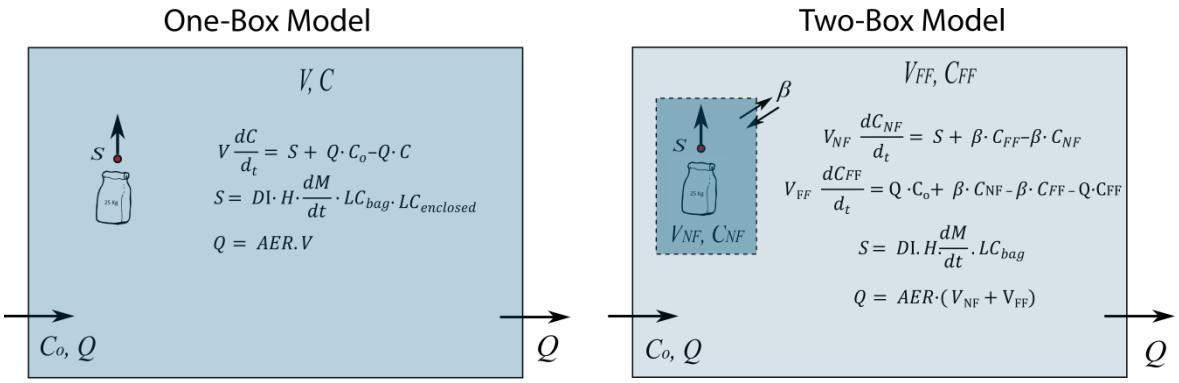

Figure 3.10 One- and two-box models layout.

3.5.1. One-box model

In the one-box model, the mass balance concentration inside the model volume is described as a function of time:

$$V\frac{dC}{d_t} = S + Q\cdot C_o - Q\cdot C \qquad \text{Eq. (3.3)}$$

$$Q = ACH\cdot V \qquad \text{Eq. (3.4)}$$

where S (mass/particles min^{-1}) is the emission source, Q (m^3 h^{-1}) the air flow, ACH (h^{-1}) air changes per hour, V (m^3) the box volume, C the concentration (inside de box and outgoing) and C_o initial and incoming concentration.

3.5.2. Two-box model

In the two-box model, mass balance concentration inside the model volume (NF and FF volume) is described as a function of the time:

- Mass balance in the NF:

$$V_{NF}\ \frac{dC_{NF}}{d_t} = S + \beta \cdot C_{FF} - \beta \cdot C_{NF} \qquad \text{Eq. (3.5)}$$

- Mass balance in the FF:

$$V_{FF}\ \frac{dC_{FF}}{d_t} = Q \cdot C_o + \beta \cdot C_{NF} - \beta \cdot C_{FF} - Q \cdot C_{FF} \qquad \text{Eq. (3.6)}$$

$$Q = ACH \cdot\ (V_{NF} + V_{FF}) \qquad \text{Eq. (3.7)}$$

where S_M or S_N (mass/particles min^{-1}, respectively) is the emission source in the NF, C_{NF} and C_{FF} are NF and FF concentrations, V_{NF} and V_{FF} (m^3) the volume in NF and FF, and β air flow between NF and FF. C_o, Q and ACH were described in Eq. (3.3 and 3.4).

3.5.3. Emission rate

The particle emission rate (S_M or S_N) can be calculated using different approaches, depending on the type of process (mechanic, thermal...) and on the information available (Figure 3.1l).

l) <u>Powdered materials: dustiness index</u>

For dust emissions from powder materials handling, the particle emission rate can be estimated by means of the dustiness index as:

$$S(t) = DI \cdot H \cdot \frac{dM(t)}{dt} \cdot LC \qquad \text{Eq. (3.8)}$$

where DI (mg kg^{-1} or particles kg^{-1}) is the respirable dustiness index of the material, H (dimensionless) is the handling energy factor for the process under study, dM(t)/dt (kg min^{-1}) is the mass flow of the powder (e.g. inorganic fertilizer), and LC (dimensionless) is the protection factor of localized controls. H needs to be assumed (Lidén 2006,

Schneider and Jensen 2007, Koivisto *et al.* 2015), and LC can be experimentally detremined, theoretically calculated or extracted from the literature (Fransman *et al.* 2008, Hewett and Ganser 2017, Goede *et al.* 2018).

2) Experimental exposure concentrations

When estimation of the emission rates from the dustiness index is not possible (e.g. no powders involved in the process or during a thermal process), two different methods can be used, which estimate emission rates by means of measured particle/mass concentrations.

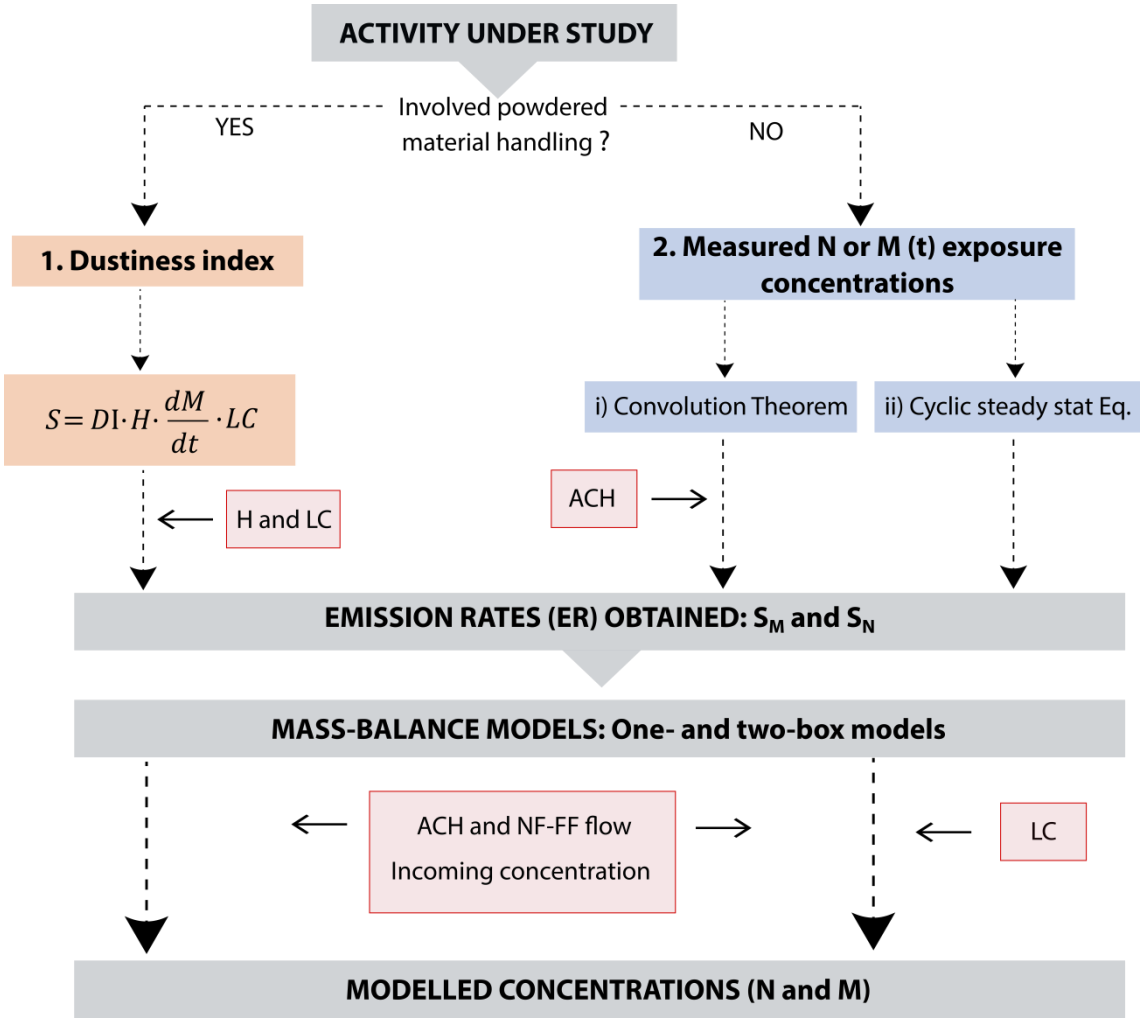

Figure 3.11 One- and two-box models application working flow. N (cm^{-3}): particle number concentration as a function of time (t). M ($\mu g\ m^{-3}$): particle mass concentration as a function of time (t). ACH (h^{-1}): air changes per hour. LC: local controls efficiency. NF: near-field. FF: far-field. H: handling energy factor.

i) Convolution theorem

Assuming that concentrations are fully mixed, particle concentrations can be described with a mass balance of aerosol particles in a single compartment (Hewett and Ganser 2017):

$$\frac{dN(t)}{dt} = \lambda N_{BG}(t) + \frac{S_N(t)}{V} - \lambda N(t) \qquad \text{Eq. (3.9)}$$

where N (cm^{-3}) is the particle concentration, λ (min^{-1}) is the ventilation rate, N_{BG} (cm^{-3}) is the background particle concentration coming from outdoors and surrounding compartments, S_N (min^{-1}) is the particle emission rate of the source, and V (m^3) is the volume of the room. Particle losses were considered only due to ventilation.

When particle emissions from ventilation and indoor sources are negligible (i.e. $S_{tot}(t) \approx 0$ min^{-1}, e.g. during background measurements) the particle concentration decay curve may be described as follows:

$$N(t) = N_{t=0} \cdot e^{-\gamma \cdot t} \qquad \text{Eq. (3.10)}$$

where γ (min^{-1}) is the total particle decay rate.

According to the convolution theorem, particle concentrations during the activity are a convolution of the particle sources and particle losses as follows (Schripp *et al.* 2008):

$$S_{tot}(t) \cdot N(t) = V \int_0^t \left(Q N_{BG}(t) + \varepsilon_C S_N(t)\right) \cdot N(t-\tau) d\tau \qquad \text{Eq. (3.11)}$$

where Q (m^3 h^{-1}) is the air flow and ε_C (dimensionless) is the protection factor due to enclosure or LEV.

Particle emission term can be solved with a numerical deconvolution as:

$$S_{tot}(t) = V \frac{N(t) - N(t-\Delta t) \cdot e^{-\gamma \cdot \Delta t}}{\Delta t} \qquad \text{Eq. (3.12)}$$

ii) Steady state equation for cyclic process

In addition, S (cm^{-3}) was calculated using the actual particle concentrations monitored, by applying the modified steady state equation for cyclic process (Hewett and Ganser 2017):

$$S_N = \frac{\bar{C} . V}{t_{ESD}} \qquad \text{Eq. (3.13)}$$

where $\bar{C}$ (cm^{-3}) is the mean concentration during the activity (in this case thermal spraying), V (cm^3) is the room volume and t_{ESD} (min) is the spray duration. Assumptions

when using this equation are that particle concentration before the process starts is lower than during spraying, particle removal processes are negligible, and concentrations are fully mixed.

3.6. Risk assessment

3.6.1. ICRP inhalation deposition model

The simplification of the ICRP model described by Hinds (1999) was used to calculate particle regional deposition due to inhalation in the three main regions of the respiratory tract: head-airways, tracheobronchial and alveolar. The model was applied in terms of particle number, surface area and particle mass. Regional deposition refers to the mean probability of an inhaled particle to be deposited in a certain region of the respiratory tract (head airways, trachea bronchi and alveolar) by collection onto airway surfaces (Heyder *et al.* 1986).

The input for the model is the particle size distribution in terms of particle number; subsequently particle surface area and mass concentration were calculated trough the equations described below.

Particle active surface area was calculated by applying particle size distribution to the equation (3.14) described in Heitbrink *et al.* (2009) as in Koivisto *et al.* (2012b):

$$s = \frac{3\pi\lambda D_b}{C_c(D_b)\delta} \qquad \text{Eq. (3.14)}$$

where λ_{air} (0.066 μm) is the mean free path for air, and δ (0.905) is the scattering parameter for air. D_b is the mobility diameter and C_c the slip correction factor for the corresponding aerodynamic or mobility particle size.

The particle mass was additionally calculated by using mobility particle diameter and effective density as in Koivisto *et al.* (2012b):

$$m = \rho_{eff} \frac{\pi}{6} D_b^3 \qquad \text{Eq. (3.15)}$$

where ρ_{eff} (g cm^{-3}) is the effective density. When particle density was unknown, 1 g cm^{-3} was assumed for simplicity.

The regional inhalation dose rate was obtained by multiplying particle size concentrations by the ICRP human respiratory tract model deposition probability (ICRP, 2011) (see figure 1.9). The respiratory volume most widely used is 25 l min^{-1}, corresponding to male respiration during light exercise (Koivisto *et al*. 2012b). However, other respiratory volumes can also be used according to what best fits in each specific case study. In the model, particles were assumed to be spherical and to preserve their size during inhalation.

3.6.2. Risk assessment tools

As previously described there are multiple empirical models and control banding tools currently in use for exposure assessment purposes. In this PhD Thesis, three of them were used and tested for different industrial scenarios assessed. ART and Stoffenmanager were selected as examples of empirical risk assessment models, given that they are recommended by the ECHA (ECHA 2016b) as higher tier I, they are mostly complete in terms of specifications, and they are widely used (Landberg *et al.* 2015, 2017, Riedmann *et al.* 2015, Bekker *et al.* 2016, Savic *et al.* 2018). In addition, NanoSafer v1.1beta was used as it is a recently launched control banding tool with focus on NP (Kristensen *et al*. 2010; Jensen *et al.* under preparation).

- Stoffenmanager® v.7.1: is a risk priorisation web-based tool which consists of a control banding tool (inhalation and dermal), and general and REACH specific quantitative inhalation exposure models (Van Tongeren *et al.* 2017). It is considered between a tier 1 and tier 2 tool (ECHA, 2016; Landberg et al., 2017; Spinazzè et al., 2017; Van Tongeren et al., 2017), and its general assumptions are based on Marquart *et al*. (2008) while the rationale of the algorithm is based on Cherrie and Schneider (1999) and adapted as described in Tielemans *et al*. (2008b). To assess inhalation exposure to engineered NPs, Stoffenmanager has a specific nano-module.

- The Advanced REACH tool (ART v.1.5): is a tier 2 mechanistic exposure modelling tool with a higher level of detail than Stoffenmanager. It also follows a Bayesian approach that combines the mechanistic model with measurements of exposure (Landberg *et al.* 2017). Similarly to Stoffenmanager, ART is also based on Cherrie and Schneider (1999) with Tielemans *et al*. (2011) modifications. It is described and explained in detail in Fransman *et al*. (2011), and it has been tested and calibrated in Schinkel *et al*. (2011). Stoffenmanager and ART dimensionless total exposure score equations can be found in Riedmann *et al*. (2015).

- The NanoSafer v.1.1beta: is a control-banding and risk management tool (Kristensen *et al*. 2010; Jensen et al. in preparation) specifically designed for manufactured nanomaterials and NP release activities (e.g. powder handling and fugitive/point-source emissions), which is currently being refined and further developed under caLIBRAte Project (http://www.nanocalibrate.eu/home). Hazard assessment and case-specific exposure potentials are combined into an integrated assessment of risk levels (control bands) with associated risk management recommendations. NanoSafer scores can be translated to concentrations by using simple equations (Jensen *et al.* 2014):

$$C_{acute} = 2 \cdot OEL \cdot NS_{acute}, \quad \text{Eq. (3.16)}$$

$$C_{8h\,TWA} = OEL \cdot NS_{8h\,TWA}, \quad \text{Eq. (3.17)}$$

where C_{acute} and $C_{8h\ TWA}$ are estimated acute and 8h TWA concentrations, NS_{acute} and $NS_{8h\ TWA}$ are NanoSafer scores for acute and 8h TWA. OEL value use will be the OEL for bulk material stablished when:

$$Volume\ specific\ surface\ area\ (VSSA) < 30\ m^2 cm^{-3}, \quad \text{Eq. (3.18)}$$

and OEL_{nano} when:

$$VSSA > 30\ m^2 cm^{-3}, \quad \text{Eq. (3.19)}$$

OEL_{nano} is estimated from bulk OEL as:

$$OEL_{nano} = OEL \cdot \frac{30 \cdot \frac{1}{\delta_{nano}}}{SSA_{nano}}, \quad \text{Eq. (3.20)}$$

where OEL is the stablished OEL for the bulk material, δ (g cm^{-3}) is the specific density of the nanomaterial and SSA (m^2 g^{-1}) is the specific surface area of the nanomaterial.

The three tools consider different input parameters (Table 3.3), and therefore provide different output results as well Table 3.4. For material-related inputs, ART has higher specifications regarding the type of material, dustiness and humidity, whereas NanoSafer focuses more on the type of particle and their physical-chemical characteristics. The other main difference is that Stoffenmanager and NanoSafer consider material health and safety, whereas ART leaves this part out if its scope, and focuses only in exposure concentrations.

Table 3.3 Comparison of input parameters for the three risk assessment models applied.

INPUT		ART	Stoffenmanager	NanoSafer
Material	**CAS**	*YES*	*For components*	*YES*
	Type substance (Physical properties)	*YES*	*YES*	*NO*
	Dustiness	*Enter value or Drop-down level*	*Chose type of material*	*Enter value or Drop-down level*
	Humidity	*Drop-down levels*	*NO*	*NO*
	% of product	*YES*	*% For components*	*NO*
	Health and Safety	*NO*	*YES*	*YES*
	Nano Specifications	*NO*	*NO (specific nano-module)*	*Modified surface, nano, fullerene...*
	Primary particle	*NO*	*NO*	*Shape, Size, SA*
	Density	*NO*	*NO*	*YES*
	Solubility	*NO*	*NO*	*YES*
Process	**Source position**	*BZ/FF*	*BZ/FF*	*NF/FF*
	Type of process	*Only mechanical process*	*Mechanical, thermal...*	*Only mechanical process*
	Type of handling	*YES*	*NO*	*NO*
	Energy	*Drop height*	*NO*	*Energy level*
	Emission controls	*Containment, LEV, glove box, segregation/enclosure*	*PPE, LEV, segregation/enclosure*	*Recommended emission controls (in the Output)*
	Maintenance	*YES*	*YES*	*NO*
	Duration	*YES*	*YES*	*YES (cycle timing)*
	Background	*YES (with specific processes)*	*NO (non-activity period)*	*NO*
	Frequency	*NO*	*Nº days and nº workers*	*NO*
	Amount of material	*NO*	*NO*	*YES (enter value)*
Room	**Volume**	*Drop-down values or description*	*Drop-down values*	*Enter value*
	ACH	*Drop-down values or description*	*Type of ventilation (description)*	*Enter value or drop-down values*

Regarding process characterization, main differences between the tools are that 1) ART and Stoffenmanager allow to assess whether emissions take place in the breathing zone

or not, whereas in NanoSafer NF-FF values are provided; 2) ART and Stoffenmanager are designed only for mechanical processes, whereas Stoffenmanager considers thermal processes as well; 3) type of handling and energy levels are not considered in Stoffenmanager; and 4) in NanoSafer no emission controls are considered as one of the purposes of the tool is to provide recommendations regarding type of control measures to be applied in a specific scenario. Further developments of the tool are expected to include control measures in the risk assessment evaluation. For the case scenarios of this Thesis, local controls reductions were included considering factors applied in the ART tool. Finally, room characteristics can be better detailed in NanoSafer as it requires specific values as input, whereas ART and Stoffenmanager have only drop-down default values.

The ART tool output is a full-shift predicted concentration in terms of mass. Conversely, the NanoSafer does not provide concentration but instead produces a hazard level, exposure potential (very high, high, moderate, low…) and protection recommendations with an efficiency percentage. Finally, Stoffenmanager's output is an in-between result, providing task and full-shift concentration (for material and components) and a risk level.

Table 3.4 Comparison of output parameters for the three risk assessment models applied.

Output		
ART	**Stoffenmanager**	**NanoSafer**
Task and full-shift mass concentrations	*Task and Full-shift concentrations for material and components, and risk level of exposure*	*Hazard level, risk level of exposure and recommendations*

Results

Chapter 4

4. RESULTS

This chapter presents the results of this PhD Thesis in the form of four research publications (papers), which discuss the objectives presented in chapter 2 (Objectives and Structure). While all four publications address the first objective (Worker exposure assessment and particle emissions), the rest of the objectives are dealt with in the different papers. **Publication I** tackles objective 3 (Dustiness as an exposure prediction tool) on the basis of mechanical handling of powders in a pilot plant. In **Publication II,** handling (packing) of ceramic materials at industrial scale was used as a base to study objectives 2i and ii (related to the use of tools and metrics for exposure assessment), 3 (Dustiness as tool for exposure prediction), and 5 (Evaluation of risk assessment and control banding tools). **Publication III** expands on the research presented in Publication II by assessing the performance of mass-balance models when challenged with low concentrations of micron-sized particles, in an industrial scenario during mechanical handling (packing) of a fertilizer. Finally, in **Publication IV** mass-balance models are tested in the framework of high number concentrations of NPs (unintentionally released), sourcing from thermal spraying of ceramic coatings at industrial scale.

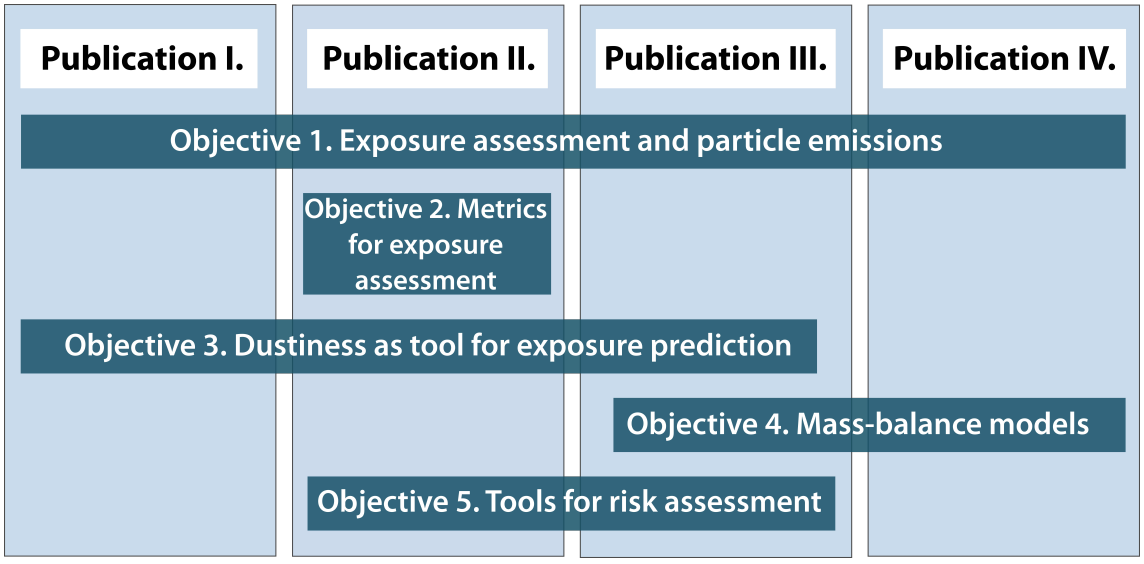

Figure 4.1 Objectives addressed in each research publication.

4.1. Publication I: On the relationship between exposure to particles and dustiness during handling of powders in industrial settings

Authors:

Ribalta C[1,2]., Viana M[1]., López-Lilao A[3]., Estupiñá S[3]., Minguillón M.C[1]., Mendoza J[4]., Díaz J[4]., Dahmann D[5]., Monfort. E[3].

[1]Institute of Environmental Assessment and Water Research (IDÆA-CSIC), C/ Jordi Girona 18, 08034 Barcelona, Spain.

[2]Barcelona University, Chemistry Faculty, C/ de Martí i Franquès, 1-11, 08028 Barcelona, Spain

[3]Institute of Ceramic Technology (ITC)- AICE - Universitat Jaume I, Campus Universitari Riu Sec, Av. Vicent Sos Baynat s/n, 12006 Castellón, Spain.

[4]Scientific and Technological Centres Barcelona University (CCiTUB), C/ Lluís Solé i Sabaris, 1-3, 08028 Barcelona, Spain

[5]Institute for the Research on Hazardous Substances (IGF), Waldring 97, 44789 Bochum, Germany.

Published in:

Annals of Work Exposures and Health, 63(1): 107-123, 2019

doi: 10.1093/annweh/wxy092

Accepted date: 16 October 2018

Journal Impact Factor / 5-Year Impact Factor: 1.615 / 2.101

On the relationship between exposure to particles and dustiness during handling of powders in industrial settings

Ribalta C[1,2]., Viana M[1]., López-Lilao A[3]., Estupiñá S[3]., Minguillón M.C[1]., Mendoza J[4]., Díaz J[4]., Dahmann D[5]., Monfort. E[3].

[1]Institute of Environmental Assessment and Water Research (IDÆA-CSIC), C/ Jordi Girona 18, 08034 Barcelona, Spain.
[2]Barcelona University, Chemistry Faculty, C/ de Martí i Franquès, 1-11, 08028 Barcelona, Spain
[3]Institute of Ceramic Technology (ITC)- AICE - Universitat Jaume I, Campus Universitario Riu Sec, Av. Vicent Sos Baynat s/n, 12006 Castellón, Spain.
[4]Scientific and Technological Centres Barcelona University (CCiTUB), C/ Lluís Solé i Sabaris, 1-3, 08028 Barcelona, Spain
[5]Institute for the Research on Hazardous Substances (IGF), Waldring 97, 44789 Bochum, Germany.

Abstract

Exposure to ceramic powders, which is frequent during handling operations, is known to cause adverse health effects. Finding proxy parameters to quantify exposure is useful for efficient and timely exposure assessments. Worker exposure during handling of five materials (a silica sand (S1), three quartzes (Q1, Q2 and Q3) and a kaolin (K1)) with different particle shape (prismatic and platy) and sizes (3.4 - 120 µm) was assessed. Materials handling was simulated using a dry pendular mill under two different energy settings (low and high). Three repetitions of two kilos of material were carried out per material and energy conditions with a flow rate of 8 - 11 kg/h. The performance of the dustiness index as a predictor of worker exposure was evaluated correlating material's dustiness indexes (with rotating drum and continuous drop) with exposure concentrations. Significant impacts on worker exposure in terms of inhalable and respirable mass fractions were detected for all materials. Mean inhalable mass concentrations during background were always lower than 40 µg/m^3 whereas during material handling under high energy settings mean concentrations were 187, 373, 243, 156 and 430 µg/m^3 for S1, Q1, Q2, Q3 and K1 respectively. Impacts were not significant with regard to particle number concentration: background particle number concentrations ranged between 10620 – 46421 /cm^3 while during handling under high energy settings they were 20880 - 40498 /cm^3. Mean lung deposited surface area during background ranged between 27 - 101 µm^2/cm^3 whereas it ranged between 22 - 42 µm^2/cm^3 during materials handling. TEM images evidenced the presence of nanoparticles (≤ 100 nm) in the form of aggregates (300 nm - 1 µm) in the worker area, and a slight reduction on mean particle size during handling was detected. Dustiness and exposure concentrations showed a high degree of correlation (R^2 = 0.77 - 0.97) for the materials and operating conditions assessed, suggesting that dustiness could be considered a relevant predictor for workplace exposure. Nevertheless, the relationship between dustiness and exposure is complex and should be assessed for each process, taking into account not only material behaviour but also energy settings and workplace characteristics.

Keywords: indoor air, prediction of exposure, airborne dust, exposure assessment, particulate matter, industrial settings, nanoparticles

Introduction

Exposure to airborne particles is a growing field of research due to its complexity and intrinsic difficulty with regard to standardization. This is linked to the large variety of sources, processes and hazardous materials involved. The ceramic industry is a relevant case study, as it results in personal exposures in ambient and indoor air to a wide range of potentially hazardous raw materials and because during the manufacturing cycle a wide variety of bulk materials is used. In most cases, these materials are dry micro-sized (or even nano-sized) powders. As described by Brouwer et al. (2004), the aerosolization of submicrometer particles in workplaces is not limited to nanotechnology facilities. New technologies such as laser ablation, laser thermal treatment or inkjet printing, and green materials developments such as bactericidal and easy-clean surfaces, are currently being introduced in the traditional ceramic sectors (Gabaldón-Estevan et al., 2014; Llop et al., 2014; Monfort, 2012). The use of these new technologies as well as the growing and emerging markets represent new challenges in terms of occupational health (Fonseca et al., 2016; Fonseca et al., 2015; Viana et al., 2017; Voliotis et al., 2014).

Particulate matter (PM) as well as ultrafine particles (UFP) can penetrate deep in the human respiratory tract, the finest fractions reaching the alveolar region (Brunekreef & Forsberg, 2005; Pope & Dockery, 2006). Respiratory-related disease in the ceramic industry due to inhalable dust has already been reported (Alim et al., 2015; Dehghan et al., 2009; Neghab et al., 2009). In Spain, concentration limit values have been established for particulate matter exposure (not otherwise specified) as 10000 μg/m^3 and 3000 μg/m^3 for inhalable and respirable mass fractions, respectively (INSH, 2017).

The number of studies dealing with exposure is relatively low when compared with the wide variety of possible exposure scenarios in industrial settings (Brouwer et al., 2009). However, exposure assessment is a key component of risk assessment, which is generally combined with toxicological studies (Kuhlbusch et al., 2011). Thus, it is essential to determine exposure under different real world industrial scenarios as well as to predict exposure and establish efficient risk management strategies. In recent years many efforts were carried out to control and reduce exposure, although less attention was paid to the production processes and material handling (Lidén, 2006). In this framework, dustiness has risen as a valuable tool for occupational safety (Hamelmann & Schmidt, 2003), as it is a measure of a material's tendency to generate airborne dust during handling. However, discussions are ongoing about the use of the dustiness index as a direct predictor for worker exposure (Dubey et al., 2017; Fonseca et al., 2018) because dust emissions are known to depend on powder properties, the amount of material handled, the process, and local controls (Fransman et al., 2011). Certain authors (Brouwer, 2006; Class et al., 2001; Fonseca et al., 2018; Heitbrink et al., 1990) found no clear or limited relationship between exposure and dustiness, although they pointed out the importance of this parameter for risk assessment. On the other hand, Breum et al. (2003) despite finding a clear positive relation between dustiness and exposure, did not use their results for exposure prediction. Finally, some factors should be taken into account when establishing the relation between dustiness and exposure: 1) two standard methods are described in (EN 15051); 2) dustiness depends mainly on material particle size distribution, humidity, density, morphology and specific surface area (SSA) (Hamelmann & Schmidt, 2003; Lidén, 2006; López-Lilao et al., 2016, 2015); and 3) dustiness tests should mimic as closely as possible the actual process energy applied (Evans et al., 2013). As a result, dustiness is currently used as an input for exposure modelling (Levin et al., 2014; Schneider and Jensen, 2007) and by materials producers to

modify products in order to reduce dust generation (Lidén, 2006), rather than as a direct exposure predictor.

In this context, the present work aims to 1) assess exposure to airborne particles during handling of five highly used ceramic materials, paying special attention to material characteristics (size and particle shape) as well as to the influence of operating conditions (energy input); 2) assess dustiness indexes of the output materials to understand their emission mechanisms; and 3) correlate actual exposure concentrations with dustiness indexes, with the final goal to contribute on the understanding of the potential use of dustiness as a predictor of worker exposure.

Methodology

Experimental setup and instrumentation

The experiments took place in the pilot plant of the Institute of Ceramic Technology (ITC), Castellón, Spain during 4 days in October 2016. The pilot plant is divided into two connected rooms of 406 m^2 and 182 m^2 partly separated by a wall, which allows for air exchange at two different points (Figure 1). The plant is operated on a regular basis by 5 or more workers carrying out different activities. Material handling took place in room 1. The exterior door leading outdoors was kept open, as this is the plant's normal procedure.

Worker exposure to airborne particles was monitored during handling of powder materials during a process which included feeding of the materials to a dry pendular mill and extracting the powders from it. In order to study only handling (and not milling) emissions, a mill not altering the primary particle size but instead only modifying the size of the aggregates was selected, so that the process resembled the one that would occur during the handling operations. To verify this, the primary particle diameters of the input and output materials were determined by laser diffraction (wet method, see section 2.3) and no significant differences were observed. Modifying the primary particle size would have required additional mechanical action (Evans et al., 2013), which was not applied in this case. The mill selected for this purpose was a pilot-plant scale Poittemill PM-LB, with a nominal output capacity around 20 kg/h.

Particle mass, number concentration and alveolar lung deposited surface area (LDSA) were monitored as well as particle size distribution and morphological/chemical characterization. Three sampling locations were selected (Figure 1):

- Worker area: the devices were placed at a distance from the emission source similar to where the worker is standing (1 m from the floor and 50 cm from the emission source). The location is representative of the breathing zone, even if it may not be considered strictly as such. Devices used were: a butanol Condensation Particle Counter (CPC, TSI Model 3775; sample flow rate 1.5 l/min) to measure particle number concentration (4 - 1500 nm, 1 minute time resolution); an electrical mobility spectrometer (NanoScan SMPS, TSI Model 3910; sample flow rate 0.7 l/min) to measure particle size distribution in 13 channels (10 - 420 nm, 1 minute time resolution); a miniature diffusion size classifier (DiSCmini Matter Aerosol, Testo; sample flow rate 1 l/min) to measure particle number concentration, mean particle size and lung deposited surface area (LDSA) (10 - 700 nm, 1 minute time resolution); and a Mini Laser Aerosol Spectrometer (Grimm, Mini-LAS 11R; sample flow rate 1.2 l/min) to measure particle mass concentration (0.25 - 32 µm, 31 channels, 1 minute time resolution). In addition, TEM grids (Qunatifolil ® Au grids with 1 µm diameter holes - 4 µm separation of 200 mesh) were placed in a sampling cassette (SKC INC., USA, inlet diameter 1/8 in. and filter diameter 25 mm) following the sampling setup described by Tsai et al., (2008). The Cassette was connected to a Leland pump (3 l/min). Sampling was performed in the worker area and indoor locations during handling for each material and for two energy

settings of the pendular mill (low and high; see 2.2). Chemical and morphological analysis was later carried out by TEM J2100 coupled with an energy-dispersive X-ray (EDX) spectrometer.

- Indoor: a monitoring location inside the plant far from the processes of study but still connected by air flows. It was representative of the pilot plant's background concentrations. Devices used were a DiSCmini (see above) and a Mini Wide Range Aerosol Spectrometer (Mini-WRAS 1371; Grimm; sample flow rate 1.2 l/min) to measure particle mass concentration, particle number concentration and particle size distribution from

mainly to discuss about indoor and outdoor influence over the worker area measurements.

All online instruments were time-synchronized and inter-compared overnight. Calibration of the Grimm laser spectrometers (Mini-LAS and Mini-WRAS) followed the procedures recommended by the manufacturer and are occasionally calibrated with regard to gravimetric reference samples. It should be noted that this kind of calibration is not carried out with the same aerosol as monitored in the present work, which would be the advisable procedure for any workplace exposure assessment (PD CEN/TR 16013 - 2:2010).

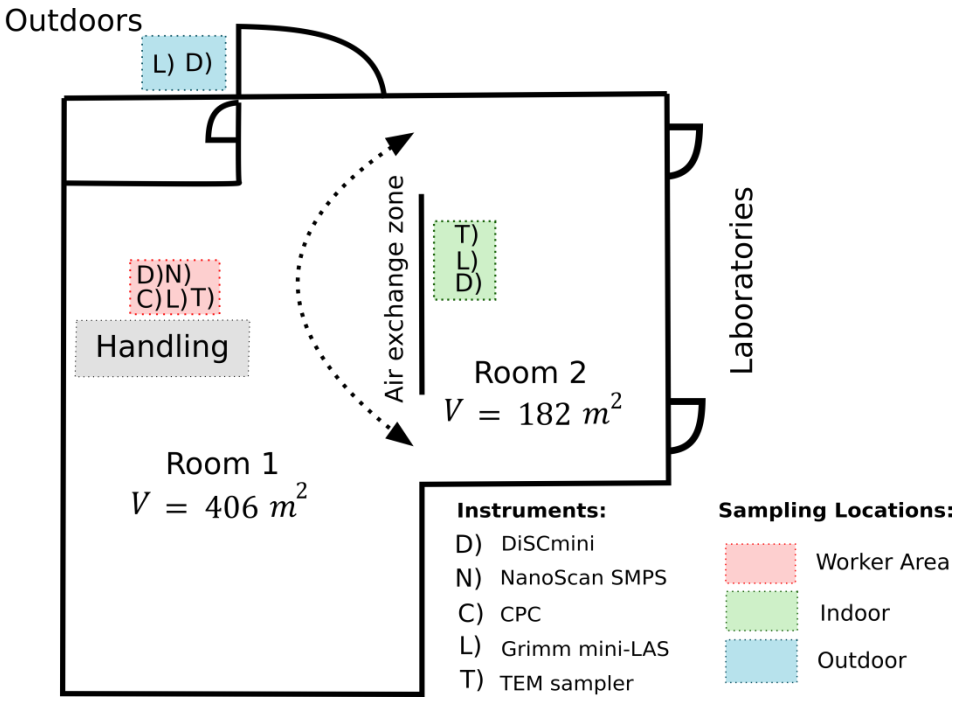

Figure 1. ITC pilot plant layout. Monitoring locations as well as devices used during the handling process are indicated.

10 nm to 35 µm in 41 channels with a 1 minute time resolution. Additionally, TEM particle collection was carried out (see above).

- Outdoor: an outside monitoring location was set close to the main entrance of the plant. Devices used were a DiSCmini and a Grimm Mini-LAS (see above).

Indoor and outdoor monitoring points are not going to be extensively discussed. They are used

Devices started monitoring between 30 and 60 minutes before the start of the process (pre-activity), and the average results in this period before the process were used as a background particle concentration (Brouwer et al., 2009; Demou et al., 2008).

Worker area exposures were considered statistically significant when the following

approach, described by Asbach et al. (2012) and Kaminski et al. (2015), was fulfilled:

Mean value during operation > BG + 3*(σBG)

where BG is the mean temporal background concentration (pre-activity) and σBG is the standard deviation of the background concentration.

Target materials, operations and conditions

Five different micronized materials, widely used in the ceramic industry, were selected (Table 1 and Table S1, Supporting information): Silica sand, S1 (d_{50} = 120 µm; CAS: 14940-68-2), three types of quartz, Quartz Q1, Quartz Q2 and Quartz Q3 (d_{50} 3.4 - 12.1 µm; CAS: 14808-60-7), and kaolin, K1 (d_{50} = 5.7 µm; CAS: 1332-58-7) sieved through a 5 mm mesh. Materials particle size distribution (d_{50}) determination was carried out by using laser diffraction; methodology described in more detail in section 2.3. According to the aspect ratio (AR) silica sand and quartz particles were considered to be prismatic (ca. spherical), while kaolin was platy (plate-like) shaped (micrographs of Q2 and K1, Figure S1, Supporting information). Because the moisture content of powders can affect material dustiness and exposure (Levin et al., 2015; Lidén, 2006) and also, due to pendular mill working requirements, all materials were previously dried using an oven at 105 - 110 ºC during at least 24h.

High energy (HE) (frequently used) and low energy (LE) operating conditions were tested, being representative for this industrial sector. Operating conditions are determined by air and material flow rate, aspiration intensity, milling speed and particle separation (Table 2).

Three repetitions were carried out for each material and condition. Approximately 2 kg of material were manually fed by the pilot plant worker into the mill grinding chamber for each repetition. All the materials were processed for 12 - 15 minutes (material flow 8 - 11 kg/h; Table 2), the exact time depending on how long it took for the material to be introduced in the mill's chamber due to its flowability. At the end of each repetition the output material was manually collected and stored for subsequent chemical and dustiness analysis.

Finally, cleaning operations were also monitored.

Materials characterisation

Input and output materials were characterized:

- Specific surface area (SSA) was assessed according to the BET method by nitrogen absorption (Brunauer et al., 1928).

- Materials flowability was assessed by using the Hausner ratio (HR); the quotient of the bulk density of the packed particle bed (by tapping) and the aerated bulk density of the particle bed, obtained by dropping powder into a container without stirring or vibration. In this regard, where the bigger the HR the lower the followability (Mallol et al., 2008).

- Particle Size Distribution (PSD) was determined by laser diffraction (d_{laser}) wet method (ISO 13320-1, 2009) using the Mastersizer 2000 that analyse the sample by the theory of Fraunhofer and Mie with a size resolution of 0.02 - 2000 µm and by and X-ray gravitational sedimentation using the Sedigraph method from Micrometrics (d_{stokes}).

- The aspect ratio (AR), a particle shape factor defined as the ratio of the particle's major dimension and minor dimension, was determined by the Parslow-Jennings method for oblate spheroids (Jennings & Parslow, 1988; Otterstedt & Brandreth, 2013). This method is based on the fact that d_{laser} and $d_{sedigraph}$ (previously described) have different dependence on aspect ratio and, therefore, we can only obtain the same diameter in the case of spherical particles.

$$\frac{d_{stokes}}{d_{laser}} = \sqrt{\frac{2\,.\,AR.\arctan\sqrt{(AR^2-1)}}{AR.\sqrt{(AR^2-1)}+\ln\left[AR+\sqrt{(AR^2-1)}\right]}} \quad (1)$$

where AR is the aspect ratio, d_{stokes} the diameter of a sphere with the same density and setting velocity as the particle of interest (µm), and d_{laser} is the diameter of the sphere of same diameter as the cross-sectional projection of the particle (µm).

TEM-EDX (Markowicz & Grieken, 2001; Williams & Carter, 2009).

Dustiness tests

Dustiness tests were performed for all materials and conditions (high and low energy) tested, before and after the handling process (input and output materials). The two dustiness tests described by the EN 15051 (2013) (Continuous drop method; López-Lilao et al., 2016), and

Table 1. Material type, material code, particle shape and most common uses in the ceramic industry are given. Particle size distribution: PSD in terms of di: diameter below which lies i% by volume of total particles, specific surface area: SSA, Hausner ratio: HR and aspect ratio: AR are described for each material. Inhalable mass fraction and classification level are shown for the two dustiness methods (continuous drop and rotating drum). Moisture of all the samples before the start of the manipulation process was <0.5%.

Material type	Code	Shape	Uses	d_{50} (µm)	d_{10} (µm)	d_{90} (µm)	SSA (m^2/g)	HR	AR	w_I (mg/kg) C.D	w_I (mg/kg) R.D
Zirconium silica sand	S1	Prismatic	Ceramics production	120	NDA	NDA	NDA	1.12	4.3	463 (Very Low)	NDA
Quartz	Q1	Prismatic	Materials preparation, forming, glazing or firing	12.1	1.4	37.0	1.4	1.64	3.3	4593 (Moderate)	202 (Very Low)
Quartz	Q2	Prismatic	Pigment production for the colouration of glazes	5.8	1.1	18.8	2.7	1.52	5.7	3855 (Low)	164 (Very Low)
Quartz	Q3	Prismatic	Used in rubber compounds	3.4	1.0	8.4	4.4	1.57	3.8	3029 (Low)	64 (Very Low)
Kaolin caobar	K1	Platy (plate-like) or ribbon-like	Traditional ceramics production. Cement and metallurgical industries	5.7	1.4	15.7	9.6	1.83	20	10012 (Moderate)	410 (Low)

This factor is a measure of the irregularity of particle shape, i.e. deviation from a spherical shape. For prismatic, platy, and ribbon-like particles the aspect ratios were 1 - 5, 4 - 15, and 5 - 100, respectively (Otterstedt & Brandreth, 2013). Therefore, the selected quartzes and sands can be considered prismatic particles and the kaolin can be classified as platy or ribbon-like particle.

In addition, airborne particles collected on Au Quantifoil ® grids during handling were morphologically and chemically characterised by

rotating drum method (Pensis et al., 2009) were performed following the standard, although with only two repetitions/material (Figure S2).

Statistical analysis and data treatment

Log-normality and homogeneity were assessed with the Shapiro-Wilk and Levene's test, respectively and, as data did not fulfil normality assumptions, the non-parametric Mann-Whitney "U" Test was performed in order to determine statistically significant differences between mean

airborne particle diameters measured with the NanoScan.

Operating condition	Air flow rate (m^3/h)	Material flow rate (kg/h)	Milling speed (rpm)	Particle separation (rpm)
Low Energy	1600	8-11	1200	600
High Energy	1800	8-11	2250	1800

Table 2. Table 2. Milling parameters for low and high energy settings are described, aspiration intensity, mill speed and particle separation. Material process flow rate, for both energy settings, are also described.

Results and Discussion

Exposure assessment

Mean background concentrations (pre-activity) for the inhalable fraction were below 40 µg/m^3 for all the materials except for S1 (92.1 µg/m^3) and Q1 (58.9 µg/m^3) (Table 3). Outdoor, indoor and background concentrations for $PM_{2.5}$ were representative of $PM_{2.5}$ outdoor concentrations (20 - 30 µg/m^3; Pérez et al., 2008). Outdoor air to indoor micro-sized particle concentration was deemed negligible (Figure S3, Supporting information).

As expected, particle mass concentrations in the worker area, for all the materials, increased during handling (Table 3, Figure 2 and S4, Supporting information). Previous studies have already seen impacts on dust concentrations in both particle number and mass during material handling on paint factories pouring (Koivisto et al., 2015; Koponen et al., 2015), during bag filling of black carbon production (Kuhlbusch, et al., 2004), and during weighing bulk CNTs and sanding epoxy containing CNTs (Cena & Peters, 2011). Particle mass concentrations, for all repetitions, showed a marked cycle that consisted on a peak during material feeding and then a decrease, showing a clear impact on coarse particles due to handling for high and low energy settings (Figure 2 and S4, Supporting information). Mean inhalable mass concentrations during low energy settings were 189.5, 80.8, 106.8 and 319.1 µg/ m^3 for Q1, Q2, Q3 and K1 respectively whereas during high energy settings they were 373.0, 243.6, 156.0 and 429.6 µg/ m^3 (Table 3). Koponen et al. (2015) also described cyclic behaviour for materials pouring, with a concentration peak at the beginning of the activity. Hence, in some cases the number of repetitions can be more critical than the amount of material processed and thus the repetitions (start and stop) of a process is a factor that should be taken into account for exposure assessment models (Koponen et al., 2015). The time-weighted averages (TWA) for exposure levels are shown in Table S2, Supporting information. The highest value for the inhalable mass fraction was 429.6 µg/m^3 during K1 handling. This is well below the inhalable (10000 µg/m^3) and respirable (3000 µg/m3) OELs (INSH, 2017). Additional information regarding the calculation of the TWAs is provided in Table S2 (Supporting information).

On the contrary, the impact of handling on fine particles, measured with the CPC, was lower than for micro-sized particles. The trend observed for particle number concentration during handling suggests a more cumulative trend than for mass, especially for high energy conditions (Figure 2 and Figure S4, Supporting information). However, a significant increase in mean number concentration was not observed for any of the materials except for S1. This was probably due to the more frequent coagulation/adsorption processes of ultrafine particles onto coarse particles, which resulted in lower particle number concentrations. Recommended exposure concentrations during handling were not exceeded in any case, again with the exception of S1 which was on the limit of 40000 /cm^3 (Van Broekhuizen et al., 2012). Alveolar lung deposited surface area, monitored with DiSCmini (Table 3) was seen to decrease during materials handling when compared with pre-activity values (background). Mean LDSA

during background concentrations ranged between 27.1 - 100.9 $\mu m^2/cm^3$ whereas during materials handling they ranged between 22.1 - 42.3 $\mu m^2/cm^3$. Concerning mill cleaning operations, the highest 1-min peak concentrations for nano- and micro-sized particles when considering background + handling + cleaning were recorded during the cleaning operation, specifically during vacuuming (Figure 2 and S4, and Table S3, Supporting information). The maximum 1-min peak recorded during the cleaning operation for inhalable mass fraction of material Q1 was 13824 $\mu g/m^3$. Regarding particle number concentrations, maximum 1-min peak concentrations of 81247, 64443 and 77385 $/cm^3$ were recorded for Q2, Q3 and K1 (materials with lower d_{50}), respectively (Table S3, Supporting information). On the other hand, mean concentrations during cleaning were higher than the corresponding background concentrations for both inhalable and respirable mass fractions and for all materials except S1. However, there is no significant increase of mean number concentration for any of the materials when comparing with their respective background concentrations.

Table 3. Mean particle number, mass concentration and LDSA during handling of the powders at low and high energy settings. NDA: no data available.

Material	Measurement point	Low Energy				High Energy			
		Particle number ($\#/cm^3$)	LDSA ($\mu m^2/cm^3$)	Inhalable fraction ($\mu g/m^3$)	Respirable fraction ($\mu g/m^3$)	Particle number ($\#/cm^3$)	LDSA ($\mu m^2/cm^3$)	Inhalable fraction ($\mu g/m^3$)	Respirable fraction ($\mu g/m^3$)
S1	Background	NDA	NDA	NDA	NDA	10620 (9179-16431)	NDA	92.1 (14.6-1168.3)	11.0 (7.7-20.1)
	Worker area	NDA	NDA	NDA	NDA	**40498 (30713-49155)**	NDA	187.2 (57.7-454.8)	**39.1 (18.4-105.9)**
Q1	Background	24439 (19249-29660)	46.1 (29.8-156.3)	58.9 (20.3-599.2)	20.9 (16.0-52.6)	42686 (25421-51461)	48.2 (28.8-69.4)	39.6 (19.0-299.8)	22.2 (17.3-91.1)
	Worker area	30310 (24624-36399)	30.8 (27.5-40.4)	189.5 (76.0-337.0)	70.7 (40.6-126.9)	28059 (22427-40300)	22.1 (18.4-27.2)	**373.0 (126.2-1074.1)**	48.0 (22.5-89.7)
Q2	Background	29036 (15904-47210)	27.1 (20.7-43.6)	15.2 (3.8-135.1)	5.9 (3.6-15.7)	29036 (15904-47210)	27.1 (20.7-43.6)	15.2 (3.8-135.1)	5.9 (3.6-15.7)
	Worker area	15033 (10149-23264)	22.7 (17.0-40.5)	80.8 (11.8-1660.5)	**16.9 (7.7-122.5)**	23091 (16805-30928)	26.9 (20.5-31.1)	**243.6 (61.7-1069.3)**	**29.3 (11.7-83.9)**
Q3	Background	33064 (24959-43430)	100.9 (68.1-132.6)	34.1 (15.0-343.6)	19.9 (13.1-32.7)	33064 (24959-43430)	100.9 (68.1-132.6)	34.1 (15.0-343.6)	19.9 (13.1-32.7)
	Worker area	21756 (17223-35332)	42.3 (29.1-59.7)	106.8 (22.1-1031.7)	22.9 (12.0-68.6)	34214 (24961-48730)	39.1 (28.5-168.0)	**156.0 (21.0-1052.8)**	**37.9 (12.0-331.9)**
K1	Background	46421 (30470-53894)	72.6 (43.2-104.5)	13.0 (5.8-34.7)	5.5 (4.0-8.0)	46421 (30470-53894)	72.6 (43.2-104.5)	13.0 (5.8-34.7)	5.5 (4.0-8.0)
	Worker area	24002 (15419-49458)	22.8 (18.2-35.2)	**319.1 (70.6-1705.3)**	**66.8 (25.6-370.9)**	20880 (14149-26659)	27.3 (16.8-39.9)	**429.6 (136.0-999.3)**	**87.4 (58.6-162.0)**

Yeganeh et al. (2008) observed an increase of $PM_{2.5}$ during a similar sweeping operation of a fullerenes production reactor, while an increase in number concentration was also not observed, which is consistent with our results. On the other hand,

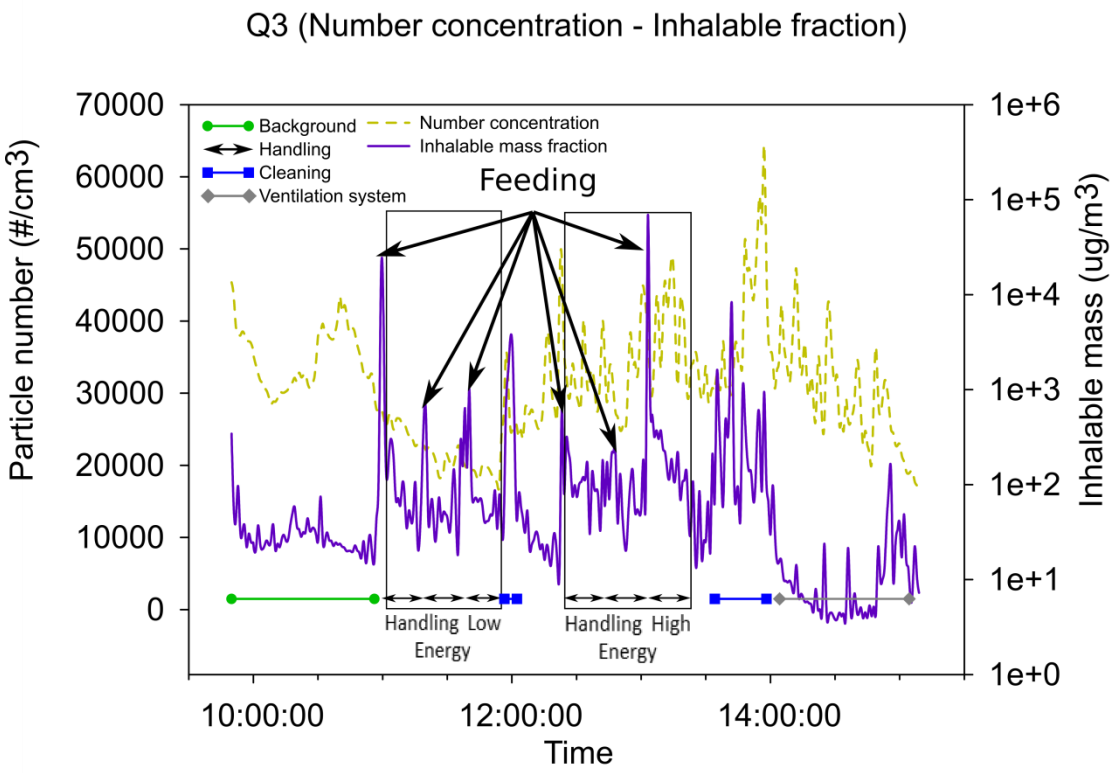

Figure 2. Time series of particle number concentration (monitored with CPC) and inhalable mass fraction in log scale (monitored with mini-LAS) for the Q3 material. Background, exhaust, cleaning and handling repetitions for low and high energy settings are marked on the bottom of the graph.

Demou et al. (2008) detected increases in particle number concentration during reactor cleaning operations, especially when vacuuming (maxim of 50000 /cm^3), identifying the vacuuming operation as an important short-term source of particles during cleaning. Other authors such as Fujitani et al. (2008) and Maynard et al. (2004) also reported the influence of vacuuming on particle number concentration and although the particle source is not clear, two main hypotheses were established by Maynard et al. (2004): (1) particle increase is due to materials aerosolization or (2) particles are generated on the unit's carbon brush motor, which seems to be the most probable reason in this case. In the present study, the maximum 1-min peaks recorded during the cleaning operation coincided with vacuuming, supporting the results of the previous studies despite differences in materials, processes and devices used.

Additionally, a case study regarding the use of a general ventilation system as a potential mitigation strategy in the pilot plant has been assessed and it is described in the Supporting information (Figure S5, Supporting information).

Material differences and influence of operating conditions

Generally particle mass concentrations increased when energy setting was set from low to high except for material Q1 (which decreased from 70.7 µg/m^3 under low energy settings to 48.0 µg/m^3 under high energy settings) (Figure 3, Table 3). For the inhalable mass fraction, significant increases with respect to the background concentrations were found during handling with high energy conditions (Figure 3b) for all materials, except for S1, ranging from 4.6 to 33.1 times the background concentrations. Contrarily, for low energy settings (Figure 3a), a significant increase was only seen for K1 (24.6 times higher than the background concentration), and in general, increases when comparing with the background values were lower than when using high energy conditions. When using high energy, increases between 25.7 to 66.8%

in inhalable mass concentrations were found comparing with low energy concentrations. Jensen et al. (2015) tested two different working styles (careful and careless) for sanding of glass- and carbon fibre-reinforced composites, and found increases in particle concentrations between 1.1 and 14.1% when working in the careless style compared with careful working style. Results from Jensen et al. (2015) and the ones herein suggest that operating conditions play an important role

shaped; mean particle diameters of 5.7 µm and highest SSA) followed by Q1 and Q2 (both prismatic, c.a. spherical) with mean particle diameter of 12.1 and 5.8 µm, respectively and with the lowest SSA values. Thus, no clear relationship between exposure concentrations and particle size, SSA or shape could be identified with the samples monitored. Regarding the respirable mass fraction, significant increases were found when using high energy conditions for Q2, Q3, K1 and S1 (Figure

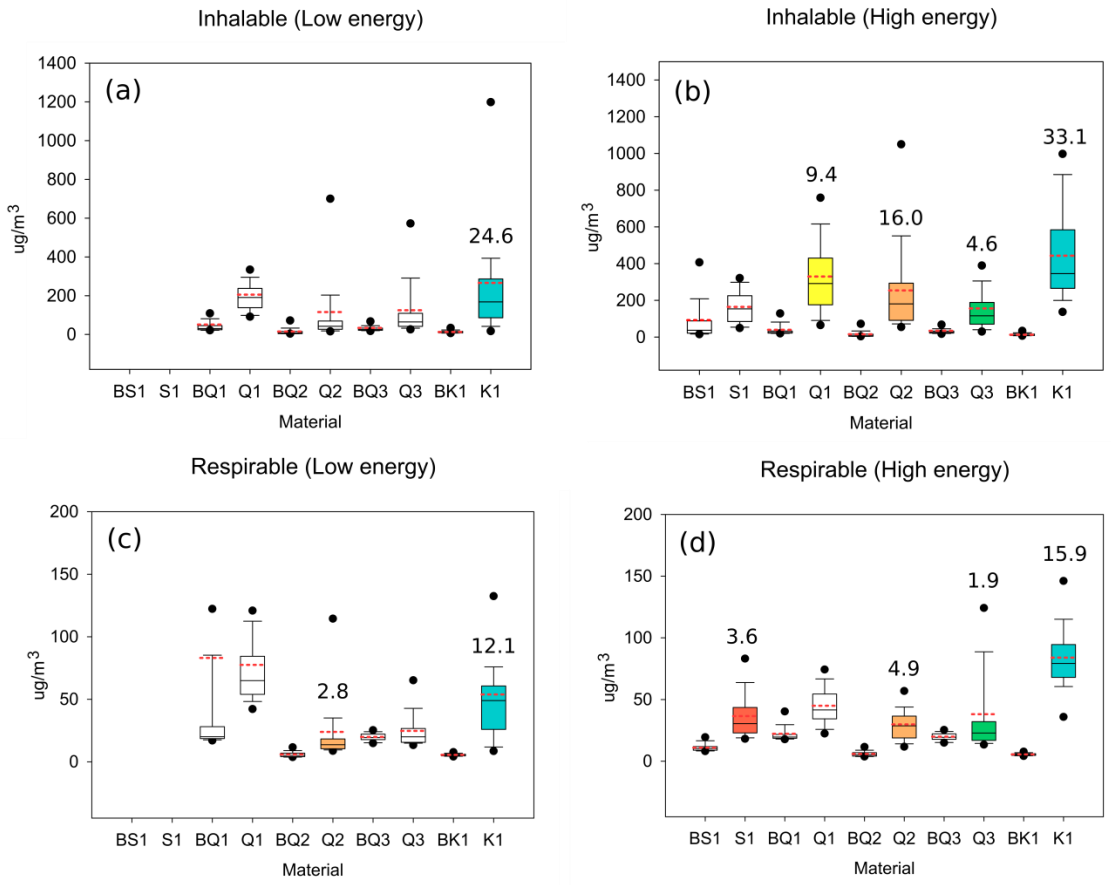

Figure 4. Vertical box plot for respirable and inhalable concentrations of the five materials during handling with high energy settings and each respective background concentration (pre-activity). The boundary of the box closest to zero indicates the 25th percentile and the farthest from zero the 75th percentile. Solid line within the box indicates the median value. Dotted line within the box indicates the mean value. Errors bars above and below indicates the 10th and 90th percentiles. Coloured box indicate significant differences when comparing with each background concentration. Values on the top of each box indicate the increase comparing with its corresponding background concentration (only when statistically significant differences were detected).

on worker exposure concentrations and therefore should be always considered when implementing corrective measures as well as for exposure prediction. On the other hand, the material with the highest inhalable mass exposure was K1 (platy

3d). On the other hand, when using low energy conditions, the respirable mass fraction only showed a significant increase for Q2 and K1 (Figure 3c). Again, also for respirable mass concentrations, higher exposure values were

observed under high energy settings. The two materials with higher exposure concentrations for low and high energy settings were K1 and Q2, respectively, both with material particle d_{50} around 5 µm (Table 1), but K1 with platy shape and Q2 prismatic. Various authors (López-Lilao et al., 2016, 2015; Pensis et al., 2009; Upton et al., 1990) reported that materials emission patterns do not follow a linear correlation with particle size, and that the assumption that finer materials have higher emissions is not always true. Materials with high content of ultrafine particles and comparably narrow size distribution have high cohesive forces and as a consequence material dustiness is lower than that of materials with a relatively larger mean particle diameter but with low ultrafine particles content. These materials show higher dustiness given that cohesive forces are less strong and ultrafine particles are easily released.

In general, particle number concentrations did not show an increase with respect to the background (pre-activity), except for S1, which was the only material showing a significant increase probably due to sources other than handling (Figure 2, 4 and S4, Supporting information). The presence of ultrafine particles from various sources is frequent in industrial settings (Viitanen et al., 2017). On the other hand, when comparing low and high energy settings, particle number concentration for all the prismatic (c.a. spherical) materials increased with the energy settings while it decreased for the platy (plate-like) shaped material K1 (from 24002 to 20880 /cm^3) (Figure 4, Table 3). Contrarily to what happened with the mass fractions, K1 is the material showing the lowest particle number concentration (Figures 3 and 4). Thus, for the materials and conditions assessed, handling of powder materials did not generate statistically significant emissions in terms of particle number concentrations.

However, results presented in Figures 5 and 6 indicate that handling may have had an impact on the mean size of the emitted ultrafine particles. This is supported by the TEM images in Figure 7 (see section 3.2.3). According to Figure 5, for S1, Q2, Q3 and K1, when using high energy conditions, mean particle size underwent a statistically significant reduction compared to background mean particle sizes (reductions in diameter in the order of 12 - 43%). However, interferences from other processes may have influenced this decrease for the S1 material (43% decrease). Under low energy conditions this influence was lower, as the reduction was only statistically significant for 2 materials. It may be hypothesised that handling allowed the release of the smaller particles contained in the materials due to aggregates breaking. Further work would be necessary to confirm this hypothesis.

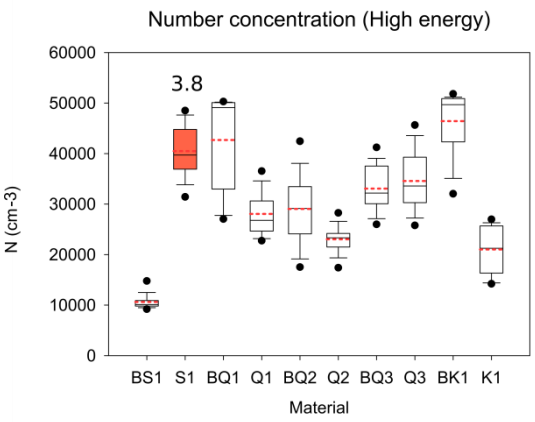

Figure 4. Vertical box plot for particle number concentrations of the five materials during handling with high energy settings and each respective background concentration (pre-activity). The boundary of the box closest to zero indicates the 25th percentile and the farthest from zero the 75th percentile. Solid line within the box indicates the median value. Dotted line within the box indicates the mean value. Errors bars above and below indicates the 10th and 90th percentiles. Coloured box indicate significant differences when comparing with each background concentration. Values on the top of each box indicate the increase comparing with its corresponding background concentration (only when statistically significant differences were detected).

When assessing the particle size distribution (Figure 6, instead of the mean diameter in Figure 5), results show only slight differences during

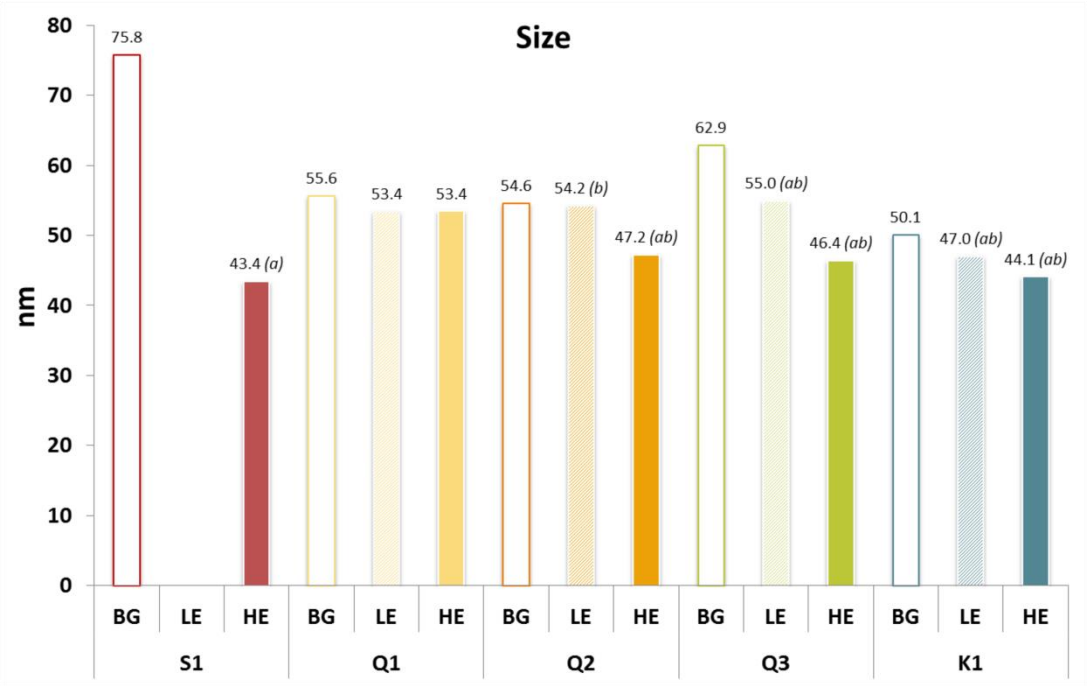

Figure 5. Mean particle diameter, as measured with the NanoScan in the worker area for the background period and during handling under low and high energy settings and for the five study materials. Letters in italics on the top of the bars indicate (a) significant differences between handling conditions (low and high energy settings) with respect to its background mean particle size and (b) significant differences between low and high energy settings mean particle size. The non-parametric Mann-Whitney "U" test was used to test statistically significant differences. Mean particle size differences between materials were not tested.

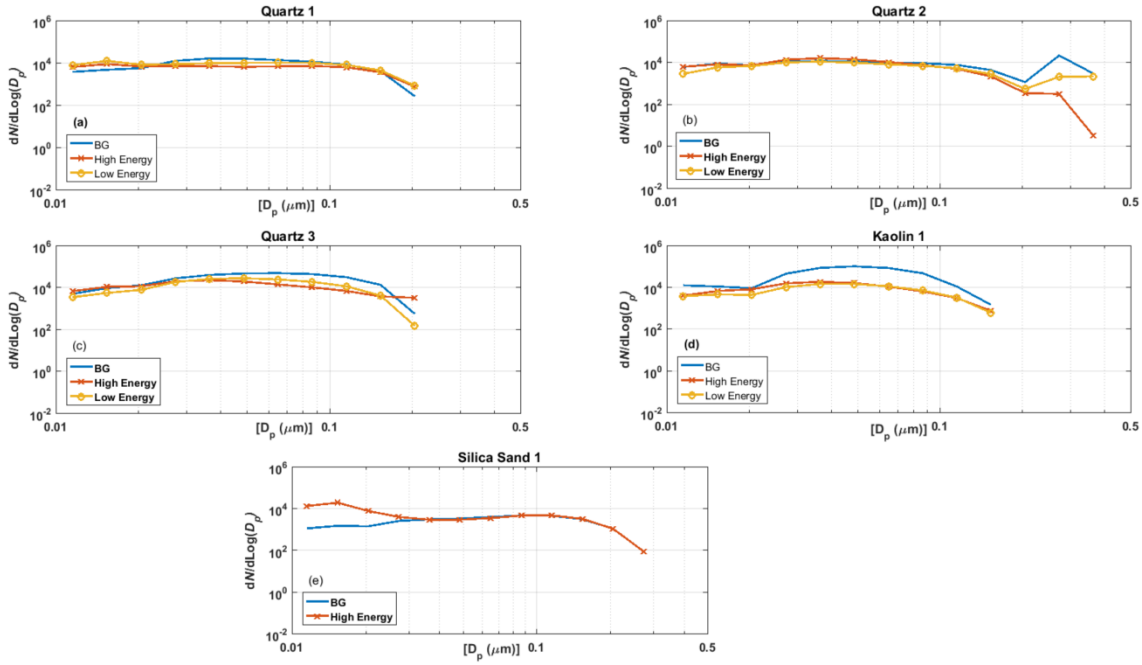

Figure 6. Particle number size distribution in the worker area (monitored with NanoScan) during handling under low and high energy settings, and during background conditions.

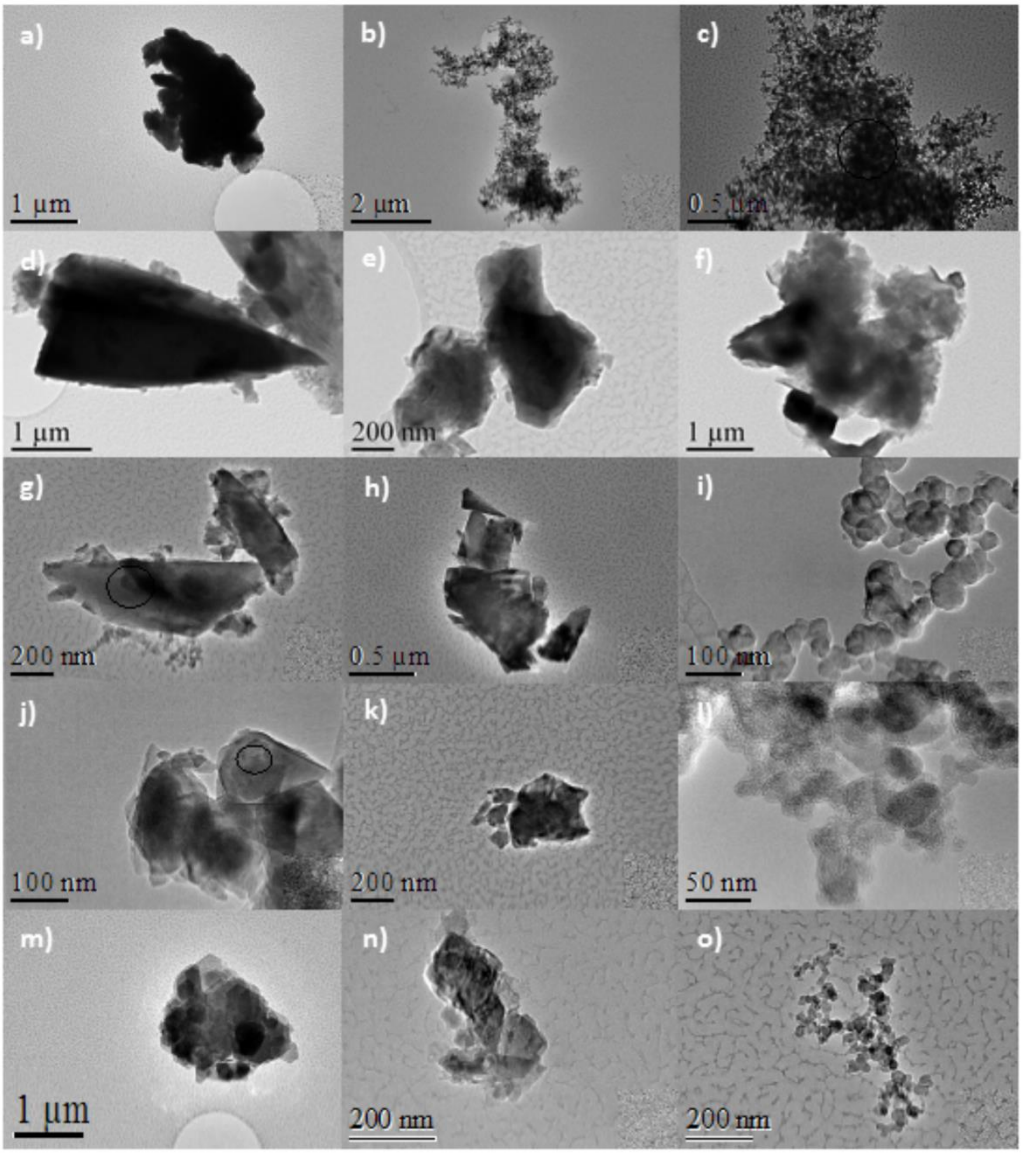

Figure 7. TEM images obtained from the worker area during handling of SI1 (images a, b and c), Q1 (images d, e and f), Q2 (images g, h and i), Q3 (images j, k and l) and K1 (images m, n and o) when using high energy settings. a) main elements Fe, Si, Al; b) agglomerate of C nanoparticles; c) agglomerate of C nanoparticles; d) SiO2 particle; e) agglomerate of SiO2 particles; f) SiO2 with other elements; g) agglomerate of SiO2 particles; h) SiO2 particles with smaller ones surrounding; i) nanoparticles (main elements: K, C and Na); j) aggregates of SiO2 ultrafine particles; k) SiO2 particle (mean diameter 200 nm) with smaller ones surrounding it (mean diameter <100 nm); l) nanoparticles (main elements: C, Na); m) agglomerate of particles (main elements: Si, Al and O) with mean particle diameter < 500 nm; n) agglomerates of particles of different compositions (translucid particles: Si, Fe, O and Ca, darker particles: Ca and O); and o) nanoparticles (main element: C). dominated.

background (pre-activity), and handling (low and high energy conditions). For Q1, Q3 and K1 materials, a slight dominance of finer particles was seen compared to during background, where the size distribution was dominated by coarser particles. Only during S1 a clear increase of particles under 30 nm was observed (probably due to interferences from other processes, as stated above).

Exposure characterization – TEM and EDX analysis

TEM images of the sampled particles during handling were analysed in order to characterise the emitted particles (Figure 7; the EDX analyses are shown in Figure S6, Supporting Information). Particles during handling under high energy

conditions of S1 were mainly formed by Si, Al, and Fe showing a compact structure (Figure 7a and S6a, Supporting information). Aside from this, large nanoparticle aggregates (main element C) were also detected suggesting the contamination by another process (a furnace being switched on or even diesel soot from outdoor air, e.g., Figure 7b, 7c and Figure S6b, Supporting information). This was also the case for materials Q2, Q3 and K1 (Figures 7i, 7l, 7o and Figure S6h S6k and S6n, Supporting information). Particles observed in Q1, Q2 and Q3 samples were mainly SiO_2 particles (0.5 - 2 µm, < 1 µm and 200 nm respectively) (Figures 7d, 7e, 7f, 7g, 7h and 7k, and S6c, S6d, S6e, S6f, S6g and S6j, Supporting information). However, smaller particles (< 100 nm) were also observed in form of aggregates (Figure 7g, 7j, 7k 7n and S6f, S6i, S6j, Supporting information). For K1, aggregates of particles < 500 nm (main elements: Si, Fe, O and Ca) presenting a platy shape were observed (Figure 7m, 7n, S6l and S6m, Supporting information). This analysis supports the conclusion extracted above whereby it was observed that, while micron-scale particles dominated emissions during handling, nano-scaled particles forming aggregates were also emitted and may potentially impact worker exposure.

Comparison between dustiness and exposure concentrations

Materials dustiness index was assessed for Q1, Q2, Q3 and K1 materials after being handled under low and high energy settings (Table 1). In addition, for high energy conditions the material S1 was also included using the continuous drop method. Dustiness concentrations are usually provided in terms of inhalable and/or respirable mass fraction using mg/kg as units. Inhalable dustiness results were then correlated with inhalable mass fraction exposure concentrations during handling (Figure 8) aiming to assess the potential ability of the dustiness index to predict exposure concentrations. Inhalable dustiness indexes obtained ranged between 463 and 10012 mg/kg for the continuous drop method, and 64 and 410 mg/kg for the rotating drum. K1 and Q1 were the materials showing higher dustiness indexes followed by Q2 and Q3, (Table 1, Figure 8). The lowest dustiness value was found for S1. Pensis et al. (2009) reported that dustiness is dependent on material nature as well as d_{50}. Moreover, López-Lilao et al. (2016) concluded, after examining quartz dustiness, that for quartzes with d_{50} < 25 µm an increase of mean particle size corresponds to an increase of dustiness while for quartzes with d_{50} > 25 µm the opposite effect takes place. Taking this into account, the results in Table 1 and Figure 8 seem to agree with those findings, with Q1 having the highest dustiness of the three analysed quartzes. According to the literature, significant correlations may be observed between particle SSA and dustiness when comparing different quartzes (López-Lilao et al., 2016) and different kaolin samples (López-Lilao et al., 2015). Previous works (López Lilao et al., 2017) have shown that, for approximately spherical and dry materials, coarser mean diameters present a higher potential for release of fine particles. Thus, dustiness depends on the amount of fine particles and the material's ability to release such fine particles. However, dustiness does not only depend on particle SSA and establishing a relationship between these parameters is complex (Pensis et al., 2009; Plinke et al., 1995, 1992). In addition, in Evans et al. (2013), where dustiness of different fine and nanoscale powders was analysed, no correlation between SSA and dustiness was found, suggesting that primary particle size, in their specific case, was not the key factor when determining material dustiness. Thus, it is evident that the current literature presents contradicting results. The present study shows that the highest exposure concentrations and dustiness indexes were measured for materials with very different SSA values (e.g., kaolin (K1) and quartz (Q1), 9.6 and 1.4 m^2/g respectively) and different particle shapes (e.g., platy kaolin and prismatic quartz). These results confirm the difficulty to establish a general

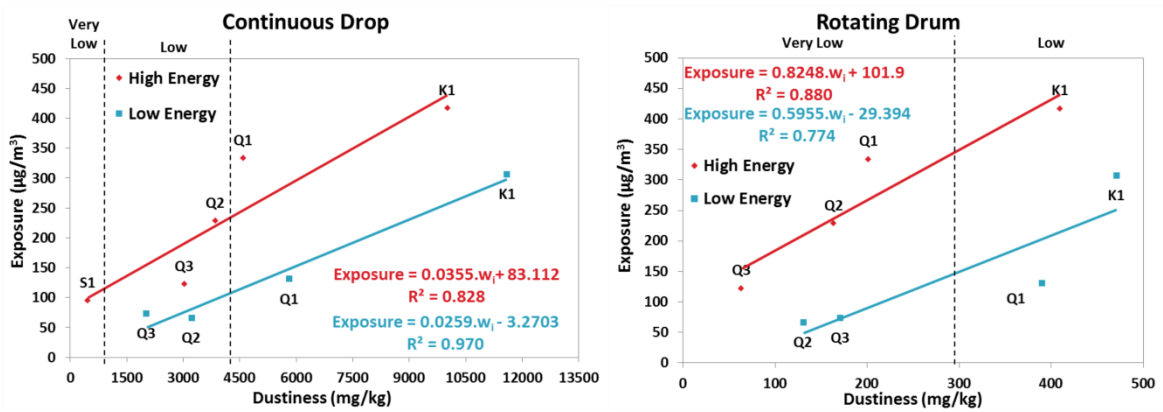

Figure 8. Correlation between exposure concentrations during handling and dustiness (inhalable mass fraction) using Q1, Q2, Q3 and K1. SI1 was only used for high energy settings and with the continuous drop method due to availability issues. a) Continuous drop dustiness test b) Rotating drum dustiness test. Dustiness index classification values according to EN 15051 for each method is shown (dotted bars).

relationship between dustiness and materials physical-chemical characteristics. As shown in Figure 8, R^2 correlation values dustiness – exposure ranged between 0.77 and 0.97 when using the inhalable fraction for both energy settings and dustiness methods. The best correlation was obtained for the continuous drop method with the low energy settings (R^2 = 0.97); contrarily, the worst correlation was obtained for the rotating drum method with low energy settings (R^2 = 0.77). For high energy settings, correlations obtained were R^2 0.83 and 0.88 for continuous drop and rotating drum method, respectively. The results indicate that continuous drop can reproduce slightly better what happened under low energy handling settings and rotating drum can reproduce better the processes taking place under high energy handling settings given that materials suffer a similar process inside the rotating drum than inside the mill. The continuous drop method uses fresh material continuously whereas the rotating drum method does not, and the material in the continuous drop is just falling and being resuspended with air flow while in the rotating drum method the material suffers rotating forces. Thus, it can be expected that both methods provide different results. Pensis et al. (2009) evaluated both EN dustiness methods and studied the correlation between them when using the inhalable and respirable fractions, and found weak correlations between methods for both mass fractions. However, here a strong correlation between methods (continuous drop and rotating drum) was found when considering the inhalable fraction (R^2 = 0.78; data not shown). Results obtained herein regarding dustiness – exposure correlations suggest that dustiness could be considered a predictor of exposure for the materials and particle sizes tested. Other authors have previously reported good exposure – dustiness correlations. Heitbrink et al. (1989) found significant correlations between two dustiness testers and worker exposure during bag packing. Breum et al. (2003) also found good correlation between exposure during installation of cellulosic fibres and rotating drum dustiness results. Contrarily, Class et al. (2001) found limited correlation of exposure during manufacturing of insulation wools and ceramic fibres with the dustiness shaking box test, as well as Brouwer et al. (2006), who found a correlation of 0.70 between rotating drum dustiness values and worker exposure during sweeping/cleaning and scooping/weighing/adding. Finally, some other authors did not find a clear correlation as it the case of Heitbrink et al. (1990) who reported very limited correlation, and only good correlation after some adjustments during bag dumping and filling. Recently, Fonseca et al. (2018) did also not find a clear correlation during laboratory spilling of nano-scaled materials with mini-rotating drum dustiness results. To come to the point, no clear

relationship dustiness – exposure has yet been clearly stablished so that dustiness could be used as a direct predictor of worker exposure. However, dustiness is one of the parameters frequently included in equations for exposure prediction (Levin et al., 2014; Schneider et al., 2011) although prediction modelling for particulate matter is not always as precise as expected (Fonseca et al., 2017; Koivisto et al., 2015). Thus, it is important to continue working on modelling, dustiness test performance as well as to understand which are the key factors to predict worker exposure.

Conclusions

Personal exposure during handling of 5 different powder materials, as well as material dustiness, were assessed and compared in a real-world industrial setting in the ceramic industry. Particles between 4 nm and 32 µm were monitored in terms of number and mass concentration. Results evidence that handling of powder materials had a significant impact on exposure in terms of particle mass, and that this impact was larger under high energy settings: the mean inhalable mass fraction under low energy settings 80.8 - 319.1 µg/m^3, and 156.0 - 429.6 µg/m^3 under high energy settings. Therefore, the modification of the energy settings can be an effective mitigation strategy for this kind of process. On the contrary, emissions in terms of particle number concentrations (mean particle number concentration during handling 15033 – 40498 /cm^3) were not significant (pre-activity concentrations = 10620 – 46421 /cm^3). However, the assessment of the particle diameter plus the analysis of TEM images evidenced the release of nanoparticles to workplace air and that these nanoparticles may have a potential impact on worker exposure. Dustiness indexes were calculated for all the materials assessed with the two standard methods (continuous drop and rotating drum). A high degree of correlation between dustiness and exposure concentrations was found during handling (R^2 = 0.77 -0.97), for inhalable mass fraction and for low (R^2 = 0.77 - 0.97) and high (R^2 = 0.83 - 0.88) energy settings. These results suggest that dustiness may be considered a relevant predictor of workplace exposure for the materials, particle sizes, energy settings and dustiness methods evaluated. Proxy parameters such as dustiness for exposure characterisation may be useful tools to deliver timely and efficient exposure assessments. However, due to this parameter's complexity, the relationship between dustiness and exposure should be assessed for each industrial processes taking into account operational settings as well as materials physical-chemical properties and workplace characteristics.

Acknowledgements

This research was founded by the Spanish MINECO (CGL2015-66777-C2-1-R, 2-R), Generalitat de Catalunya AGAUR 2014 SGR33, the Spanish Ministry of the Environment (13CAES006) and FEDER (European Regional Development Fund) "Una manera de hacer Europa". M.C. Minguillón acknowledges the Ramón y Cajal Fellowship awarded by the Spanish Ministry of Economy, Industry and Competitiveness. The authors also acknowledge the company MOLARIS for their support with technical information on the mill used. The authors declare no conflict of interest relating to the material presented in this Article.

References

Alim, M. A., Biswas, M. K., Biswas, G., Hossain, M. A., & Ahmad, S. A. (2015). Respiratory health problems among the ceramic workers in Dhaka. *Faridpur Medical College Journal*, *9*(1), 19. http://doi.org/10.3329/fmcj.v9i1.23617

Asbach, C., Kuhlbusch, T. A. J., Kaminski, H., Stahlmecke, B., Plitzko, S., Götz, U., … Dahmann, D. (2012). Standard Operation Procedures For assessing exposure to nanomaterials, following a tiered approach.

Breum, N. O., Schneider, T., Jørgensen, O., Rasmussen, T. V., & Skibstrup Eriksen, S. (2003). Cellulosic Building Insulation versus Mineral Wool, Fiberglass or Perlite: Installer's Exposure by

Inhalation of Fibers, Dust, Endotoxin and Fire-retardant Additives. *Ann. Occup. Hyg*, *47*(8), 653–669. http://doi.org/10.1093/annhyg/meg090

British Standards Institute. (2009). Particle size analysis — Laser diffraction methods, BS ISO 13320-1:1999.

Brouwer, D. H., Gijsbers, J. H. J., & Lurvink, M. W. M. (2004). Personal Exposure to Ultrafine Particles in the Workplace: Exploring Sampling Techniques and Strategies. *Annals of Occupational Hygiene*, *48*(5), 439–453. http://doi.org/10.1093/annhyg/meh040

Brouwer, D. H., Links, I. H. M., De Vreede, S. A. F., & Christopher, Y. (2006). Size selective dustiness and exposure; simulated workplace comparisons. *Annals of Occupational Hygiene*, *50*(5), 445–452. http://doi.org/10.1093/annhyg/mel015

Brouwer, D., Van Duuren-Stuurman, B., Berges, M., Jankowska, E., Bard, D., & Mark, D. (2009). From workplace air measurement results toward estimates of exposure–Development of a strategy to assess exposure to manufactured nano-objects. *Journal of Nanoparticle Research*, *11*(8), 1867–1881. http://doi.org/10.1007/s11051-009-9772-1

Brunauer, S., Emmert, P. H., & Teller, E. (1928). Adsorption of gases in multimolecular layers. J. Am. Chem. Soc, 60, 309-319. *Journal of the American Chemical Society*, 309–319.

Brunekreef, B., & Forsberg, B. (2005). Epidemiological evidence of effects of coarse airborne particles on health. *European Respiratory Journal*, *26*(2), 309–318. http://doi.org/10.1183/09031936.05.00001805

Cena, L. G., & Peters, T. M. (2011). Characterization and Control of Airborne Particles Emitted During Production of Epoxy/Carbon Nanotube Nanocomposites. *Journal of Occupational and Environmental Hygiene*, *8*(2), 86–92. http://doi.org/10.1080/15459624.2011.545943

Class, P., Deghilage, P., & Brown, R. C. (2001). Dustiness of different high-temperature insulation wools and refractory ceramic fibres. *Annals of Occupational Hygiene*, *45*(5), 381–4.

Dehghan, F., Mohammadi, S., Sadeghi, Z., & Attarchi, M. (2009). Respiratory Complaints and Spirometric Parameters in Tile and Ceramic Factory Workers. *Tanaffos*, *8*(4), 19–25.

Demou, E., Peter, P., & Hellweg, S. (2008). Exposure to manufactured nanostructured particles in an industrial pilot plant. *Annals of Occupational Hygiene*, *52*(8), 695–706. http://doi.org/10.1093/annhyg/men058

Dubey, P., Ghia, U., & Turkevich, L. A. (2017). Computational fluid dynamics analysis of the Venturi Dustiness Tester. *Powder Technology*, *312*, 310–320. http://doi.org/10.1016/j.powtec.2017.02.030

European Committee for Standardization (CEN). (2013). *Workplace exposure: Measurement of the dustiness of bulk materials; Part1: Requirements and choice of test methods; Part 2: Rotating drum method; Part 3: Continuous drop method (EN 15051). [Stantdard] Brussels, Belgium, 2013.*

Evans, D. E., Turkevich, L. A., Roettgers, C. T., Deye, G. J., & Baron, P. A. (2013). Dustiness of fine and nanoscale powders. *Annals of Occupational Hygiene*, *57*(2), 261–277. http://doi.org/10.1093/annhyg/mes060

Fonseca, A. S., Koivisto, A. J., Koponen, I. K., Jensen, A. C. Ø., Kling, K. I., Levin, M., ... Jensen, K. A. (2017). Goodness of dustiness index for predicting human exposure to airborne nanomaterials. *In New Tools and Approaches for Nanomaterial Safety Assessment - Book of Abstracts [#1552] Malaga, Spain.* Retrieved from http://orbit.dtu.dk/files/128854576/BOOK_OF_ABSTRACTS.pdf

Fonseca, A. S., Kuijpers, E., Kling, K. I., Levin, M., Koivisto, A. J., Nielsen, S. H., … Koponen, I. K. (2018). Particle release and control of worker exposure during laboratory-scale synthesis, handling and simulated spills of manufactured nanomaterials in fume hoods. *Journal of Nanoparticle Research*, *20*(2). http://doi.org/10.1007/s11051-018-4136-3

Fonseca, A. S., Maragkidou, A., Viana, M., Querol, X., Hämeri, K., de Francisco, I., … de la Fuente, G. F. (2016). Process-generated nanoparticles from ceramic tile sintering: Emissions, exposure and environmental release. *Science of The Total Environment*, *565*, 922–932. http://doi.org/10.1016/j.scitotenv.2016.01.106

Fonseca, A. S., Viana, M., Querol, X., Moreno, N., de Francisco, I., Estepa, C., & de la Fuente, G. F. (2015). Ultrafine and nanoparticle formation and emission mechanisms during laser processing of ceramic materials. *Journal of Aerosol Science*, *88*, 48–57. http://doi.org/10.1016/j.jaerosci.2015.05.013

Fransman, W., Van Tongeren, M., Cherrie, J. W., Tischer, M., Schneider, T., Schinkel, J., … Tielemans, E. (2011). Advanced Reach Tool (ART): Development of the Mechanistic Model. *Annals of Occupational Hygiene*, *55*(9), 957–79. http://doi.org/10.1093/annhyg/mer083

Fujitani, Y., Kobayashi, T., Arashidani, K., Kunugita, N., & Suemura, K. (2008). Measurement of the Physical Properties of Aerosols in a Fullerene Factory for Inhalation Exposure Assessment. *Journal of Occupational and Environmental Hygiene*, *5*(6), 380–389. http://doi.org/10.1080/15459620802050053

Gabaldón-Estevan, D., Criado, E., & Monfort, E. (2014). The green factor in European manufacturing: A case study of the Spanish ceramic tile industry. *Journal of Cleaner Production*, *70*, 242–250. http://doi.org/10.1016/j.jclepro.2014.02.018

Hamelmann, F., & Schmidt, E. (2003). Methods of Estimating the Dustiness of Industrial Powders – A Review. *KONA Powder and Particle Journal*, *21*(March), 7–18. http://doi.org/10.14356/kona.2003006

Heitbrink, W. A., Todd, W. F., & Fischbach, T. J. (1989). Correlation of tests for material dustiness with worker exposure from the bagging of powders. *Applied Industrial Hygiene*, *4*(1), 12–16. http://doi.org/10.1080/08828032.1989.10389884

Heitbrink, W. A., Tood, W. F., Cooper, T. C., & O'Brien, D. M. (1990). The Application of Dustiness Tests to the Prediction of Worker Dust Exposure. *American Industrial Hygiene Association Journal*, *51*(4), 217–223. http://doi.org/10.1080/15298669091369565

INSH. (2017). *LEP 2017. Instituto Nacional de Seguridad e Higiene en el Trabajo.* http://doi.org/10.1017/CBO9781107415324.004

Jensen, A. C. Ø., Levin, M., Koivisto, A. J., Kling, K. I., Saber, A. T., & Koponen, I. K. (2015). Exposure assessment of particulate matter from abrasive treatment of carbon and glass fibre-reinforced epoxy-composites – Two case studies. *Aerosol and Air Quality Research*, *15*(5), 1906–1916. http://doi.org/10.4209/aaqr.2015.02.0086

Jennings, B.R., and K. Parslow. (1988). Particle size measurement: the equivalent spherical diameter.. *Proceedings of the Royal Society of London A*, 419. p.137–149

Kaminski, H., Beyer, M., Fissan, H., Asbach, C., & Kuhlbusch, T. A. J. (2015). Measurements of nanoscale TiO2 and Al2O3 in industrial workplace environments – Methodology and results. *Aerosol and Air Quality Research*, *15*(1), 129–141. http://doi.org/10.4209/aaqr.2014.03.0065

Koivisto, A. J., Jensen, A. C. Ø., Levin, M., Kling, K. I., Maso, M. D., Nielsen, S. H., … Koponen, I. K. (2015). Testing the near field/far field model performance for prediction of particulate matter emissions in a paint factory. *Environ. Sci.: Processes Impacts*, *17*(1), 62–73. http://doi.org/10.1039/C4EM00532E

Koponen, I. K., Koivisto, A. J., & Jensen, K. A. (2015). Worker exposure and high time-resolution analyses of process-related submicrometre particle concentrations at mixing stations in two paint factories. *Annals of Occupational Hygiene*, *59*(6), 749–763. http://doi.org/10.1093/annhyg/mev014

Kuhlbusch, T. A., Asbach, C., Fissan, H., Göhler, D., & Stintz, M. (2011). Nanoparticle exposure at nanotechnology workplaces: A review. *Particle and Fibre Toxicology*, *8*(1), 22. http://doi.org/10.1186/1743-8977-8-22

Kuhlbusch, T. A. J., Neumann, S., & Fissan, H. (2004). Number Size Distribution, Mass Concentration, and Particle Composition of PM_{1}, $PM_{2.5}$, and PM_{10} in Bag Filling Areas of Carbon Black Production. *Journal of Occupational and Environmental Hygiene*, *1*(10), 660–671. http://doi.org/10.1080/15459620490502242

Levin, M., Koponen, I. K., & Jensen, K. A. (2014). Exposure Assessment of Four Pharmaceutical Powders Based on Dustiness and Evaluation of Damaged HEPA Filters. *Journal of Occupational and Environmental Hygiene*, *11*(3), 165–177. http://doi.org/10.1080/15459624.2013.848038

Levin, M., Rojas, E., Vanhala, E., Vippola, M., Liguori, B., Kling, K. I., … Jensen, K. A. (2015). Influence of relative humidity and physical load during storage on dustiness of inorganic nanomaterials: implications for testing and risk assessment. *Journal of Nanoparticle Research*, *17*(8), 337. http://doi.org/10.1007/s11051-015-3139-6

Lidén, G. (2006, July). Dustiness testing of materials handled at workplaces. *Annals of Occupational Hygiene*. http://doi.org/10.1093/annhyg/mel042

Llop et al., 2014. (2014). The Ceramic Industry in Spain: Challenges and Opportunities in Times of Crisis. Retrieved from

http://repositori.uji.es/xmlui/handle/10234/123013

López-Lilao, A., Bruzi, M., Sanfélix, V., Gozalbo, A., Mallol, G., & Monfort, E. (2015). Evaluation of the Dustiness of Different Kaolin Samples. *Journal of Occupational and Environmental Hygiene*, *12*(8), 547–554. http://doi.org/10.1080/15459624.2015.1019079

López-Lilao, A., Escrig, A., Orts, M. J., Mallol, G., & Monfort, E. (2016). Quartz dustiness: A key factor in controlling exposure to crystalline silica in the workplace. *Journal of Occupational and Environmental Hygiene*, *13*(11). http://doi.org/10.1080/15459624.2016.1183011

López Lilao, A., Sanfélix Forner, V., Mallol Gasch, G., & Monfort Gimeno, E. (2017). Particle size distribution: A key factor in estimating powder dustiness. *Journal of Occupational and Environmental Hygiene*, *14*(12), 975–985. http://doi.org/10.1080/15459624.2017.1358818

Mallol, G., Amorós, J. L., Orts, M. J., & Llorens, D. (2008). Densification of monomodal quartz particle beds by tapping. *Chemical Engineering Science*, *63*(22), 5447–5456. http://doi.org/10.1016/j.ces.2008.07.032

Markowicz, A. A., & Grieken, R. E. Van. (2001). *Handbook of X-Ray Spectrometry*. Marcel Dekker.

Maynard, A. D., Baron, P. A., Foley, M., Shvedova, A. A., Kisin, E. R., & Castranova, V. (2004). Exposure to Carbon Nanotube Material: Aerosol Release During the Handling of Unrefined Single-Walled Carbon Nanotube Material. *Journal of Toxicology and Environmental Health, Part A*, *67*(1), 87–107. http://doi.org/10.1080/15287390490253688

Monfort, E. (2012). What tole do ceramic tiles play in green procurement and sustainable building? *In: Qualicer 2012 - World Congress on ceramic tile quality* (pp. 1–22). Retrieved from http://www.qualicer.org/recopilatorio/ponencias/pdfs/2012167.pdf

Neghab, M., Zadeh, J. H., & Fakoorziba, M. R. (2009). Respiratory toxicity of raw materials used in ceramic production. *Industrial Health*, *47*(1), 64–9. Retrieved from http://www.ncbi.nlm.nih.gov/pubmed/19218759

Otterstedt, J. E., & D. A., Brandreth. (2013). Small particles technology. *Springer Science & Business Media*.

PD CEN/TR 16013-2:2010 - Workplace exposure. Guide for the use of direct-reading instruments for aerosol monitoring. Evaluation of airborne particle concentrations using optical particle counters. (n.d.).

Pensis, I., Mareels, J., Dahmann, D., & Mark, D. (2009). Comparative Evaluation of the Dustiness of Industrial Minerals According to European Standard EN 15051, 2006. *Annals of Occupational Hygiene*, *54*(2), 204–16. http://doi.org/10.1093/annhyg/mep077

Pérez, N., Pey, J., Querol, X., Alastuey, A., López, J. M., & Viana, M. (2008). Partitioning of major and trace components in PM10-PM2.5-PM1 at an urban site in Southern Europe. *Atmospheric Environment*, *42*(8), 1677–1691. http://doi.org/10.1016/j.atmosenv.2007.11.034

Petavratzi, E., Kingman, S. W., & Lowndes, I. S. (2007). Assessment of the dustiness and the dust liberation mechanisms of limestone quarry operations. *Chemical Engineering and Processing: Process Intensification*, *46*(12), 1412–1423. http://doi.org/10.1016/j.cep.2006.11.005

Plinke, M. A. E., Leith, D., Boundy, M. G., & Löffler, F. (1995). Dust Generation from Handling Powders in Industry. *American Industrial Hygiene Association Journal*, *56*(3), 251–257. http://doi.org/10.1080/15428119591017088

Plinke, M. A. E., Maus, R., & Leith, D. (1992). Experimental examination of factors that affect dust generation by using Heubach and MRI testers. *American Industrial Hygiene Association Journal*, *53*(5), 325–330. http://doi.org/10.1080/15298669291359726

Pope, C. A., & Dockery, D. W. (2006). Health Effects of Fine Particulate Air Pollution: Lines that Connect. *Journal of the Air & Waste Management Association*, *56*(6), 709–742. http://doi.org/10.1080/10473289.2006.10464485

Schneider, T., Brouwer, D. H., Koponen, I. K., Jensen, K. A., Fransman, W., Van Duuren-Stuurman, B., … Tielemans, E. (2011). Conceptual model for assessment of inhalation exposure to manufactured nanoparticles. *Journal of Exposure Science and Environmental Epidemiology*, *21*(5), 450–463. http://doi.org/10.1038/jes.2011.4

Schneider, T., & Jensen, K. A. (2007). Combined Single-Drop and Rotating Drum Dustiness Test of Fine to Nanosize Powders Using a Small Drum. *Annals of Occupational Hygiene*, *52*(1), 23–34. http://doi.org/10.1093/annhyg/mem059

Tsai, S.-J., Ashter, A., Ada, E., Mead, J. L., Barry, C. F., & Ellenbecker, M. J. (2008). Airborne Nanoparticle Release Associated with the Compounding of Nanocomposites using Nanoalumina as Fillers. *Aerosol and Air Quality Research*, *x*(x).

Upton, S., Hall, D., & Marsland, G. (1990). Some experiments on material dustiness. *Aeorosol Society Annual Conference, University of.* Retrieved from https://scholar.google.com/scholar_lookup?publication_year=1990&pages=325-330&issue=5&author=S.L.+Uptonauthor=D.J.+Hallauthor=G.W.+Marsland&title=Some+experiments+on+material+dustiness

Van Broekhuizen, P., Van Veelen, W., Streekstra, W. H., Schulte, P., & Reijnders, L. (2012). Exposure limits for nanoparticles: Report of an international workshop on nano reference values. *Annals of Occupational Hygiene* (Vol. 56, pp. 515–524). Edinburgh Napier University,. http://doi.org/10.1093/annhyg/mes043

Viana, M., Fonseca, A. S., Querol, X., López-Lilao, A., Carpio, P., Salmatonidis, A., & Monfort, E. (2017). Workplace exposure and release of ultrafine particles during atmospheric plasma spraying in the ceramic industry. *Science of The Total Environment*, *599*, 2065–2073. http://doi.org/10.1016/j.scitotenv.2017.05.132

Viitanen, A. K., Uuksulainen, S., Koivisto, A. J., Hämeri, K., & Kauppinen, T. (2017). Workplace measurements of ultrafine particles-A literature review. *Annals of Work Exposures and Health*. http://doi.org/10.1093/annweh/wxx049

Voliotis, A., Bezantakos, S., Giamarelou, M., Valenti, M., Kumar, P., & Biskos, G. (2014). Nanoparticle emissions from traditional pottery manufacturing. *Environmental Science: Processes & Impacts*, *16*(6), 1489. http://doi.org/10.1039/c3em00709j

Williams, D. B., & Carter, C. B. (2009). The Transmission Electron Microscope. In *Transmission Electron Microscopy* (pp. 3–22). Boston, MA: Springer US. http://doi.org/10.1007/978-0-387-76501-3_1

Yeganeh, B., Kull, C. M., Hull, M. S., & Marr, L. C. (2008). Characterization of airborne particles during production of carbonaceous nanomaterials. *Environmental Science and Technology*, *42*(12), 4600–4606. http://doi.org/10.1021/es703043c

4.1.1. Additional Results Publication I: On the relationship between exposure to particles and dustiness during handling of powders in industrial settings

After publication, the work presented in Publication I was completed by adding data for two types of clays, with plate-like primary particle shape. This was carried out because, of the materials studied in Publication I, the one presenting highest inhalable and respirable exposure mass concentration during handling was the Kaolin, with plate-like primary particles. Thus, two plate-like clays (white (C1) and red (C2) clay), with similar particle diameter as the other materials, were added to the study at a later stage (Figure 4.2). The two clays were subjected to the same process as the rest of the materials.

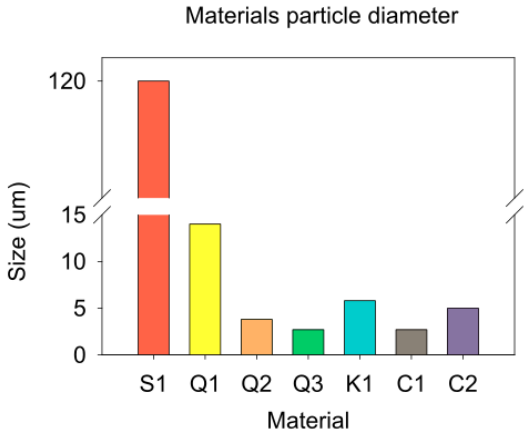

Figure 4.2 Particle size for all materials

Particle mass concentrations during handling (under low and high energy settings) of C1 material ranged between 727 and 1061 µg m^{-3}, for the inhalable fraction, and 161 and 240 µg m^{-3} for the respirable one, with increases between 51 and 86 times the background concentration (Figure 4.3). For C2, monitored particle mass concentrations during material handling at low and high energy settings ranged between 1059-1319 µg m^{-3} and 280-300 µg m^{-3}, with increases 17-27 and 16-19 times the background concentration for the inhalable and respirable fractions, respectively (Figure 4.3). From all 7 studied materials the three presenting higher mass concentration exposure were the three plate-like shaped, even though primary particle size was similar to the rest of materials. Therefore, it seems that exposure could be related to primary particle shape. Further research is necessary to understand this pattern and confirm this hypothesis.

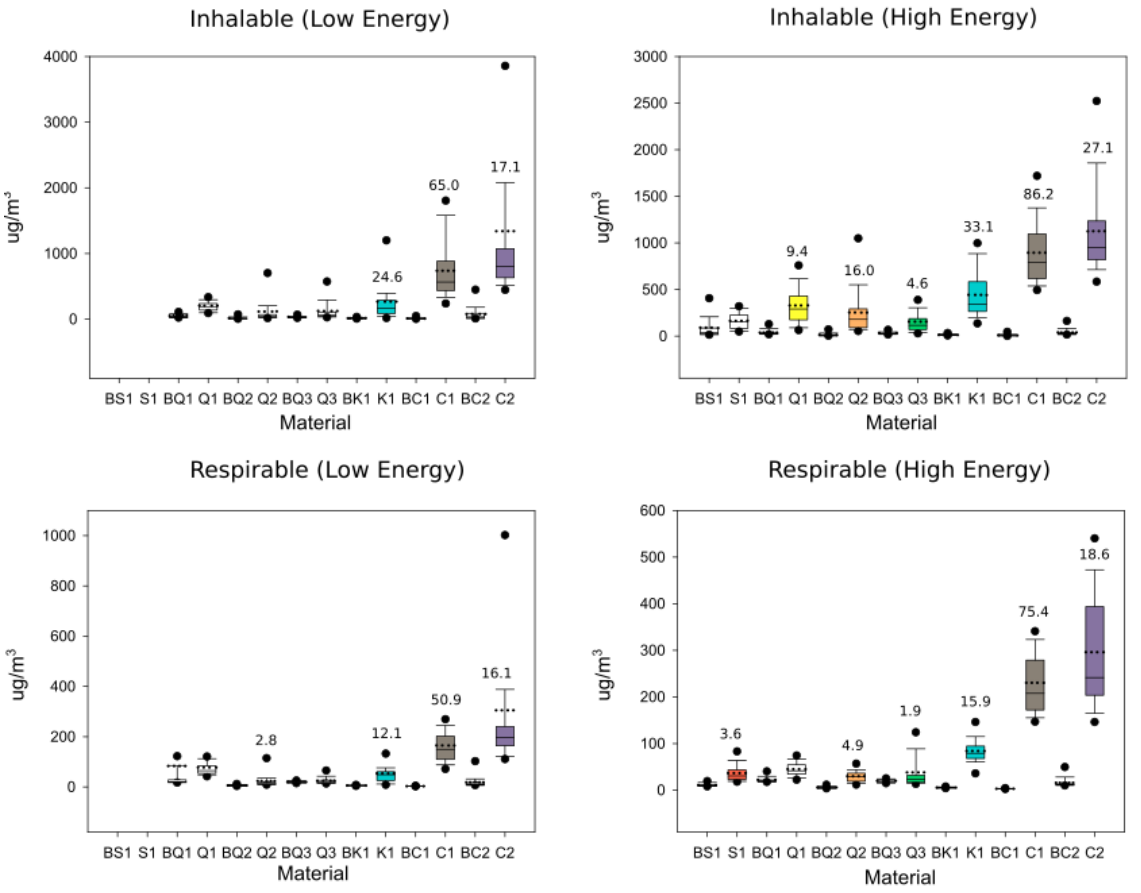

Figure 4.3 Figure 3 from Publication I where the two clays are included.

The exposure results from the two clays were also added and used for dustiness-exposure correlations (Figure 4.4). When including C1 and C2 to the high energy settings correlation, exposure correlation with dustiness was 0.97 and 0.99 for the C.D and the R.D methods, respectively. Conversely, for the low energy correlation, exposure-dustiness correlation with the C.D and R.D methods was 0.83 and 0.80, respectively. In these new correlations, especially for the low energy settings, the two clays appear as outliers. These results agree with those found by Evans *et al.* (2017), where dustiness of several materials was assessed by using the R.D and the Venturi methods, and the two nano-clay materials were seen as clear outliers. Also in Evans *et al.* (2017), a certain correlation between the two dustiness methods used was found. In this work, good correlation between methods was also found (R^2 = 0.78) (Figure 4.5).

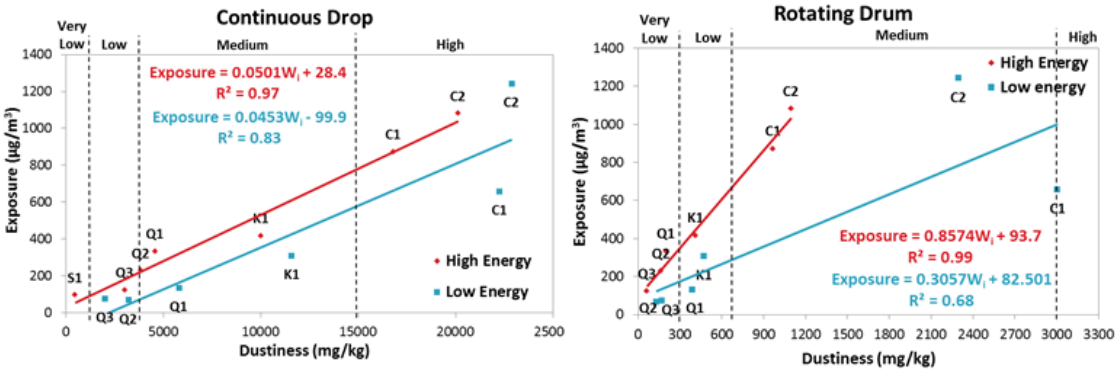

Figure 4.4 Figure 8 from Publication I where the two clays are included.

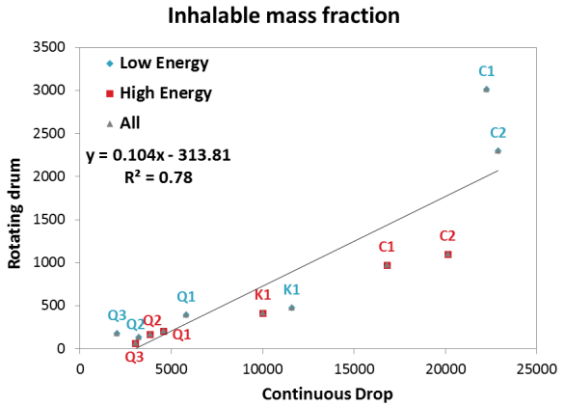

Figure 4.5 Correlation between R.D and C.D dustiness indexes. R.D: rotating drum. C.D: continuous drop.

4.2. Publication II: Health risk assessment from exposure to particles during packing in working environments

Authors:

Ribalta C[1,2*]., López-Lilao A[3]., Estupiñá S[3]., Fonseca A.S[4]., Tobías A[1]., García-Cobos A[3]., Minguillón M.C[1]., Monfort. E[3]., Viana M[1].

[1]Institute of Environmental Assessment and Water Research (IDÆA-CSIC), C/ Jordi Girona 18, 08034 Barcelona, Spain.

[2]Barcelona University, Chemistry Faculty, C/ de Martí i Franquès, 1-11, 08028 Barcelona, Spain

[3]Institute of Ceramic Technology (ITC)- AICE - Universitat Jaume I, Campus Universitario Riu Sec, Av. Vicent Sos Baynat s/n, 12006 Castellón, Spain.

[4]National Research Centre for the Working Environment (NRCWE), Lersø Parkallé 105, Copenhagen DK-2100, Denmark

Published in:

Science of the Total Environment, 671: 474-487, 2019

doi: 10.1016/j.scitotenv.2019.03.347

Please cite this article as: Ribalta, C., López-Lilao, A., Estupiñá, S., Fonseca, A.S., Tobías, A., García-Cobos, A., Minguillón, M.C., Monfort, E., and Viana, M., 2019. Health risk assessment from exposure to particles during packing in working environments. *Science of The Total Environment*, 671, 474–487.

Accepted date: 22 March 2019

Journal Impact Factor / 5-Year Impact Factor: 4.610 / 4.984

Science of the Total Environment 671 (2019) 474–487

Contents lists available at ScienceDirect

Science of the Total Environment

journal homepage: www.elsevier.com/locate/scitotenv

Health risk assessment from exposure to particles during packing in working environments

C. Ribalta [a,b,*], A. López-Lilao [c], S. Estupiñá [c], A.S. Fonseca [d], A. Tobías [a], A. García-Cobos [c], M.C. Minguillón [a], E. Monfort [c], M. Viana [a]

[a] Institute of Environmental Assessment and Water Research (IDÆA-CSIC), C/ Jordi Girona 18, 08034 Barcelona, Spain
[b] Barcelona University, Chemistry Faculty, C/ de Martí i Franquès, 1-11, 08028 Barcelona, Spain
[c] Institute of Ceramic Technology (ITC)- AICE - Universitat Jaume I, Campus Universitario Riu Sec, Av. Vicent Sos Baynat s/n, 12006 Castellón, Spain
[d] National Research Centre for the Working Environment (NRCWE), Lersø Parkallé 105, Copenhagen DK-2100, Denmark

HIGHLIGHTS

- Worker exposure to particles during packing of 7 ceramic materials was assessed.
- ICRP modelling revealed that particle deposition occurred mainly in the head airways.
- Risk assessment models generally overestimated measured exposure concentrations.
- Source enclosure effectively reduced exposure and health risk.
- Dustiness correlated with exposure when emissions were driven by material properties.

GRAPHICAL ABSTRACT

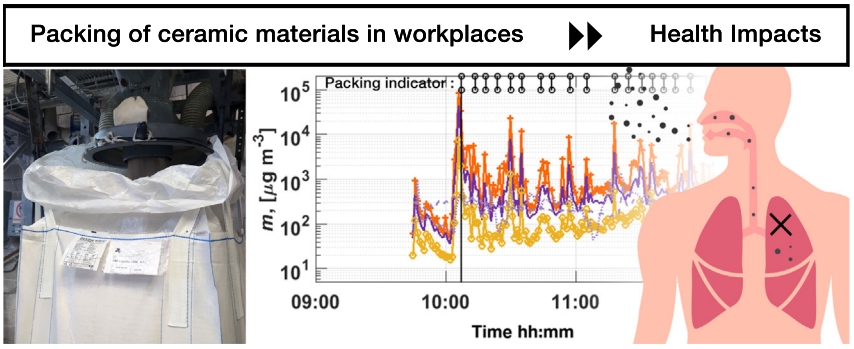

ARTICLE INFO

Article history:
Received 14 January 2019
Received in revised form 22 February 2019
Accepted 22 March 2019
Available online 26 March 2019

Editor: Pavlos Kassomenos

Keywords:
Exposure
Non-communicable disease
Workplace
Human health impacts
Modelling
Ventilation

ABSTRACT

Packing of raw materials in work environments is a known source of potential health impacts (respiratory, cardiovascular) due to exposure to airborne particles. This activity was selected to test different exposure and risk assessment tools, aiming to understand the effectiveness of source enclosure as a strategy to mitigate particle release. Worker exposure to particle mass and number concentrations was monitored during packing of 7 ceramic materials in 3 packing lines in different settings, with low (L), medium (M) and high (H) degrees of source enclosure. Results showed that packing lines L and M significantly increased exposure concentrations (119–609 μg m^{-3} respirable, 1150–4705 μg m^{-3} inhalable, 24,755–51,645 cm^{-3} particle number), while non-significant increases were detected in line H. These results evidence the effectiveness of source enclosure as a mitigation strategy, in the case of packing of ceramic materials. Total deposited particle surface area during packing ranged between 5.4 and 11.8 × 10^5 μm^2 min^{-1}, with particles depositing mainly in the alveoli (51–64%) followed by head airways (27–41%) and trachea bronchi (7–10%). The comparison between the results from different risk assessment tools (Stoffenmanager, ART, NanoSafer) and the actual measured exposure concentrations evidenced that all of the tools overestimated exposure concentrations, by factors of 1.5–8. Further research is necessary to bridge the current gap between measured and modelled health risk assessments.

* Corresponding author at: Institute of Environmental Assessment and Water Research (IDÆA-CSIC), C/ Jordi Girona 18, 08034 Barcelona, Spain.
E-mail address: carla.ribalta@idaea.csic.es (C. Ribalta).

https://doi.org/10.1016/j.scitotenv.2019.03.347
0048-9697/

1. Introduction

Exposure to particulate matter (PM) is known to cause adverse health effects such as respiratory and cardiovascular non-communicable diseases (Landrigan et al., 2017). The finest fractions (with aerodynamic particle diameter Dp ≤ 2.5 μm) are considered the most harmful for human health (Gakidou et al., 2017; Landrigan et al., 2017; World Health Organization, 2016). In workplace settings, ceramic industry workers are known to suffer from work-related asthma due to airborne dust inhalation (Kurt et al., 2018). Elements such as Cr, Cd or Pb were detected in ceramic workers blood and urine samples in higher amounts than in control workers, causing a diminution of lung function and oxidative stress (Hormozi et al., 2018; Shouroki et al., 2015). Workers in the ceramic sector can also be exposed to respirable crystalline silica (RCS) dust which was found to cause silicosis and oxidative damage in workers (Anlar et al., 2017; Nardi et al., 2018). Moreover, RCS has been recently classified as carcinogenic for humans (Directive 2017/2398/EC). Reducing worker exposure to RCS is paramount and efforts are being carried out to reduce not only exposure but also toxicity (e.g., by using organosilane coatings; Ziemann et al. (2017).

Industrial bag filling, packing and pouring processes are high exposure risk activities in the ceramic sector. Studies in different industrial sectors report from very low to high levels of worker exposure to particles, e.g., during pouring and packing of fertilizers, paint pigments, TiO_2, carbon black, fullerenes and carbon nanofibers (Ding et al., 2017; Evans et al., 2013, 2010; Fujitani et al., 2008; Koivisto et al., 2012a, 2012b; Koivisto et al., 2015; Koponen et al., 2015; Kuhlbusch et al., 2004; Ribalta et al., 2019a, 2019b), as well as packing and pouring of cement materials (Notø et al., 2018; Peters et al., 2008). The literature is increasing and emissions are known to be influenced by numerous parameters including powder properties, amount of material handled, type of processes, localized controls and number of repetitions (Fransman et al., 2011; Koponen et al., 2015; Van Tongeren et al., 2011). However, additional studies are still necessary. Specifically, studies providing real–world experimental data on dust emissions from different packing lines and materials are especially valuable to quantitatively assess the relevance of process parameters, as well as to generate input data which may be subsequently used in workplace air modelling approaches. An example of this kind of work may be found in Koponen et al. (2015), where particle release was studied during pouring of different materials and amounts, and using different types of mixing tanks.

In this context, packing of 7 widely used raw materials in the ceramic industry with potential impacts on human health was studied in 3 industrial packing lines equipped with different mitigation measures. A discussion on different methods available to determine the statistical significance of particle emissions is presented (Asbach et al., 2012 and Kaminski et al., 2015; ARIMA time series approach in Klein Entink et al. (2011); and more conventional statistical tests, e.g., *t*-test, Mann-Whitney "U" test, ANOVA, Fonseca et al., 2018), assessing their applicability to high-variability, coarse particle emission scenarios. Finally, monitored concentrations are compared to results from 3 of the most widely used screening tools for risk assessment (Stoffenmanager, ART and NanoSafer v1.1). Stoffenmanager and ART, are tools recommended by the ECHA (ECHA, 2016) for tier 1–2 risk assessment of chemical hazards (Fransman et al., 2011; Tielemans et al., 2008a).

This work aims to (1) monitor real-world occupational exposure concentrations to particles during packing of different materials in a ceramic industry plant; (2) report inhalation doses in terms of particle number, mass and surface area to link exposure to health outcomes; (3) explore the applicability of different methods to determine the statistical significance of coarse particle emissions, and (4) contribute to reducing the gap between measured and modelled exposure concentrations, with the aim to improve the performance of human risk assessment models in real world scenarios.

2. Methodology

2.1. Work environment

The measurements were carried out during packing of 7 ceramic materials (2 clays, 2 feldspars, 2 kaolin and 1 quartz) in 3 different packing lines, between the 14th and 28th of February 2018 at 2 industrial settings, named as #1 and #2 (for confidentiality reasons) and located in the vicinity of Valencia, Spain (Fig. 1). All materials are highly used in the ceramic industry, and thus representative of this sector. The 3 packing lines are representative of 3 different levels of source containment, with low, medium and high mitigation strategies and referred to as L, M and H respectively.

- Industrial plant #1 (Fig. 1(a)): Packing lines L and M were located in plant #1 which has a total volume (total surface area x height) of 2100 m^3 (Fig. 1). Packing of big bags (1200 kg) was carried out through a cylindrical opening at a 400–800 kg min^{-1} flow depending on the material being packed. Packing line L was not enclosed and had no closing system to attach the bag to the feed funnel whereas packing line M was not enclosed but had a partially closing system to attach the bag to the feed funnel preventing release of airborne dust; (Supplemental Fig. S1(a) and (b)). Both packing lines were equipped with a local exhaust ventilation system (LEV), with a flow rate of 18,000 m^3 h^{-1} (value provided by the company), and a subsequent bag filter. Additionally, plant #1 was naturally ventilated with air coming from outdoors via doors (flow rate 187–725 m^3 h^{-1}, experimentally measured) which were always open. Experimentally determined total air exchange per hour (ACH) was 9 h^{-1}. Packing lines L and M were not operated at the same time.
- Industrial plant #2 (Fig. 1(b)): with a total volume (total surface area × height) of 420 m^3 (Fig. 1), it contained packing line H where packing of small bags (20–25 kg) was carried out through a lateral cylindrical opening at 75 kg min^{-1} flow. The packing line was not enclosed but the bag was completely attached to the feed funnel during the bag filling process (Supplemental Fig. S1(d)), and was equipped with a LEV system (flow rate of 2400 m^3 h^{-1}, value provided by the company) and a subsequent bag filter, meaning that particle emissions were much more mitigated than in lines L and M in industrial plant #1. In addition, the plant #2 was naturally ventilated through a pair of doors (flow rate 386–437 m^3 h^{-1}, experimentally measured) with a total experimentally determined ACH of 7 h^{-1}.

During packing, worker's tasks were to (1) manually place a pallet and an empty bag in the packing area (Supplemental Fig. S1(a) and (b)); (2) control and guarantee the correct functioning of the line during the packing process, with the worker standing at approximately 2 m from the emission source, and (3) manually close the bag except in packing line H (Supplemental Fig. S1(c)). Diesel-powered forklifts were used to move the filled bags to the storage area; this task was usually carried out by another worker.

A summary of the packing lines operated each day, the materials used and the number of repetitions monitored, is described in Table 1.

2.2. Materials

Clay 1 and clay 2 consist of >90% of clay (CAS: 999999–99-4). The main components of Feldspar 1 and 2 (> 90%) is feldspar (CAS: 68476–25-5) with a RCS content between 1 and 10%, determined using the SWeRF method. The main component of Quartz 1 is quartz >95% (CAS: 014808–60-7). Kaolin 1 and 2 are composed by >90% kaolinite (CAS: 1332-58-7) and < 1% quartz. The true and bulk density of all materials is between 2.5 and 2.6 and 0.9–1.5 g cm^{-3}, respectively. Materials characteristics and chemical composition are shown in Table 1 and Supplemental Table S1.

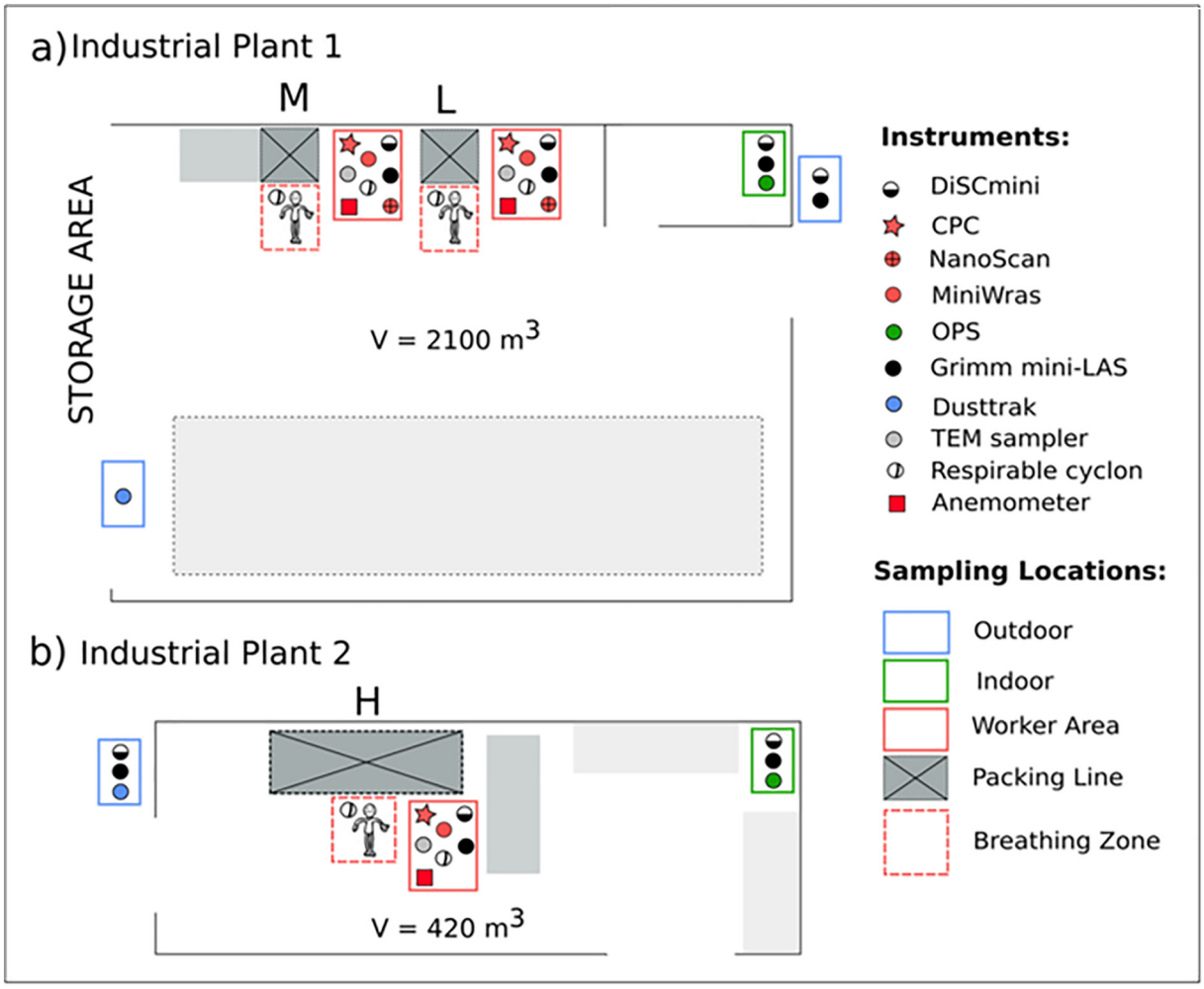

Fig. 1. Industrial setting 1(a) and 2 (b) layouts. NanoScan was only used during Clay 1 packing due to technical problems.

2.3. Dustiness

Material dustiness was assessed by using the continuous drop (C.D) standard method (EN 15051) (CEN, 2013) (Supplemental Fig. S2).

The C.D device, made of stainless steel, consists of a cylindrical pipe through which air circulates in an upward direction with a volume flow rate of 53 l min^{-1} (López-Lilao et al., 2015). Sampling heads for inhalable (designed by Institut für Gefahrstoff-Forschung-IGF) and respirable (FSP-2, BGIA) fractions are located slightly above the discharge position of the material. Samples for gravimetric measurements of inhalable and respirable fractions were collected on cellulose thimbles, single thickness, 10 × 50 mm and PVC filters of 37 mm and 5 μm of porosity respectively.

The experiments were repeated 2 times to ensure results repeatability and total duration of each test was 10 min.

2.4. Real time measurements

Particle number and mass concentrations were monitored in real time by using mobility and optical particle sizers, aerosol photometers, diffusion chargers and a condensation particle counter (Table 2). Air flows in the plant (WA) were experimentally measured with a Weather Transmitter WXT536, WXT530 Series, Vaisala, Helsinki, Finland. The uncertainties of the portable instruments are reported in Viana et al. (2015). Calibration of the Grimm laser spectrometers (Mini-LAS and Mini-WRAS) followed the procedures recommended by the manufacturer and were also

Table 1
Description of daily activity and material characteristics. S.D.: standard deviation. DL: detection limit. RCS: respirable crystalline silica. C.D: continuous drop method. W_I: Inhalable fraction. W_R: Respirable fraction. * indicates respirable cyclone minutes of measurement.

Material	Activity description					Material characteristics		
	Industrial plant	Packing Line	Batch Rep.	Day (02/2018)	Process time (min)	C.D (mg kg^{-1}) $W_I \pm$ S.D./ $W_R \pm$ S.D	d_{50} (μm)	Moisture (%)
Clay 1	#1	L	3	14th	174	1733 ± 880/6 ± 1	13	11
Feldspar 1	#1	M	3	20th	342 (243*)	10,246 ± 253/59 ± 2	31–39	0.2
Quartz 1	#1	M	2	21th	264	8891 ± 1002/43 ± 17	30–38	0.1
Clay 2	#1	L	2	22th	287	5,170,918±/16 ± 1	10	13
Kaolin 1	#1	L	2	23th	162	18,886 ± 174/44 ± 5	13	11
Feldspar 2	#2	H	2	26th	350	9651 ± 235/77 ± 0	22	0.3
Kaolin 2	#2	H	2	28th	309	12,325 ± 235/104 ± 1	8	0.7

calibrated with regard to gravimetric reference samples collecting ambient aerosols. It should be noted that this kind of calibration was therefore not carried out with the same aerosol as monitored in the present work, which would be the advisable procedure for any workplace exposure assessment (PD CEN/TR 16013-2:2010). Monitoring was conducted in the worker area (WA), indoors, and outdoors (Fig. 1). The instruments were placed on a portable table at approximately 1 m height (instrument inlets being at 1.5 m above the ground level and at 1.5–2 m from the emission source), and were used without connecting any tubing to the inlets Thus, measurements were considered representative of exposure but not strictly breathing zone (Asbach et al., 2012). All instruments were synchronized prior to the measurements and intercompared (Supplemental Table S2).

In the industrial plant #1, particle concentrations were measured for 2/3 batch repetitions of 20 bags each (each batch was between 1 and 2 h). Conversely, in the industrial plant #2, concentrations were measured for 4 to 5 h of continuous activity (packing). Total packing for all materials lasted between 3 and 5 h (162–350 min) (Table 1). Additionally, 20–30 min of pre-activity concentrations was measured for each day. During the lunch break, which was between 12:00–15:00 h, packing was not ongoing.

2.5. Particle collection and analysis

Particles emitted during packing were collected in the WA onto Au grids (Quantifolil ® with 1 μm diameter holes – 4 μm separation of 200 mesh). The grids were attached to polycarbonate filters placed in a sampling cassette (SKC INC., USA, 1/8 in. inlet diameter and 25 mm filter Ø). The cassette was connected to a Leland pump with an operating flow rate of 3 l min^{-1}. The morphology and primary particle size of the particles collected were determined using a field emission scanning electron microscope (FESEM) FEI CUANTA 200F.

Respirable mass concentration was gravimetrically determined in the WA by pre- and post- weighing by using a CIP 10 (Arelco ARC) sampler with a flow rate of 10 l min^{-1} and air filtration by a rotating porous foam filter (Görner et al., 2010; Görner et al., 2009). Respirable mass fraction in the worker breathing zone (BZ) was determined by pre- and post- weighing using a Dorr-Oliver Nylon Cyclone Assembly with a Mixed Cellulose Ester Membranes, 0.80 μm pore size, 25 mm Ø (EDM Millipore™ MF-Millipore™) connected to a pump (Apex, Casella) operating at a 1.7 l min^{-1} flow (Supplemental Fig. S1(c)). BZ filters were baked in an oven, re-suspended in ultrapure water and tragacanth, and redeposited onto PVC filters (25 mm Ø) following the national occupational health and safety institute's (INSHT) method based on membrane filter/ X-ray diffraction (MTA/MA -056/A06). Filters were left for at least 2 h in a dryer prior to quantification. Exposure to RCS was quantified by the X-ray diffraction technique, using a BRUKER theta-theta model D8 Advance diffractometer with copper radiation (Kα λ = 1.54183 Å) and VÅntec solid-state detector. Data were recorded from 2θ of 26° to 28°, with a step size of 0.07° and acquisition time of 3 s. Certified reference materials were used for quantification and validation (BCR-66, SRM 1878a y SRM 2950-2957).

2.6. Data processing

8-Hour time weighted average (8 h TWA) WA concentrations for online mass measurements were calculated as follows:

$$TWA = \frac{t_1C_1 + t_2C_2 + \ldots + t_nC_n}{t_1 + t_2 + \ldots + t_n} \quad (1)$$

where C_n is the mean concentration during a specific operation and t_n is the time of the specific operation, and compared to 8 h TWA limit values for unspecified dusts (respirable mass concentration, 3000 μg m^{-3} and inhalable mass concentration, 10,000 μg m^{-}) and RCS (50 μg m^{-3}) (INSH, 2018). Note that sampling periods were different for each material thus; temporal background concentrations were used to complete the 8 h TWA. 8 h TWA RCS was calculated by applying the content of RCS in percentage obtained with the gravimetrical analysis, to calculated 8 h TWA respirable mass concentration.

Table 2
Description, settings and location of the instrumentation used. * NanoScan was only use during Clay 1 monitoring due to technical problems. PSD: particle size distribution.

Instrument	Location	Manufacturer	Sample flow rate (l min^{-1})	Information	Particle size range	Concentration range	Time resolution
Butanol Condensation Particle Counter (CPC TSI Model 3775)	Worker Area	TSI Inc., Shoreview, MN, USA	1.5	Particle number concentration	4-1500 nm	0–10^7 cm^{-3}	6-s
Mini Wide Range Aerosol Spectrometer (Mini-WRAS 1371)	Worker Area (For Clay 1 in Indoor)	Grimm Aerosol Technik, Ainring, Germany	1.2	Particle mass and number concentration and PSD	10 nm-35 μm	0.1–10^4 μg m^{-3} 3×10^3-5×10^5 cm^{-3} (electrical) 0-3×10^6 l^{-1} (optical)	1-min
Miniature diffusion size classifier (DiSCmini Matter Aerosol AG)	Worker Area, Indoor and Outdoor	Testo, Wohlen, Switzerland	1	Particle number concentration, mean particle size and alveolar lung deposited surface area	10-700 nm	10^3–10^6 cm^{-3}	1-s
Mini Laser Aerosol Spectrometer (Grimm Mini-LAS)	Worker Area, Indoor and Outdoor	Grimm Aerosol Technik, Ainring, Germany	1.2	Particle mass concentration	0.25-32 μm	0.1–10^4 μg m^{-3}	6-s
Optical Particle Sizer (OPS, TSI Model 3330)	Indoor	TSI Inc., Shoreview, MN, USA	1	PSD	0.3–10 μm (16 channels)	0- 3×10^3 cm^{-3}	1-min
*Electrical Mobility spectrometer (NanoScan SMPS TSI Model 3910)	Worker Area (Only for Clay 1)	TSI Inc., Shoreview, MN, USA	0.7	Particle number concentration and PSD	10-420 nm (13 channels)	0–10^5 cm^{-3}	1-min
Light scattering laser photometer (DustTrak™ DRX aerosol monitor TSI Model 8533)	Outdoor	TSI Inc., Shoreview, MN, USA	3	Particle mass concentration	PM_{10}, PM_4, $PM_{2.5}$ and PM_1	0.001–150 mg m^{-3}	1-min

Conversely to particle number concentration for which a specific approach has been designed (Asbach et al., 2012), for particle mass there is no specific method to determine statistically significant increases other than conventional statistical tests. Therefore, the need was identified to test the performance of different methods which could be useful to establish guidelines in occupational exposure assessment studies. Here, 3 methods to determine statistically significant increases in exposure during packing, compared to pre-activity periods, were tested:

1) The approach described by Asbach et al. (2012) and Kaminski et al. (2015) for particle number, from now on referred to as nanoGEM approach:

$$\text{Mean concentration during packing} > BG \pm 3 * (\sigma BG) \quad (2)$$

where BG is the mean temporal background (pre-activity) concentration and σBG is the standard deviation of the background concentration.

2) Conventional statistical methods; two-sample *t*-test and Mann-Whitney "U" test, parametric and non-parametric tests for independent samples.

Log-normality and variance homogeneity were assessed by using the Kolmogorov-Smirnov and Levene's (absolute) test respectively, and by histogram plotting. In general, data did not fully fulfil normality assumptions. However, for datasets >30–40 samples, the violation of normality assumptions should not be a major problem (Ghasemi and Zahediasl, 2012; Pallant, 2007). Therefore, in order to determine statistically significant differences between measured concentrations during background and packing the two-sample *t*-test (from now on referred to as t-test) was performed (unequal variances) as well as the non-parametric Mann-Whitney "U" Test (Wilcoxon rank-sum test) (from now on referred to as MW "U" test), both for independent samples and typically used as in e.g. (Fonseca et al., 2018; Ribalta et al., 2019b).

3) Autoregressive Integrated Moving Average (ARIMA) time series approach. ARIMA models are used for nanoparticle exposure assessment in Klein Entink et al. (2011) and proposed in the EN 17058:, 2018 (standard for workplace exposure- assessment of exposure by inhalation of nano-objects and their aggregates and agglomerates) as the golden standard method for number concentration and other metrics analyses. The ARIMA models are the most general type of models used for analyzing time series while considering the autocorrelation between samples. Examples of the ARIMA analysis performed are shown in Annex A (Supplemental Material).

2.7. Particle inhalation dose

The inhalation dose of deposited particles in the respiratory tract during inspiration and expiration was quantified in terms of particle number concentration, particle active surface area and mass. Particle active surface area was calculated for particles up to 750 nm (cut-off diameter at 679 nm) by using particle size distribution (PSD) (Heitbrink et al., 2009; Keller et al., 2001) as in Koivisto et al. (2012a). Particle mass was calculated by using mobility particle diameter and effective density as in Koivisto et al. (2012a). Particle density during packing was assumed to be 2.55 g cm^{-3} as it is the materials' mean density (López Lilao et al., 2017) described by the provider, and 1.5 g cm^{-3} during background (Martins et al., 2015). The regional inhalation dose rate, calculated for head airways, tracheobronchial and alveolar regions, was obtained by applying WA particle size concentrations to simplified deposition fraction probability equations for the ICRP human respiratory tract model (Cousins et al., 2011) as described by Hinds (1999). The respiratory volume used was 25 l min^{-1}, corresponding to male respiration during light exercise (Koivisto et al., 2012b). In the model, particles were assumed to be spherical and to preserve their size during inhalation.

2.8. Risk assessment using online tools (Stoffenmanager, ART and NanoSafer)

Stoffenmanager® v.7.1, is a risk priorisation web-based tool which consists of a control banding tool (inhalation and dermal), with a part designed for exposure to engineered nanoparticles (inhalation) and general and REACH specific quantitative inhalation exposure parts (van Tongeren et al., 2017). It is between tier 1 and 2 tool as recommended by ECHA (ECHA, 2016; Landberg et al., 2017; Spinazzè et al., 2017; van Tongeren et al., 2017), and its general assumptions are based on Marquart et al. (2008) whereas the rationale of the algorithm is based on Cherrie and Schneider (1999) and adapted as described in Tielemans et al. (2008a).

The Advanced REACH tool (ART), is a tier 2 mechanistic exposure modelling tool with a higher level of detail than the Stoffenmanager and recommended by the ECHA (ECHA, 2016). It also has a Bayesian approach that combines the mechanistic model with measurements of exposure (Landberg et al., 2017). Similarly to Stoffenmanager, ART is also based on Cherrie and Schneider (1999) approach with Tielemans et al. (2008b) modifications. It is described and explained in detail in Fransman et al. (2011) and has been tested and calibrated in Schinkel et al. (2011).

Stoffenmanager and ART dimensionless total exposure score equations can be found in Riedmann et al. (2015).

The NanoSafer v1.1 is a control-banding and risk management tool (Kristensen et al., 2010; Jensen et al., in preparation) for manufactured nanomaterials. In addition to manufactured nanomaterials, the tool can also be used to assess and manage emissions from nanoparticle-forming processes such as powder handling and fugitive/point-source emissions. Hazard assessment and case-specific exposure potentials are currently combined into an integrated assessment of risk levels expressed in control bands with associated risk management recommendations and e-learning on how to reduce exposure or risk thereof. The tool is currently intended for small and medium-size companies and laboratories with no or limited experience in working with nanomaterials and/or insufficient resources to perform a full precautionary risk assessment. Further developments in future aim to expand the application domains and include assessment with risk management measures as part of calibrate project (http://www.nanocalibrate.eu/home).

3. Results and discussion

3.1. Worker exposure monitoring

Worker exposure is here analyzed considering the packing line type and the material being packed. In the following sections, results are discussed considering statistical significance obtained only when using the nanoGEM approach. Discussion regarding differences when using different statistical tests will be done in a separate section 3.6.

The results for Clay 2 from line L, Feldspar 1 from line M and Feldspar 2 from line H are discussed in detail in this section, while the results from the rest of the materials are shown in Supplemental Material-Fig. S3, S4, S5 and S6. The case studies in this section were selected due to their representativeness and due to the fact that statistically significant exposure concentrations were recorded. Measured concentrations for all materials are shown in Table 3.

3.1.1. Packing line L (low mitigation strategies)

In packing line L, located in the industrial plant #1, packing of Clay 1, Clay 2 and Kaolin 1 was monitored (Table 1). For Clay 1 and Kaolin 1, 2 batches of 20 bags of 1200 kg each were monitored whereas for the Clay

2, 20 pallets consisting of 3 bags (400 kg each; total 1200 kg) were monitored.

Packing of Clay 2 in line L (Fig. 2 and Table 3) increased total particle number concentrations significantly (34806–36,253 cm^{-3}) compared to background concentrations (18,348 ± 3412 cm^{-3}). However, these increases seem to be related to outdoor influence (Supplemental Table S3). In addition, statistically significant increases of inhalable (1524–1998 μg m^{-3}) and respirable (135–139 μg m^{-3}) mass concentrations were monitored, with increases from pre-activity concentrations of 1317–1791 μg m^{-3} for inhalable and 117–121 μg m^{-3} for respirable fractions. BZ and WA respirable dust concentrations gravimetrically analyzed were 226 μg m^{-3} and 230 μg m^{-3}, respectively, which are slightly higher than online respirable concentrations measured by the mini-LAS. RCS exposure was 73.6 μg m^{-3} (32.7% of total respirable dust) (Table 3). Arithmetic mean particle dimeter (10 nm-35 μm, Mini-WRAS particle count) during packing was 82.2–82.7 nm whereas during pre-activity it was 79.2 ± 4.2 nm. Clear peaks for particle mass (Fig. 2(b) and (c)) can be identified coinciding with the start of a new pallet (of 1200 kg) being packed which will contain 3 bags of 400 kg. Therefore, peaks are not related to the start of pouring but to the action of manually placing the pallet in the packing area, otherwise we would be able to detect the peaks in between related to the start and stop for the next bag of 400 kg. Cyclic process in which the start of the process presents the maximum peak concentration have been described for industrial pouring (Koponen et al., 2015) and pilot plant milling (Ribalta et al., 2019b). Therefore, the type of handling and number of repetitions can be as critical as the amount of material being handled or even more, as pointed out by Koponen et al. (2015).

PSD in Fig. 3(a) shows that packing of Clay 2 increased particle concentrations for particle diameters >0.5 μm. The same was observed for Kaolin 1 (Fig. 3(b)) which had a similar behavior than Clay 2, showing also statistically significantly increased concentrations during packing of particle number and mass (respirable and inhalable) concentrations (Supplemental Fig. S4). SEM images for Clay 2 show clay platy particles (> 1 μm dimeter) together with diesel agglomerates (Supplemental Fig. S7(a) and (b)). Clay 1 PSD is not shown due to a power shortage. In general, Clay 1 (Supplemental Fig. S3) differs from the other 2 materials as no significant increases were detected. This is in agreement with the dustiness indexes, Clay 1 presenting the lowest value of the 3 materials (1733 ± 880 mg kg^{-1}). Table 1 shows the C.D dustiness results in terms of inhalable (W_I) and respirable (W_R) mass fractions (mg kg^{-1}). In sum, line L (with low mitigation strategies) generated statistically significant impacts on exposure in terms of particle number and mass (respirable and inhalable) for 2 of 3 materials (Clay 2 and Kaolin 1).

3.1.2. Packing line M (medium mitigation strategies)

Packing of Feldspar 1 (3 batches of 20 bags of 1200 kg each) (Fig. 4) and Quartz 1 (2 batches of 20 bags of 1200 kg each) (Supplemental Fig. S5) in line M (industrial plant #1) was monitored.

During packing of Feldspar 1 (Fig. 4), total particle number concentration measured with the CPC (26777–51,645 cm^{-3}) was similar to pre-activity (42,038 ± 5595 cm^{-3}). The same was true for the respirable mass fraction (119–577 μg m^{-3} during packing vs. 212 ± 70 μg m^{-3} during background) but with a significant increase during batch 1 (Table 3). Contrarily, the inhalable mass fraction was found to be significantly higher during all packing repetitions (1412–3416 μg m^{-3}) when compared to pre-activity concentrations (643 ± 224 μg m^{-3}) with increases between 770 and 2773 μg m^{-3}. As occurred during packing in line L, peaks can be identified at the beginning of each bag being packed (Fig. 4(b) and (c)) especially from 16:00 to 18:00 of particles 1–5 μm (Fig. 4(b)). Peaks were less marked during the morning shift due to another indoor process which was slightly covering up packing emissions. Particle mean diameter (10 nm-35 μm) during packing was 80.2–84.9 nm whereas during pre-activity was 80.9 ± 2.4 nm. During packing in line M, the concentration of particles >2 μm increased when packing Feldspar 1 (Fig. 3(c)) whereas the concentration of particles between 0.01 and 0.5 μm increased when packing Quartz 1 (Fig. 3(d)). SEM images for Feldspar 1 show high concentrations of feldspar particles (> 2 μm diameter) and diesel agglomerates (Supplemental Fig. S7(c) and (d)). Conversely, for Quartz 1, quartz particles observed were > 1 μm diameter (Supplemental Fig. S7(g) and (h)). During packing, Quartz 1 presented lower mass concentrations than Feldspar 1

Table 3
Mean ± S.D. (standard deviation) of each batch in the worker area and for each day. Bold values are those which are significantly higher than pre-activity (BG) concentrations using the nanoGEM approach. BZ: breathing zone. DL: detection limit. NaN: Not available number. *The pump stopped during the sampling. Mini-WRAS arithmetic mean particle size is calculated by using particle count distribution.

Sampling		CPC (cm^{-3})	MiniWras (nm)	Mini-LAS (μg m^{-3})		Gravimetric Respirable Mass (μg m^{-3}) (RCS μg m^{-3})	
		N_{TOT}	Size	Inhalable	Respirable	BZ	WA
Clay 1_L Day 1	BG	42,410 ± 32,660	50 ± 9	986 ± 1000	212 ± 260	–	–
	Batch 1	37,896 ± 12,825	51 ± 7	1847 ± 2571	144 ± 139	101 (<DL)	182
	Batch 2	34,535 ± 6339	56 ± 6	1697 ± 2390	166 ± 202		
	Batch 3	NaN	NaN	1370 ± 1434	162 ± 165		
Feldspar 1_M Day 2	BG	42,038 ± 5595	81 ± 2	643 ± 224	212 ± 70	–	–
	Batch 1	51,645 ± 15,528	80 ± 5	**3416 ± 4868**	**577 ± 713**	1065 (75)	313
	Batch 2	39,969 ± 68,776	83 ± 27	**2180 ± 4965**	270 ± 623		
	Batch 3	26,777 ± 11,431	85 ± 19	**1412 ± 1564**	119 ± 104		
Quartz 1_M Day 3	BG	23,291 ± 6988	94 ± 21	3529 ± 3324	353 ± 351	–	–
	Batch 1	24,755 ± 4862	83 ± 9	1714 ± 2094	153 ± 135	468 (161)	186
	Batch 2	**46,670 ± 17,666**	74 ± 5	1150 ± 625	209 ± 99		
Clay 2_L Day 4	BG	18,348 ± 3412	79 ± 4	207 ± 208	40 ± 26	–	–
	Batch 1	**36,253 ± 7974**	82 ± 12	**1998 ± 3403**	**139 ± 148**	226 (74)	230
	Batch 2	**34,806 ± 4002**	83 ± 5	**1524 ± 1469**	**135 ± 122**		
Kaolin 1_L Day 5	BG	15,721 ± 2185	86 ± 3	92 ± 114	18 ± 9	–	–
	Batch 1	**40,565 ± 10,218**	80 ± 7	**2647 ± 3486**	**242 ± 206**	36*[1] (< DL)	321
	Batch 2	**42,331 ± 3358**	87 ± 7	**4705 ± 4224**	**609 ± 471**		
Feldspar 2_H Day 6	BG	69,673 ± 29,930	76 ± 5	1824 ± 1270	333 ± 179	–	–
	Batch 1	43,049 ± 10,829	87 ± 25	4264 ± 17,531	701 ± 2607	17* (< DL)	437
	Batch 2	19,476 ± 10,503	**97 ± 11**	1573 ± 1628	289 ± 228		
Kaolin 2_H Day 7	BG	12,484 ± 6143	90 ± 19	898 ± 806	148 ± 134	–	–
	Batch 1	**71,996 ± 127,876**	74 ± 10	830 ± 762	137 ± 141	< DL*	55
	Batch 2	**50,504 ± 28,475**	69 ± 7	283 ± 193	53 ± 26		

*[1] Worker wearing the cyclone was carrying out other activities not related to packing which may have influenced in the low concentrations registered on the BZ that day.

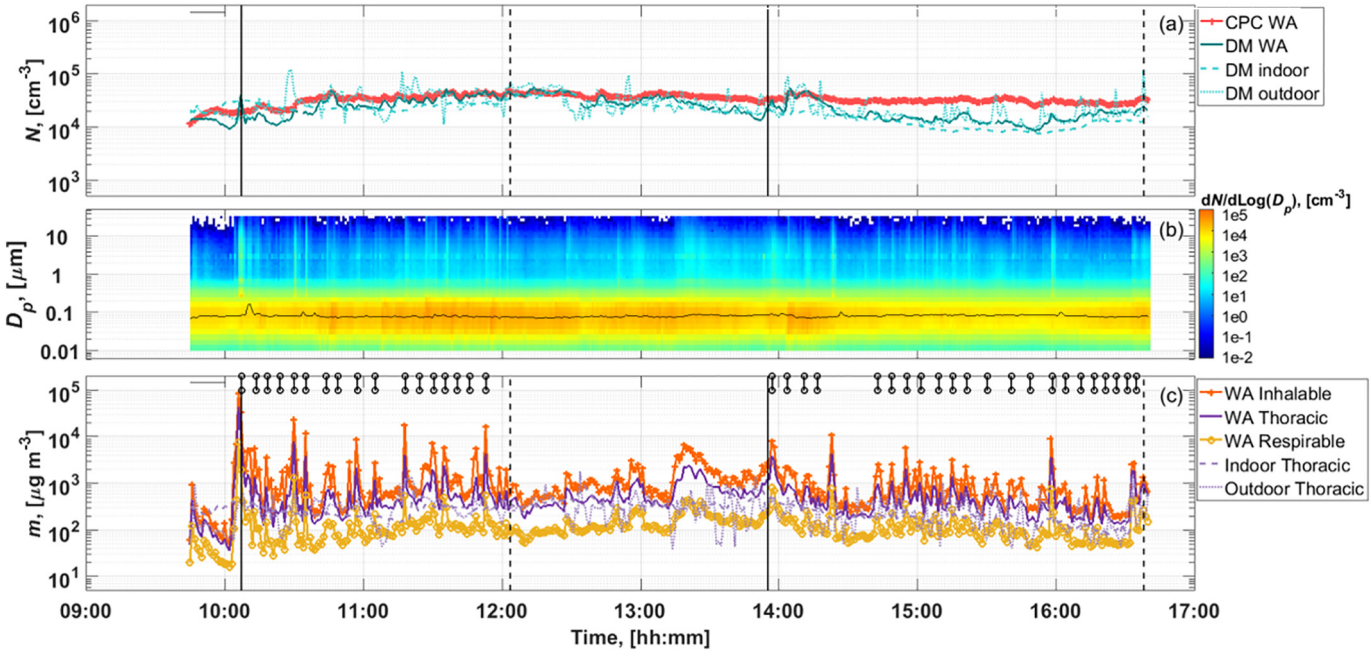

Fig. 2. Particle concentration at the worker area during packing of Clay 2: (a) particle number concentration time series (CPC and DM; DiSCmini); (b) particle size distribution time series measured with the MiniWras, solid black line shows MiniWras d_{50}; (c) mass concentration time series measured by Grimm mini-LAS. Black vertical lines indicate start (solid line) and stop (dashed line) of each batch. Vertical top black lines mark the start of each bag being packed. Horizontal grey line shows the background period.

which is in agreement with dustiness indexes Quartz 1 < Feldspar 1. In general Quartz 1 (Supplemental Fig. S5) behaved differently than Feldspar 1, showing only a significant increase in particle number during one batch (Table 3). When, comparing WA with indoor measures during packing, WA was seen to have slightly lower particle number concentration than the indoor location but higher mass concentrations

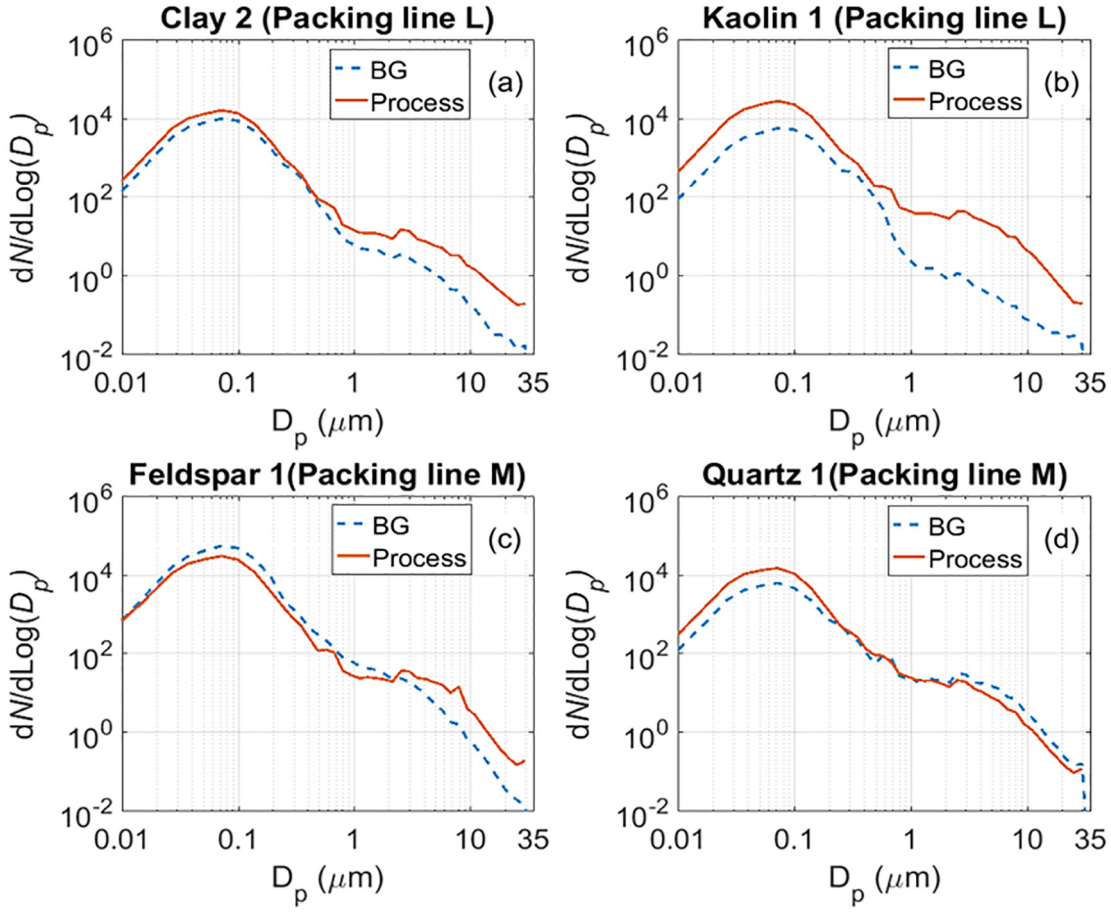

Fig. 3. Particle size distribution in the worker area during pre-activity and packing in packing line L for Clay 2 (a) and Kaolin 1 (b) and packing line M for Feldspar 1 (c) and Quartz 1 (d).

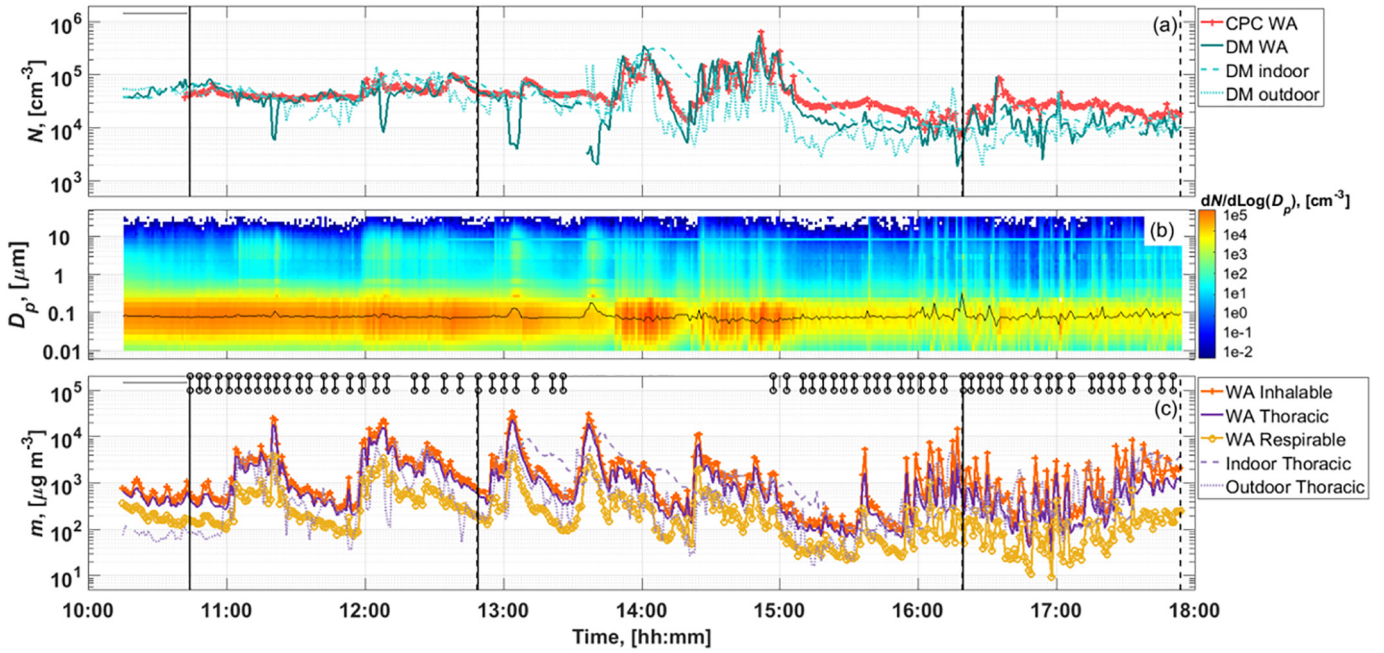

Fig. 4. Particle concentration at the worker area during packing of Feldspar 1: (a) particle number concentration time series (CPC and DM; DiSCmini); (b) particle size distribution time series measured with the MiniWras, solid black line shows MiniWras d_{50}; (c) mass concentration time series measured by Grimm mini-LAS. Black vertical lines indicate start (solid line) and stop (dashed line) of each batch. Vertical top black lines mark the start of each bag being packed. Horizontal grey line shows the background period.

(Supplemental Table S3). Before Quartz 1 pre-activity period, maintenance tasks were carried out in the plant, which probably influenced pre-activity and indoor concentrations.

BZ and WA respirable dust concentrations for Feldspar 1 and Quartz 1 gravimetrically analyzed were 1065 μg m^{-3} and 313 μg m^{-3}, and 468 μg m^{-3} and 186 μg m^{-3} respectively (Table 3). Conversely, in line L respirable dust in BZ and WA were approximately in the same range (see 3.1.1). Near field online measurements were seen to underestimate worker exposure when compared with personal exposure (Koivisto et al., 2015; Koponen et al., 2015) although this is not always the case as found by (Janssen et al., 1998). Here, BZ mass concentrations were seen to be higher than WA concentrations only for Feldspar 1 and Quartz 1, both materials packed in line M. The difference between line L and M results could be explained by the fact that materials packed in packing line M were the ones with a higher dustiness index and during pouring the level of mitigation strategies is "medium", additionally main exposure of the worker to the material was when the worker manually closed the bag and not during material pouring into the bag (when closing there was no extraction system and the worker was directly on the emission source).

RCS exposure in the BZ was 74.6 (7% of total respirable mass concentration) and 160.5 (34.3% total respirable mass concentration) μg m^{-3} for Feldspar 1 and Quartz 1 respectively (Table 3). RCS content during Quartz 1 packing was lower than expected as during dustiness tests respirable silica content represented 97–100% of the total respirable dust collected (Supplemental Table S4), which shows that worker exposure measured was not only due to Quartz 1 packing.

3.1.3. Packing line H (high mitigation strategies)

In packing line H (industrial plant #2), packing of Feldspar 2 (Fig. 5) and Kaolin 2 (Supplemental Fig. S6) in bags of 20–25 kg was monitored during 5 to 6 h. This line had the most stringent mitigation measures of all three lines, with the opening of the bag fully enclosed and automated system.

Packing of Feldspar 2 did not significantly increase particle number or mass concentrations (Fig. 5 and Table 3). Particle number concentrations measured with the CPC during pre-activity was 69,673 ± 29,930 cm^{-3} whereas during packing they ranged between 19,476–43,049 cm^{-3}. Mean inhalable and respirable mass concentrations during pre-activity were 1824 ± 1270 and 333 ± 179 μg m^{-3} and, although during batch 1 mass concentrations increased (4264 ± 17,531 and 701 ± 2607 μg m^{-3} for inhalable and respirable fractions), those were not statistically significant, most likely due to the fact that they were related to unexpected events during packing e.g. broken bags during pouring (Fig. 5 (c)). If only the period between 12:00 and 14:00 is considered (where no events occurred), then inhalable and respirable concentrations were 1127 ± 617 μg m^{-3} and 187 ± 93 μg m^{-3} respectively. WA respirable dust concentration was 437 μg m^{-3}. Particle mean dimeter (10 nm-35 μm) during packing and pre-activity was 87.2–97.3 nm and 76.2 ± 4.6 nm, respectively. Conversely, Kaolin 2 did not behave the same way, showing significant increases for particle number, although this was due to outdoor and indoor influence (Supplemental Table S3), and mass concentration remained the same during packing than during pre-activity.

In packing line H, the 2 materials did not behave exactly the same, but no significant increases were detected for particle mass concentration for any of them. Kaolin 2 had higher dustiness index than Feldspar 2 but conversely showed lowest concentrations during packing. This is in line with the fact that line H is the one with the strongest mitigation strategies. However, it is important to highlight that high respirable mass concentrations (up to 20,000 μg m^{-3}) were detected during specific events such as bags breaking, which may impact worker exposure but would not be detected if only 8 h TWA was considered. This highlights the relevance of real-world and time-resolved particle monitoring in occupational risk assessment.

3.2. 8 h time-weighted average (8 h TWA)

Particle number concentrations increased significantly only during Clay 2, Kaolin 1 and during 1 repetition of the Quartz 1. However, those increases were always below 40,000 cm^{-3}, the nano-reference value used as precautionary approach in this specific case (non-biodegradable granular nanomaterials in the range of 1–100 nm and density < 6 kg l^{-1}) (Van Broekhuizen et al., 2012).

Increases of inhalable and respirable mass concentrations were found during packing for Feldspar 1, Clay 2 and Kaolin 1. However, 8 h

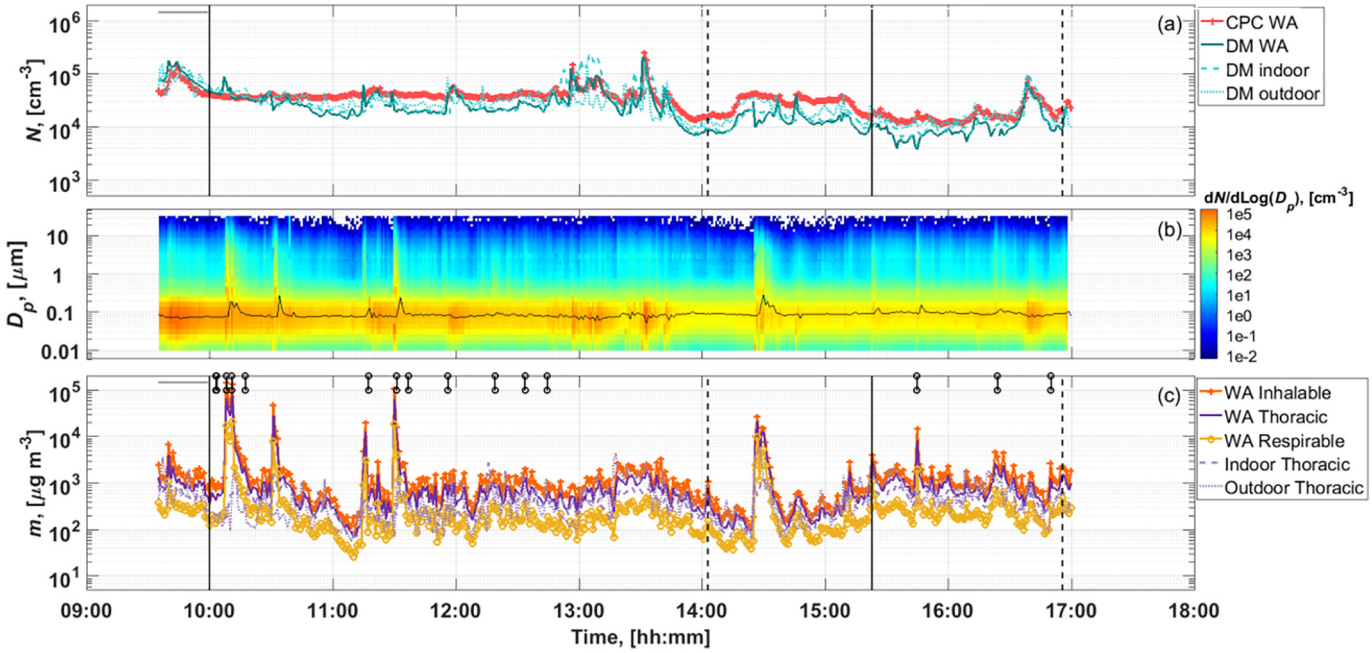

Fig. 5. Particle concentration at the worker area during packing of Feldspar 2: (a) particle number concentration time series (CPC and DM; DiSCmini); (b) particle size distribution time series measured with the MiniWras, solid black line shows MiniWras d_{50}; (c) mass concentration time series measured by Grimm mini-LAS. Black vertical lines indicate start (solid line) and stop (dashed line) of each batch. Vertical top black lines mark specific events (bags being broken or other accidents). Horizontal grey line shows the background period.

TWA concentrations (Table 4) did not exceed in any case the limit values for particles not otherwise specified of inhalable (8 to 28 times <10,000 μg m^{-3}) and respirable (4 to 14 times <3000 μg m^{-3}) mass fractions (INSH, 2018). RCS exposure limit value (50 μg m^{-3}) was also not exceeded. RCS exposure in the WA for Feldspar 1, Quartz 1 and Clay 2 was 16, 43 and 35 μg m^{-3} (3, 1.2 and 1.4 times lower than the occupational limit, respectively). Thus, although RCS 8 h TWA was not exceeded and considering that values correspond to a 5 to 6 h packing shift, it is important to mention that a 7 or 8 h packing could lead to exceed the RCS exposure limit values.

3.3. Inhalation dose

Inhalation dose rates were estimated for each day using size distribution data from the MiniWras with the exception of Clay 1, for which PSD was obtained using the NanoScan SMPS. Thus, it should be noted that results for Clay 1 are not directly comparable with the rest.

Total deposited particle surface area during packing ranged between 5.4 and 11.8 × 10^5 μm^2 min^{-1}. The main deposition region during packing was the alveoli (50.8–63.7%) followed by head airways (26.6–41.3%)

Table 4
Calculated 8 h TWA (including pre-activity concentrations) for inhalable and respirable mass fractions in the worker area is provided. Risk assessment results conducted with the ART (Mechanistic and Bayesian), Stoffenmanager and NanoSafer v1.1. Ratios of mass predicted and mass measured are shown in brackets. Material, sampling time and inhalable dustiness index using the continuous drop (C.D) is provided. WA: worker area. NF: near-field. RCS: respirable crystalline silica. DL: detection limit. W_I: inhalable fraction. W_R: respirable fraction.

Sampling time "min" $W_{I/R}$ mg kg^{-1}	WA Respirable 8 h TWA (μg m^{-3}) (WA RCS μg m^{-3})[a]	WA Inhalable 8 h TWA (μg m^{-3})	ART (inhalable μg m^{-3}) C.D based		Stoffenmanager (inhalable μg m^{-3})	NanoSafer v1.1 (respirable (NF/FF, 8 h TWA) μg m^{-3})
			Mechanistic	Bayesian		
Clay 1_L 174 min C.D W_I = 1733 C.D W_R = 6	129 (< DL)	1454	300 (160–570) [−4.9]	2200 (1500–3300) [1.5]	2710 [1.9]	1698/143 [13]/[1.1]
Feldspar 1_M 342 min C.D W_I = 10,246 C.D W_R = 59	227 (16)	1679	1600 (860–3100) [−1.1]	4000 (2900–5500) [2.4]	4420 [2.6]	16,698/1407 [74]/[6.2]
Quartz 1_M 264 min C.D W_I = 8891 C.D W_R = 43	126 (43)	1317	900 (480–1700) [−1.5]	3400 (2500–4700) [2.6]	2100 [1.6]	12,171/1025 [97]/[8.1]
Clay 2_L 287 min C.D W_I = 5170 C.D W_R = 16	108 (35)	780	3300 (1700–6200) [4.2]	4700 (3500–6400) [6.0]	2290 [2.9]	4530/382 [42]/[3.5]
Kaolin 1_L 162 min C.D W_I = 18,886 C.D W_R = 44	166 (< DL)	1538	1800 (980–3500) [1.2]	4100 (3000–5500) [2.7]	2950 [1.9]	12,453/1049 [75]/[6.3]

[a] 8 h TWA RCS was calculated by applying the content of RCS in percentage obtained with the gravimetrical analysis, to calculated 8 h TWA respirable mass concentration.

and trachea bronchi (7.3–9.6%) (Fig. 6). However, deposition in the trachea bronchi and alveolar regions during packing was reduced when compared to pre-activity, whereas it increased in the head airways (between 1.2 and 23%). The same occurred with particle number and mass, which showed increases in particles deposited in the head airways during packing (0.8–4.9% and 0.1–5.4%, respectively) and reductions in the trachea bronchi and alveolar regions. These results are in agreement with the mean PSD of packing emissions which are mainly coarse.

It is important to point out that surface dose analysis as estimated here can only be applied for particles up to 750 nm (Heitbrink et al., 2009; Keller et al., 2001), but PSD for some of the materials (Feldspar 1, Clay 2 and Kaolin 1) was >1 μm. This should be considered as a limitation. Hygroscopicity was not considered, which can lead to over- or under-estimations of particle deposition in the respiratory tract depending on the dry and humid size of the particles(Martonen and Clark, 1983; Asgharian, 2004; Winkler-Heil et al., 2014; Ching and Kajino, 2018; Salamtonidis et al., under review, JAS).

In this model, the 3 metrics (number, mass and surface area) were included based on Wang et al. (2010) and Koivisto et al. (2012a, 2012b). Even though percentages of deposited particles in the different regions were different, similar results were obtained indicating that airborne emitted particles during packing increased deposition in the head airways.

3.4. Risk assessment modelling

Different web-based tools have been developed in order to provide risk assessment of chemical hazards (Fransman et al., 2011; Kristensen et al., 2010; Tielemans et al., 2008a; Jensen et al., in preparation). Tier 1–2 risk assessment tools Stoffenmanager and ART have been tested in different scenarios including dust emissions (Bekker et al., 2016; Landberg et al., 2017, 2015; Riedmann et al., 2015; Savic et al., 2018) and they are recommended by ECHA (ECHA, 2016). However, there is controversy regarding whether or not web-based tools results are sufficiently robust to be used with decision-making regulatory purposes (Raul and Dwyer, 2003; Koivisto et al., 2019). In general, models are seen to overestimate actual exposures (van Tongeren et al., 2017; Savic et al., 2018) although underestimations have been reported (Landberg et al., 2017). In addition, prediction accuracy depends on many factors such as the type of process or the concentration ranges, and further studies are required to fully understand the performance of online modelling tools.

Here, 8 h TWA inhalable concentrations were compared to ART (Mechanistic and Bayesian), and Stoffenmanager, and respirable concentrations were compared to NanoSafer v1.1 estimations (Table 4). Differences between packing lines L and M could be included in the ART with the option "open process/handling that reduces contact between product and adjacent air". Conversely, this differentiation could not be included in Stoffenmanager and NanoSafer v1.1. Examples of the reports provided by the tools are shown in Supplemental Annex B (Supplemental Material). Only packing lines L and M were considered for risk assessment modelling due to the complexity to differentiate between packing lines when using the web-based tools.

The ART mechanistic model was found to underestimate exposure in 3 out of 5 cases (Clay 1, Feldspar 1 and Quartz 1). For Feldspar 1 and Quartz 1 underestimation was slight (< 2 factor) whereas for Clay 1, exposure was underestimated by a factor of 4.9. 8 h TWA concentrations were overestimated for Clay 2 and Kaolin 1 with a factor of 4.2 and 1.2 respectively. To sum up, ART predicted concentrations with an accuracy of ±2 factor in three cases. ART Bayesian predicted exposures within a factor < 2 for Clay 1, overestimated exposure for Feldspar 1, Quartz 1, Kaolin 1 and Clay 2 (factors 2–6). Finally, Stoffenmanager overestimated measured exposure concentrations by a factor between 1.6 and 2.9 for all materials. The risk assessment results obtained with the ART and Stoffenmanager are in line with the literature, where models are seen to both, over and under estimate actual exposures depending on the case study (van Tongeren et al., 2017; Savic et al., 2017; Landberg et al., 2017).

Results of the exposure assessment modelling by using NanoSafer v1.1 (test date: December 4, 2018) are summarized in Table 4. The hazard estimates in NanoSafer showed that the 5 tested materials ranged from 0.2 to 0.8 (finite four-step linear scale ranging from 0 to 1 with increase in hazard level at 0.25, 0.5 and 0.75 points). Only for Feldspar 1 and Quartz 1, specific risk sentences were listed and adopted from the bulk material. In consequence, these materials scored the highest hazard score and the other three materials (Clay 1, Clay 2, and Kaolin 1) scored the lowest possible hazard score of 0.2.

The exposure score in NanoSafer ranges from 0 to ∞ and the exposure risk level increases in five steps at 0.1, 0.25, 0.5, and 1.0, where occupational exposure limit (OEL) is exceeded when the exposure risk level is larger than 1. For the five cases modelled the exposure potential ranks Feldspar 1 > Kaolin 1 > Quartz 1 > Clay 2 > Clay 1. In all the cases except for Clay 1, the exposure potential exceeded the OEL (3000 μg m^{-3}), which resulted in a risk level (RL) of 5; a special high exposure-related risk level. In Clay 1 (packing line L), the exposure score was 0.57 resulting in a final RL4. These risk levels (RL4 and RL5)

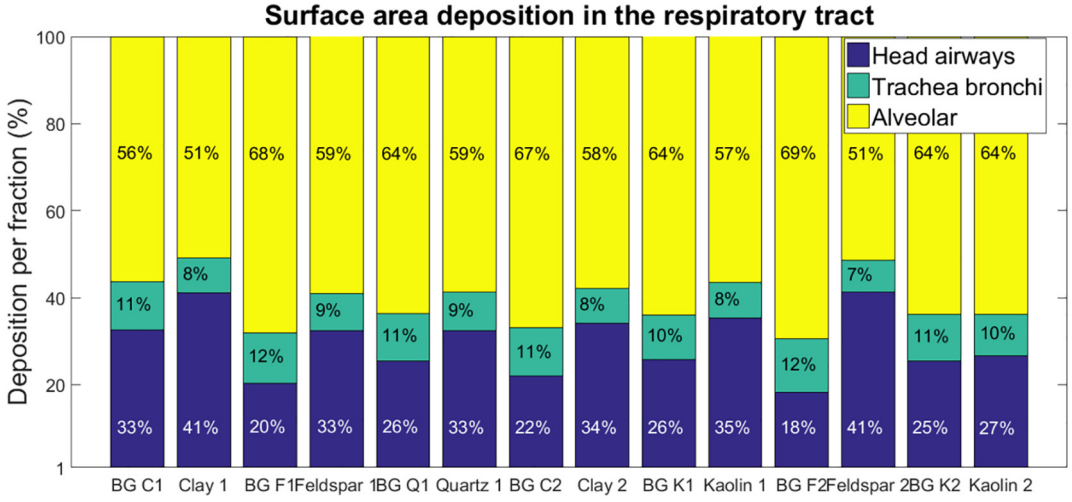

Fig. 6. Percentage of surface deposited area in the respiratory tract per region during packing and pre-activity for of all materials. Abbreviations codes are: BG, background (pre-activity period); C1, Clay 1; F1, Feldspar 1; Q1, Quartz 1; C2, Clay 2; K1, Kaolin 1; F2, Feldspar 2; K2, Kaolin 2.

were associated with general recommendations for risk management such as:

RL4: High toxicity suspected and/or high exposure potential. Use highly efficient local exhaust ventilation, fume-hood, glove-box etc. Make sure to have the personal respiratory protection equipment (PP3 or higher quality) available in case of accidents.

RL5: Very high toxicity suspected and/or moderate to very high exposure. The work should be conducted under strict dust release control, such as in a fume-hood, separate enclosure etc. Air-supplied respirators or highly efficient filter masks (PP3 or higher quality) may be used as a supplement and must be readily available in case of accidents. Expert advice is recommended.

In overall, NanoSafer overestimated WA measured concentrations for all materials with a factor between 13 and 97 when near-field (NF) output concentrations were considered, and between 1 and 8 when far-field (FF) output concentrations were considered. WA was located between 1.5 and 2 m from the emission source which is in the limit of the NF defined by NanoSafer (2 m). This explains why the ratios of mass predicted and mass measured are closer to 1 if FF concentrations are considered.

3.5. Dustiness-exposure concentration correlation

The use of the dustiness index as an exposure predictor metric has been explored by several authors (Brouwer et al., 2006; Evans et al., 2013; Levin et al., 2014; Ribalta et al., 2019b). Following the EN 15051 dustiness classification with the C.D method, the material showing the highest exposure to inhalable mass concentration (Kaolin 1) was also the material with highest inhalable dustiness index (18,886 ± 174 mg kg^{-1}), which was followed by Kaolin 2, Feldspar 1, Feldspar 2, Quartz 1 and Clay 2.

Correlation between exposure during materials being packed in line L (low mitigation strategy) and their dustiness index (using inhalable fraction) was relatively high (R^2 0.80) (Fig. 7(a)). However, this correlation was low for packing lines M and H, which have moderate to high mitigation strategies (R^2 0.27) (Fig. 7(b)). Thus, results seem to suggest that a clear correlation dustiness exposure exists when materials characteristics (e.g. dustiness) dominate over process characteristics (e.g. degree of source enclosure). Conversely, when emissions depend more on process characteristics correlation is not straightforward.

The respirable mass-based dustiness indices varied over 1 order of magnitude with Kaolin 2 and Feldspar 2 having the highest (104 ± 1 mg kg^{-1} and 77 ± 0 mg kg^{-1}) (Table 1). According to the EN 15051, the respirable dustiness tests reveal that 4 powders are categorized as very low (Clay 1) and low (Clay 2, Quartz 1, and Kaolin 1) and 3 (Feldspar 1, Feldspar 2, and Kaolin 2) are in the category of powders with moderate dustiness. When considering correlations for the respirable fraction, these were similar but less robust than for the inhalable fraction ($R^2 = 0.55$ for packing line L and $R^2 = 0.02$ for packing lines M and H, data not shown).

Current discussions are ongoing regarding this topic (Dubey et al., 2017; Fonseca et al., 2018; Ribalta et al., 2019b) as yet no clear direct relationship dustiness-exposure has been established. In Fonseca et al. (2018) no clear correlation during laboratory spilling of nano-scaled materials under a fume hood with the small-rotating drum dustiness results was found, whereas in Ribalta et al. (2019b) good correlations between dustiness (measured with the continuous drop and rotating drum) were found during handling of different coarse ceramic materials. Earlier studies also found correlation (Breum et al., 2003; Brouwer et al., 2006; Heitbrink et al., 1989) although, some others did not (Class et al., 2001; Heitbrink et al., 1990).

3.6. Statistical significance variations depending on the statistical method used

The nanoGEM approach, a specific user-friendly approach, was designed in order to assess the statistical significance of exposure impacts for particle number. However, no specific approach is available, other than statistical tests, for particle mass concentration. Thus, different approaches were tested for the current dataset, in terms of particle number and mass.

Results (Table 5) showed that with respect to currently available and frequently used nanoGEM method, the *t*-test and the MW "U" test provided slightly more conservative results. The *t*-test differs only in 1 case for inhalable mass and 1 case for respirable mass out of 21 cases. Similarly, the MW "U" test differs in 1 and 2 cases for inhalable and respirable mass fractions, respectively. Conversely, for particle number, all 3 methods provided the same results. Therefore, using the t-test or the MW "U" test for mass could provide slightly more conservative results to the point of view of exposure assessment. However, this could come as the cost of using a less friendly-user approach.

With regard to the method proposed as "golden standard by the EN 17058:2018" (ARIMA), in 6 cases results were less conservative (no significant exposures were identified in contrast to the other tests) than results obtained when using the other tests. Considering the obtained results, ARIMA models are complex to apply and require expert knowledge, and they did not identify exposures to mass in the case studies.

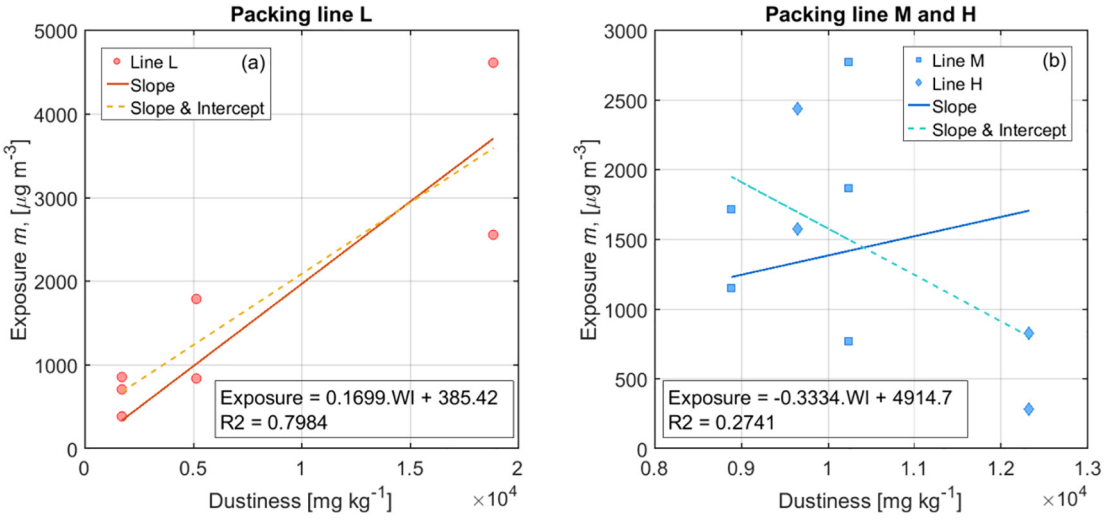

Fig. 7. Continuous drop dustiness index correlated with exposure for materials packed in line L (a), and M and H (b). Inhalable fraction is used.

Finally, it was observed that using the nanoGEM approach could lead to a slight underestimation of the statistical significance when the pre-activity dataset is characterized by a high variability, which is frequent in industrial monitoring, especially for particle mass concentration. This is not usually the case in laboratory experiments. However, it should be noted that the nanoGEM methodology was not designed to be applied to particle mass concentrations. As a result, the nanoGEM criterion may be applicable to assess the significance of particle emissions in terms of mass concentrations taking into account the above limitation. The design of a method tailored to particle mass concentrations would be advisable.

4. Conclusions

Exposure and health impacts were assessed during industrial packing of 7 materials in 3 lines with different levels of mitigation (low, medium and high). The main conclusions extracted are summarized below:

4.1. Impact of enclosure strategies on exposure

It may be concluded that packing in packing line L and M had a significant impact on worker exposure with regard to particles in the 11.5 nm – 35 μm size range, significantly increasing worker exposure and reaching high respirable (135–609 μg m^{-3} for packing line L and 119–577 μg m^{-3} for packing line M) and inhalable (1370–4705 μg m^{-3} for packing line L and 1150–3416 μg m^{-3} for packing line M) mass concentrations. However, 8 h TWA limits were not exceeded in any case. RCS exposure limits were also not exceeded but values were close to the limit, indicating a potential risk of exposure. Conversely, packing in line H, which had the highest mitigation strategies, was seen to have an impact, only during accidental spills e.g. bags being broken, with respirable mass concentration reaching 20,000 μg m^{-3}. Therefore, the degree of source enclosure showed a clear inverse relationship with the exposure concentrations monitored evidencing the effectiveness of mitigation strategies in place. In addition, results highlight the relevance of real-world and time-resolved exposure assessments in occupational exposure, as 8 h TWA is unable to detect time-resolved high exposures which may significantly impact workers' health. In this case study, where micro-sized materials (d_{50} 8–40 μm) where packed, airborne particles emitted were seen to deposit mainly in the head airways of the human respiratory tract, indicating that risk of penetration to the alveolar region is low.

Table 5
Statistically significant increases by using the nanoGEM approach, two-sample *t*-test, Mann-Whitney (MW) "U" test and the ARIMA model. X* indicates that only one of the cases was significantly higher. Significant decreases are not considered. N_{TOT} (total particle number) measured with CPC. Inhalable and respirable masas measured with Mini-LAS.

Sampling	Metric	nanoGEM	*t*-test	MW "U" test	ARIMA
Clay 1_L	N_{TOT}	–	–	–	–
Day 1	Inhalable mass	–	X	–	–
	Respirable mass	–	–	–	–
Feldspar 1_M	N_{TOT}	–	–	–	–
Day 2	Inhalable mass	X	X	X	–
	Respirable mass	X*	X	X*	–
Quartz 1_M	N_{TOT}	X*	X*	X	–
Day 3	Inhalable mass	–	–	–	–
	Respirable mass	–	–	–	–
Clay 2_L	N_{TOT}	X	X	X	–
Day 4	Inhalable mass	X	X	X	–
	Respirable mass	X	X	X	–
Kaolin 1_L	N_{TOT}	X	X	X	X
Day 5	Inhalable mass	X	X	X	X
	Respirable mass	X	X	X	X
Feldspar 2_H	N_{TOT}	–	–	–	–
Day 6	Inhalable mass	–	–	X*	–
	Respirable mass	–	–	X*	–
Kaolin 2_H	N_{TOT}	X	X	X	X
Day 7	Inhalable mass	–	–	–	–
	Respirable mass	–	X*	X*	–

4.2. Exposure assessment tools

the dustiness index (inhalable fraction) of the materials tested correlated with exposure concentrations during packing in packing line L (R^2 0.80), but no correlation was found for packing in lines M and H (R^2 0.27). Thus, it may be concluded that dustiness can be a useful metric for exposure prediction when materials properties are the main determinant of worker exposure. However, when process properties (e.g. degree of enclosure) play a more important role, correlation is not straightforward and parametrization is needed.

In addition, 4 different approaches were tested to assess the statistical significance of exposure concentrations (in terms of particle number and mass): *t*-test, Man-Whitney (MW) test, the ARIMA models (referred to as the golden standard in EN 17058:2018), and the frequently used nanoGEM approach. The comparison between methods evidenced that (a) the ARIMA method is the least conservative of the 4; (b) the t-test, MW test and nanoGEM approach provided the same results for 18 out of 21 cases analyzed; (c) for the 3 remaining cases, the differences obtained referred to exposures in terms of particle mass, and never to particle number concentrations, which is expected considering that nanoGEM was designed to be used for particle number and not mass concentrations, (d) the nanoGEM approach may lead to underestimations when assessing scenarios with highly variable background concentrations (in terms of particle mass). From the point of view of usability, the nanoGEM method was seen to be the most practical and the least time and resource consuming.

4.3. Risk assessment modelling

3 models were tested: ART, Stoffenmanager and NanoSafer. Only in 3 out of 5 cases, ART estimated the measured exposure within a factor ± 2 and for the 5 cases it was within the inter-quartile confidence interval. The Stoffenmanager web-based tool overestimated all predictions, and only in three cases it was by a factor < 2. NanoSafer overestimated measured exposure respirable mass concentrations in all case scenarios within a factor between 13 and 97, and 1 and 8 when NF and FF concentrations were considered, respectively.

Acknowledgments

This research was founded by the Spanish MINECO (CGL2015-66777-C2-1-R, 2-R), Generalitat de Catalunya AGAUR 2017 SGR41, the Spanish Ministry of the Environment (13CAES006), and FEDER (European Regional Development Fund) "Una manera de hacer Europa". Additional support was provided by caLIBRAte project funded by the European Union's Horizon 2020 research and innovation programme under grant agreement No 686239. M.C. Minguillón acknowledges the Ramón y Cajal Fellowship awarded by the Spanish Ministry of Economy, Industry and Competitiveness.

The authors also acknowledge the company in which the measurements were carried out for their support. The authors declare no conflict of interest relating to the material presented in this article.

Appendix A. Supplementary data

Supplementary data to this article can be found online at https://doi.org/10.1016/j.scitotenv.2019.03.347.

References

Anlar, H.G., Bacanli, M., İritaş, S., Bal, C., Kurt, T., Tutkun, E., Hinc Yilmaz, O., Basaran, N., 2017. Effects of occupational silica exposure on Oxidative stress and immune system parameters in ceramic workers in Turkey. J. Toxicol. Environ. Heal. Part A 80, 688–696. https://doi.org/10.1080/15287394.2017.1286923.

Asbach C, Kuhlbusch TAJ, Kaminski H, Stahlmecke B, Plitzko S, Götz U, Voetz M, Kiesling H-J, Dahmann D, 2012. Standard Operation Procedures for Assessing Exposure to Nanomaterials, following a tiered approach.

Asgharian, B., 2004. A model of deposition of hygroscopic particles in the human lung. Aerosol Sci. Technol. 38, 938–947. https://doi.org/10.1080/027868290511236.

Bekker, C., Voogd, E., Fransman, W., Vermeulen, R., 2016. The validity and applicability of using a generic exposure assessment model for occupational exposure to nano-objects and their aggregates and agglomerates. Ann. Occup. Hyg. 60, 1039–1048. https://doi.org/10.1093/annhyg/mew048.

Breum, N.O., Schneider, T., Jørgensen, O., Valdbjørn Rasmussen, T., Skibstrup Eriksen, S., 2003. Cellulosic building insulation versus mineral wool, fiberglass or perlite: Installer's exposure by inhalation of fibers, dust, endotoxin and fire-retardant additives. Ann. Occup. Hyg. 47, 653–669. https://doi.org/10.1093/annhyg/meg090.

Brouwer, D.H., Links, I.H.M., De Vreede, S.A.F., Christopher, Y., 2006. Size selective dustiness and exposure. simulated workplace comparisons. Ann. Occup. Hyg. 50, 445–452. https://doi.org/10.1093/annhyg/mel015.

Cherrie, J.W., Schneider, T., 1999. Validation of a new method for structured subjective assessment of past concentrations. Ann. Occup. Hyg. 43, 235–245. https://doi.org/10.1016/S0003-4878(99)00023-X.

Ching, J., Kajino, M., 2018. Aerosol mixing state matters for particles deposition in human respiratory system. Sci. Rep. 8, 8864. https://doi.org/10.1038/s41598-018-27156-z.

Class, P., Deghilage, P., Brown, R.C., 2001. Dustiness of different high-temperature insulation wools and refractory ceramic fibres. Ann. Occup. Hyg. 45, 381–384.

Cousins, C., Boice Jr., J., Cooper, U.J., Lee, U.J., Lochard, K.J., 2011. Annals of the ICRP Published on Behalf of the International Commission on Radiological Protection International Commission on Radiological Protection Members of the 2010–2013 Main Commission of ICRP. https://doi.org/10.1016/S0146-6453(11)00010-8.

Ding, Y., Kuhlbusch, T.A.J., Van Tongeren, M., Jiménez, A.S., Tuinman, I., Chen, R., Alvarez, I.L., Mikolajczyk, U., Nickel, C., Meyer, J., Kaminski, H., Wohlleben, W., Stahlmecke, B., Clavaguera, S., Riediker, M., 2017. Airborne engineered nanomaterials in the workplace—a review of release and worker exposure during nanomaterial production and handling processes. J. Hazard. Mater. 322, 17–28. https://doi.org/10.1016/j.jhazmat.2016.04.075.

Dubey, P., Ghia, U., Turkevich, L.A., 2017. Computational fluid dynamics analysis of the Venturi dustiness tester. Powder Technol. 312, 310–320. https://doi.org/10.1016/j.powtec.2017.02.030.

ECHA, 2016. Guidance on information requirements and chemical safety assessment. Chapter R. 14: Occupational exposure assessment. doi:https://doi.org/10.2823/678250.

EN 17058:2018, 2018. Workplace exposure - Assessment of exposure by inhalation of nano-objects and their aggregates and agglomerates.

European Committee for Standardization (CEN), 2013. Workplace exposure: measurement of the dustiness of bulk materials; Part1: requirements and choice of test methods; part 2: rotating drum method; part 3: continuous drop method (EN 15051). [Stantdard] Brussels. Belgium 2013.

Evans, D.E., Ku, B.K., Birch, M.E., Dunn, K.H., 2010. Aerosol monitoring during carbon nanofiber production: Mobile direct-Reading sampling. Ann. Occup. Hyg. 54, 514–531. https://doi.org/10.1093/annhyg/meq015.

Evans, D.E., Turkevich, L.A., Roettgers, C.T., Deye, G.J., Baron, P.A., 2013. Dustiness of fine and nanoscale powders. Ann. Occup. Hyg. 57, 261–277. https://doi.org/10.1093/annhyg/mes060.

Fonseca, A.S., Kuijpers, E., Kling, K.I., Levin, M., Koivisto, A.J., Nielsen, S.H., Fransman, W., Fedutik, Y., Jensen, K.A., Koponen, I.K., 2018. Particle release and control of worker exposure during laboratory-scale synthesis, handling and simulated spills of manufactured nanomaterials in fume hoods. J. Nanopart. Res. 20, 48. https://doi.org/10.1007/s11051-018-4136-3.

Fransman, W., Van Tongeren, M., Cherrie, J.W., Tischer, M., Schneider, T., Schinkel, J., Kromhout, H., Warren, N., Goede, H., Tielemans, E., 2011. Advanced reach tool (ART): development of the mechanistic model. Ann. Occup. Hyg. 55, 957–979. https://doi.org/10.1093/annhyg/mer083.

Fujitani, Y., Kobayashi, T., Arashidani, K., Kunugita, N., Suemura, K., 2008. Measurement of the physical properties of aerosols in a fullerene factory for inhalation exposure assessment. J. Occup. Environ. Hyg. 5, 380–389. https://doi.org/10.1080/15459620802050053.

Gakidou, E., Afshin, A., Abajobir, A.A., Al., A. et, 2017. Global, regional, and national comparative risk assessment of 84 behavioural, environmental and occupational, and metabolic risks or clusters of risks, 1990–2016: a systematic analysis for the global burden of disease study 2016. Lancet 390, 1345–1422. doi:https://doi.org/10.1016/S0140-6736(17)32366-8

Ghasemi, A., Zahediasl, S., 2012. Normality tests for statistical analysis: a guide for non-statisticians. Int. J. Endocrinol. Metab. 10, 486–489. https://doi.org/10.5812/ijem.3505.

Görner, P., Wrobel, R., Simon, X., 2009. High efficiency CIP 10-I personal inhalable aerosol sampler. J. Phys. Conf. Ser. 151, 012061. https://doi.org/10.1088/1742-6596/151/1/012061.

Görner, P., Görner, G., Simon, X., Wrobel, R., Kauffer, E., Witschger, O., 2010. Laboratory study of selected personal inhalable aerosol samplers. Ann. Occup. Hyg 54, 165–187. https://doi.org/10.1093/annhyg/mep079.

Heitbrink, W.A., Todd, W.F., Fischbach, T.J., 1989. Correlation of tests for material dustiness with worker exposure from the bagging of powders. Appl. Ind. Hyg. 4, 12–16. https://doi.org/10.1080/08828032.1989.10389884.

Heitbrink, W.A., Tood, W.F., Cooper, T.C., O'Brien, D.M., 1990. The application of dustiness tests to the prediction of worker dust exposure. Am. Ind. Hyg. Assoc. J. 51, 217–223. https://doi.org/10.1080/15298669091369565.

Heitbrink, W.A., Evans, D.E., Ku, B.K., Maynard, A.D., Slavin, T.J., Peters, T.M., 2009. Relationships among particle number, surface area, and respirable mass concentrations in automotive engine manufacturing. J. Occup. Environ. Hyg. 6, 19–31. https://doi.org/10.1080/15459620802530096.

Hinds, W.C., 1999. Aerosol technology: properties, behavior, and measurement of airborne particles. Wiley-Interscience Publication. Wiley. https://doi.org/10.1016/0021-8502(83)90049-6.

Hormozi, M., Mirzaei, R., Nakhaee, A., Izadi, S., Dehghan Haghighi, J., 2018. The biochemical effects of occupational exposure to lead and cadmium on markers of oxidative stress and antioxidant enzymes activity in the blood of glazers in tile industry. Toxicol. Ind. Health 34, 459–467. https://doi.org/10.1177/0748233718769526.

INSH, 2018. Límites de Exposición Profesional para Agentes Químicos en España 2018.

Janssen, N.A., Hoek, G., Harssema, H., Brunekreef, B., 1998. Personal sampling of airborne particles: method performance and data quality. J. Expo. Anal. Environ. Epidemiol. 8, 37–49.

Jensen, K.A., Saber, A.T., Kristensen, H.V., Liguori, B., Jensen, A.C.Ø., Koponen, I.K., et al. NanoSafer version 1.1: A web-based precautionary risk assessment and management tool for manufactured nanomaterials using first order modeling (manuscript in preparation).

Kaminski, H., Beyer, M., Fissan, H., Asbach, C., Kuhlbusch, T.A.J., 2015. Measurements of nanoscale TiO2 and Al2O3 in industrial workplace environments ??? Methodology and results. Aerosol Air Qual. Res. 15, 129–141. https://doi.org/10.4209/aaqr.2014.03.0065.

Keller, A., Fierz, M., Siegmann, K., Siegmann, H.C., Filippov, A., 2001. Surface science with nanosized particles in a carrier gas. J. Vac. Sci. Technol. A Vacuum, Surfaces, Film. 19, 1–8. https://doi.org/10.1116/1.1339832.

Klein Entink, R.H., Fransman, W., Brouwer, D.H., 2011. How to statistically analyze nano exposure measurement results: using an ARIMA time series approach. J. Nanopart. Res. 13, 6991–7004. https://doi.org/10.1007/s11051-011-0610-x.

Koivisto, A.J., Aromaa, M., Mäkelä, J.M., Pasanen, P., Hussein, T., Hämeri, K., 2012a. Concept to estimate regional inhalation dose of industrially synthesized nanoparticles. ACSNano 6, 1195–1203.

Koivisto, A.J., Lyyränen, J., Auvinen, A., Vanhala, E., Hämeri, K., Tuomi, T., Jokiniemi, J., 2012b. Industrial worker exposure to airborne particles during the packing of pigment and nanoscale titanium dioxide. Inhal. Toxicol. 24, 839–849. https://doi.org/10.3109/08958378.2012.724474.

Koivisto, A.J., Jensen, A.C.Ø., Levin, M., Kling, K.I., Maso, M.D., Nielsen, S.H., Jensen, K.A., Koponen, I.K., 2015. Testing the near field/far field model performance for prediction of particulate matter emissions in a paint factory. Environ. Sci. Process. Impacts 17, 62–73. https://doi.org/10.1039/C4EM00532E.

Koivisto, A.J., Kling, K.I., Hänninen, O., Jayjock, M., Löndahl, J., Wierzbicka, A., Fonseca, A.S., Uhrbrand, K., Boor, B.E., Jiménez, A.S., Hämeri, K., Maso, M.D., Arnold, S.F., Jensen, K.A., Viana, M., Morawska, L., Hussein, T., 2019. Source specific exposure and risk assessment for indoor aerosols. Sci. Total Environ. 668, 13–24. https://doi.org/10.1016/j.scitotenv.2019.02.398.

Koponen, I.K., Koivisto, A.J., Jensen, K.A., 2015. Worker exposure and high time-resolution analyses of process-related submicrometre particle concentrations at mixing stations in two paint factories. Ann. Occup. Hyg. 59, 749–763. https://doi.org/10.1093/annhyg/mev014.

Kristensen, H.V., Hansen, S.V., Holm, G.R., 2010. Nanopartikler i arbejdsmiljøet: Viden og inspiration om håndtering af nanomaterialer. [Internet] Available from: http://nanosafer.i-bar.dk/media/Nanopartikler_i_arbejdsmiljoet_samlet.pdf.

Kuhlbusch, T.A.J., Neumann, S., Fissan, H., 2004. Number size distribution, mass concentration, and particle composition of PM_1, $PM_{2.5}$, and PM_{10} in bag filling areas of carbon black production. J. Occup. Environ. Hyg. 1, 660–671. https://doi.org/10.1080/15459620490502242.

Kurt, O.K., Ergun, D., Basaran, N., 2018. Can the ceramic industry be a new and hazardous sector for work-related asthma? Respir. Med. 137, 176–180. https://doi.org/10.1016/j.rmed.2018.03.012.

Landberg, H.E., Berg, P., Andersson, L., Bergendorf, U., Karlsson, J.-E., Westberg, H., Tinnerberg, H., 2015. Comparison and evaluation of multiple Users' usage of the exposure and risk tool: Stoffenmanager 5.1. Ann. Occup. Hyg. 59, 821–835. https://doi.org/10.1093/annhyg/mev027.

Landberg, H.E., Axmon, A., Westberg, H., Tinnerberg, H., 2017. A study of the validity of two exposure assessment tools: Stoffenmanager and the advanced REACH tool. Ann. Work Expo. Heal. 61, 575–588. https://doi.org/10.1093/annweh/wxx008.

Landrigan, P.J., Fuller, R., Acosta, N.J.R., Adeyi, O., Arnold, R., Basu, N., Baldé, A.B., Bertollini, R., Bose-O'Reilly, S., Boufford, J.I., Breysse, P.N., Chiles, T., Mahidol, C., Coll-Seck, A.M., Cropper, M.L., Fobil, J., Fuster, V., Greenstone, M., Haines, A., Hanrahan, D., Hunter, D., Khare, M., Krupnick, A., Lanphear, B., Lohani, B., Martin, K., Mathiasen, K.V., McTeer, M.A., Murray, C.J.L., Ndahimananjara, J.D., Perera, F., Potočnik, J., Preker, A.S., Ramesh, J., Rockström, J., Salinas, C., Samson, L.D., Sandilya, K., Sly, P.D., Smith, K.R., Steiner, A., Stewart, R.B., Suk, W.A., van Schayck, O.C.P., Yadama, G.N., Yumkella, K., Zhong, M., 2017. The Lancet Commission on pollution and health. Lancet 391. https://doi.org/10.1016/S0140-6736(17)32345-0.

Levin, M., Koponen, I.K., Jensen, K.A., 2014. Exposure assessment of four pharmaceutical powders based on dustiness and evaluation of damaged HEPA filters. J. Occup. Environ. Hyg. 11, 165–177. https://doi.org/10.1080/15459624.2013.848038.

López Lilao, A., Sanfélix Forner, V., Mallol Gasch, G., Monfort Gimeno, E., 2017. Particle size distribution: a key factor in estimating powder dustiness. J. Occup. Environ. Hyg. 14, 975–985. https://doi.org/10.1080/15459624.2017.1358818.

López-Lilao, A., Bruzi, M., Sanfélix, V., Gozalbo, A., Mallol, G., Monfort, E., 2015. Evaluation of the dustiness of different kaolin samples. J. Occup. Environ. Hyg. 12, 547–554. https://doi.org/10.1080/15459624.2015.1019079.

Marquart, H., Heussen, H., Le Feber, M., Noy, D., Tielemans, E., Schinkel, J., West, J., Van Der Schaaf, D., 2008. "Stoffenmanager", a web-based control banding tool using an exposure process model. Ann. Occup. Hyg. https://doi.org/10.1093/annhyg/men032.

Martins, V., Cruz Minguillón, M., Moreno, T., Querol, X., de Miguel, E., Capdevila, M., Centelles, S., Lazaridis, M., 2015. Deposition of aerosol particles from a subway microenvironment in the human respiratory tract. J. Aerosol Sci. 90, 103–113. https://doi.org/10.1016/j.jaerosci.2015.08.008.

Martonen, T.B., Clark, M.L., 1983. The deposition of hygroscopic phosphoric acid aerosols in ciliated airways or man. Toxicol. Sci. 3, 10–15. https://doi.org/10.1093/toxsci/3.1.10.

Determinación de sílice libre cristalina (cuarzo, cristobalita, tridimita) en aire -Método del filtro de membrana / Difracción de rayos X MTA/MA -056/A06, n.d.

Nardi, J., Nascimento, S., Göethel, G., Gauer, B., Sauer, E., Fão, N., Cestonaro, L., Peruzzi, C., Souza, J., Garcia, S.C., 2018. Inflammatory and oxidative stress parameters as potential early biomarkers for silicosis. Clin. Chim. Acta 484, 305–313. https://doi.org/10.1016/j.cca.2018.05.045.

Notø, H., Nordby, K.-C., Skare, Ø., Eduard, W., 2018. Job tasks as determinants of thoracic aerosol exposure in the cement production industry. Ann. Work Expo. Heal. 62, 88–100. https://doi.org/10.1093/annweh/wxx085.

Pallant, J., 2007. SPSS Survival Manual, a Step by Step Guide to Data Analysis Using SPSS for Windows. McGraw-Hill Companies.

PD CEN/TR 16013-2:2010 - Workplace exposure. Guide for the use of direct-reading instruments for aerosol monitoring. Evaluation of airborne particle concentrations using optical particle counters, n.d. doi:10.3403/30209359

Peters, T.M., Elzey, S., Johnson, R., Park, H., Grassian, V.H., Maher, T., O'Shaughnessy, P., 2008. Airborne monitoring to distinguish engineered nanomaterials from incidental particles for environmental health and safety. J. Occup. Environ. Hyg. 6, 73–81. https://doi.org/10.1080/15459620802590058.

Raul, A.C., Dwyer, J.Z., 2003. Regulatory Daubert: a proposal to enhance judicial review of agency science by incorporating Daubert principles into administrative law. Law Contemp. Probl.

Ribalta, C., Koivisto, A.J., López-Lilao, A., Estupiñá, S., Minguillón, M.C., Monfort, E., Viana, M., 2019a. Testing the performance of one and two box models as tools for risk assessment of particle exposure during packing of inorganic fertilizer. Sci. Total Environ. 650, 2423–2436. https://doi.org/10.1016/j.scitotenv.2018.09.379.

Ribalta, C., Viana, M., López-Lilao, A., Estupiñá, S., Minguillón, M.C., Mendoza, J., Díaz, J., Dahmann, D., Monfort, E., 2019b. On the relationship between exposure to particles and dustiness during handling of powders in industrial settings. Ann. Work Expo. Heal. 63, 107–123. https://doi.org/10.1093/annweh/wxy092.

Riedmann, R.A., Gasic, B., Vernez, D., 2015. Sensitivity analysis, dominant factors, and robustness of the ECETOC TRA v3, Stoffenmanager 4.5, and ART 1.5 occupational exposure models. Risk Anal. 35, 211–225. https://doi.org/10.1111/risa.12286.

Savic, N., Gasic, B., Vernez, D., 2018. ART, Stoffenmanager, and TRA: a systematic comparison of exposure estimates using the TREXMO translation system. Ann. Work Expo. Heal. 62, 72–87. https://doi.org/10.1093/annweh/wxx079.

Schinkel, J., Warren, N., Fransman, W., van Tongeren, M., McDonnell, P., Voogd, E., Cherrie, J.W., Tischer, M., Kromhout, H., Tielemans, E., 2011. Advanced REACH tool (ART): calibration of the mechanistic model. J. Environ. Monitor. 13, 1374. https://doi.org/10.1039/c1em00007a.

Shouroki, F.K., Shahtaheri, S.J., Golbabaei, F., Barkhordari, A., Rahimi-Froushani, A., 2015. Biological monitoring of glazers exposed to lead in the ceramics industry in Iran. Int. J. Occup. Saf. Ergon. 21, 359–364. https://doi.org/10.1080/10803548.2015.1085751.

Spinazzè, A., Lunghini, F., Campagnolo, D., Rovelli, S., Locatelli, M., Cattaneo, A., Cavallo, D.M., 2017. Accuracy evaluation of three modelling tools for occupational exposure assessment. Ann. Work Expo. Heal. 61, 284–298. https://doi.org/10.1093/annweh/wxx004.

Tielemans, E., Noy, D., Schinkel, J., Heussen, H., Van Der Schaaf, D., West, J., Fransman, W., 2008a. Stoffenmanager exposure model: development of a quantitative algorithm. Ann. Occup. Hyg. 52, 443–454. https://doi.org/10.1093/annhyg/men033.

Tielemans, E., Schneider, T., Goede, H., Tischer, M., Warren, N., Kromhout, H., Van Tongeren, M., Van Hemmen, J., Cherrie, J.W., 2008b. Conceptual model for assessment of inhalation exposure: defining modifying factors. Ann. Occup. Hyg. 52, 577–586. https://doi.org/10.1093/annhyg/men059.

van Tongeren, M., Lamb, J., Cherrie, J.W., MacCalman, L., Basinas, I., Hesse, S., 2017. Validation of lower tier exposure tools used for REACH: comparison of tools estimates with available exposure measurements. Ann. Work Expo. Heal. 61, 921–938. https://doi.org/10.1093/annweh/wxx056.

Van Broekhuizen, P., Van Veelen, W., Streekstra, W.H., Schulte, P., Reijnders, L., 2012. Exposure Limits for Nanoparticles: Report of an International Workshop on Nano Reference Values, in: Annals of Occupational Hygiene. Edinburgh Napier University, pp. , pp. 515–524 https://doi.org/10.1093/annhyg/mes043.

Van Tongeren, M., Fransman, W., Spankie, S., Tischer, M., Brouwer, D., Schinkel, J., Cherrie, J.W., Tielemans, E., 2011. Advanced REACH tool: development and application of the substance emission potential modifying factor. Ann. Occup. Hyg. 55, 980–988. https://doi.org/10.1093/annhyg/mer093.

Viana, M., Rivas, I., Reche, C., Fonseca, A.S., Pérez, N., Querol, X., Alastuey, A., Álvarez-Pedrerol, M., Sunyer, J., 2015. Field comparison of portable and stationary instruments for outdoor urban air exposure assessments. Atmos. Environ. 123, 220–228. https://doi.org/10.1016/j.atmosenv.2015.10.076.

Wang, Y.F., Tsai, P.J., Chen, C.W., Chen, D.R., Hsu, D.J., 2010. Using a modified electrical aerosol detector to predict nanoparticle exposures to different regions of the respiratory tract for workers in a carbon black manufacturing industry. Environ. Sci. Technol. 44, 6767–6774. https://doi.org/10.1021/es1010175.

Winkler-Heil, R., Ferron, G., Hofmann, W., 2014. Calculation of hygroscopic particle deposition in the human lung. Inhal. Toxicol. 26, 193–206. https://doi.org/10.3109/08958378.2013.876468.

World Health Organization, 2016. Ambient Air Pollution: A Global Assessment of Exposure and Burden of Disease. World Heal. Organ. 1–131. https://doi.org/9789241511353.

Ziemann, C., Escrig, A., Bonvicini, G., Ibanez, M.J., Monfort, E., Salomoni, A., Creutzenberg, O., 2017. Organosilane-based coating of quartz species from the traditional ceramics industry: evidence of Hazard reduction using in vitro and in vivo tests. Ann. Work Expo. Heal. 61, 468–480. https://doi.org/10.1093/annweh/wxx014.

4.2.1. Additional Results Publication II: Health risk assessment from exposure to particles during packing in working environments

The work presented in this paper was expanded for this PhD Thesis by performing the risk assessment for the materials packed in packing line H (high mitigation strategies applied) with the ART, Stoffenmanager and the NanoSafer tools.

Table 4.1 Calculated 8h TWA (including pre-activity concentrations) for inhalable and respirable mass fractions based on exposure measurements conducted in the worker area (WA). Risk assessment results conducted with the ART (Mechanistic and Bayesian), Stoffenmanager and NanoSafer v1.1 using Continuous drop (C.D) index. NF: near-field. FF: far-field.

8h TWA values	WA Respirable (µg m^{-3})	WA Inhalable (µg m^{-3})	ART (inhalable µg m^{-3})		Stoffenmanager (inhalable µg m^{-3})	NanoSafer (respirable (NF-FF) µg m^{-3})
			Mechanistic	Bayesian		
Feldspar 2	386	2512	1400 (740-2600)	3800 (2800-5100)	680	46481-14522
Kaolin 2	149	709	1200 (650-2300)	3700 (2700-5100)	600	9573-2991

The ART mechanistic model underestimated measured exposure inhalable mass concentrations for Feldspar 2 and overestimated exposure for Kaolin 2, but within a ratio range of 0.6-1.7. Conversely, ART Bayesian overestimated exposure for both materials, with a ratio < 2 only for Feldspar 2. Stoffenmanager underestimated exposure for both materials with ratios 0.3 and 0.8 for Feldspar 2 and Kaolin 2, respectively. Conversely, NanoSafer, as with the other materials of this study, highly overestimated exposures for both materials. It should be noted, as discussed in chapter 3 (Methodology), that NanoSafer was developed to model mainly risks due to NP exposures, although it should be able to assess and manage emissions from powder handling and point source emissions. NanoSafer is at present undergoing test and calibration phases. Therefore, the results provided by this model should not be considered as final and are fully directly applicable to this case study.

Additionally, the ART tool was applied by using R.D dustiness index instead of the C.D index. The same was not conducted with Stoffenmanager (as the tool do not have the option to introduce a dustiness index or level categorization), or NanoSafer (as the input required is respirable dustiness index and difference between C.D W_R and R.D W_R is very small, 6-104 vs. 13-80 mg Kg^{-1}, respectively). The ART mechanistic model underestimated

exposure in all cases with ratios modelled/measured < 0.2. Conversely, ART Bayesian predicted concentrations within a ratio range 0.5-2.0 in 5 out of 11 cases, with underestimations for 9 out of 11 cases.

Table 4.2 Calculated 8h TWA (including pre-activity concentrations) for inhalable mass fraction in the worker area. Risk assessment results conducted with the ART (Mechanistic and Bayesian using Rotating drum (R.D) index. WA Inhalable: exposure concentrations measured in the worker area (WA).

Packing Line	Material	WA Inhalable (µg m^{-3})	ART (inhalable µg m^{-3})	
			Mechanistic	Bayesian
Low	Clay 1	1454	39 (20-74)	420 (230-820)
	Clay 2	780	97 (52-190)	940 (530-1700)
	Kaolin 1	1538	55 (29-110)	570 (310-1100)
Medium	Feldspar 1	1679	25 (13-48)	310 (170-650)
	Quartz 1	1317	27 (14-52)	330 (180-670)
High	Feldspar 2	2512	140 (73-270)	1300 (770-2200)
	Kaolin 2	709	120 (65-240)	1200 (660-1900)

4.3. Publication III: Testing the performance of one and two box models as tools for risk assessment of particle exposure during packing of inorganic fertilizer

Authors:

Carla Ribalta[1,2], Antti J. Koivisto[3], Ana López-Lilao[4], Sara Estupiñá[4], María C. Minguillón[1], Eliseo Monfort[4], Mar Viana[1].

[1]Institute of Environmental Assessment and Water Research (IDÆA-CSIC), C/ Jordi Girona 18, 08034 Barcelona, Spain.

[2]Barcelona University, Chemistry Faculty, C/ de Martí i Franquès, 1-11, 08028 Barcelona, Spain

[3]National Research Centre for the Working Environment, Lersø Parkallé 105, Copenhagen DK-2100, Denmark.

[4]Institute of Ceramic Technology (ITC)- AICE - Universitat Jaume I, Campus Universitario Riu Sec, Av. Vicent Sos Baynat s/n, 12006 Castellón, Spain.

Published in:

Science of the Total Environment, 650: 2423–2436, 2019

doi: 10.1016/j.scitotenv.2018.09.379

Please cite this article as: Ribalta, C., Koivisto, A.J., López-Lilao, A., Estupiñá, S., Minguillón, M.C., Monfort, E., and Viana, M., 2019. Testing the performance of one and two box models as tools for risk assessment of particle exposure during packing of inorganic fertilizer. *Science of The Total Environment*, 650, 2423–2436.

Accepted date: 28 September 2018

Journal Impact Factor / 5-Year Impact Factor: 4.610 / 4.984

Science of the Total Environment 650 (2019) 2423–2436

Contents lists available at ScienceDirect

Science of the Total Environment

journal homepage: www.elsevier.com/locate/scitotenv

Testing the performance of one and two box models as tools for risk assessment of particle exposure during packing of inorganic fertilizer

Carla Ribalta [a,b,*], Antti J. Koivisto [c], Ana López-Lilao [d], Sara Estupiñá [d], María C. Minguillón [a], Eliseo Monfort [d], Mar Viana [a]

[a] Institute of Environmental Assessment and Water Research (IDÆA-CSIC), C/ Jordi Girona 18, 08034 Barcelona, Spain
[b] Barcelona University, Chemistry Faculty, C/ de Martí i Franquès, 1-11, 08028 Barcelona, Spain
[c] National Research Centre for the Working Environment, Lersø Parkallé 105, Copenhagen DK-2100, Denmark
[d] Institute of Ceramic Technology (ITC) - AICE - Universitat Jaume I, Campus Universitario Riu Sec, Av. Vicent Sos Baynat s/n, 12006 Castellón, Spain

HIGHLIGHTS

- Occupational exposure to particles during industrial packing was assessed.
- No significant increases were found during packing of a granulate fertilizer.
- One and two box models predicted adequately actual worker exposure.
- Including outdoor concentrations in models was seen to improve their performance.
- Models parametrization was seen to be a key issue to adequately predict exposure.

GRAPHICAL ABSTRACT

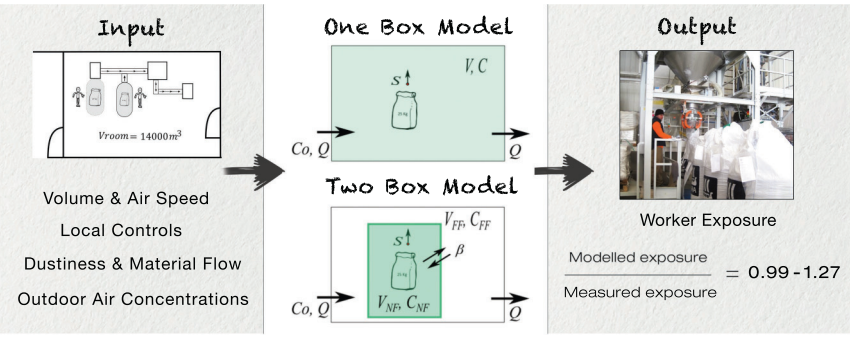

ARTICLE INFO

Article history:
Received 24 April 2018
Received in revised form 28 September 2018
Accepted 28 September 2018
Available online 2 October 2018

Keywords:
Indoor aerosol modelling
Exposure prediction
Occupational exposure
Industrial packing
Risk management

ABSTRACT

Modelling of particle exposure is a useful tool for preliminary exposure assessment in workplaces with low and high exposure concentrations. However, actual exposure measurements are needed to assess models reliability. Worker exposure was monitored during packing of an inorganic granulate fertilizer at industrial scale using small and big bags. Particle concentrations were modelled with one and two box models, where the emission source was estimated with the fertilizer's dustiness index. The exposure levels were used to calculate inhaled dose rates and test accuracy of the exposure modellings. The particle number concentrations were measured from worker area by using a mobility and optical particle sizer which were used to calculate surface area and mass concentrations. The concentrations in the worker area during pre-activity ranged 63,797–81,073 cm^{-3}, 4.6×10^6 to 7.5×10^6 μm^2 cm^{-3}, and 354 to 634 μg m^{-3} (respirable mass fraction) and during packing 50,300 to 85,949 cm^{-3}, 4.3×10^6 to 7.6×10^6 μm^2 cm^{-3}, and 279 to 668 μg m^{-3} (respirable mass fraction). Thus, the packing process did not significantly increase the exposure levels. Chemical exposure was also under control based on REACH standards. The particle surface area deposition rate in respiratory tract was up to 7.6×10^6 μm^2 min^{-1} during packing, with 52%–61% of deposition occurring in the alveolar region. Ratios of the modelled and measured concentrations were 0.98 ± 0.19 and 0.84 ± 0.12 for small and big bags, respectively, when using the one box model, and 0.88 ± 0.25 and 0.82 ± 0.12, when using the two box model. The modelling precision improved for both models when outdoor particle concentrations were included. This study shows that exposure concentrations in a low emission industrial scenario, e.g.

* Corresponding author at: Institute of Environmental Assessment and Water Research (IDÆA-CSIC), C/ Jordi Girona 18, 08034 Barcelona, Spain.
E-mail address: carla.ribalta@idaea.csic.es (C. Ribalta).

https://doi.org/10.1016/j.scitotenv.2018.09.379

during packing of a fertilizer, can be predicted with a reasonable accuracy by using the concept of dustiness and mass balance models.

1. Introduction

Industrial bag filling, packing and pouring processes have been pointed out as activities with high potential to emit airborne particles. Studies in different industrial sectors had reported from very low to high levels of worker exposure to particles, e.g.; during pouring and packing of paint pigments, packing of TiO_2, carbon black, fullerenes and carbon nanofibers (Ding et al., 2017; Fujitani et al., 2008; Koivisto et al., 2015, 2012a; Koponen et al., 2015; Kuhlbusch et al., 2004; Evans et al., 2010) as well as packing and pouring of cement materials (Notø et al., 2018; Peters et al., 2008). Additionally, differences in particle release have been observed when pouring different materials, different amounts, and using different types of mixing tanks (Koponen et al., 2015). Thus, every case is specific and further research is needed in order to understand emission patterns during packing and pouring.

Exposure to particulate matter (PM) is known to cause various adverse health effects, such as respiratory and cardiovascular diseases (Landrigan et al., 2017). Current epidemiological and toxicological studies consider $PM_{2.5}$ (with aerodynamic particle diameter $D_p \leq 2.5$ μm) as the most harmful component for human health (Gakidou et al., 2017; Landrigan et al., 2017; World Health Organization, 2016). Inhalation by humans of dust from inorganic complex fertilizers, which are the object of the present study, results in health effects which might be detected especially after long-term exposures. Inorganic complex fertilizers generally contain basic nutrients (nitrogen, phosphorus, potassium) as well as secondary and micronutrients (calcium, magnesium, boron, manganese) (Roy et al., 2006). Specifically, the fertilizer under study in this work is composed by ammonium nitrate, potassium nitrate and calcium fluoride. Ammonium nitrate, when inhaled, was seen to cause possibly meaningful pulmonary function changes (Kleinman et al., 1980) and to be irritating, cause coughing, bronchospasm, laryngospasm and laryngeal edema even at low concentrations (Gorguner and Akgun, 2003). Additionally, the clinical examination of workers of the ammonium nitrate production showed frequent cases of chronic bronchitis and radiculoneuropathy (Tsimakuridze et al., 2005). On the other hand, ammonium nitrate is known to be potentially explosive when confined. Potassium nitrate, has been seen to be irritating for the respiratory tract (INCHEM, 2001). Therefore, the study of packing of an inorganic fertilizer is of interest as workers can be exposed to relatively high concentrations of airborne fertilizer particles, which might cause respiratory health effects.

Exposure prediction models have been proposed as valuable risk assessment tools. Since the initial application of exposure prediction models, several research papers have been published regarding their theoretical aspects (Ganser and Hewett, 2017; Hewett and Ganser, 2017; Hussein and Kulmala, 2008; Nazaroff, 2004; Nazaroff and Cass, 1989). The two box model is a well-accepted exposure assessment tool in the risk assessment field as, even with its simplified assumptions, it is able to adequately simulate actual conditions for various processes including volatile compounds and PM emissions (Arnold et al., 2017; Jayjock et al., 2011). In the chemical industry, models have been tested in a variety of cases (Nicas, 2016; Sahmel et al., 2009 and references therein). However, when testing the models for PM in actual industrial environments, the number of studies decreases (Boelter et al., 2009; Johnson et al., 2011; Jones et al., 2011; Koivisto et al., 2015; Lopez et al., 2015). Recently, Arnold et al. (2017) conducted a study where the one and two box models, were evaluated under highly controlled conditions. Predicted exposure results for three industrial solvents when using near and far field models was categorized excellent and good to excellent under the ASTM Standard 5157 criteria (Arnold et al., 2017). However, in order to implement prediction models as trustable tools for worker risk assessment, additional real-world cases (including low and high exposure concentration scenarios) need to be evaluated, in order to validate model performance under real-world settings. Especially, performance of models on low concentration scenarios is relevant since real industrial exposure concentrations (especially for nanomaterials) are frequently low (Fonseca et al., 2018; Koivisto et al., 2012a; Koponen et al., 2015; Kuhlbusch et al., 2004). Thus, if models are to be used as tools for risk assessment, testing their performance in low emission and concentration scenarios is paramount. This, will favour understanding of the uncertainties related to critical parameters, such as the source characterization, local controls, and air mixing (Jayjock et al., 2011; Sahmel et al., 2009).

The objectives of the present study were 1) to perform a worker exposure and risk assessment study of packing of an inorganic complex fertilizer in an industrial plant, and 2) to test the one box and two box models performance in a real-world setting in order to contribute to the better understanding and validation of exposure prediction models. A real industrial case scenario, characterized by low particle emissions and subsequently low exposure concentrations, was selected for this purpose with the aim to test the applicability of models at the lower end of the particle concentration range. In this way, results are expected to be extrapolable to industrial settings dealing with nanomaterial exposures, which are typically low (e.g., Koivisto et al., 2012a; Kuhlbusch et al., 2004).

2. Methodology

2.1. Fertilizer chemical composition

The main chemical components of the fertilizer under study (commercial complex inorganic fertilizer) were ammonium nitrate; NH_4NO_3 (15–20%), potassium nitrate; KNO_3 (12.5–15%) and calcium fluoride; CaF_2 (2–3%), according to the material's safety data sheet. The fertilizer was granulated in 2.5 to 5 mm diameter spherical pellets. The product is not classified as hazardous according to regulation EC 1272/2008. However, it may intensify fire (oxidizer) it causes serious eye irritation, the inhalation of its degradation products may cause health hazards, and serious effects may be derived following exposure (material's safety data sheet). According to the European Chemicals Association (ECHA), Derived No Effect Level (DNEL) for long term inhalation are 37.6 mg m^{-3} for ammonium nitrite, 36.7 mg m^{-3} for potassium nitrite and 5 mg m^{-3} for calcium fluoride. For calcium fluoride, the EU occupational exposures limit (OEL) time-weighted average (TWA) is 2.5 mg m^{-3}. Recommended controls are good general ventilation, the use of safety glasses with side-shields, chemical resistant gloves and respiratory protection in case of inadequate ventilation (material's safety data sheet).

2.2. Work environment and packing process

The measurements were carried out during packing of a fertilizer in two different packing lines between the 23th and 26th of January 2017 at an industrial facility located in Castellón, Spain.

The packing hall was only naturally ventilated and the replacement air came from outdoors and from adjacent industrial hall via doors, which were always open (Fig. 1). The packing lines were for small bags (25 kg) and big bags (600 kg) where the studied fertilizer was

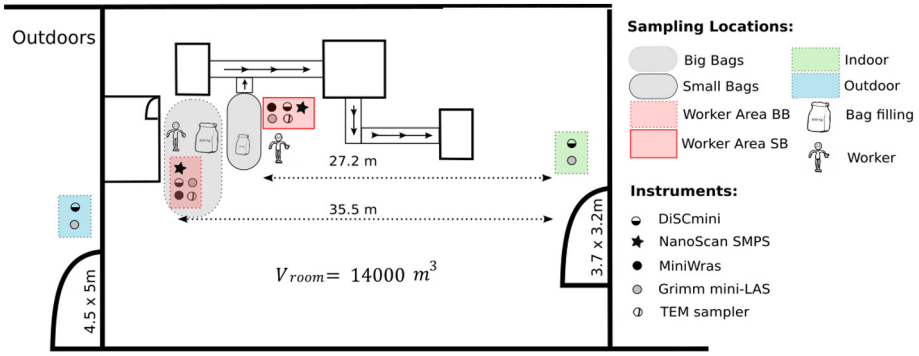

Fig. 1. Packing industrial unit layout. Measurement locations as well as devices used during packing operation are pointed out. BB: big bags. SB: small bags.

poured into the bags from a silo by using a feed funnel. Fig. S1 in the Supporting information shows photos from the packing lines. The two packing lines were not operated at the same time. Two-day measurements were conducted at both packing lines, small bags day 1 (SB1), small bags day 2 (SB2), big bags day 1 (BB1) and big bags day 2 (BB2). In small bags, packing was carried out through an opening fitting the bag width (33–35 cm) and subsequently mechanically sealed. The fertilizer was poured at a flow of 250 kg min^{-1} and the drop height was 5 cm from the feed funnel to the bag opening. Total material drop height was approximately 0.6 m. The packing process was fully automated and the process area was partially enclosed. In big bags, packing was carried out through a cylindrical opening (20 cm diameter) and at a 175 kg min^{-1} flow; material drop height was 20 cm from the feed funnel to the bag opening. Total material drop height was approximately 1.3 m. In that case, the bag was manually closed by the worker, who was standing in front of the bag at approximately 0.5 m distance.

During small and big bags filling, workers tasks were to control and guarantee the correct functioning of the lines as well as to move the filled bags to the storage area using an electric forklift. Occasionally, diesel-powered forklifts were performing truck loading and unloading operations in the hall.

2.3. Aerosol measurements and sampling

Particle number and mass concentrations were monitored in real time in the worker area (WA), indoors, and outdoors (Fig. 1). All online instruments were synchronized prior to the measurements and intercompared overnight between experiments. Particle concentrations during packing were measured for approximately 2 h. Additionally, 30 min of pre-activity concentrations were measured for each day except for BB2.

In the worker area, the instruments were placed on a portable table at approximately 1 m height (instrument inlets being at 1.5 m above the ground level), at 0.5 m from the emission source and 1 m from the worker (Figs. 1 and S1, Supporting information). The monitoring instruments were:

- An electrical mobility spectrometer (NanoScan, SMPS TSI Model 3910; sample flow rate 0.7 l min^{-1}) to measure particle number concentration and particle size distribution in 13 channels from 10 to 420 nm with a 1 minute time resolution
- A Mini Wide Range Aerosol Spectrometer (Mini-WRAS 1371; sample flow rate 1.2 l min^{-1}) to measure particle mass concentration, particle number concentration and particle size distribution from 10 nm to 35 μm in 41 channels with a 1 minute time resolution
- A miniature diffusion size classifier (DiSCmini Matter Aerosol, Testo; sample flow rate 1 l min^{-1}) to measure particle number concentration, mean particle size and alveolar lung deposition surface area (LDSA) in a range of 10 to 700 nm with a 1 minute time resolution
- A Mini Laser Aerosol Spectrometer (Grimm, Mini-LAS 11R; sample flow rate 1.2 l min^{-1}) to measure particle mass concentration from 0.25 to 32 μm in 31 channels with a 1 minute time resolution.

The indoor and outdoor concentrations were monitored by using a DiSCmini and a Grimm Mini-LAS, with the same settings as described above.

During the packing process, particles emitted were collected onto Au grids (Quantifolil ® with 1 μm diameter holes – 4 μm separation of 200 mesh). The grids were attached to polycarbonate filters that were placed in a sampling cassette (SKC INC., USA, inlet diameter 1/8 in. and filter diameter 25 mm). The cassette was connected to a Leland pump with an operating flow rate of 3 l min^{-1}. The morphology and primary particle size of the particles collected were determined using a transmission electron microscope (TEM, Jeol, JEM 1220, Tokyo, Japan) coupled with an energy-dispersive X-ray (EDX) spectrometer. Particle samples for subsequent chemical characterization were not collected due to the short sampling times (3–4 h), as the samples would not have been representative of full 8-hour shifts. This should be considered a limitation of the study.

The worker area particle number size distributions measured by the NanoScan and MiniWras were combined according to Koivisto et al. (2012a) to obtain a wide range for particle size distribution from 10 nm to 35 μm. NanoScan size channels between 11.5 and 86.6 nm were used while channels ranging from 139 nm to 35 μm were taken from the MiniWras. Between 86.6 nm and 139 nm a combined channel (108.6 nm) was created. Upper channels from NanoScan (>115.5 nm) were not used as it is known to not have a good resolution for particles >200 nm (Fonseca et al., 2016), while MiniWras was seen to not accurately measure particles under 50 nm; therefore, MiniWras lower channels were not used (see Fig. S2, Supporting information) and explanation. Here, due to channels cut, ultrafine particles are defined as $D_p < 86.60$ nm, fine particles as 86.60 nm < Dp < 943.0 nm and coarse particles as >943.0 nm.

Increases and reductions in exposure during packing when comparing with pre-activity levels were considered statistically significant when the following approach (Asbach et al., 2012; Kaminski et al., 2015) was fulfilled:

$$\text{Mean concentration during packing} > BG \pm 3 * (\sigma BG)$$

where BG is the mean temporal background (pre-activity) concentration and σBG is the standard deviation of the background concentration.

2.4. Dustiness

Material dustiness was assessed by using the continuous drop standard method (EN 15051). The continuous drop device, made of stainless

steel, consisted of a cylindrical pipe through which air circulated in an upward direction with a volume flow rate of 53 l min^{-1}. Concentric to the cylindrical pipe there was an inner pipe, slightly shorter than the cylindrical pipe, through which material was dropped at a flow rate of 6 to 10 g min^{-1}, so that the powdered material was released into a countercurrent airflow (López-Lilao et al., 2015). Total material drop height during the test is approximately 1.2 m. Two sampling heads for inhalable (approximately PST; designed by Institut für Gefahrstoff-Forschung-IGF) and respirable (approximately PM_4; FSP-2, BGIA) fractions were located slightly above the discharge position of the material. Samples for gravimetric measurements of inhalable and respirable fractions were collected on cellulose thimbles, single thickness, 10 × 50 mm 25/pk and PVC filters of 37 mm and 5 μ of porosity respectively. The experiment, which lasted for 10 min, was repeated two times to ensure results repeatability. Between experiment repetitions, the sampling heads for inhalable and respirable fractions were superficially cleaned while the rest of the device was thoroughly cleaned only at the end of the test.

2.5. Exposure modelling

2.5.1. One- and two-box dispersion models

Exposure modelling was performed by using a one box model (Hewett and Ganser, 2017) and a two box model (Ganser and Hewett, 2017). Fig. 2 shows the models schemes and the mass balance

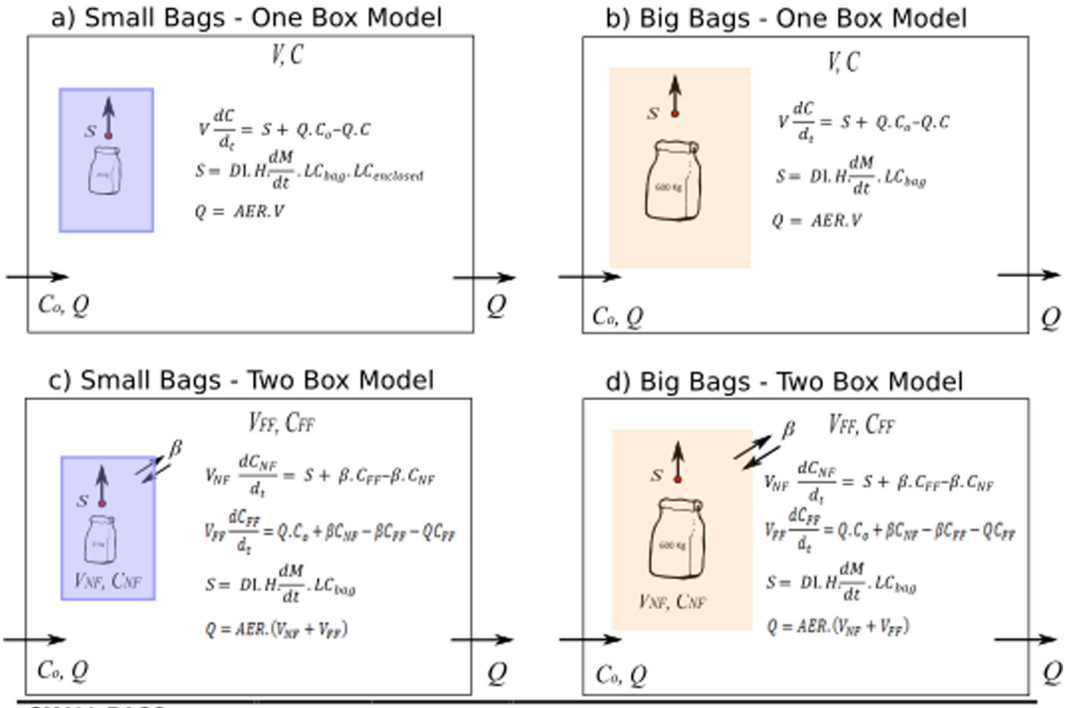

SMALL BAGS			
Respirable dustiness index	*DI*	16 mg/kg	Very low dustiness index
Mass flow	*dM/dt*	250 kg/min	Mass flow value
Handling energy	*H*	0.5	Drop height is approximately half of the dustiness test drop height
Local emission controls	LC_{bag} $LC_{enclosed}$	0.6 0.5	0.6 = bag acts as a protection (reduction of the emissions of a 40%) 0.5 = process enclosed (reduction of the emissions of a 50%)
Room volume	V_{room}/V_{FF}	14000 m^3	Big industrial unit
Air Exchange rate	*AER*	7 ACH	Medium ventilation rate
Near field volume	V_{NF}	6 m^3	Volume of the enclosed space, it does not include the worker area
Near field air flow	β	0.75 m^3/min	Low air exchange NF-FF (enclosed process)
BIG BAGS			
Respirable dustiness index	*DI*	16 mg/kg	Very low dustiness index
Mass flow	*dM/dt*	175 kg/min	Mass flow value
Handling energy	*H*	1	1 is equivalent to the drop height in the dustiness test
Local emission controls	LC_{bag}	0.6	0.6 = bag acts as a protection (reduction of the emissions of a 40%)
Room volume	V_{room}/V_{FF}	14000 m^3	Big industrial unit
Air Exchange rate	*AER*	7 ACH	Medium ventilation rate
Near field volume	V_{NF}	25m^3	Volume of the bagging line were the process of bag filling is taking place
Near field air flow	β	30 m^3/min	High air exchange NF-FF (opened process)

Fig. 2. One box and two box model description and parameters values (table). For small bags, one box model (a) and two box model (c) and for big bags, one box model (b) and two box model (d).

equations. The models assume that 1) particles are fully mixed at all times; 2) mass is created by a source inside the plant (near field in two box model) and by concentrations coming from outdoors; 3) there are no other particle losses than the natural ventilation. The models were used to calculate the respirable fraction. Particle losses by sedimentation may be considered negligible for this size fraction.

2.5.2. Emission source

The emission (S) from the packing process is described based on the dustiness index as:

$$S(t) = DI \cdot H \cdot \frac{dM(t)}{dt} \cdot LC \quad (1)$$

where *DI* is the respirable dustiness index of the fertilizer expressed in mg kg^{-1} or particles kg^{-1}, *H* is the handling energy factor for the process, d*M*/d*t* (kg min^{-1}) is the mass flow of the fertilizer, and *LC* is the protection factor of localized controls. The respirable dustiness index of the fertilizer was obtained using the continuous drop method, as it is the method that adapts better to the process under study (Pujara, 1997; Ribalta et al., 2018).

2.5.3. Modelling parametrization

The input parameters needed to run the model and experimentally unavailable in this case study are the handling energy factor (H), local control factors (LC), and the air flow rate (β) between near field (NF) and far field (FF) (for two box model only).

By definition, *H*, links the energy applied during the process with the energy applied during the dustiness test (Schneider and Jensen, 2007) and can range from 0 to 1 (Koivisto et al., 2015; Lidén, 2006). The parameter *H* has been defined for the rotating drum dustiness test by Van Tongeren et al. (2011) for the Advanced REACH tool. However, currently the scaling of the source by using handling energy factor is not yet well understood and works are ongoing in order to parameterize the *H* factor. Here, taking into account the previous cited works and based on our experimental knowledge of the bagging facility, *H* was assumed to be 0.5 for small bags as the drop height during small bags packing was approximately 50% of the drop height in dustiness tests, and 1 for the big bags as the material drop height was similar to the dustiness drop height (see Sections 2.2 and 2.4). With regard to local controls (LC), two main controls were detected. For both small and big bags, the bag itself was estimated in this work to reduce particle release by 40% (applied in the emission rate equation as ($LC_{bag} = 0.6$). In addition, for small bags one box model, the effect of the enclosure was taken into account and applied in the model reducing emission by 50% ($LC_{enclosed} = 0.5$) (Fransman et al., 2008). Finally, β was estimated after testing the range values reported by Baldwin and Maynard (1998) and Arnold et al. (2017) taking into account the characteristics from our case scenarios. A sensitivity analysis for different β was carried out and is reported in the section below (Table 1). Small bags NF volume was 6 m^3 (2 × 2 × 1.5 m) corresponding to the size of the enclosure and for big bags 25 m^3 (3.5 × 3 × 2.5 m), as this is the volume of the packing area including the bag and the worker. For small bags β was set at 0.75 m^3 min^{-1} (0.0125 m s^{-1}) as the air flow rate was considered to be low due to the enclosure of the packing line (enclosure opening of 1 m^2, free surface area (FSA)). In this case, for the two box model, as the effect of the enclosure was introduced by the NF-FF β, the local control regarding the enclosure ($LC_{enclosed}$) in the emission rate equation was suppressed. Big bags FSA is 28 m^3 as the top, bottom and one of the four sides are covered. For big bags, the air flow rate was considered to be higher as there was no enclosure or division between NF and FF, so β was set to 30 m^3 min^{-1} (0.036 m s^{-1}). The model schemes and parameters are listed in Fig. 2. The air exchange rate (AER) between indoor and outdoor air was experimentally calculated considering outdoor wind speed during the measurement period (obtained from the local air quality monitoring network), the size of the outdoors door, and the size of the industrial unit. This resulted in a mean air exchange rate of around 7 h^{-1} for the entire period.

2.6. Calculated active surface area and mass concentrations

The particle active surface area was calculated by applying particle size distribution obtained from NanoScan and MiniWras data combination to Eq. (2) described in Heitbrink et al. (2009) as in Koivisto et al. (2012b).

$$s = \frac{3\pi\lambda D_b}{C_c(D_b)\delta} \quad (2)$$

where λ is the mean free path for air, 0.066 μm, and δ is the scattering parameter for air, 0.905. D_b is the mobility diameter and C_c the slip correction factor for the corresponding aerodynamic or mobility particle size.

The particle mass was additionally calculated by using mobility particle diameter and effective density as in Koivisto et al. (2012b)

$$m = \rho_{eff} \frac{\pi}{6} D_b^3 \quad (3)$$

where ρ_{eff} is the effective density. As fertilizer and airborne particles density was unknown, 1 g cm^{-3} was assumed for simplicity.

2.7. Calculated regional inhalation dose rate

The inhalation dose of deposited particles in the respiratory system during inspiration and expiration was quantified. The regional inhalation dose rate was obtained by multiplying particle size concentrations

Table 1
Sensitivity analysis for different air flow values for small and big bags with ratios (modelled values/measured values). Variation (%) of the modelled concentration when using the higher and lower air flow value is reported. $\beta = \frac{1}{2} \cdot SA \cdot S$; where *SA* is the surface area.

β (m^3 min^{-1})	S (m s^{-1})	SB1 ratio		SB2 ratio		β (m^3 min^{-1})	S (m s^{-1})	BB1 ratio		BB2 ratio	
		With outdoor	Without outdoor	With outdoor	Without outdoor			With outdoor	Without outdoor	With outdoor	Without outdoor
0.36	0.006	0.69	0.63	0.68	0.39	–	–	–	–	–	–
0.5	0.004	0.87	0.81	0.81	0.51	–	–	–	–	–	–
0.75	0.013	1.11	1.06	0.99	0.70	9.4	0.011	1.08	0.70	0.99	0.88
1	0.017	1.30	1.25	1.15	0.86	12.75	0.015	1.10	0.71	1.00	0.89
1.5	0.025	1.56	1.50	1.40	1.1	15	0.018	1.10	0.71	1.01	0.90
1.8	0.030	1.66	1.60	1.51	1.21	–	–	–	–	–	–
2.4	0.040	1.80	1.75	1.67	1.36	30 (33.6)	0.036 (0.04)	1.12	0.73	1.02	0.91
3	0.05	1.89	1.84	1.79	1.50	–	–	–	–	–	–
Variation (%)		36.4	34.6	38.0	25.8	Variation (%)		3.0	4.5	2.6	2.9

on the worker area (NanoScan and MiniWras data combination) by the ICRP human respiratory tract model deposition probability (Eckerman et al., 2011). The respiratory volume used was 25 l min^{-1}, corresponding to male respiration during light exercise (Koivisto et al., 2012b). The regional dose was calculated for head airways, tracheobronchial and alveolar regions by using simplified deposition fraction equations for the ICRP model as described by Hinds (1999). In the model, particles were assumed to be spherical and to preserve their size during inhalation.

2.8. Chemical risk assessment

A chemical risk assessment was conducted by using Stoffenmanager® v.7.1 (hereinafter referred to as Stoffenmanager), which is a risk prioritisation web-based tool consisting of a control banding tool (inhalation and dermal), with a part designed for exposure to engineered nanoparticles (inhalation) and general and REACH specific quantitative inhalation exposure parts (van Tongeren et al., 2017). Stoffenmanager is recommended by ECHA for Tier 2 regulatory exposure assessment (ECHA, 2016a; Spinazzè et al., 2017; van Tongeren et al., 2017). Stoffenmanager background and general assumptions are based on Marquart et al. (2008) whereas the rationale of the algorithm is based on Cherrie and Schneider (1999) but adapted in several ways as described by Tielemans et al. (2008). Stoffenmanager has been validated for different scenarios involving handling of powders, solids, low-volatile and volatile liquids using >6000 measurements (Stoffenmanager®) and in 10 scientific studies (Bekker et al., 2016; Lamb et al., 2015; Landberg et al., 2017, 2015; Riedmann et al., 2015; Savic et al., 2018, 2016; Schinkel et al., 2010; Spinazzè et al., 2017; van Tongeren et al., 2017).

The relative chemical composition of the main components of the fertilizer (ammonium nitrate, 20%; potassium nitrate, 15%; calcium fluoride, 3%) was used to calculate likely inhalable concentrations for each chemical component, based on the total measured inhalable mass concentrations. Subsequently, concentrations were compared with the Derived No Effect Level (DNEL) and risk assessment was applied using the ECHA guidance (ECHA, 2016b) approach which defines risk characterization:

- Controlled risk: [concentration]/DNLE < 1
- Uncontrolled risk: [concentration]/DNLE > 1.

3. Results

3.1. Material morphology and characterization

Samples collected onto Au TEM grids were observed and characterized using TEM-EDX. In the samples collected during SB2 (Fig. 3a, b, c, d and e) and BB1 (Fig. 3f, g, h and i) experiments, particles which main elements were O, Na, K, Ca, Cr and Zn were detected proving the presence of fertilizer particles in the worker area (Fig. 3a, b, c, d, f, g and h). A few differences were observed between both samples. Fertilizer particles size was between 1 μm up to >35 μm in both samples, although in BB1 there was a bigger proportion of bigger particles (Fig. 3f) whereas in SB2 a bigger proportion of smaller ones (Fig. 3c). Additionally, agglomerates of nanoparticles, with particle size < 50 nm and main components O and C, were found on both samples indicating the presence of diesel combustible particles in the worker area, coming from the diesel forklift (Fig. 3d, e, h and i). Those agglomerates were occasionally seen in the BB1 samples (Fig. 3h and i), whereas in the SB2 they were highly abundant (Fig. 3c, d and e) owing to a higher activity of diesel forklifts inside the plant (96.2%; Table 2).

3.2. Dustiness indices

Material dustiness was assessed using the continuous drop method and results were given in terms of inhalable and respirable mass fractions (mg kg^{-1}) gravimetrically analyzed. Following the EN 15051 dustiness classification for continuous drop, the fertilizer under study was classified as a material with low and very low dustiness indices, with

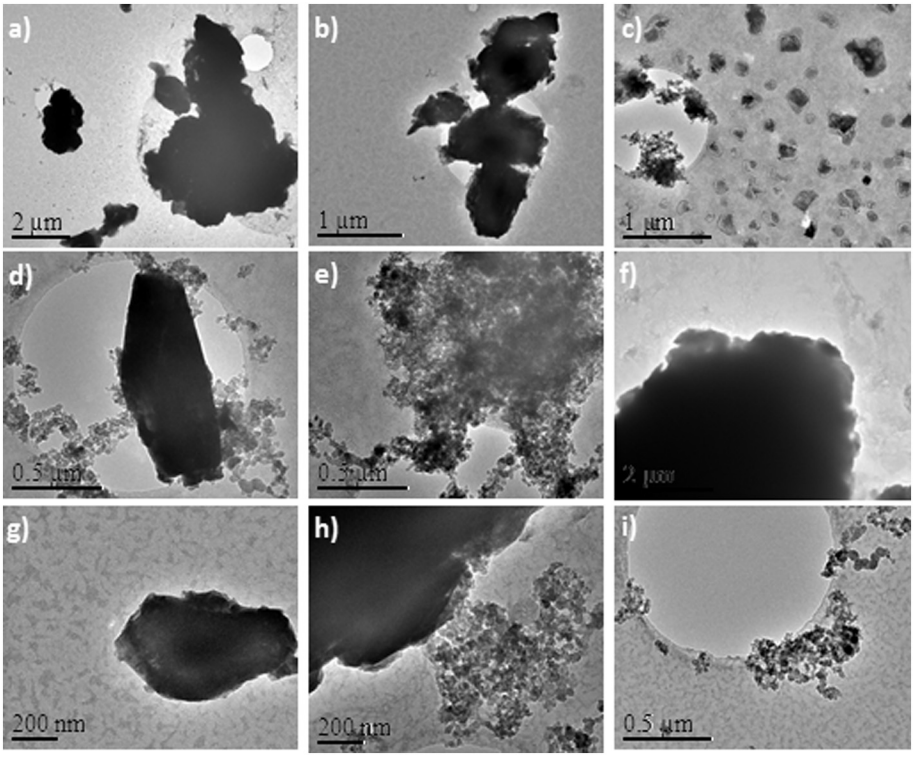

Fig. 3. TEM images of the collected particles during the fertilizer bag filling process with small (a, b, c, d and e), and big bags (f, g, h and i).

Table 2
Pre-activity, total process time, and total time for each activity (packing, electric forklift and diesel forklift) shown in hh:mm. The percentage of time of each activity (packing, electric forklift and diesel forklift) with respect to the total length of the process is included in brackets. Background period (pre-activity) not included. <5 minute difference between stop and start of the next activity was counted as the same period activity.

Process	Background time	Packing process time	Material pouring time (%)	Electric forklift time (%)	Diesel forklift time (%)
SB1	00:41	02:26	02:03 (84.2%)	00:02 (1.4%)	00:44 (30.2%)
SB2	00:46	01:20	01:16 (95.0%)	00:42 (53.2%)	01:17 (96.2%)
BB1	00:36	01:23	00:46 (55.9%)	00:26 (32.1%)	00:31 (38.4%)
BB2	–	02:43	00:36 (22.1%)	00:40 (24.9%)	02:05 (77.1%)

1026 ± 210 mg kg^{-1} and 16 ± 3 mg kg^{-1} for inhalable and respirable fractions, respectively.

3.3. Concentrations

3.3.1. Worker area concentrations

The measurements started 34 to 46 min prior to the packing process. Packing lasted between 1 h 20 min and 2 h 43 min (Table 2). For BB2 no background concentrations could be recorded. During SB1 (Fig. S3), total particle number and inhalable mass concentrations during packing were similar to background concentrations (Table 3 and Fig. S3). Concentrations of fine particles (100 nm–1 μm) and thoracic and respirable mass concentrations were lower during packing compared with pre-activity levels (Table 3, Fig. S3, Supporting information), which resulted from decreasing background concentrations during the pre-activity period (see Fig. S3). Thus, it was concluded that during SB1 experiments no significant impacts on particle exposure were detected. Similarly, during SB2 (Fig. 4) experiments no statistically significant differences were observed in terms of mass concentrations between the pre-activity and activity periods (Table 3, Fig. 4). These results are in agreement with the low dustiness index of the fertilizer material. Conversely, during SB2 total particle number concentration did increase significantly with regard to pre-activity levels (on average for total particle number, 17340 cm^{-3}) (Table 3, Fig. 4). This increase may have been linked to diesel emissions from a diesel forklift which operated inside the plant during this period, as will be discussed below. In addition, very few differences were observed in particle size distributions between the pre-activity and activity particle size distributions for SB1 and SB2 (Fig. 5a and b). In Koivisto et al. (2012a) measurements during packing of TiO_2 into small and large bags did not have an impact on particle concentrations except when opening the enclosed packing machine. Impacts on worker exposure when packing silicon nanoparticles were also not detected probably because the packing line was hermetically sealed (Wang et al., 2012).

During BB1 (Fig. 6), particle number and mass concentrations were again similar to pre-activity concentrations, showing slightly higher (non-statistically significant) mean concentrations (Table 3). Total particle number concentrations increased by 4876 cm^{-3} and respirable mass concentration by 314 μg m^{-3} (Table 3, Fig. 6). During the BB2 experiments (Fig. S4) pre-activity concentrations were not available because the activity was initiated before the monitoring instrumentation was ready, and therefore worker exposure can only be discussed comparing with indoor background concentrations. As in the case of SB1 and SB2 very few differences were observed in particle size distribution between the pre-activity and BB1 packing periods. Only slight increases in particles < 30 nm and >10 μm were observed (Fig. 5c). Contrarily, in Koivisto et al. (2012a), packing of TiO_2 into large bags was seen to increase particles > 500 nm. Even so, the present results were to be expected as when classifying the fertilizer according to its dustiness index, it was sorted as a material with very low and low capacity to generate airborne dust for inhalable and respirable fractions, respectively.

As described above, particle number concentrations increased significantly only during two of the four experiments, i.e., SB2 and BB1. However, those increases were not clearly related to the packing activity as no specific relation was seen with the start and stop of the process (Figs. 4 and 6). Increases of ultrafine particles in comparison with the background were always below 40,000 cm^{-3}, the suggested reference limit value in this specific case (non-biodegradable granular nanomaterials in the range of 1–100 nm and density < 6 kg l^{-1}) (Van Broekhuizen et al., 2012).

Inhalable and respirable mass concentrations did not exceed in any case the limit values for particles not otherwise specified of 10 and 3 mg m^{-3}, respectively (INSH, 2018). Thus, it may be concluded that packing activity of the specific fertilizer did not have a significant impact on worker exposure with regard to particles in the 11.5 nm–35 μm size range. It should be pointed out that in this study worker exposure concentrations do not correspond strictly to the worker breathing zone (because instruments were not worn by the workers), which are expected to be higher (Koivisto et al., 2015; Koponen et al., 2015). Additionally,

Table 3
Mean number concentration and mass concentrations during background period (BG) (pre-activity) and packing process in the worker area (WA). N_{TOT} (Dp: 10 nm–35 μm), N_{UPF} (Dp< 86.60 nm), N_{FP} (86.60 nm < Dp < 943.0 nm), N_C (Dp > 943.0 nm). Mass concentrations are shown in terms of inhalable, thoracic and respirable fractions measured with the Grimm monitor. Calculated dose rates in particle number, $\dot{n}$, and surface area, $\dot{s}$, and regional deposition in percentages on head airways, trachea bronchi and alveolar. Values in bold indicate statistically significant differences compared with background concentrations.

	Small bags day 1 (SB1)		Small bags day 2 (SB2)		Big bags day 1 (BB1)		Big bags day 2 (BB2)	
	BG	Packing	BG	Packing	BG	Packing	BG	Packing
N_{TOT} [cm^{-3}]	67,254 ± 11,076	63,108 ± 29,592	63,797 ± 5435	**81,137 ± 42,448**	81,073 ± 8719	85,949 ± 29,748	–	50,290 ± 40,893
N_{UPF} [cm^{-3}]	61,083	59,900	58,646	**75,912**	73,641	77,945	–	46,359
N_{FP} [cm^{-3}]	6121	**3188**	5129	5197	7383	7935	–	3922
N_C [cm^{-3}]	50	**20**	22	**28**	50	**68**	–	14
Inhalable [μg m^{-3}]	1987 ± 214	2025 ± 975	1866 ± 1141	1276 ± 550	1650 ± 588	1864 ± 556	–	1047 ± 923
Thoracic [μg m^{-3}]	1487 ± 138	**1053 ± 435**	1147 ± 315	962 ± 345	1183 ± 367	1507 ± 381	–	787 ± 721
Respirable [μg m^{-3}]	634 ± 64	**279 ± 131**	362 ± 74	318 ± 109	354 ± 105	668 ± 153	–	528 ± 898
$\dot{n}$, ·10^6 [min^{-1}]	770	857	834	1035	882	1122	–	682
$\dot{s}$, ·10^6 [μm^2 min^{-1}]	6.4	4.3	4.6	6.0	7.5	7.6	–	3.3
$\dot{s}$, ·head airways [%]	30.7	26.3	27.1	26.2	28.0	36.0	–	24.7
$\dot{s}$, ·trachea bronchi [%]	12.7	14.2	13.9	14.0	13.3	12.5	–	14.2
$\dot{s}$, ·alveolar [%]	56.6	59.5	59.0	59.8	58.7	51.5	–	61.1

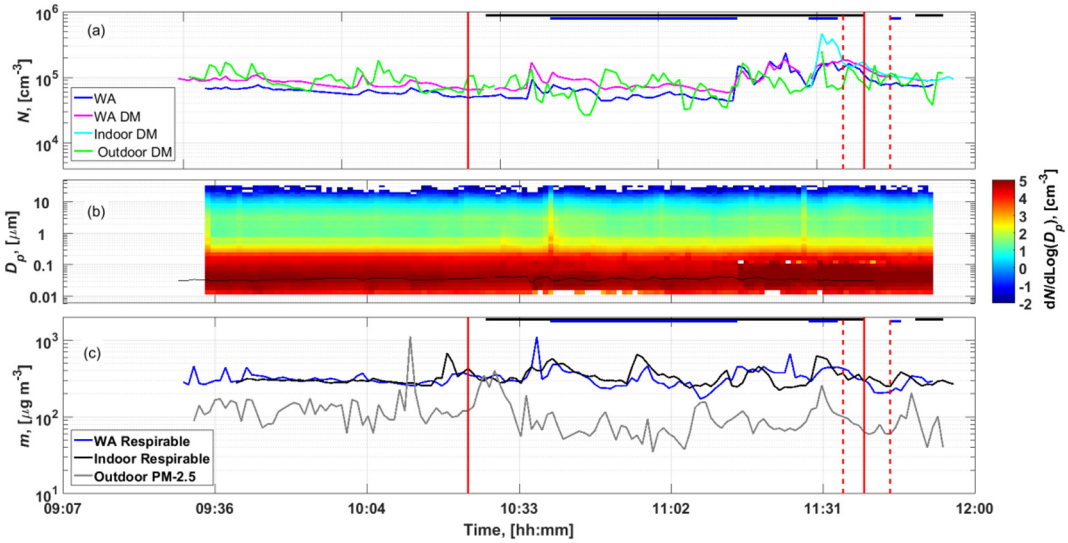

Fig. 4. Particle concentration at packing area (WA) during small bags 2 (SB2): (a) particle number concentration time series; (b) particle size distribution time series measured with the MiniWras and the NanoScan, solid black line shows DiSCmini (DM) D_{50}; (c) mass concentration time series. Red vertical lines indicate start (solid line) and stop (dashed line) of the packing operation and horizontal black and blue lines in the top of the graphs indicate diesel and electric forklifts activity respectively.

the measurements were carried out for a maximum of 2.5 h and therefore not representative of the 8 h necessary to calculate the 8 h time weighted average over a full shift.

Packing processes and similar industrial activities such as material pouring have been previously studied among different types of industries with results indicating that packing, pouring or dumping processes usually lead to slight increases in worker exposure concentrations. Packing of carbon black in bags of 25 kg and 1000 kg was shown to increase airborne particles > 400 nm and mass concentrations (Ding et al., 2017; Kuhlbusch et al., 2004). Fullerenes packing increased particle number > 1000 nm (Fujitani et al., 2008). Evans et al. (2010) also found that dumping of carbon nanofibers into a drum resulted in an increase of respirable mass concentrations. In the case of the cement industry, Notø et al. (2018) found that packing was associated with an increase of worker exposure to the thoracic mass fraction of 12% and 33% when working less than and more than half a shift, respectively. On the contrary, pouring of cement at a construction site was seen to have highly variable and low percentages of inhalable mass exposure, probably because of workers performing pouring operations also carried out other activities (Peters et al., 2008). In comparison to these studies, the fertilizer packing case presented in this work seemed to have one of the lowest impacts on worker exposure to particle mass and number concentrations.

3.3.2. Outdoor concentrations

The packing hall was connected by two doors (Fig. 1) to outdoors and to another industrial unit. In both sites other processes were occasionally ongoing. Thus, influence of outdoors and other processes taking

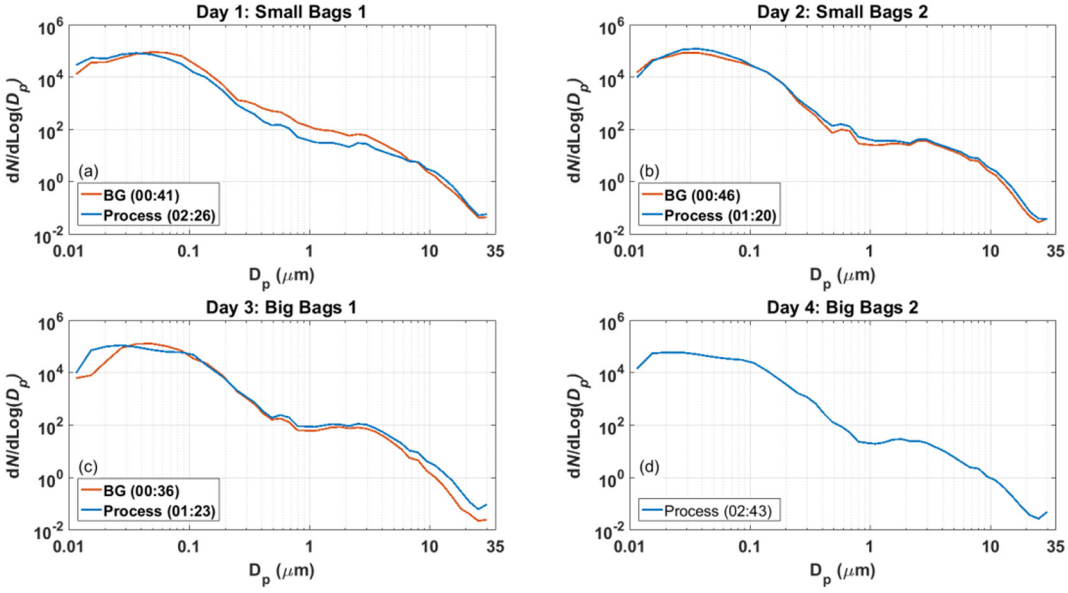

Fig. 5. Average particle size distributions measured by NanoScan and MiniWras during pre-activity and packing processes for (a) small bags day 1, SB1; (b) small bags day 2, SB2; (c) big bags day 1, BB1 and (d) big bags day 2, BB2.

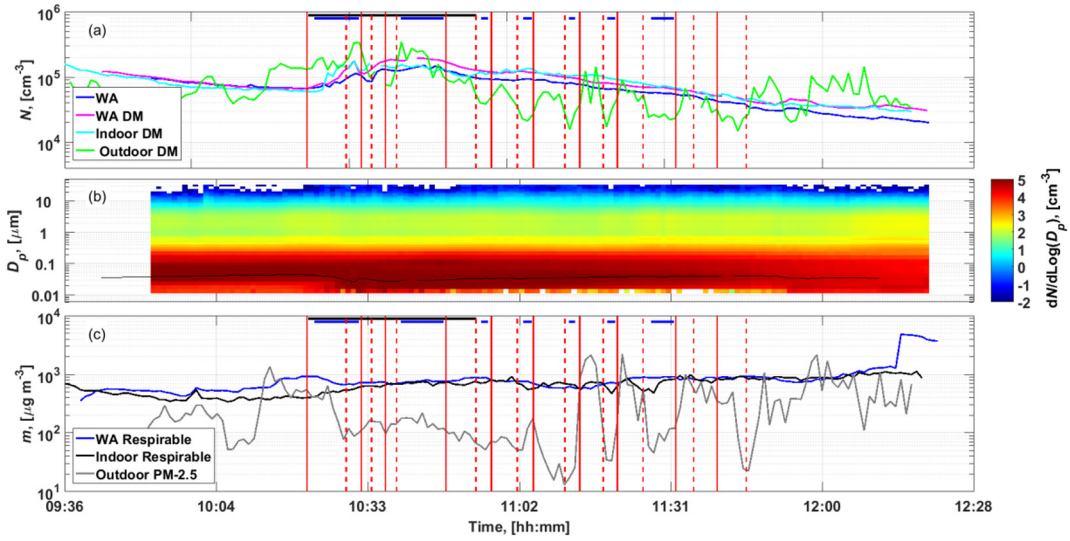

Fig. 6. Particle concentration at packing area (WA) during big bags day 1 (BB1): (a) particle number concentration time series; (b) particle size distribution time series measured with the MiniWras and the NanoScan, solid black line shows DiSCmini (DM) D_{50}; (c) mass concentration time series. Red vertical lines indicate start (solid line) and stop (dashed line) of the packing operation and horizontal black and blue lines in the top of the graphs indicate diesel and electric forklifts activity respectively.

place in the adjacent industrial unit were to be expected. Outdoor particle number concentrations as well as PM_{10} mass were usually lower or in a similar range as the worker area and indoor concentrations (thoracic mass fraction) (Tables S1 and S2, Supporting information). Regarding mean particle size, it was usually smaller in the outdoor location than in the indoor and worker area by 10–20 nm (Table S1, Supporting information) due to the influence of outdoor traffic emissions. Mean particle size remained more or less constant between pre-activity and packing periods in the worker area (38–32, 28–37, 33–37, 41–44 nm), indoor (43–37, 38–43 nm) and outdoor (23–20, 31–31, 29–32 nm) measurement points for all days. In general, outdoor concentrations seemed to follow a different pattern from the rest of the locations even if with some exceptions where similar peaks in outdoor, indoor and worker area were observed (e.g., Figs. 4, 11:30; S3, 15:10; S4, 12:15). Numerous studies have reported the infiltration of outdoor particles into diverse indoor environments, especially through windows and doors when they are open (Bennett and Koutrakis, 2006; Hussein et al., 2009; Koponen et al., 2001; Reche et al., 2014; Rivas et al., 2015; Wang et al., 2010). In Wang et al. (2010), outdoor infiltration was detected in a similar packing industrial unit where indoor and outdoor areas were connected by opened doors as in the present study.

3.3.3. Forklifts activity

Electric and diesel forklift activity was recorded and is shown on the top of Figs. 4, 6, S3 and S4 and as a percentage of total recorded time in Table 2. On certain occasions, increases in particle number concentrations in the worker area and indoor seemed to be related to the use of the diesel forklift while in others this relationship was more difficult to establish. For example, the highest statistically significant increase in mean particle number concentration in the worker area was for SB2, also having the highest percentage of diesel forklift activity 96.2% (Table 2). Moreover, when an increase in number concentration linked to the activity of a diesel forklift was seen in the worker area it was also seen in the outdoor and indoor measurement points. This is probably due to the fact that the diesel forklift was used to load and unload trucks, which means that the forklift was moving from outdoor to indoor having to drive by all the measurement points (worker area, indoor and outdoor). Diesel and propane forklifts have been previously identified as a common source of ultrafine particles (20–50 nm) in activities such as warehouse bagging and packing (Ding et al., 2017; Huang et al., 2010; Kuhlbusch et al., 2004; Tsai et al., 2011; Viitanen et al., 2017; Wang et al., 2010).

In terms of particle mass concentration, no increases were detected linked to diesel forklift emissions. However, during the SB2 packing period, two peaks at 10:40 and 11:30 (Fig. 4b) of particles at around 1 μm were identified, which coincided with the start of an electric forklift. This may have resulted from coarse particle resuspension, as observed previously (Huang et al., 2010).

3.4. Regional inhalation dose rates

Inhalation dose rates were estimated for each day using combined data from NanoScan and MiniWras (Tables 3 and S3). Particle number dose rates ($\dot{n}$) during packing ranged between 682×10^6 and 1122×10^6 min^{-1}. Increases (between 87×10^6 and 240×10^6 min^{-1}) during the packing process were obtained when comparing with pre-activity periods for all days. Surface dose ($\dot{s}$) analysis was calculated as well as respiratory tract deposition percentages. From the total surface area of the deposited particles during packing ($3.3–7.6 \times 10^6$ μm^2 min^{-1}), 52–61% was estimated to deposit in the alveolar region, 13–14% in the trachea bronchi and 25–36% in the head airways (Table 3). The percentage for the alveolar region is lower than that found by Wang et al. (2010), who determined the percentage of deposited surface area in the alveolar region to be 80% during packing in a carbon black manufacturing industry. No increases in the total surface deposited area during packing were observed when compared with the pre-activity periods except for SB2. In addition, an increase on the percentage on the alveolar and trachea bronchi regions during packing was observed for SB1, whereas for the rest, percentages remained approximately the same. This increase in number and surface deposited area is most likely due to the diesel forklift activity or another process taking place near the packing area and not due to the packing process itself, which emits coarser particles as described in previous sections. The day with the highest percentage of diesel forklift activity (SB2) showed the highest increase in total surface deposited area (4.6×10^6 and 6.0×10^6 μm^2 min^{-1} for pre-activity and process respectively). Higher percentages of deposited particles were detected in the alveolar and head airways regions. Particles deposition on the tracheobronchial area is dominated by particles with diameters

under 10 nm. Here, instruments used have a lower limit at around 20 nm. Thus, when analyzing tracheobronchial estimations the previous fact must be considered.

Particle number deposition percentages on the alveolar region ranged between 66 and 69%, similar range as in Wang et al. (2010), who found it to be 64% during packing in a carbon black manufacturing industry. As pointed out in Wang et al. (2010) the use of both metrics, number concentration and surface area, is advisable as, when used separately, different results may be obtained. In Koivisto et al. (2012b) inhalation dose rates as well as percentages of deposited particles in the respiratory tract were calculated for nanoparticle production process in terms of particle number, mass and active surface area. Increases in number concentration and surface area were detected when comparing pre-activity period with process. For that specific case, number concentration was found to be the metric defining better the particles emitted during the process whereas surface area was found to describe process and background particles (Koivisto et al., 2012b).

3.5. Risk assessment: chemical exposure

Chemical risk assessment during fertilizer packing was assessed using Stoffenmanager and by comparing measured inhalable mass concentrations of the different fertilizer components with ECHA (European Chemicals Agency) DNEL values (Table 4). Stoffenmanager results reports can be found in Tables S4 and S5, Supporting information. Stoffenmanager predicted concentrations for the packing task (pre-activity concentrations not considered) and risk assessment ratios are shown in Table 4 together with actual online total inhalable concentrations and likely components concentrations with its calculated risk assessment ratios (see Section 2.8). For small and big bags, predicted and measured concentrations for the chemical components were in all cases below the established DNEL. For small bags, the ammonium nitrate predicted concentration was 360 μg m^{-3} whereas measured were 410 and 260 μg m^{-3} for SB1 and SB2 respectively. Ratios [concentration]/DNLE were 0.011 or <0.01, well below 1 indicating that the chemical risk is controlled (<1) according to the REACH classification (ECHA, 2016b). Similarly, for the big bags, ratios [concentration]/DNLE for ammonium nitrate of 0.022 for predicted and <0.01 for measured (BB1 and BB2) were obtained. For potassium nitrate, predicted concentrations for small and big bags were 270 and 620 μg m^{-3} respectively, whereas measured concentrations ranged between 160 and 300 μg m^{-3} with ratios [concentration]/DNLE ranging between 0.004 and 0.016 (<1). Similarly, calcium fluoride [concentration]/DNLE ratios for small and big bags were <1 (0.006–0.024) with concentrations ranging between 30 and 120 μg m^{-3}. Therefore, under the REACH approach for risk assessment, exposure to the chemical components of the fertilizer in the present study should be considered under control.

3.6. Prediction models

Exposure concentrations were modelled using the one and two box models including and excluding outdoor concentrations. Worker area monitored concentrations were compared to one box modelled results, and to FF modelled concentrations when using the two box model, as worker area monitoring instruments were not placed inside the limits of the defined NF area.

As described in Section 2.5.3, a sensitivity analysis was carried out to identify the optimal air flow rate between NF and FF (β) in the two box model for this industrial setting. The range of values tested was obtained from the literature (Baldwin and Maynard, 1998; Arnold et al., 2017), and the results of this analysis are summarized in Tables 1 and 4. For small bags, a range of S = 0.006–0.05 m s^{-1}, where S is wind speed inside the plant, corresponding to β = 0.36–3 m^3 min^{-1} was tested. Modelled concentrations were seen to variate between 26 and 38%. On the other hand, for big bags a range of S = 0.0125–0.04 m s^{-1} corresponding to β = 9.4–30 m^3 min^{-1} was tested, and modelled concentrations were seen to variate < 5%. Results evidenced that for small bags, higher β (e.g., 3 m^3 min^{-1}) resulted in modelled/measured ratios up to 1.89, whereas lower β largely underestimated modelled concentrations (ratios = 0.39–0.69 for β = 0.36 m^3 min^{-1}). As a result, a β of 0.75 m^3 min^{-1} was selected for the small bag scenarios. In a similar analysis, for the big bag scenarios β was 30 m^3 min^{-1} (Table 1), although as explained β does not seem to be a critical parameter for this scenario.

With the parametrization selected, for the one box setup including outdoor concentrations, modelled concentrations (325, 404, 759 and 546 μg m^{-3} for SB1, SB2, BB1 and BB2, respectively) (Table 5) were able to reproduce actual exposure measurements (279, 318, 668 and 528 μg m^{-3} for SB1, SB2, BB1 and BB2, respectively) (Table 3). Predicted concentrations were only slightly higher than the measured values (Tables 3 and 4). The ratio ($m_{modelled}/m_{measured}$) was 1.22 ± 0.07 for the small bags and 1.09 ± 0.08 for big bags (Table 5). For the two box model including outdoors, modelled concentrations (311, 316, 745 and 538 μg m^{-3} for SB1, SB2, BB1 and BB2, respectively) (Table 5) were higher than measured concentrations with a ratio ($m_{modelled}/m_{measured}$) of 1.05 ± 0.08 for small bags and 1.07 ± 0.07 for big bags (Table 5).

Modelled concentrations without adding outdoor concentrations (Table 5) were generally lower than measured concentrations (and only slightly higher in 2 cases; SB1 one and two box model

Table 4
Stoffenmanager tool results for the small and big bags case scenarios (task concentration) in terms of total and component (ammonium nitrate, potassium nitrate and calcium fluoride) inhalable concentrations. Actual online measured inhalable concentrations and likely component concentrations calculated using composition percentages of the fertilizer. DNLE values for each fertilizer component. Risk assessment (Risk ass.) is calculated following the REACH approach: [concentration]/DNLE < 1, controlled risk; [concentration]/DNLE > 1, uncontrolled risk. SB: small bags; BB: big bags.

		Total inhalable [μg m^{-3}]	Ammonium nitrate (20%) [inhalable μg m^{-3}]	Potassium nitrate (15%) [inhalable μg m^{-3}]	Calcium fluoride (3%) [inhalable μg m^{-3}]
8 h TWA	DNLE	–	37,600	36,700	5000
Stoffenmanager results	Small bags	1800	360	270	54
	Small bags risk ass.	–	<0.01	<0.01	0.011
	Big bags	4110	820	620	120
	Big bags risk ass.	–	0.022	0.017	0.025
Small bags actual online measured concentrations	Small bags 1 (SB1)	2025	410	300	60
	Risk ass. SB1	–	0.011	<0.01 (0.008)	0.012
	Small bags 2 (SB2)	1276	260	190	40
	Risk ass. SB2	–	<0.01 (0.007)	<0.01 (0.005)	<0.01 (0.008)
Big bags actual online measured concentrations	Big bags 1 (BB1)	1864	370	280	60
	Risk ass. BB1	–	(0.010)	<0.01 (0.008)	0.011
	Big bags 2 (BB2)	1047	210	160	30
	Risk ass. BB2	–	<0.01 (0.006)	<0.01 (0.004)	<0.01 (0.006)

Table 5
One box and two box modelled respirable concentration results including and without including outdoor concentrations. Ratios between modelled and measured concentrations for each specific case are shown in brackets. Last two columns are mean ratio values (and standard deviation) for small and big bags (SB and BB). Last row shows the measured respirable fraction concentrations in the workers area and the spatial background.

[μg m^{-3}] ($ratio_{modelled/measured}$)	SB1	SB2	BB1	BB2	Ratio mean ± (s.d.)	
					Small bags	Big bags
One box with outdoor	325 (1.16)	404 (1.27)	759 (1.14)	546 (1.03)	1.22 (0.07)	1.09 (0.08)
Two box with outdoor (FF)	311 (1.11)	316 (0.99)	745 (1.12)	538 (1.02)	1.05 (0.08)	1.07 (0.07)
One box	310 (1.11)	270 (0.85)	501 (0.75)	488 (0.92)	0.98 (0.19)	0.84 (0.12)
Two box (FF)	296 (1.06)	223 (0.70)	487 (0.73)	480 (0.90)	0.88 (0.25)	0.82 (0.12)
Measured respirable fraction in worker area	279	318	668	528	–	

including outdoor). The ratio ($m_{modelled}/m_{measured}$) for the one box model was 0.98 ± 0.19 for the small bags and 0.84 ± 0.12 for the big bags. The ratio ($m_{modelled}/m_{measured}$) for the two box model was of 0.88 ± 0.25 for the small bags and 0.82 ± 0.12 for big bags. Thus, the model underestimated exposure concentrations when outdoor contributions were not included. Commonly, model testing assumes that the initial concentration is zero and that the supplied air is free of contaminants (Zhang et al., 2009). However, as discussed in Section 3.3.2, the infiltration of outdoor contaminants is frequent, especially when having open doors as in this case. In the industrial setting under study, modelled concentrations without including outdoor were underestimated in 6 of the 8 cases. This kind of underestimation has been considered detrimental in risk assessment (Arnold et al., 2017). On the other hand, modelled concentrations when including outdoor slightly overestimated measured concentrations and had higher precision. These more conservative results were considered preferable from a risk assessment point of view.

Arnold et al. (2017) highlighted the importance of making the right model selection when applying them to real cases. The use of the two box model in a well-mixed environment can lead to an overestimation of the FF and especially of the NF modelled concentrations, whereas using a one box model to estimate concentrations in a NF-FF environment can lead to an underestimation. In the industrial setting under study, the big bags scenario seemed to be clearly a one box case scenario due to the absence of an enclosure. However, both models provided similar predictions, the one box model resulting in only slightly higher concentrations. In general, overestimation by models has been described for both, one and two box models (Jensen et al., 2018; Johnson et al., 2011; Koponen et al., 2015; Sahmel et al., 2009).

4. Discussion: parametrization of exposure models

Evidently, the results obtained regarding modelled concentrations are highly dependent on model parameters (Mølgaard et al., 2014) such as the handling energy factor, local controls, air exchange rate (AER) and NF-FF air flow (β), which are not yet fully parametrized (Cherrie et al., 2011; Jayjock et al., 2011; Sahmel et al., 2009; Baldwin and Maynard, 1998; Keil and Zhao, 2017) and are often challenging to estimate (Zhang et al., 2009). Sensitivity analyses such as the one presented in Table 1 are also valuable.

In the case of the AER and β, experimental data were not available for this case study and they were thus obtained from the literature and tested by means of a sensitivity analysis. β was seen to be a key parameter when modelling the small bags case scenario while it was not critical for the big bags case scenario. That may be explained by the fact that the small bags case scenario was a real two box case (with an actual enclosure and with a small surface area for the air flow between NF and FF) whereas for the big bags there was no real separation between NF and FF and consequently the theoretical free surface area used in the model was much higher.

Local controls prevent dispersion of the aerosolized particles in the room air or remove the particles from air, e.g. enclosures or local extraction systems (Fransman et al., 2008). When having to consider extractions systems, local control values associated can be relatively easy to determine, but in cases like enclosures or barriers it is more complex especially without having actual exposure concentrations. Local exhaust ventilation efficiency can be calculated by a relatively simple equation (Hewett and Ganser, 2017) although some unknown parameters are required. For cases such as the present study when there is no possibility to experimentally establish a value, Fransman et al. (2008) conducted a review with values proposed for different local controls. Here, enclosure local control and bag protection was included in the equation by using values reviewed in Fransman et al. (2008). The output modelled concentrations were seen to correctly predict measured concentrations when using the reported values.

Finally, the emission source characterization is one of the main sources of uncertainty in the model, as it is strongly case-specific. This is one of the reasons why studies dealing with real-world scenarios are highly necessary in the literature. As in the present study, emission source characterization can be based on the dustiness index which may be obtained by standard methods (Lidén, 2006). However, the handling energy factor must be considered (Koivisto et al., 2015; Lidén, 2006; Schneider and Jensen, 2007) and it is still not completely parametrized. When the dustiness concept cannot be used, equations to estimate emission rates have been described (Hewett and Ganser, 2017; Sachse et al., 2012) and used on real scenarios by using mass equation balance and a convolution theorem (Koivisto et al., 2018a; Koivisto et al., 2018b). However, unlike the other parameters, literature regarding emission rates is still limited.

Thus, although here good estimations were obtained, it is important to keep in mind that uncertainties can be considerable when some of the parameters (e.g. local controls or β) are unknown and must be literature based or estimated. Therefore, an appropriate selection of the parameters is essential.

Additionally, an important consideration to be discussed at this point is that the models do not consider particle losses due to sedimentation. Cherrie et al. (2011) found that for particles < 10 μm the impact of deposition might be reasonably ignored, but for particles with a higher aerodynamic diameter the deposition impact may be important. Fig. 5 shows that most of the emitted particles during packing were under 10 μm. However, for BB1, a slight increase of particles > 10 μm during packing was observed.

Stoffenmanager overestimated total inhalable exposure levels by a factor of 1.4 to 3.9 with the exception of SB1 in which the prediction was accurate. This is in line with findings by Landberg et al. (2017) who showed that Stoffenmanager overestimates low exposures and underestimates high exposures, and Spinazzè et al. (2017) who showed that ca. 50% of the simulations overestimated the exposure levels for solvents. The overestimation may be party related to the error in the general ventilation multipliers that are used to describe dilution of the concentrations (Koivisto et al., 2018c). However, a better explanation is that Stoffenmanager is a non-physical model that does not follow principal laws of physics, such as mass balance and it does not describe the reality well (Koivisto et al., 2018c).

Based on the above considerations, it may be concluded that the use of the one box and two box models in the industrial setting tested can satisfactorily predict low particle concentration exposures, especially when input parameters are sufficiently robust. In Sahmel et al. (2009),

the steady state model, similar to the one box model used here, was seen to correctly perform concentration modelling when choosing the appropriate factors. However, in industrial settings many considerations must be taken into account and what is clearly observed in a laboratory scale or controlled settings cannot be directly extrapolated to the industrial world. To this end, the parameters used in this work and the coefficients applied, described in Section 2.5, may be useful as input for future modelling studies.

5. Conclusions

Packing of a fertilizer into small (respirable fraction range 279–318 μg m^{-3}) and big bags (respirable fraction range 487–668 μg m^{-3}) was not seen to significantly increase worker exposure compared with pre-activity concentrations in terms of inhalable and respirable concentrations. However, increases in particle number concentrations were observed, quite likely related to the diesel forklift activity. A statistically significant increase in ultrafine particles was observed for SB2 (58,646 cm^{-3} during pre-activity; 75,912 cm^{-3} during packing). According to REACH standards, the chemical risk due to exposure to fertilizers in the present study should be considered under control. It should be noted, however, that personal exposure samples were not collected in this work, and that chemical exposures were quantified based on the fertilizer's chemical composition. This dataset was used to test the performance of one and two box models as tools for risk assessment under real-world industrial settings.

The one and two box models were tested in a real industrial exposure case scenario, where low exposure concentrations were detected, during packing of a fertilizer into small and big bags, with and without enclosure. Both models seemed to be able to predict low exposure concentrations. When outdoor concentrations were not included in the models, modelled concentrations slightly underestimated actual concentrations, with ratios modelled/measured ranging between 0.82 ± 0.12 and 0.98 ± 0.19 for the respirable size fraction. The use of outdoor concentrations as an input for the models was seen to improve model performance, resulting in slight overestimations of measured concentrations what was estimated as preferable from a risk assessment point of view. In addition, higher precision between repetitions was achieved when including outdoor contributions (ratio modelled/measured 1.05 ± 0.08 to 1.22 ± 0.07). Thus, it was concluded that including outdoor concentrations in the model resulted in an improved model performance, which may be considered a step forward in the application of risk assessment models.

With regard to the selection of the one or two box models, similar results for the small and big bags case scenarios were obtained. However, slightly better results were obtained when using the two box model for the small bags scenario (one box model 1.22 ± 0.07; two box model 1.05 ± 0.08), whereas both models provided similar results for the big bags (1.09 ± 0.08 and 1.07 ± 0.07 respectively). Thus, it may be concluded that, even in complex real-world settings where low exposure concentrations are monitored, the simplest approach of the one box model may provide good results if it is adequately parametrized. Model parametrization is in itself a key issue: the selection of parameters such as the handling energy factor, the local controls and especially the NF-FF air flow in the two box model were seen to be critical for the model's performance. Here, NF-FF air flow, local controls efficiency as well as handling energy factor were assumed based on literature databases, and relatively accurate predictions were obtained. Therefore, reporting measured or tested values for these parameters is seen as necessary to expand the use and applicability of prediction models for risk assessment.

Stoffenmanager estimated that the packing process increases exposure levels from 2000 to 4000 μg m^{-3} for small and big bags even though the packing did not elevate the concentrations in detectable amounts (1000–2000 μg m^{-3}, measured concentrations). Thus, in this case, using Stoffenmanager for assessing risk management measures would not be recommended.

Acknowledgments

This research was founded by the Spanish MINECO (CGL2015-66777-C2-1-R, 2-R), Generalitat de Catalunya AGAUR 2017 SGR41, the Spanish Ministry of the Environment (13CAES006), FEDER (European Regional Development Fund) "Una manera de hacer Europa" and H2020 project caLIBRAte (Work Package 7). M.C. Minguillón acknowledges the Ramón y Cajal Fellowship awarded by the Spanish Ministry of Economy, Industry and Competitiveness. The authors also acknowledge the company in which the measurements were carried out for their support. The authors declare no conflict of interest relating to the material presented in this article.

Appendix A. Supplementary data

Supplementary data to this article can be found online at https://doi.org/10.1016/j.scitotenv.2018.09.379.

References

Arnold, S.F., Shao, Y., Ramachandran, G., 2017. Evaluating well-mixed room and near-field–far-field model performance under highly controlled conditions. J. Occup. Environ. Hyg. 14, 427–437. https://doi.org/10.1080/15459624.2017.1285492.

Asbach, C., Kuhlbusch, T.A.J., Kaminski, H., Stahlmecke, B., Plitzko, S., Götz, U., Voetz, M., Kiesling, H.-J., Dahmann, D., 2012. Standard Operation Procedures for Assessing Exposure to Nanomaterials, Following a Tiered Approach.

Baldwin, P.E.J., Maynard, A.D., 1998. A survey of wind speeds in indoor workplaces. 42, 303–313.

Bekker, C., Voogd, E., Fransman, W., Vermeulen, R., 2016. The validity and applicability of using a generic exposure assessment model for occupational exposure to nano-objects and their aggregates and agglomerates. Ann. Occup. Hyg. 60, 1039–1048. https://doi.org/10.1093/annhyg/mew048.

Bennett, D.H., Koutrakis, P., 2006. Determining the infiltration of outdoor particles in the indoor environment using a dynamic model. Aerosol Sci. 37, 766–785. https://doi.org/10.1016/j.jaerosci.2005.05.020.

Boelter, F.W., Simmons, C.E., Berman, L., Scheff, P., 2009. Two-zone model application to breathing zone and area welding fume concentration data. J. Occup. Environ. Hyg. 6, 289–297. https://doi.org/10.1080/15459620902809895.

Cherrie, J.W., Schneider, T., 1999. Validation of a new method for structured subjective assessment of past concentrations. Ann. Occup. Hyg. 43, 235–245. https://doi.org/10.1016/S0003-4878(99)00023-X.

Cherrie, J.W., MacCalman, L., Fransman, W., Tielemans, E., Tischer, M., Van Tongeren, M., 2011. Revisiting the effect of room size and general ventilation on the relationship between near- and far-field air concentrations. Ann. Occup. Hyg. 55, 1006–1015. https://doi.org/10.1093/annhyg/mer092.

Eckerman, K., Harrison, J., Menzel, H-G., Clement, C.H., 2011. Annals of the ICRP Published on Behalf of the International Commission on Radiological Protection International Commission on Radiological Protection Members of the 2010–2013 Main Commission of ICRP. https://doi.org/10.1016/S0146-6453(11)00010-8.

Ding, Y., Kuhlbusch, T.A.J., Van Tongeren, M., Jiménez, A.S., Tuinman, I., Chen, R., Alvarez, I.L., Mikolajczyk, U., Nickel, C., Meyer, J., Kaminski, H., Wohlleben, W., Stahlmecke, B., Clavaguera, S., Riediker, M., 2017. Airborne engineered nanomaterials in the workplace—a review of release and worker exposure during nanomaterial production and handling processes. J. Hazard. Mater. 322, 17–28. https://doi.org/10.1016/j.jhazmat.2016.04.075.

ECHA, 2016a. Guidance on Information Requirements and Chemical Safety Assessment. Chapter R. 14: Occupational Exposure Assessment. https://doi.org/10.2823/678250.

ECHA, 2016b. Guidance on Information Requirements and Chemical Safety Assessment. Part E: Risk Characterisation. Eur. Chem. Agency, p. 496 (2.1).

European Committee for Standardization (CEN), 2013. Workplace Exposure: Measurement of the Dustiness of Bulk Materials; Part1: Requirements and Choice of Test Methods; Part 2: Rotating Drum Method; Part 3: Continuous Drop Method (EN 15051) ([Stantdard] Brussels, Belgium, 2013).

Evans, D.E., Ku, B.K., Birch, M.E., Dunn, K.H., 2010. Aerosol monitoring during carbon nanofiber production: mobile direct-reading sampling. Ann. Occup. Hyg. 54, 514–531. https://doi.org/10.1093/annhyg/meq015.

Fonseca, A.S., Viana, M., Pérez, N., Alastuey, A., Querol, X., Kaminski, H., Todea, A.M., Monz, C., Asbach, C., 2016. Intercomparison of a portable and two stationary mobility particle sizers for nanoscale aerosol measurements. Aerosol Sci. Technol. 50, 653–668. https://doi.org/10.1080/02786826.2016.1174329.

Fonseca, A.S., Kuijpers, E., Kling, K.I., Levin, M., Koivisto, A.J., Nielsen, S.H., Fransman, W., Fedutik, Y., Jensen, K.A., Koponen, I.K., 2018. Particle release and control of worker exposure during laboratory-scale synthesis, handling and simulated spills of manufactured nanomaterials in fume hoods. J. Nanopart. Res. 20. https://doi.org/10.1007/s11051-018-4136-3.

Fransman, W., Schinkel, J., Meijster, T., Van Hemmen, J., Tielemans, E., Goede, H., 2008. Development and evaluation of an Exposure Control Efficacy Library (ECEL). Ann. Occup. Hyg. 52, 567–575. https://doi.org/10.1093/annhyg/men054.

Fujitani, Y., Kobayashi, T., Arashidani, K., Kunugita, N., Suemura, K., 2008. Measurement of the physical properties of aerosols in a fullerene factory for inhalation exposure assessment. J. Occup. Environ. Hyg. 5, 380–389. https://doi.org/10.1080/15459620802050053.

Gakidou, E., Afshin, A., Abajobir, A.A., et al., 2017. Global, regional, and national comparative risk assessment of 84 behavioural, environmental and occupational, and metabolic risks or clusters of risks, 1990–2016: a systematic analysis for the Global Burden of Disease Study 2016. Lancet 390, 1345–1422. https://doi.org/10.1016/S0140-6736(17)32366-8.

Ganser, G.H., Hewett, P., 2017. Models for nearly every occasion: part II - two box models. J. Occup. Environ. Hyg. 14, 58–71. https://doi.org/10.1080/15459624.2016.1213393 To.

Gorguner, M., Akgun, M., 2010. Acute inhalation injury. Eur. J. Med. 42 (1), 28. https://doi.org/10.5152/eajm.2010.09.

Heitbrink, W.A., Evans, D.E., Ku, B.K., Maynard, A.D., Slavin, T.J., Peters, T.M., 2009. Relationships among particle number, surface area, and respirable mass concentrations in automotive engine manufacturing. J. Occup. Environ. Hyg. 6, 19–31. https://doi.org/10.1080/15459620802530096.

Hewett, P., Ganser, G.H., 2017. Models for nearly every occasion: part I - one box models. J. Occup. Environ. Hyg. 14, 49–57. https://doi.org/10.1080/15459624.2016.1213392.

Hinds, W.C., 1999. Aerosol Technology: Properties, Behavior, and Measurement of Airborne Particles. Wiley-Interscience Publication. Wiley https://doi.org/10.1016/0021-8502(83)90049-6.

Huang, C.H., Tai, C.Y., Huang, C.Y.U., Tsai, C.J., Chen, C.W., Chang, C.P., Shih, T.S., 2010. Measurements of respirable dust and nanoparticle concentrations in a titanium dioxide pigment production factory. J. Environ. Sci. Health A Tox. Hazard. Subst. Environ. Eng. 45, 1227–1233. https://doi.org/10.1080/10934529.2010.493792.

Hussein, T., Kulmala, M., 2008. Indoor aerosol modeling: basic principles and practical applications. Water Air Soil Pollut. Focus 8, 23–34. https://doi.org/10.1007/s11267-007-9134-x.

Hussein, T., Hruška, A., Dohányosová, P., Džumbová, L., Hemerka, J., Kulmala, M., Smolík, J., 2009. Deposition rates on smooth surfaces and coagulation of aerosol particles inside a test chamber. Atmos. Environ. 43, 905–914. https://doi.org/10.1016/j.atmosenv.2008.10.059.

ICSC 0184 - potassium nitrate. URL. http://www.inchem.org/documents/icsc/icsc/eics0184.htm, Accessed date: 26 January 2018 (WWW Document, n.d.).

INSH, 2018. LEP 2017. Instituto Nacional de Seguridad e Higiene en el Trabajo https://doi.org/10.1017/CBO9781107415324.004.

Jayjock, M.A., Armstrong, T., Taylor, M., 2011. The daubert standard as applied to exposure assessment modeling using the two-zone (Nf/ff) model estimation of indoor air breathing zone concentration as an example. J. Occup. Environ. Hyg. 8, D114–D122. https://doi.org/10.1080/15459624.2011.624387.

Jensen, A., Dal Maso, M., Koivisto, A., Belut, E., Meyer-Plath, A., Van Tongeren, M., Sánchez Jiménez, A., Tuinman, I., Domat, M., Toftum, J., Koponen, I., 2018. Comparison of geometrical layouts for a multi-box aerosol model from a single-chamber dispersion study. Environment 5, 52. https://doi.org/10.3390/environments5050052.

Johnson, M., Lam, N., Brant, S., Gray, C., Pennise, D., 2011. Modeling indoor air pollution from cookstove emissions in developing countries using a Monte Carlo single-box model. Atmos. Environ. 45, 3237–3243. https://doi.org/10.1016/j.atmosenv.2011.03.044.

Jones, R.M., Simmons, C.E., Boelter, F.W., 2011. Comparing two-zone models of dust exposure. J. Occup. Environ. Hyg. 8, 513–519. https://doi.org/10.1080/15459624.2011.598762.

Kaminski, H., Beyer, M., Fissan, H., Asbach, C., Kuhlbusch, T.A.J., 2015. Measurements of nanoscale TiO2 and Al2O3 in industrial workplace environments—methodology and results. Aerosol Air Qual. Res. 15, 129–141. https://doi.org/10.4209/aaqr.2014.03.0065.

Keil, C., Zhao, Y., 2017. Interzonal airflow rates for use in near-field far-field workplace concentration modeling. J. Occup. Environ. Hyg. 14 (10), 793–800. https://doi.org/10.1080/15459624.2017.1334903.

Kleinman, M.T., Linn, W.S., Bailey, R.M., Jones, M.P., Hackney, J.D., 1980. Effect of ammonium nitrate aerosol on human respiratory function and symptoms. Environ. Res. 21, 317–326. https://doi.org/10.1016/0013-9351(80)90033-X.

Koivisto, A.J., Lyyränen, J., Auvinen, A., Vanhala, E., Hämeri, K., Tuomi, T., Jokiniemi, J., 2012a. Industrial worker exposure to airborne particles during the packing of pigment and nanoscale titanium dioxide. Inhal. Toxicol. 24, 839–849. https://doi.org/10.3109/08958378.2012.724474.

Koivisto, A.J., Aromaa, M., Mäkelä, J.M., Pasanen, P., Hussein, T., Hämeri, K., 2012b. Concept to estimate regional inhalation dose of industrially synthesized nanoparticles. ACSNano 6, 1195–1203.

Koivisto, A.J., Jensen, A.C.Ø., Levin, M., Kling, K.I., Maso, M.D., Nielsen, S.H., Jensen, K.A., Koponen, I.K., 2015. Testing the near field/far field model performance for prediction of particulate matter emissions in a paint factory. Environ. Sci. Processes Impacts 17, 62–73. https://doi.org/10.1039/C4EM00532E.

Koivisto, A.J., Jensen, A.C.Ø., Kling, K.I., Kling, J., Budtz, H.C., Koponen, I.K., Tuinman, I., Hussein, T., Jensen, K.A., Nørgaard, A., Levin, M., 2018a. Particle emission rates during electrostatic spray deposition of TiO2 nanoparticle-based photoactive coating. J. Hazard. Mater. 341, 218–227. https://doi.org/10.1016/j.jhazmat.2017.07.045.

Koivisto, A.J., Kling, K.I., Fonseca, A.S., Bluhme, A.B., Moreman, M., Yu, M., Costa, A.L., Giovanni, B., Ortelli, S., Fransman, W., Vogel, U., Jensen, K.A., 2018b. Dip coating of air purifier ceramic honeycombs with photocatalytic TiO2 nanoparticles: a case study for occupational exposure. Sci. Total Environ. 630, 1283–1291. https://doi.org/10.1016/j.scitotenv.2018.02.316.

Koivisto, A.J., Jensen, A.C.Ø., Koponen, I.K., 2018c. The general ventilation multipliers calculated by using a standard Near-Field/Far-Field model. J. Occup. Environ. Hyg. 15, D38–D43. https://doi.org/10.1080/15459624.2018.1440084.

Koponen, I.K., Asmi, A., Keronen, P., Puhto, K., Kulmala, M., 2001. Indoor air measurement campaign in Helsinki, Finland 1999 - the effect of outdoor air pollution on indoor air. Atmos. Environ. 35, 1465–1477. https://doi.org/10.1016/S1352-2310(00)00338-1.

Koponen, I.K., Koivisto, A.J., Jensen, K.A., 2015. Worker exposure and high time-resolution analyses of process-related submicrometre particle concentrations at mixing stations in two paint factories. Ann. Occup. Hyg. 59, 749–763. https://doi.org/10.1093/annhyg/mev014.

Kuhlbusch, T.A.J., Neumann, S., Fissan, H., 2004. Number size distribution, mass concentration, and particle composition of PM_1, $PM_{2.5}$, and PM_{10} in bag filling areas of carbon black production. J. Occup. Environ. Hyg. 1, 660–671. https://doi.org/10.1080/15459620490502242.

Lamb, J., Hesse, S., Miller, B.G., MacCalman, L., Schroeder, K., Cherrie, J., van Tongeren, M., 2015. Evaluation of Tier 1 Exposure Assessment Models Under REACH (eteam) Project Final Overall Project Summary Report Evaluation of Tier 1 Exposure Assessment Models Under REACH (eteam) Project Final Overall Project Summary Report.

Landberg, H.E., Berg, P., Andersson, L., Bergendorf, U., Karlsson, J.-E., Westberg, H., Tinnerberg, H., 2015. Comparison and evaluation of multiple users' usage of the exposure and risk tool: Stoffenmanager 5.1. Ann. Occup. Hyg. 59, 821–835. https://doi.org/10.1093/annhyg/mev027.

Landberg, H.E., Axmon, A., Westberg, H., Tinnerberg, H., 2017. A study of the validity of two exposure assessment tools: Stoffenmanager and the Advanced REACH Tool. Ann. Work Expo. Heal. 61, 575–588. https://doi.org/10.1093/annweh/wxx008.

Landrigan, P.J., Fuller, R., Acosta, N.J.R., Adeyi, O., Arnold, R., Basu, N., Baldé, A.B., Bertollini, R., Bose-O'Reilly, S., Boufford, J.I., Breysse, P.N., Chiles, T., Mahidol, C., Coll-Seck, A.M., Cropper, M.L., Fobil, J., Fuster, V., Greenstone, M., Haines, A., Hanrahan, D., Hunter, D., Khare, M., Krupnick, A., Lanphear, B., Lohani, B., Martin, K., Mathiasen, K.V., McTeer, M.A., Murray, C.J.L., Ndahimananjara, J.D., Perera, F., Potočnik, J., Preker, A.S., Ramesh, J., Rockström, J., Salinas, C., Samson, L.D., Sandilya, K., Sly, P.D., Smith, K.R., Steiner, A., Stewart, R.B., Suk, W.A., van Schayck, O.C.P., Yadama, G.N., Yumkella, K., Zhong, M., 2017. The Lancet Commission on pollution and health. Lancet, 391 https://doi.org/10.1016/S0140-6736(17)32345-0.

Lidén, G., 2006. Dustiness testing of materials handled at workplaces. Ann. Occup. Hyg. https://doi.org/10.1093/annhyg/mel042.

Lopez, R., Lacey, S.E., Jones, R.M., 2015. Application of a two-zone model to estimate medical laser-generated particulate matter exposures. J. Occup. Environ. Hyg. 12, 309–313. https://doi.org/10.1080/15459624.2014.989361.

López-Lilao, A., Bruzi, M., Sanfélix, V., Gozalbo, A., Mallol, G., Monfort, E., 2015. Evaluation of the dustiness of different kaolin samples. J. Occup. Environ. Hyg. 12, 547–554. https://doi.org/10.1080/15459624.2015.1019079.

Marquart, H., Heussen, H., Le Feber, M., Noy, D., Tielemans, E., Schinkel, J., West, J., Van Der Schaaf, D., 2008. "Stoffenmanager", a web-based control banding tool using an exposure process model. Ann. Occup. Hyg. 52, 429–441. https://doi.org/10.1093/annhyg/men032.

Mølgaard, B., Ondráček, J., Štávová, P., Džumbová, L., Barták, M., Hussein, T., Smolík, J., 2014. Migration of aerosol particles inside a two-zone apartment with natural ventilation: a multi-zone validation of the multi-compartment and size-resolved indoor aerosol model. Indoor Built Environ. 23, 742–756. https://doi.org/10.1177/1420326X13481484.

Nazaroff, W.W., 2004. Indoor particle dynamics. Indoor Air 14, 175–183. https://doi.org/10.1111/j.1600-0668.2004.00286.x.

Nazaroff, W.W., Cass, G.R., 1989. Mathematical modeling of indoor aerosol dynamics. Environ. Sci. Technol. 23, 157–166. https://doi.org/10.1021/es00179a003.

Nicas, M., 2016. The near field/far field model with constant application of chemical mass and exponentially decreasing emission of the mass applied. J. Occup. Environ. Hyg. 13, 519–528. https://doi.org/10.1080/15459624.2016.1148268.

Notø, H., Nordby, K.-C., Skare, Ø., Eduard, W., 2018. Job tasks as determinants of thoracic aerosol exposure in the cement production industry. Ann. Work Expo. Heal. 62, 88–100. https://doi.org/10.1093/annweh/wxx085.

Peters, T.M., Elzey, S., Johnson, R., Park, H., Grassian, V.H., Maher, T., O'Shaughnessy, P., 2008. Airborne monitoring to distinguish engineered nanomaterials from incidental particles for environmental health and safety. J. Occup. Environ. Hyg. 6, 73–81. https://doi.org/10.1080/15459620802590058.

Pujara, C.P., 1997. Determination of Factors that Affect the Generation of Airborne Particles from Bulk Pharmaceutical Powders. PhD diss., Faculty of Purdue University, West Lafayette, IN.

Reche, C., Viana, M., Rivas, I., Bouso, L., Àlvarez-Pedrerol, M., Alastuey, A., Sunyer, J., Querol, X., 2014. Outdoor and indoor UFP in primary schools across Barcelona. Sci. Total Environ. 493, 943–953. https://doi.org/10.1016/j.scitotenv.2014.06.072.

Ribalta, C., Viana, M., López-Lilao, A., Estupiñá, S., Minguillón, M.C., Mendoza, J., Díaz, J., Dahmann, D., Monfort, E., 2018. On the relationship between exposure to particles and dustiness during handling of powders in industrial settings. Annals of Work Exposures and Health (in press).

Riedmann, R.A., Gasic, B., Vernez, D., 2015. Sensitivity analysis, dominant factors, and robustness of the ECETOC TRA v3, Stoffenmanager 4.5, and ART 1.5 occupational exposure models. Risk Anal. 35, 211–225. https://doi.org/10.1111/risa.12286.

Rivas, I., Viana, M., Moreno, T., Bouso, L., Pandolfi, M., Alvarez-Pedrerol, M., Forns, J., Alastuey, A., Sunyer, J., Querol, X., 2015. Outdoor infiltration and indoor contribution of UFP and BC, OC, secondary inorganic ions and metals in PM2.5 in schools. Atmos. Environ. 106, 129–138. https://doi.org/10.1016/j.atmosenv.2015.01.055.

Roy, R.N., Finck, A., Blair, G.J., Tandon, H.L.S., 2006. Plant nutrition for food security: a guide for integrated nutrient management. FAO Fertil. Plant Nutr. Bull. 16 (348 pp.).

Sachse, S., Silva, F., Irfan, A., Zhu, H., Pielichowski, K., Leszczynska, A., Blazquez, M., Kazmina, O., Kuzmenko, O., Njuguna, J., 2012. Physical characteristics of nanoparticles

emitted during drilling of silica based polyamide 6 nanocomposites. IOP Conf. Ser. Mater. Sci. Eng. 40, 12012. https://doi.org/10.1088/1757-899X/40/1/012012.
Sahmel, J., Unice, K., Scott, P., Cowan, D., Paustenbach, D., 2009. The use of multizone models to estimate an airborne chemical contaminant generation and decay profile: occupational exposures of hairdressers to vinyl chloride in hairspray during the 1960s and 1970s. Risk Anal. 29, 1699–1725. https://doi.org/10.1111/j.1539-6924.2009.01311.x.
Savic, N., Racordon, D., Buchs, D., Gasic, B., Vernez, D., 2016. TREXMO: a translation tool to support the use of regulatory occupational exposure models. Ann. Occup. Hyg. 60, 991–1008. https://doi.org/10.1093/annhyg/mew042.
Savic, N., Gasic, B., Vernez, D., 2018. ART, Stoffenmanager, and TRA: a systematic comparison of exposure estimates using the TREXMO translation system. Ann. Work Expo. Heal. 62, 72–87. https://doi.org/10.1093/annweh/wxx079.
Schinkel, J., Fransman, W., Heussen, H., Kromhout, H., Marquart, H., Tielemans, E., 2010. Cross-validation and refinement of the Stoffenmanager as a first tier exposure assessment tool for REACH. Occup. Environ. Med. 67, 125–132. https://doi.org/10.1136/oem.2008.045500.
Schneider, T., Jensen, K.A., 2007. Combined single-drop and rotating drum dustiness test of fine to nanosize powders using a small drum. Ann. Occup. Hyg. 52, 23–34. https://doi.org/10.1093/annhyg/mem059.
Spinazzè, A., Lunghini, F., Campagnolo, D., Rovelli, S., Locatelli, M., Cattaneo, A., Cavallo, D.M., 2017. Accuracy evaluation of three modelling tools for occupational exposure assessment. Ann. Work Expo. Heal. 61, 284–298. https://doi.org/10.1093/annweh/wxx004.
Stoffenmanager Consortium, n.d. Stoffenmanager: Online exposure and risk tool.
Tielemans, E., Noy, D., Schinkel, J., Heussen, H., Van Der Schaaf, D., West, J., Fransman, W., 2008. Stoffenmanager exposure model: development of a quantitative algorithm. Ann. Occup. Hyg. 52, 443–454. https://doi.org/10.1093/annhyg/men033.
Tsai, C.J., Huang, C.Y., Chen, S.C., Ho, C.E., Huang, C.H., Chen, C.W., Chang, C.P., Tsai, S.J., Ellenbecker, M.J., 2011. Exposure assessment of nano-sized and respirable particles at different workplaces. J. Nanopart. Res. 13, 4161–4172. https://doi.org/10.1007/s11051-011-0361-8.
Tsimakuridze, M., Saakadze, V., Tsereteli, M., 2005. The characteristic state of health of ammonia nitrate producing workers. Georgian Med. News 80–83.
Van Broekhuizen, P., Van Veelen, W., Streekstra, W.H., Schulte, P., Reijnders, L., 2012. Exposure limits for nanoparticles: report of an international workshop on nano reference values. Annals of Occupational Hygiene. Edinburgh Napier University, pp. 515–524 https://doi.org/10.1093/annhyg/mes043.
Van Tongeren, M., Fransman, W., Spankie, S., Tischer, M., Brouwer, D., Schinkel, J., Cherrie, J.W., Tielemans, E., 2011. Advanced REACH Tool: development and application of the substance emission potential modifying factor. Ann. Occup. Hyg. 55, 980–988. https://doi.org/10.1093/annhyg/mer093.
van Tongeren, M., Lamb, J., Cherrie, J.W., MacCalman, L., Basinas, I., Hesse, S., 2017. Validation of lower tier exposure tools used for REACH: comparison of tools estimates with available exposure measurements. Ann. Work Expo. Heal. 61, 921–938. https://doi.org/10.1093/annweh/wxx056.
Viitanen, A.K., Uuksulainen, S., Koivisto, A.J., Hämeri, K., Kauppinen, T., 2017. Workplace measurements of ultrafine particles-a literature review. Ann. Work Expo. Heal. https://doi.org/10.1093/annweh/wxx049.
Wang, Y.F., Tsai, P.J., Chen, C.W., Chen, D.R., Hsu, D.J., 2010. Using a modified electrical aerosol detector to predict nanoparticle exposures to different regions of the respiratory tract for workers in a carbon black manufacturing industry. Environ. Sci. Technol. 44, 6767–6774. https://doi.org/10.1021/es1010175.
Wang, J., Asbach, C., Fissan, H., Hülser, T., Kaminski, H., Kuhlbusch, T.A.J., Pui, D.Y.H., 2012. Emission measurement and safety assessment for the production process of silicon nanoparticles in a pilot-scale facility. J. Nanopart. Res. 14, 759. https://doi.org/10.1007/s11051-012-0759-y.
World Health Organization, 2016. Ambient Air Pollution: A Global Assessment of Exposure and Burden of Disease. World Heal. Organ., pp. 1–131. https://doi.org/9789241511353.
Zhang, Y., Banerjee, S., Yang, R., Lungu, C., Ramachandran, G., 2009. Bayesian modeling of exposure and airflow using two-zone models. Ann. Occup. Hyg. https://doi.org/10.1093/annhyg/mep017.

4.3.1. Additional Results Publication III: Testing the performance of one and two box models as tools for risk assessment of particle exposure during packing of inorganic fertilizer

After publication and with the aim to apply risk assessment tools to the highest number of case studies possible in this work, this publication was expanded by performing risk assessment (with 8h TWA concentrations) for the small and big bags scenarios with the ART, NanoSafer and Stoffenmanager models by using the C.D index. ART mechanistic underestimated (< 0.4) inhalable mass exposure for all cases. Conversely, ART Bayesian and Stoffenmanager underestimated exposure for the small bags scenario but overestimated (ratio 1.8-2.1 and 1.2-1.4 ART Bayesian and Stoffenmanager, respectively) the big bags scenarios. The NanoSafer was seen to highly overestimate exposure (ratio 6.7-6.8) for the big bags scenario when considering NF modelled concentrations, but to accurately predict them when considering FF modelled concentrations (ratio 1.1). Conversely, for the small bags case scenario, NanoSafer NF modelled concentrations predicted actual concentrations with a ratio 1.2-1.8, but underestimated actual concentrations when considering FF modelled concentrations.

Table 4.3 Calculated 8h TWA (including pre-activity concentrations) for inhalable and respirable mass fractions in the worker area. Risk assessment results conducted with the ART (Mechanistic and Bayesian), Stoffenmanager and NanoSafer v1.1 using Continuous drop (C.D) index. NF: near-field. FF: far-field.

Case	WA Respirable (µg m^{-3})	WA Inhalable (µg m^{-3})	ART (inhalable µg m^{-3})		Stoffenmanager (inhalable µg m^{-3})	NanoSafer (respirable (NF-FF) µg m^{-3})
			Mechanistic	Bayesian		
Small bags	526 355	1999 1768	6.5 (3.5-12)	220 (120-460)	900	623-10
Big bags	408 413	1687 1445	590 (310-1100)	3100 (2100-4400)	2006	2771-434

Additionally, the ART tool was applied by using R.D dustiness index. The same was not carried out with Stoffenmanager (as the tool does not have the option to introduce a dustiness index or level categorization), or NanoSafer (as the input required is respirable dustiness index and difference between C.D W_R and R.D W_R is very small, 16 vs. 12 mg Kg^{-1}, respectively). ART mechanistic and Bayesian models underestimated exposure in all scenarios, and only for the big bags the ART Bayesian model underestimated with a ratio modelled/measured > 0.5.

Table 4.4 Calculated 8h TWA (including pre-activity concentrations) for inhalable mass fraction based on exposure measurements conducted in the worker area (WA). Risk assessment results conducted with the ART (Mechanistic and Bayesian using Rotating drum (R.D) index.

Case	WA Inhalable (µg m^{-3})	ART (inhalable µg m^{-3})	
		Mechanistic	Bayesian
Small bags	1999 1768	0.65 (0.34-1.2)	65 (29-180)
Big bags	1687 1445	59 (31-110)	940 (570-1500)

4.4. Publication IV: Modelling of high nanoparticle exposure in an indoor industrial scenario with a one-box model

Authors:

Carla Ribalta[1,2], Antti J. Koivisto[3], Apostolos Salmatonidis[1,2], Ana López-Lilao[4], Eliseo Monfort[4], Mar Viana[1].

[1]Institute of Environmental Assessment and Water Research (IDÆA-CSIC), C/ Jordi Girona 18, 08034 Barcelona, Spain.

[2]Barcelona University, Chemistry Faculty, C/ de Martí i Franquès, 1-11, 08028 Barcelona, Spain

[3]National Research Centre for the Working Environment, Lersø Parkallé 105, Copenhagen DK-2100, Denmark.

[4]Institute of Ceramic Technology (ITC)- AICE - Universitat Jaume I, Campus Universitario Riu Sec, Av. Vicent Sos Baynat s/n, 12006 Castellón, Spain.

Published in:

International Journal of Environmental Research and Public Health, 16 (10): 1695, 2019. doi: 10.3390/ijerph16101695

Please cite this article as: Ribalta, C., Koivisto, A.J., Salmatonidis, A., López-Lilao, A., Monfort, E., and Viana, M., 2019. Modeling of High Nanoparticle Exposure in an Indoor Industrial Scenario with a One-Box Model. *International Journal of Environmental Research and Public Health*, 16 (10), 1695.

Accepted date: 11 May 2019

Journal Impact Factor / 5-Year Impact Factor: 2.145 / 2.608

International Journal of
Environmental Research and Public Health

MDPI

Article

Modeling of High Nanoparticle Exposure in an Indoor Industrial Scenario with a One-Box Model

Carla Ribalta [1,2,*], Antti J. Koivisto [3,4], Apostolos Salmatonidis [1,2], Ana López-Lilao [5], Eliseo Monfort [5] and Mar Viana [1]

1 Institute of Environmental Assessment and Water Research (IDÆA-CSIC), C/ Jordi Girona 18, 08034 Barcelona, Spain; apostolos.salmatonidis@idaea.csic.es (A.S.); mar.viana@idaea.csic.es (M.V.)
2 Chemistry faculty, University of Barcelona, C/ de Martí i Franquès, 1–11, 08028 Barcelona, Spain
3 Institute for Atmospheric and Earth System Research (INAR), University of Helsinki, PL 64, FI-00014 Helsinki, Finland; joonas.koivisto@helsinki.fi
4 Air Pollution Management, Willemoesgade 16, st tv, Copenhagen DK-2100, Denmark
5 Institute of Ceramic Technology (ITC)- AICE - Universitat Jaume I, Campus Universitario Riu Sec, Av. Vicent Sos Baynat s/n, 12006 Castellón, Spain; ana.lopez@itc.uji.es (A.L.-L.); eliseo.monfort@itc.uji.es (E.M.)
* Correspondence: carla.ribalta@idaea.csic.es

Received: 11 April 2019; Accepted: 11 May 2019; Published: 14 May 2019

Abstract: Mass balance models have proved to be effective tools for exposure prediction in occupational settings. However, they are still not extensively tested in real-world scenarios, or for particle number concentrations. An industrial scenario characterized by high emissions of unintentionally-generated nanoparticles (NP) was selected to assess the performance of a one-box model. Worker exposure to NPs due to thermal spraying was monitored, and two methods were used to calculate emission rates: the convolution theorem, and the cyclic steady state equation. Monitored concentrations ranged between 4.2×10^4–2.5×10^5 cm^{-3}. Estimated emission rates were comparable with both methods: 1.4×10^{11}–1.2×10^{13} min^{-1} (convolution) and 1.3×10^{12}–1.4×10^{13} min^{-1} (cyclic steady state). Modeled concentrations were 1.4-6 $\times 10^4$ cm^{-3} (convolution) and 1.7–7.1 $\times 10^4$ cm^{-3} (cyclic steady state). Results indicated a clear underestimation of measured particle concentrations, with ratios modeled/measured between 0.2–0.7. While both model parametrizations provided similar results on average, using convolution emission rates improved performance on a case-by-case basis. Thus, using cyclic steady state emission rates would be advisable for preliminary risk assessment, while for more precise results, the convolution theorem would be a better option. Results show that one-box models may be useful tools for preliminary risk assessment in occupational settings when room air is well mixed.

Keywords: prediction; emission rates; air exchange rate; ultrafine particles; unintentional nanoparticles; incidental nanoparticles; plasma spraying; worker exposure; particle mass concentration

1. Introduction

Thermal spraying is applied at an industrial scale to produce thermally- and mechanically-resistant coatings. A feedstock material (metal, alloy or ceramic) is projected at high temperature and velocity onto the surface to be coated. Protective coatings are widely used in the ceramic, automotive, naval, aeronautic and metallurgy industries to prevent corrosion and wear, as well as to restore different types of damaged surfaces [1–5]. From a risk assessment perspective, thermal spraying is known to generate unintentional nanoparticle (NP) emissions (with diameters < 100 nm; 10^6 cm^{-3}) at pilot-plant and industrial scales [6,7]. High particle mass concentrations have also been reported [8,9]. Similar NP emission and formation mechanisms have been identified in a large variety of industrial processes [10–17].

Identifying and modeling exposure to this kind of NPs is relevant due to their potential health impacts. Exposure to particulate matter (PM) may cause respiratory and cardiovascular diseases [18], where respirable particles (those which can penetrate into non-ciliated airways, EN 481, 1995) are considered as a harmful component for human health [18–21]. Oberdörster, (2001) [22] indicated the ability of finer size fractions (< 100 nm; NP) to penetrate deeper in the respiratory tract. In vivo studies have revealed that NPs can cross the alveolar barrier and cause pulmonary inflammation, which turns into cardiovascular risk [23] in much higher numbers than coarser particles, as they can reach deeper areas in the respiratory tract and therefore have a longer retention time [21].

Thus, unintentional NP release in workplaces is a key environmental health and safety issue which requires further research to understand the determinants of personal exposure. Mass-balance models are useful tools for this purpose, as they allow understanding of critical factors affecting exposure and could lead to efficient risk mitigation strategies [24]. Theoretical modeling aspects have been extensively discussed [25–29]. Indoor exposure assessment is frequently performed using one- and two-box models, which have been shown to predict exposure levels with relative accuracy when adequately parametrized in several environments (e.g., indoor concentrations of volatile compounds; PM concentrations in controlled and industrial scenarios [30,31]).

Key challenges for model application are source characterization, local controls and air mixing rates [30,32–36]. In addition, there is a need to test model performance under real-world conditions. Because of the large variety of indoor micro-environments and emission sources, libraries compiling model parameters would be highly useful for modeling studies [33,37]. Source characterization requires dedicated attention, as it is the main determinant of exposure. In the case of primary particle emissions, tools such as the dustiness index are available to estimate emission rates. However, as in the case of understanding exposure determinants in thermal spraying [6,7], emission rates must be quantified from measured concentrations using methods such as the convolution theorem or mathematical mass balance [27,38]. The use of estimated emission rates from actual monitored concentrations has been seen to provide good modeling results in laboratory studies [35,36,39]. However, literature related to emission rates of unintentional NP at industrial scale is limited [15,40]. As a result, emission rates for industrial sources of unintentional NP release and its use for real-world scenario modeling is highly valuable in view of the increasing use of prediction models and web-based risk assessment tools.

In this context, the aims of the present study are (1) to quantify NP emission rates for two different industrials scale thermal spraying processes; and (2) to test the performance of a one-box model in a real-world setting where high NP concentrations were monitored.

2. Materials and Methods

2.1. Work environment and Process

NP monitoring was carried out during thermal spraying of ceramic coatings in an industrial workshop (T.M. Comas, Blanes, Barcelona, Spain). Two types of spraying were applied, 1) High Velocity Oxy-Fuel coating spraying (HVOF), using low temperatures (< 3000 ºC) and high velocities; and 2) Atmospheric Plasma Spraying (APS), using high temperatures (up to 14000 ºC) [1,7,41]. Measurements were conducted over a 4-day period in April 2016. The workshop has three thermal spraying booths in an area of approximately 240 m^2 (14 m wide and 17 m in length) (Figure 1). Here, only data from booth #1 (APS) and #3 (HVOF) will be considered for the modeling approach (Figure 1 and Table S1, Supplementary material) given that booth #2 was not operated continuously. The central area of the workshop (outside the booths), from now on called the worker area (WA) is equipped with a general ventilation extraction system that consisted of three extractors with 11800 m^3 h^{-1} flow each (value provided by the company, not measured). Booth #3 and #1 were additionally equipped with a localized extraction ventilation system (LEV), but only Booth #3's LEV air flow rate was provided by the company (6500 m^3 h^{-1}). Booth #3's activity periods had a short duration and high frequency (5–10 min, 7–9 repetitions/half day) whereas in booth #1, periods had a longer duration

and lower frequency (20–30 min, 2–4 repetitions/half day). The two booths were not operated at the same time. However, certain activities such as the cooling and sanding of pieces were occasionally carried out in parallel. More details on the campaign can be found in Salmatonidis et al. (2019) [7]. In booth #1 the door was usually closed while spraying although not completely, thus allowing air mixing between the booth and the WA. In booth #3, during the activity the worker had to enter and leave the booth more frequently due to technical needs of the process and increased the air mixing between the booth and the WA.

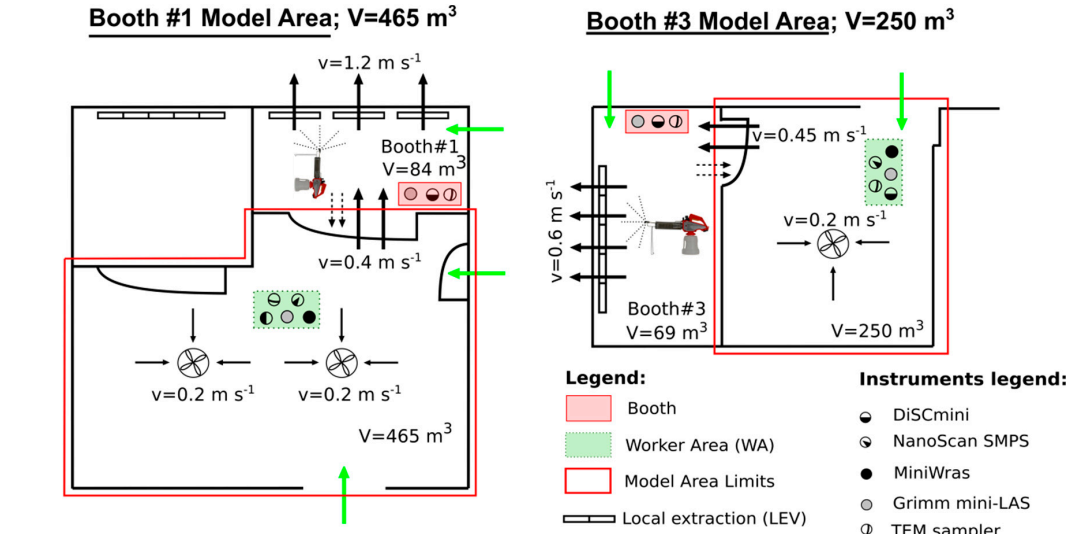

Model Area	*V*, [m3]	*Q*, [m3h-1]	ACH, [h-1]
#1	465	16078	35
#3	250	6216	25

Figure 1. Modeled areas limit, volumes (m^3), ventilation air speeds (m s^{-1}), and description of instruments deployed and their location. Green and black arrows indicate incoming air flows and ventilation extraction flows, respectively. Dashed arrow indicates air flow from booth to WA. The table shows parameterization of the one-box model: V (m^3) is volume used for modeling, Q (m^3 h^{-1}) is ventilation air volume flow through the WA, ACH (h^{-1}) is the air changes per hour calculated from measured air speeds and used for modeling.

2.2. Feedstock Material

In booth #1 (days 1 and 2), two types of commercial products (feedstock) were sprayed: Amdry 6228 (Oerlikon Metco, Pfäffikon, Switzerland) and ANVAL 50/50 (Anval) (Table S1). The Amdry 6228 formula is Al_2O_3 13TiO_2, and it consists of alumina 84% (CAS: 1344-28-1), 14% titania (CAS: 13463-67-7), and organic binder silicon dioxide (CAS: 7631-86-9). The mean aggregate size is 36.0 µm [7] and particles are considered angular/blocky. Amdry is classified as dangerous according to Directive 1999/45/EC [42] and its amendments. The ANVAL 50/50 formulation consists of 50% chromium (CAS: 7440-47-3) and 50% nickel (CAS: 7440-02-0). The powder's mean aggregate size is 76.5 µm [7]. The fact that instruments were intercompared using a different type of aerosol is acknowledged as a limitation of this work.

The feedstock sprayed in booth #3 (days 3 and 4) was a WOKA 3702–1 powder (Oerlikon Metco, Pfäffikon, Switzerland) (Table S1). Its formula is WC 20Cr_3C_2 7Ni, and it consists of 69.5% tungsten carbide (CAS: 12070–12–1), 14.5% trichromium dicarbide (CAS: 12012-35-0), 9% chromium (CAS: 7440-47-3) and 7% nickel (7440-02-0). An unspecified portion of metallic chromium and nickel may be converted during the thermal spray process to hexavalent chromium and nickel compounds, respectively, which are classified as IARC group 1 carcinogen (Safety data sheet, Supplementary material). The mean aggregate size is 34.3 µm [7] and particles are considered mainly spheroidal with

an apparent density between 3.8–4.9 g cm^{-3}. WOKA 3702–1 is classified as hazardous according to Regulation (EC) 1272/2008 [43] and it is suspected to cause cancer.

2.3. Online Measurements and Airborne Particle Collection

Mean particle diameter, and particle number and mass concentrations were monitored inside the booths and in the central WA (Figure 1). Additionally, particle size distribution was monitored in the WA.

The monitoring instruments deployed were:

- A miniature diffusion size classifier (DiSCmini Matter Aerosol, Testo; sample flow rate 1 l min^{-1}) to measure particle number concentration, mean particle size and alveolar lung deposition surface area (LDSA) in a range of 10 to 700 nm, with a 1-minute time resolution.
- A Mini Laser Aerosol Spectrometer (Grimm, Mini-LAS 11R; sample flow rate 1.2 L min^{-1}) to measure particle mass concentration from 0.25 to 32 µm in 31 channels, with a 1-minute time resolution.

Inside the spraying booths, instruments were located near the cabin extraction system, and at 1.5 m from the plasma spray nozzle.

The WA instruments were located outside the booths, at approximately 4 m from the door (Figure 1). The instruments were located between 0.5 and 1.5 m above ground. Concentrations were monitored by using a DiSCmini and a Grimm Mini-LAS (as described above), as well as:

- An electrical mobility spectrometer (NanoScan, SMPS TSI Model 3910; sample flow rate 0.7 L min^{-1}) to measure particle number concentration and size distribution in 13 channels from 10 to 420 nm, with a 1-minute time resolution.
- A Mini Wide Range Aerosol Spectrometer (Mini-WRAS 1371; sample flow rate 1.2 L min^{-1}) to measure particle mass concentration, number concentration and size distribution from 10 nm to 35 µm in 41 channels, with a 1-minute time resolution.

Particle metrics were monitored each day between 10:00 and 17:00. During the lunch breaks, from 12:45 to 13:45, processes were switched off and this period was considered to be representative of background (BG) concentrations.

Instrument intercomparison was carried out prior to the industrial measurements at an air quality monitoring station in Barcelona, Spain, using ambient air aerosols [7]. The fact that instruments were intercompared using a different type of aerosol is acknowledged as a limitation of this work.

Increases in particle number and respirable mass concentrations during spraying were considered statistically significant when the following approach, described by Asbach et al. (2012) [44] and Kaminski et al. (2015) [45], was fulfilled:

$$\text{Mean concentration during spraying} > BG \pm 3 \cdot (\sigma BG), \quad (1)$$

where BG is the mean temporal background concentration and σBG is the standard deviation of the BG concentration.

Finally, in order to complement the air flow data provided by the company, air speeds at booths LEV, central ventilation extraction, and inside the plant were experimentally measured (shown in Figure 1) with an anemometer (VelociCalc ® thermal anemometer, TSI Model 9545; TSI Inc., Shoreview, MN, USA; range 0–30 m s^{-1}; accuracy ±3% or ±0.015 m s^{-1}; resolution 0.01 m s^{-1}).

2.4. Exposure Modeling

2.4.1. Air changes per hour (ACH)

The number of air changes per hour (ACH) in the WA was calculated by using the measured air speeds in the central ventilation extraction and also next to the booth doors, as:

$$ACH = Q/V = (m^3\ h^{-1})/m^3, \quad (2)$$

where Q ($m^3\ h^{-1}$) is the total flow rate and V (m^3) is the total room volume.

2.4.2. Particle Emission Rates

Particle emissions were monitored in close proximity to the source (the spraying nozzle), with the logistical limitations characteristic of operational industrial scenarios, where measurements should be as least invasive as possible. Despite the air extraction systems in place, particle number concentrations measured inside the booths largely exceeded the instrument (DiSCmini) monitoring range (4×10^6 cm^{-3}; Figure 1 and Figure S1 in Supplementary materials). As a result, particle emissions rates could not be calculated based on data collected inside the booths. To overcome this limitation, emission rates were calculated based on the data collected in the WA, i.e., how much particles are leaking from the booth to the WA (booth is the source). This was based on the assumption that air exchange between both areas was frequent: the booth doors were sometimes wide open (when the operator had to access the inside of the booth), and when they were closed they were not fully airtight, and small holes through which cables were inserted were visible along the booth walls. As a result, particle emissions in the booths impacted concentrations in the WA significantly [7]. Similar results have been reported by other authors [46], indicating impacts on particle number concentrations up to 6 m away from the source.

In the present work, particle emission rates were estimated from concentrations measured in the WA, and thus do not strictly correspond to actual emission rates but are rather considered as transported emission rates from the booths to the WA. These transported emissions were used as input to model particle concentrations in the WA. For the sake of clarity and in the present work, transported emission rates from the booths to the WA, measured in the WA, will be referred to as emission rates.

Emission rates were calculated by using two different approaches:

Convolution Theorem

Assuming that NP concentrations are fully mixed, the WA particle concentrations can be described with a mass balance of aerosol particles in a single compartment [28]:

$$(dN(t))/dt = \lambda N_{BG}\ (t) + (S_N\ (t))/V\text{-}\lambda N(t), \quad (3)$$

where N (cm^{-3}) is the WA particle concentration, λ (min^{-1}) is the WA total particle loss rate including particle removal processes like ventilation and deposition, N_{BG} (cm^{-3}) is the background particle concentration coming from outdoors and surrounding compartments, S_N (min^{-1}) is the particle emission rate of the source, and V (m^3) is the volume of the WA room.

The one-box model [28] assumes that 1) particles are fully mixed at all times; 2) particles are created by the source and through infiltration; and 3) there are no other particle losses than mechanical ventilation. Particle losses by sedimentation may be considered negligible because of the high air exchange ratio (ACH) measured (25–35 h^{-1}, Figure 1).

When background particle emissions and indoor sources are negligible (i.e., $S_{tot}\ (t) \approx 0\ min^{-1}$), e.g., during the lunch break, the particle number concentration decay curve may be described as follows:

$$N(t) = N_{t=0} \cdot e^{-\gamma \cdot t}, \quad (4)$$

The calculated ACH varied from 25 to 35 h^{-1}, which is much higher than particle deposition rates, which are typically below 4 h^{-1} in indoor environments for particles within the measurement range in this work (10 nm to 35 µm; [47]). Thus, the only particle loss considered is through ventilation, and here it was assumed that $\lambda \approx$ ACH.

According to the convolution theorem, the particle number concentration during the activity is a convolution of the particle sources and particle losses as follows [38]:

$$S_{tot}(t) \cdot N(t) = V_0 \int^t (Q N_{BG}(t) + \varepsilon_C S_N(t)) \cdot N(t-\tau) d\tau, \quad (5)$$

where Q (m^3 h^{-1}) is the air flow and ε_C (-) is the protection factor of the booth.

The particle emission term can be solved with a numerical deconvolution as:

$$S_{tot}(t) = V \cdot (N(t) - N(t-\Delta t) \cdot e^{-\gamma \cdot \Delta t})/\Delta t, \quad (6)$$

In this work, particle emission rates were calculated for the pre-activity period when $S_N(t) = 0$ min^{-1} to estimate background particle generation rate $S_{BG}(t) = Q N_{BG}(t)$ (corresponding mainly to infiltration from outdoor air). Because the booth protection factor ε_C was not known, the plasma spray emission rate term is a combination of $\varepsilon_C S_N$ where background particle emission rate S_{BG} is subtracted.

Steady State Equation for Cyclic Processes

In addition, emission rates during the activity were also calculated using particle number concentrations (cm^{-3}) monitored in the WA with the NanoScan instrument, by applying the modified steady state equation for cyclic processes [7]:

$$S_N = \hat{C} \cdot V / t_{ESD}, \quad (7)$$

where $\hat{C}$ (cm^{-3}) is the mean concentration of particles (as number concentration) during spraying, V (cm^3) is the volume of the room, and t_{ESD} (min) is the spraying duration. Assumptions were that particle concentrations before the activity were lower than during the activity, particle removal processes were negligible, and that particle concentrations were fully mixed.

2.4.3. One-box Mass Balance Model

As particle concentrations monitored inside the booths exceeded the instrument's measurement range, applying a two-box model to estimate particle concentrations inside and outside the booths was not possible. Therefore, a one-box model was applied to calculated particle number concentrations. With the emission rates calculated in the WA, the one-box model was applied to the WA volume considering the influence of two types of ventilation systems: the central one in the WA, and the ventilation driving the air flows from the WA to the booth due to the booth's LEV (Figure 1). Booth air extraction systems were compensated with air coming from the WA (through the door and through small holes for cables) and from outdoors (through a direct pipeline connecting with outdoor air). Background particle concentrations were included in the model with the incoming air, as this was seen to improve mass-balance model performance and accuracy [33].

3. Results and Discussion

3.1. Exposure Concentrations

Particle number concentrations (Table 1) were monitored during thermal spraying in booth #1 (APS, days 1 and 2) and #3 (HVOF, days 3 and 4). Respirable particle mass concentrations varied from 130 to 709 µg m^3 inside the booths, and 93 to 172 µg m^3 in the WA (Table S2, Supplementary material), which is below the occupational exposure limits (OELs) given in the material safety data sheet (MSDS). A clear impact on particle number concentrations was observed inside the booths and

in the WA, once the spraying activity started (Figure 2 and Figures S2 and S3, Supplementary material). Additionally, chemical analyses of the airborne particles indicated that they had the same composition as the feedstock material being sprayed (more details in Salmatonidis et al., 2019 [7]). Thus, it was concluded that the spraying activities generated high concentrations of unintentionally emitted NPs. Chemical analyses of the airborne particles indicated that their composition in terms of mass was that of the raw feedstock material, and that chromium was present in the form of chromium carbide and nickel in its free form (more details in Salmatonidis et al., 2019 [7]).

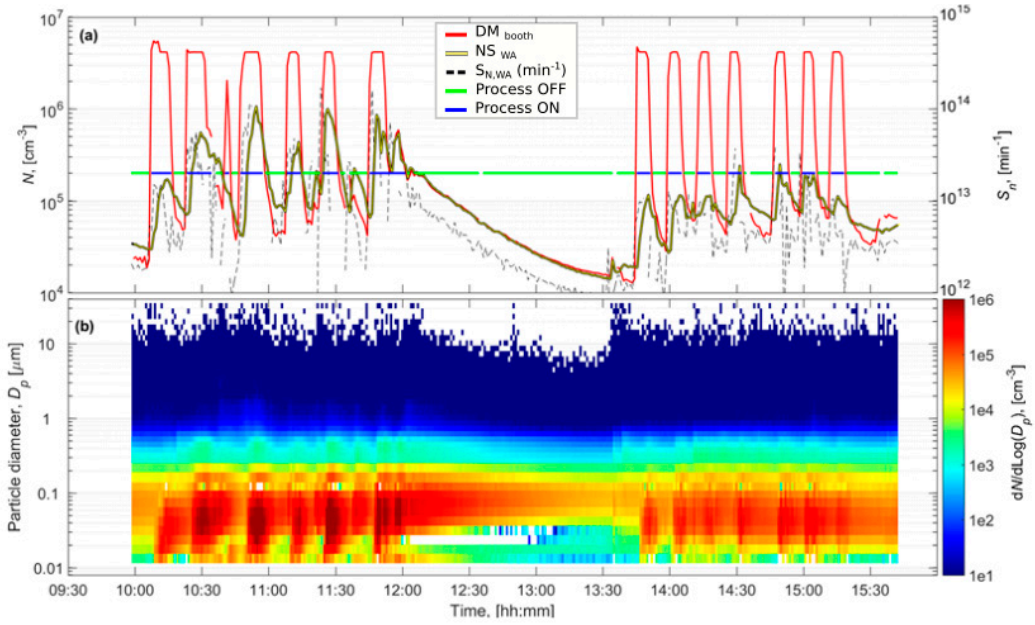

Figure 2. Booth #3, Day 3 **(a)** shows the particle number concentrations measured inside the booth by DiSCmini (DM), from worker area by NanoScan (WA) and particle emission rates solved by convolution from NanoScan WA concentrations. Blue line shows when the DM concentration was $>10^5$ cm^{-3} indicating that the plasma spray was ON and green line when the DM concentration was $<10^5$ cm^{-3} indicating that the plasma spray was OFF. Figure **(b)** shows the particle size distributions measured by the NanoScan in the WA.

The particle number concentrations, measured with the DiSCmini inside the booths during spraying, ranged between 8.5×10^5 and 3.5×10^6 cm^{-3} in booth #1, and between 1.0×10^6 and 1.9×10^6 cm^{-3} in booth #3 (Table 1), exceeding instruments detection limit (Figure 2 and Figures S1, S2 and S3, Supplementary material). The operators wore personal protective equipment (FPP3, masks in booth #3, and welding helmet with respirator in booth #1) when they entered the booths but in the WA, the operators only wore the masks intermittently. NP concentrations were approximately one order of magnitude lower than inside the booths (6.4×10^3-9.6×10^4 cm^{-3} and 1.1-3.5×10^5 cm^{-3} for booth #1 and #3, respectively). However, the impact of booth #1 emissions on WA concentrations (especially during day 1) was lower than that of booth #3 emissions (Table 1). Particle concentrations recorded in the WA by the NanoScan monitor were similar to the ones measured by the DiSCmini: 4.2-7.8×10^4 cm^{-3} and 9.0×10^4-2.5×10^5 cm^{-3}, for booth #1 and #3, respectively. Due to the similarity between both datasets, and the fact that the NanoScan provided additional information on particle size distributions, the latter dataset was used as an input for the one-box model.

In booth #3 the worker had to enter the booth between repetitions to exchange the coated surface with a new one (to be coated). As the spraying periods were short (5–10 min), the door of the booth was kept open between repetitions during Day 2/Morning, whereas during Day 2/Afternoon the door was alternatively open and closed. This explains the significantly lower concentrations measured in the WA during Day 2/Afternoon compared to during the Morning (Figure 2).

In all cases (inside the booths, and in the WA except on Day 1), particle concentrations exceeded the 40,000 cm^{-3} threshold considered the nano-reference value used in the precautionary approach [48], and they were statistically significantly higher than background concentrations [44], Eq. 1).

Table 1. Measured particle number concentration during the thermal spraying activity. Statistically significant increases are marked in bold.

Day	Shift	Booth	Worker Area (WA)		Inactivity (BG)	
		DiSCmini N (cm^{-3})	DiSCmini N (cm^{-3})	NanoScan N (cm^{-3})	DiSCmini N (cm^{-3})	NanoScan N (cm^{-3})
Booth #1 Model Area (Day 1)	Afternoon	**3.5×10^6**	6.4×10^3	4.2×10^4	1.2×10^4	1.4×10^4
Booth #1 Model Area (Day 2)	Morning Afternoon	**1.1×10^6** **8.5×10^5**	**9.6×10^4** **6.7×10^4**	**7.8×10^4** **4.9×10^4**	1.2×10^4	1.7×10^4
Booth #3 Model Area (Day 3)	Morning Afternoon	**1.9×10^6** **1.7×10^6**	**3.5×10^{5e}** **1.1×10^5**	**2.5×10^5** **9.0×10^4**	2.0×10^4	1.9×10^4
Booth #3 Model Area (Day 4)	Morning Afternoon	**1.3×10^6** **1.0×10^6**	**1.9×10^5** **1.6×10^5**	**1.5×10^5** **1.3×10^5**	4.5×10^4	3.7×10^4

3.2. Air Exchange Quantification

Air speeds were measured at the central ventilation system and at the doors of the booths, during activity periods, and were used to quantify the total air flows in the WA during spraying. The total air changes per hour (ACH, h^{-1}) were then estimated by considering the volume of each of the modeled areas (to reproduce emissions from booths #1 and #3, Figure 1). The total flows (Q) for model area #1 and #3 were 16078 and 6216 m^3 h^{-1}, respectively with ACH values of 35 and 25 h^{-1}. These values are quite high although in line with reported values in industrial environments, which typically range between 0.3-30 h^{-1} [49,50]. Additionally, air speeds were measured at the booth doors when they were open, with ACH ranging between 49–89 h^{-1} (Table S3). The latter ACH are not representative of actual working conditions, given that doors were mostly closed when the spraying guns were operating. Overall, the ACH measured indicate a high variability of the air exchange rates in the workplace, which would influence the modeling results as the ACH is, together with the emission rate, a key input parameter for the model.

3.3. Particle Emission Rates

Particle emission rates were estimated based on WA concentrations, using convolution and cyclic steady state equations (Table 2) in order to compare the results from both approaches. Results showed that emission rates from booth #1 ranged between 1.4×10^{11}–3.4×10^{12} min^{-1} using the convolution theorem, and between 1.3×10^{12}–3.0×10^{12} min^{-1} using the cyclic steady state equation. Both approaches provided similar outputs for booth #3, ranging between 7.9×10^{12}–1.2×10^{13} min^{-1}, with the convolution theorem and between 7.9×10^{12}–1.4×10^{13} with the cyclic steady state. Emission rates were higher from booth #3 than from booth #1, which is consistent with the different operational procedures (HVOF vs. APS; [7]).

Table 2. One-Box modeled concentrations using the convolution theorem and the cyclic steady state (Cyclic SS) approach to calculate emission rate (S_N) from NanoScan data. Emission rates were calculated for each day considering all activity periods, and modelings were applied for morning (M) and afternoon (A) periods (shift) separately.

Model Area		**Booth #1**			**Booth #3**			
Day		**Day 1**	**Day 2**		**Day 3**		**Day 4**	
Shift		**A**	**M**	**A**	**M**	**A**	**M**	**A**
WA NanoScan S_N	**Convolution**	1.4×10^{11}	3.4×10^{12}		1.2×10^{13}		7.9×10^{12}	
	Cyclic SS	1.3×10^{12}	3.0×10^{12}		7.9×10^{12}		1.4×10^{13}	
Modeled concentrations (cm^{-3})	**Convolution**	1.4×10^{4}	2.0×10^{4}	2.4×10^{4}	5.9×10^{4}	6.0×10^{4}	5.6×10^{4}	5.3×10^{4}
	Cyclic SS	1.7×10^{4}	2.0×10^{4}	2.4×10^{4}	4.5×10^{4}	4.6×10^{4}	7.1×10^{4}	6.5×10^{4}
WA measured (cm^{-3})	**NanoScan**	4.2×10^{4}	7.8×10^{4}	4.9×10^{4}	2.5×10^{5}	9.0×10^{4}	1.5×10^{5}	1.3×10^{5}
	DiSCmini	6.4×10^{3}	9.6×10^{4}	6.7×10^{4}	3.5×10^{5}	1.1×10^{5}	1.9×10^{5}	1.6×10^{5}
Ratio (modeled/NanoScan measured)	**Convolution**	0.33	0.26	0.49	0.24	0.67	0.37	0.41
	Cyclic SS	0.40	0.26	0.49	0.18	0.51	0.47	0.50
Ratio (modeled/DiSCmini measured)	**Convolution**	2.19*	0.21	0.36	0.17	0.55	0.29	0.33
	Cyclic SS	2.66*	0.21	0.36	0.13	0.42	0.37	0.41

* Unusually high ratios were obtained for Day 1, probably due to the low impact of particle emissions on WA concentrations (Figure S1) which led to an overestimation of low concentrations by the model.

In general, both methods provided relatively similar results despite the differences in calculations, thus supporting the robustness of the emission rates calculated. The cyclic steady state generally provided higher emission rates than the convolution theorem (from 1.8 up to 10 times higher), with the exception of Day 3 in booth #3, for which the convolution theorem provided a higher rate (by a factor of 4–16; Table 2). When using the cyclic steady state, differences between days in the same booth were smaller than when using the convolution theorem, suggesting that the convolution theorem is more case-sensitive and will, therefore, probably provide more precise modeling results. In Koivisto et al. (2018) [15], where particle number emission rates were quantified during electrostatic spray deposition of TiO2 by using the same approaches as in the present study, emission rates near the source were 2.2×10^{12} min^{-1} (convolution theorem) and 1.1×10^{12} min^{-1} (cyclic steady state). As in the present work, emission rates calculated with the two methods were mostly comparable despite differences in the calculation methods.

The emission rates quantified for the thermal spraying activities were comparable to other emission sources in the literature, e.g., dip coating (4.2×10^{11} min^{-1} and 6.6×10^{11} min^{-1}, [40], laser printing (maximum rates between 2.4×10^{9} and 1.0×10^{13}; [38,51,52]), in houses due to Tabaco ($0.84\text{-}3.76 \times 10^{11}$ min^{-1}) and cooking ($1\text{-}8 \times 10^{11}$ min^{-1}) [53–55], or NP production in academic laboratories (1.3×10^{11}–1.2×10^{12} min^{-1}; [56]), among others.

3.4. One-Box Model Performance

Worker area (WA) particle number concentrations were modeled by applying a one-box mass balance model [28]. The two types of emission rates calculated (using convolution theorem and cyclic steady state approach) were used as input, with the aim to test model performance under a real-world industrial scenario. The one-box model was applied to the booth #1 and #3 model areas, to predict particle number concentrations in the WA during thermal spraying from each of the booths. The model was tested for two days (including one morning and one afternoon shift, each) in each model area (#1 and #3).

Modeled particle number concentrations in the WA based on the NanoScan monitored concentrations ranged between $1.4\text{–}2.4 \times 10^{4}$ (convolution theorem) and $1.7\text{–}2.4 \times 10^{4}$ (cyclic steady state) while spraying in booth #1, and between $5.3\text{–}6.0 \times 10^{4}$ (convolution theorem) and $4.5\text{–}7.1 \times 10^{4}$ (cyclic steady state) while spraying in booth #3 (Table 2). When comparing these concentrations with actual measured NanoScan ones, on a case by case basis, results indicate that in all cases the model underestimated measured concentrations irrespective of the method used to calculate emission rates: ratios modeled/measured concentrations were < 0.5 for all of the study cases (with one exception, Figure 3a). When comparing modeled concentrations to measured DiSCmini concentrations in the

WA, ratios modeled/measured were consistent with those obtained with NanoScan (<0.55, except for the booth #1, day 1), also underestimating measured concentrations (Table 2 and Figure 3a). In general, higher underestimations and variability of the measured concentrations were obtained when using the DiSCmini dataset for model validation. These differences may be attributed to the fact that both instruments (NanoScan and DiSCmini) are not directly comparable as DiSCmini (corona charging principle) monitors particle diameters between 10–700 nm while NanoScan (single particle counting) monitors 20–420 nm (Fonseca et al., 2016). It should be noted that concentrations in terms of particle number are significantly higher than in terms of mass, which is a metric more frequently used with mass balance models, and both metrics are known to represent different particle properties (e.g., size, density, etc.) and therefore have different behaviors [56].

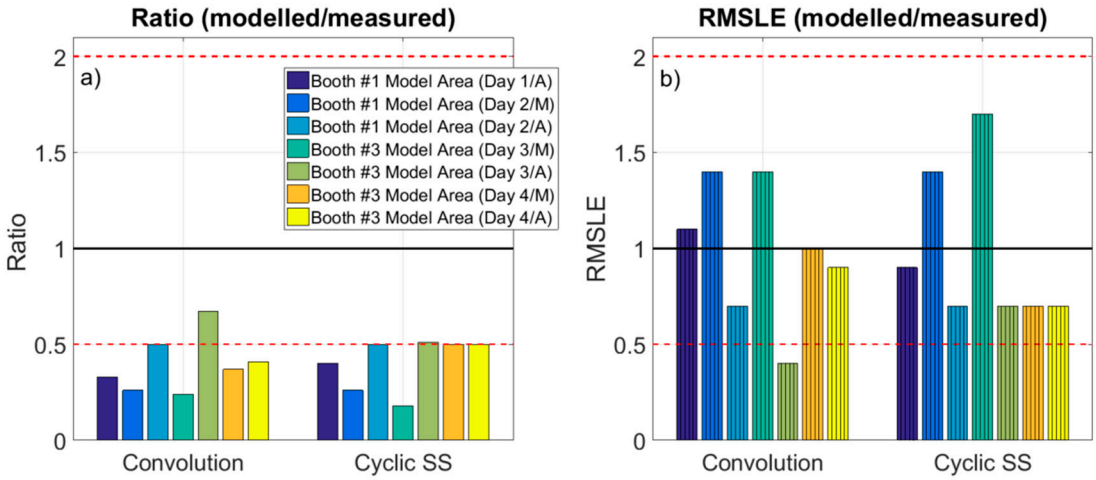

Figure 3. Ratio modeled/measured concentrations **(a)**, and RMSLE (modeled/measured) **(b)**. Ratio 0.5 and 2 are marked as reference (dashed line). Cyclic SS: cyclic steady state equation.

Because of this limitation, the assessment of the root mean squared logarithmic error (RMSLE) is proposed to not over-penalize differences between predicted and actual values, when concentrations are high [36]. This is because the RMSLE mainly takes into account the ratio of change, rather than the actual concentrations. Figure 3b shows that the RMSLE (modeled/NanoScan measured) ranged between 0.4–1.4 when using convolution emission rates and 0.7–1.7 when using cyclic steady state. The same analysis using the DiSCmini dataset resulted in RMSLE (modeled/DiSCmini measured) between 0.6–1.8 when using convolution emission rates and 0.9–2.1 when using cyclic steady state (data not shown). These ratios were compared to the benchmarks proposed by Jayjock et al. (2011) [30], which representative of modeling outputs reviewed in literature. Thus, when considering the RMSLE, only one case was outside the Jayjock et al. (2011) benchmark (0.5–2): booth #3 (Day3/A) with the convolution theorem. This would mean that, according to the ranges suggested by Jayjock et al. (2011), the performance of the one-box model for the industrial scenario assessed in this work would be considered as comparable. In the literature, several authors have reported underestimations by the one-box model [31,35,36,57,58] as it assumes homogeneous concentrations through all the room. This is consistent with our results, even though the high airflows measured in the industrial scenario allowed us to assume adequate mixing, on average. However, it is possible that full mixing was not achieved at all times and during all repetitions, and this should be considered as one of the limitations of the present work.

Model underestimations could also be related to inaccurate ACH calculation or to the underestimation of emission rates including booth protection factor. Emission rates are known to be the most critical exposure determinant, and thus should be calculated based on experimental data collected as close (physically) to the source as possible with known dilution and mixing. Otherwise, large differences may be detected depending on the location and position of the monitoring

instrumentation [36]. These authors demonstrated that emission rates can be corrected by using an adjusting coefficient to compensate for unknown flow distributions. The results presented in this work, which are based on emission rates calculated from data collected at a distance from the source (>3m), support the need for a correction coefficient to improve the emission rates calculated. Unfortunately, knowledge of air mixing is a frequent issue encountered when measurements are carried out in real-world industrial scenarios.

The results were also analyzed in terms of average RMLSE across all cases (Days 1 to 4, morning and afternoon shifts), for the booth #1 and #3 scenarios (Figure 4). Results show that when emission rates were calculated using the convolution theorem, model predictions were more closely aligned with RMLSE = 1 than when the cyclic steady state equation was used, and the ratios (especially for booth #3) presented lower variability. The results obtained when applying the convolution theorem were more case-sensitive, whereas applying the cyclic steady state required lower computational efforts. Overall, differences obtained with both parametrizations were not large. Therefore, for preliminary risk assessment and based on the data from this industrial scenario, particle emission rates calculated with the cyclic steady state equation may be sufficient, whereas for a more case-specific analysis the convolution theorem may be a better approach for emission rate calculation.

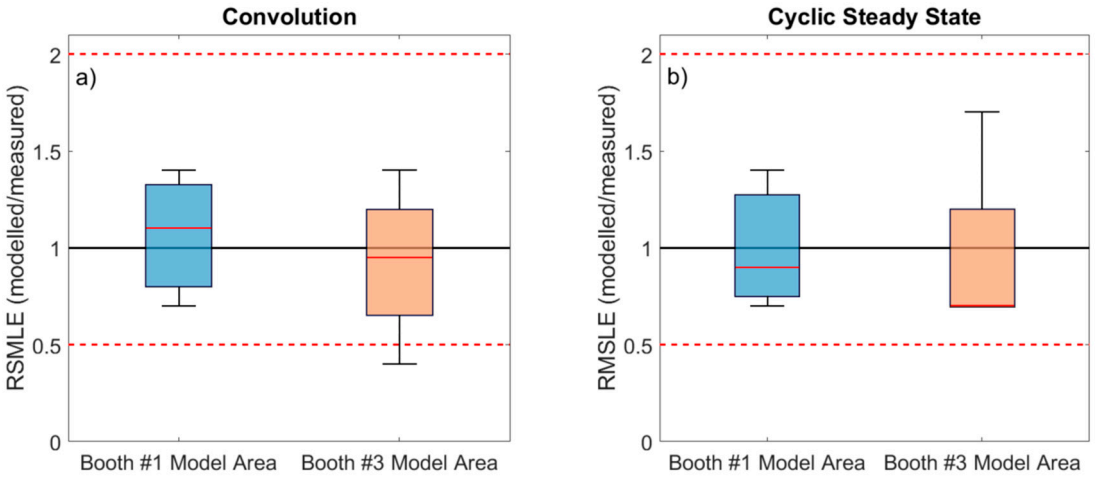

Figure 4. Vertical box plot for RMSLE modeled/measured concentrations for booth#1 and booth#3 model areas using convolution SN **(a)** and Cyclic steady state SN **(b)**. Ratio 0.5 and 2 are marked as reference (dashed line). The boundary of the box closest to zero indicates the 25th percentile and the farthest from zero the 75th percentile. The solid red line within the box indicates the median value. Error bars above and below indicate the 10th and 90th percentiles.

Finally, model performance was also evaluated with regard to the type of particles emitted, which were different in the two scenarios given that different thermal spraying techniques were used (APS in booth #1, and HVOF in booth #3). In short, particles emitted in booth #1 were mostly spherical and resulting from melting of the ceramic powder sprayed, while particles emitted in booth #3 showed more irregular morphologies resulting from mechanical impaction of the powder on the surface to be coated [7]. Modeling results for both scenarios showed only slight differences (Figure 4), which did not seem to be linked to the spraying techniques (APS and HVOF) but rather to the layout and configuration of the study area (Figure 1). In the booth #1 model area the door was always kept in a similar position (partially closed). Conversely, in the booth #3 model area, due to requirements of the spraying process the worker had to enter and exit the booth frequently, which means that the door configuration and the number of times that it was open and closed was different in every shift. The door configuration not only impacts particle transport, but also air flows (ACH). The impact of this can be clearly observed in Day 3 (Figure 2), where markedly higher concentrations were recorded in the WA during the morning (when the door was open) than in the afternoon (door closed),

while emissions at the source remained at relatively constant levels. Given that particle emission rates were calculated for full days, this intra-daily variability is considered a source of the higher variability in modeled/measured ratios (Figure 3) and RMLSE (Figure 4) observed for booth #3 (in comparison with booth #1). This result indicates that, to improve model performance, not only emission rates but also the ACH need to be calculated as precisely as possible, given that small variations can lead to significant under- or overestimations of particle concentrations and, thus, can limit the effectiveness of risk assessments and lead to impaired decision-making.

An example of the variability of model outcomes is reported in Supplementary material (Table S3 and S4), using a different door configuration (door fully open). The estimated ACH values from measured air speeds when booths doors were open ranged between 49–89 h^{-1}, which is approximately double than the ACH (25–35 h^{-1}) estimated when booths doors were closed. Modeled/measured concentrations ratios using ACH 49–89 h^{-1} ranged between 0.1–0.4, indicating higher underestimations of measured concentrations than when using ACH 25–35 h^{-1} (when ratios ranged between 0.2–0.7, Table 2). As door configurations and worker layout were not always constant, especially in booth #3 where the time during which the door was open/closed was different in every repetition, estimated ACH values used for the modeling (25–35 h^{-1}) may not be fully representative of actual ACH values for each specific repetition. In such cases, were ACH may be highly variable with time, a probabilistic approach or a sensitivity analysis as the one conducted in Ribalta et al., 2019 [33] would be highly useful.

According to the literature, mass balance models have been satisfactorily tested in real-world settings mostly in terms of particle mass [39,59–62] with ratios modeled/measured of 0.82–1.22 and 1.10 ± 2.32 during packing and pouring processes [32,33], and for vapors and sprays with ratios of 0.49–3.29 and 0.32–3.28 for chemical component emissions [30,63]. However, models have not been extensively tested for particle number concentrations, which is currently the most commonly-used metric for NP exposure, in real-work environments. In Jensen et al. [35,36], one-, two- and three-box models were tested for particle number concentrations from a brush generator in a controlled chamber experiment, with models being able to estimate concentrations within a RMSLE factor of 0.5–2 [36].

In the present work, ratios for modeled concentration were 0.2–0.7 and RMSLE 0.4–1.7, with the model clearly underestimating actual exposures. It may thus be concluded that the one-box model can provide a preliminary idea of the order of magnitude of unintentional NP concentrations, and that the accuracy of the results depends on the input parameters like ACH and particle emission rates. Therefore, the availability of a publicly-shared emission-rate library for modeling would be highly useful for preliminary risk assessments in absence of measured emission rates or particle concentrations. However, more precise modeling results require accurate quantification of the input parameters, implying that additional work in model parametrization is necessary. Model underestimations, even when ratios are within the 0.5–2 benchmark, are undesirable from a risk assessment point of view, where overestimating concentrations would be more precautionary.

4. Conclusions

An industrial scenario characterized by high concentrations of unintentionally-released NPs was selected to test the performance of a one-box mass balance model. Emission rates in terms of particle number concentration, one of the main inputs of the model, were estimated using two approaches: the convolution theorem and the cyclic steady state equation. The main conclusions extracted are:

- Nanoparticle emission rates from thermal spraying of ceramic coatings were from the booth to working area (WA) in the range 1.4×10^{11}–1.4×10^{13} min^{-1}. These emission rates are slightly higher or of a similar order of magnitude as those reported in the literature from sources such as industrial dip-coating, laser printing or even indoor cooking in homes.
- Both approaches for emission rate calculation provided comparable rates, which were slightly lower when the convolution theorem was used. The cyclic steady state approach required lower computational efforts.

- The one-box model underestimated concentrations measured in the WA irrespective of the method used for emission-rate calculation. The ratios modeled/measured concentrations were 0.2–0.7 (using the convolution theorem) and 0.2–0.5 (using the cyclic steady state equations). When correcting high concentrations by using the root mean squared logarithmic error (RMSLE), ratios were 0.4–1.4 (convolution) and 0.7–1.7 (cyclic steady state).
- Even though both model parametrizations showed similar performance on average, the use of emission rates calculated with the convolution theorem improved results on a case by case basis (results were more case-sensitive). Thus, emission rates calculated with the cyclic steady state approach would be advisable for preliminary risk assessment, while for more precise case-specific results, the convolution theorem would be the better option.
- An additional key input affecting model performance was seen to be the estimation of the air exchange per hour (ACH). This parameter was strongly impacted by the position of the door of the booth where emissions were generated, which should be taken into account carefully in modeling exercises.
- In sum, with adequate parametrization, one-box mass balance models may provide useful guidance regarding the order of magnitude of expected particle number concentrations in industrial scenarios, and thus be used as a preliminary risk assessment tools.

Supplementary Materials: The following are available online at http://www.mdpi.com/1660-4601/16/10/1695/s1, Figure S1: Booth #1, Day 1 a) shows particle number concentrations measured inside the booth by DiSCmini (DM), from worker area by NanoScan (WA) and particle emission rates solved by convolution from NanoScan WA concentrations, Figure S2: Booth #1, Day 2 a) shows particle number concentrations measured inside the booth by DiSCmini (DM), from worker area by NanoScan (WA) and particle emission rates solved by convolution from NanoScan WA concentrations, Figure S3: Booth #3, Day 4 a) shows particle number concentrations measured inside the booth by DiSCmini (DM), from worker area by NanoScan (WA) and particle emission rates solved by convolution from NanoScan WA concentrations, Table S1: Sampling day, booth, technic used (HVOF or APS), and feedstock materials summary, Table S2: Respirable mass concentration during the thermal spraying activity, Table S3: Parameterization of the single box model considering booth door open: V (m3) is volume used for modeling, Q (m3 h–1) is ventilation air volume flow through the Worker Area and ACH (h–1) is the air changes per hour calculated from measured air speeds, Table S4: One Box modeled concentrations considering booth door open, and using the convolution theorem and the cyclic steady state (Cyclic SS) approach to calculate emission rate (SN) from NanoScan data.

Author Contributions: All of the authors contributed substantially to the conception and design of the study. C.R., E.M. and M.V. contributed to conceptualization; C.R., A.J.K. and A.S. methodology; C.R. and A.J.K. data analysis; C.R., A.J.K. and A.L-L. writing—original draft preparation; C.R., A.J.K., A.L-L., E.M. and M.V. writing—review and editing; E.M. and M.V. supervision.

Funding: This research was funded by the Spanish MINECO (CGL2015-66777-C2–1-R, 2-R), and through project PCIN-2015–173-C02-01, under the frame of SIINN, the ERA-NET for a Safe Implementation of Innovative Nanoscience and Nanotechnology, by SIINN-ERANET project CERASAFE (id.:16). Additional support was provided by Generalitat de Catalunya AGAUR 2017 SGR41, the Spanish Ministry of the Environment (13CAES006), FEDER (European Regional Development Fund) "Una manera de hacer Europa".

Acknowledgments: The authors acknowledge TM COMAS (http://www.tmcomas.com) for their committed cooperation.

Conflicts of Interest: The authors declare no conflict of interest relating to the material presented in this article.

References

1. Lima, R.S.; Marple, B.R. From APS to HVOF spraying of conventional and nanostructured titania feedstock powders: A study on the enhancement of the mechanical properties. *Surf. Coat. Technol.* **2004**, *200*, 3428–3437. [CrossRef]
2. Tan, J.C.; Looney, L.; Hashmi, M.S.J. Component repair using HVOF thermal spraying. *J. Mater. Process. Technol.* **1999**, *92–93*, 203–208. [CrossRef]
3. Toma, F.-L.; Stahr, C.C.; Berger, L.-M.; Saaro, S.; Herrmann, M.; Deska, D.; Michael, G. Corrosion Resistance of APS- and HVOF-Sprayed Coatings in the Al_2O_3-TiO_2 System. *J. Therm. Spray Technol.* **2010**, *19*, 137–147. [CrossRef]

4. Barbezat, G. Application of thermal spraying in the automobile industry. *Surf. Coat. Technol.* **2006**, *201*, 2028–2031.
5. Fauchais, P.L.; Heberlein, J.V.R.; Boulos, M.I. *Thermal Spray Fundamentals*; Springer: New York, NY, USA, 2014; ISBN 978-0-387-28319-7.
6. Viana, M.; Fonseca, A.S.; Querol, X.; López-Lilao, A.; Carpio, P.; Salmatonidis, A.; Monfort, E. Workplace exposure and release of ultrafine particles during atmospheric plasma spraying in the ceramic industry. *Sci. Total Environ.* **2017**, *599–600*, 2065–2073. [CrossRef]
7. Salmatonidis, A.; Ribalta, C.; Sanfélix, V.; Bezantakos, S.; Biskos, G.; Vulpoi, A.; Simion, S.; Monfort, E.; Viana, M. Workplace Exposure to Nanoparticles during Thermal Spraying of Ceramic Coatings. *Ann. Work Expo. Health* **2019**, *63*, 91–106. [CrossRef] [PubMed]
8. Petsas, N.; Kouzilos, G.; Papapanos, G.; Vardavoulias, M.; Moutsatsou, A. Worker Exposure Monitoring of Suspended Particles in a Thermal Spray Industry. *J. Therm. Spray Technol.* **2007**, *16*, 214–219. [CrossRef]
9. Huang, H.; Li, H.; Li, X. Physicochemical Characteristics of Dust Particles in HVOF Spraying and Occupational Hazards: Case Study in a Chinese Company. *J. Therm. Spray Technol.* **2016**, *25*, 971–981. [CrossRef]
10. Ding, Y.; Kuhlbusch, T.A.J.; Van Tongeren, M.; Jiménez, A.S.; Tuinman, I.; Chen, R.; Alvarez, I.L.; Mikolajczyk, U.; Nickel, C.; Meyer, J.; et al. Airborne engineered nanomaterials in the workplace—A review of release and worker exposure during nanomaterial production and handling processes. *J. Hazard. Mater.* **2017**, *322*, 17–28. [CrossRef]
11. Fonseca, A.S.; Maragkidou, A.; Viana, M.; Querol, X.; Hämeri, K.; de Francisco, I.; Estepa, C.; Borrell, C.; Lennikov, V.; de la Fuente, G.F. Process-generated nanoparticles from ceramic tile sintering: Emissions, exposure and environmental release. *Sci. Total Environ.* **2016**, *565*, 922–932. [CrossRef]
12. Fonseca, A.S.; Viana, M.; Querol, X.; Moreno, N.; de Francisco, I.; Estepa, C.; de la Fuente, G.F. Ultrafine and nanoparticle formation and emission mechanisms during laser processing of ceramic materials. *J. Aerosol Sci.* **2015**, *88*, 48–57. [CrossRef]
13. Fujitani, Y.; Kobayashi, T.; Arashidani, K.; Kunugita, N.; Suemura, K. Measurement of the Physical Properties of Aerosols in a Fullerene Factory for Inhalation Exposure Assessment. *J. Occup. Environ. Hyg.* **2008**, *5*, 380–389. [CrossRef] [PubMed]
14. Koivisto, A.J.; Aromaa, M.; Koponen, I.K.; Fransman, W.; Jensen, K.A.; Mäkelä, J.M.; Hämeri, K.J. Workplace performance of a loose-fitting powered air purifying respirator during nanoparticle synthesis. *J. Nanopart. Res.* **2015**, *17*, 177. [CrossRef]
15. Koivisto, A.J.; Jensen, A.C.Ø.; Kling, K.I.; Kling, J.; Budtz, H.C.; Koponen, I.K.; Tuinman, I.; Hussein, T.; Jensen, K.A.; Nørgaard, A.; et al. Particle emission rates during electrostatic spray deposition of TiO_2 nanoparticle-based photoactive coating. *J. Hazard. Mater.* **2018**, *341*, 218–227. [CrossRef] [PubMed]
16. Kuhlbusch, T.A.J.; Neumann, S.; Fissan, H. Number Size Distribution, Mass Concentration, and Particle Composition of PM 1, PM 2.5, and PM 10 in Bag Filling Areas of Carbon Black Production. *J. Occup. Environ. Hyg.* **2004**, *1*, 660–671. [CrossRef]
17. Viitanen, A.-K.; Uuksulainen, S.; Koivisto, A.J.; Hämeri, K.; Kauppinen, T. Workplace Measurements of Ultrafine Particles—A Literature Review. *Ann. Work Expo. Health* **2017**, *61*, 749–758. [CrossRef]
18. Landrigan, P.J.; Fuller, R.; Acosta, N.J.R.; Adeyi, O.; Arnold, R.; Basu, N.; Baldé, A.B.; Bertollini, R.; Bose-O'Reilly, S.; Boufford, J.I.; et al. The Lancet Commission on pollution and health. *Lancet* **2018**, *391*, 462–512. [CrossRef]
19. GBD 2016 Risk Factors Collaborators. Global, regional, and national comparative risk assessment of 84 behavioural, environmental and occupational, and metabolic risks or clusters of risks, 1990–2016: A systematic analysis for the Global Burden of Disease Study 2016. *Lancet* **2017**, *390*, 1345–1422. [CrossRef]
20. World Health Organization. *Ambient Air Pollution: A Global Assessment of Exposure and Burden of Disease*; World Health Organization: Geneva, Switzerland, 2016; pp. 1–131.
21. Fröhlich, E.; Salar-Behzadi, S. Toxicological Assessment of Inhaled Nanoparticles: Role of in Vivo, ex Vivo, in Vitro, and in Silico Studies. *Int. J. Mol. Sci.* **2014**, *15*, 4795–4822. [CrossRef]
22. Oberdörster, G. Pulmonary effects of inhaled ultrafine particles. *Int. Arch. Occup. Environ. Health* **2001**, *74*, 1–8. [CrossRef]

23. Saber, A.T.; Jacobsen, N.R.; Jackson, P.; Poulsen, S.S.; Kyjovska, Z.O.; Halappanavar, S.; Yauk, C.L.; Wallin, H.; Vogel, U. Particle-induced pulmonary acute phase response may be the causal link between particle inhalation and cardiovascular disease. *Wiley Interdiscip. Rev. Nanomed. Nanobiotechnol.* **2014**, *6*, 517–531. [CrossRef] [PubMed]
24. Hussein, T.; Wierzbicka, A.; Löndahl, J.; Lazaridis, M.; Hänninen, O. Indoor aerosol modeling for assessment of exposure and respiratory tract deposited dose. *Atmos. Environ.* **2015**, *106*, 402–411. [CrossRef]
25. Nazaroff, W.W.; Cass, G.R. Mathematical modeling of indoor aerosol dynamics. *Environ. Sci. Technol.* **1989**, *23*, 157–166. [CrossRef]
26. Nazaroff, W.W. Indoor particle dynamics. *Indoor Air* **2004**, *14*, 175–183. [CrossRef] [PubMed]
27. Hussein, T.; Kulmala, M. Indoor Aerosol Modeling: Basic Principles and Practical Applications. *Water Air Soil Pollut. Focus* **2008**, *8*, 23–34. [CrossRef]
28. Hewett, P.; Ganser, G.H. Models for nearly every occasion: Part I—One box models. *J. Occup. Environ. Hyg.* **2017**, *14*, 49–57. [CrossRef]
29. Ganser, G.H.; Hewett, P. Models for nearly every occasion: Part II—Two box models. *J. Occup. Environ. Hyg.* **2017**, *14*, 58–71. [CrossRef]
30. Jayjock, M.A.; Armstrong, T.; Taylor, M. The daubert standard as applied to exposure assessment modeling using the two-zone (NF/FF) model estimation of indoor air breathing zone concentration as an example. *J. Occup. Environ. Hyg.* **2011**, *8*, D114–D122. [CrossRef]
31. Koivisto, A.J.; Kling, K.I.; Hänninen, O.; Jayjock, M.; Löndahl, J.; Wierzbicka, A.; Fonseca, A.S.; Uhrbrand, K.; Boor, B.E.; Jiménez, A.S.; et al. Source specific exposure and risk assessment for indoor aerosols. *Sci. Total Environ.* **2019**, *668*, 13–24. [CrossRef]
32. Koivisto, A.J.; Jensen, A.C.Ø.; Levin, M.; Kling, K.I.; Maso, M.D.; Nielsen, S.H.; Jensen, K.A.; Koponen, I.K. Testing the near field/far field model performance for prediction of particulate matter emissions in a paint factory. *Environ. Sci. Process. Impacts* **2015**, *17*, 62–73. [CrossRef]
33. Ribalta, C.; Koivisto, A.J.; López-Lilao, A.; Estupiñá, S.; Minguillón, M.C.; Monfort, E.; Viana, M. Testing the performance of one and two box models as tools for risk assessment of particle exposure during packing of inorganic fertilizer. *Sci. Total Environ.* **2019**, *650*, 2423–2436. [CrossRef]
34. Sahmel, J.; Unice, K.; Scott, P.; Cowan, D.; Paustenbach, D. The Use of Multizone Models to Estimate an Airborne Chemical Contaminant Generation and Decay Profile: Occupational Exposures of Hairdressers to Vinyl Chloride in Hairspray During the 1960s and 1970s. *Risk Anal.* **2009**, *29*, 1699–1725. [CrossRef]
35. Jensen, A.; Dal Maso, M.; Koivisto, A.; Belut, E.; Meyer-Plath, A.; Van Tongeren, M.; Sánchez Jiménez, A.; Tuinman, I.; Domat, M.; Toftum, J.; et al. Comparison of Geometrical Layouts for a Multi-Box Aerosol Model from a Single-Chamber Dispersion Study. *Environments* **2018**, *5*, 52. [CrossRef]
36. Jensen, A.C.Ø.; Poikkimäki, M.; Brostrøm, A.; Dal Maso, M.; Nielsen, O.J.; Rosenørn, T.; Butcher, A.; Koponen, I.K.; Koivisto, A.J. The Effect of Sampling Inlet Direction and Distance on Particle Source Measurements for Dispersion Modeling. *Aerosol Air Qual. Res.* **2019**, *39*, 40.
37. Koivisto, A.J.; Jensen, A.C.Ø.; Kling, K.I.; Nørgaard, A.; Brinch, A.; Christensen, F.; Jensen, K.A. Quantitative material releases from products and articles containing manufactured nanomaterials: Towards a release library. *NanoImpact* **2017**, *5*, 119–132. [CrossRef]
38. Schripp, T.; Wensing, M.; Uhde, E.; Salthammer, T.; He, C.; Morawska, L. Evaluation of Ultrafine Particle Emissions from Laser Printers Using Emission Test Chambers. *Environ. Sci. Technol.* **2008**, *42*, 4338–4343. [CrossRef]
39. Glytsos, T.; Ondráček, J.; Džumbová, L.; Eleftheriadis, K.; Lazaridis, M. Fine and coarse particle mass concentrations and emission rates in the workplace of a detergent industry. *Indoor Built Environ.* **2014**, *23*, 881–889. [CrossRef]
40. Koivisto, A.J.; Kling, K.I.; Fonseca, A.S.; Bluhme, A.B.; Moreman, M.; Yu, M.; Costa, A.L.; Giovanni, B.; Ortelli, S.; Fransman, W.; et al. Dip coating of air purifier ceramic honeycombs with photocatalytic TiO2 nanoparticles: A case study for occupational exposure. *Sci. Total Environ.* **2018**, *630*, 1283–1291. [CrossRef] [PubMed]
41. Lima, R.S.; Marple, B.R. Optimized HVOF titania coatings. *J. Therm. Spray Technol.* **2003**, *12*, 360–369. [CrossRef]
42. European Parliment and Council. *Directive 1999/45/EC*; European Parliment and Council: Brussels, Belgium, 1999.
43. Eurpean Parliament and Council. *(EC) 1272/2008*; European Parliment and Council: Brussels, Belgium, 2008.

44. Asbach, C.; Kuhlbusch, T.; Kaminski, H.; Stahlmecke, B.; Plitzko, S.; Götz, U.; Voetz, M.; Kiesling, H.-J.; Dahmann, D. *Standard Operation Procedures for Assessing Exposure to Nanomaterials, Following a Tiered Approach*; Federal Ministry of Education and Research: Bonn, Germany, 2012.
45. Kaminski, H.; Beyer, M.; Fissan, H.; Asbach, C.; Kuhlbusch, T.A.J. Measurements of Nanoscale TiO2 and Al2O3 in Industrial Workplace Environments—Methodology and Results. *Aerosol Air Qual. Res.* **2015**, *15*, 129–141. [CrossRef]
46. Jensen, A.C.Ø.; Levin, M.; Koivisto, A.J.; Kling, K.I.; Saber, A.T.; Koponen, I.K. Exposure Assessment of Particulate Matter from Abrasive Treatment of Carbon and Glass Fibre-Reinforced Epoxy-Composites—Two Case Studies. *Aerosol Air Qual. Res.* **2015**, *15*, 1906–1916. [CrossRef]
47. He, C.; Morawska, L.; Gilbert, D. Particle deposition rates in residential houses. *Atmos. Environ.* **2005**, *39*, 3891–3899. [CrossRef]
48. Van Broekhuizen, P.; Van Veelen, W.; Streekstra, W.H.; Schulte, P.; Reijnders, L. Exposure Limits for Nanoparticles: Report of an International Workshop on Nano Reference Values. *Ann. Occup. Hyg.* **2012**, *56*, 515–524. [PubMed]
49. Baldwin, P.E.J.; Maynard, A.D. A Survey of Wind Speeds in Indoor workplaces. *Ann. Occup. Hyg.* **1998**, *42*, 303–313. [CrossRef]
50. Koivisto, A.J.; Jensen, A.C.Ø.; Koponen, I.K. The general ventilation multipliers calculated by using a standard Near-Field/Far-Field model. *J. Occup. Environ. Hyg.* **2018**, *15*, D38–D43. [CrossRef] [PubMed]
51. He, C.; Morawska, L.; Taplin, L. Particle emission characteristics of office printers. *Environ. Sci. Technol.* **2007**, *41*, 6039–6045. [CrossRef]
52. Koivisto, A.J.; Hussein, T.; Niemelä, R.; Tuomi, T.; Hämeri, K. Impact of particle emissions of new laser printers on modeled office room. *Atmos. Environ.* **2010**, *44*, 2140–2146. [CrossRef]
53. Afshari, A.; Matson, U.; Ekberg, L.E. Characterization of indoor sources of fine and ultrafine particles: A study conducted in a full-scale chamber. *Indoor Air* **2005**, *15*, 141–150. [CrossRef]
54. He, C.; Morawska, L.; Hitchins, J.; Gilbert, D. Contribution from indoor sources to particle number and mass concentrations in residential houses. *Atmos. Environ.* **2004**, *38*, 3405–3415. [CrossRef]
55. Hussein, T.; Glytsos, T.; Ondráček, J.; Dohányosová, P.; Ždímal, V.; Hämeri, K.; Lazaridis, M.; Smolík, J.; Kulmala, M. Particle size characterization and emission rates during indoor activities in a house. *Atmos. Environ.* **2006**, *40*, 4285–4307. [CrossRef]
56. Demou, E.; Stark, W.J.; Hellweg, S. Particle emission and exposure during nanoparticle synthesis in research laboratories. *Ann. Occup. Hyg.* **2009**, *53*, 829–838. [PubMed]
57. Arnold, S.F.; Shao, Y.; Ramachandran, G. Evaluating well-mixed room and near-field–far-field model performance under highly controlled conditions. *J. Occup. Environ. Hyg.* **2017**, *14*, 427–437. [CrossRef] [PubMed]
58. Keil, C.B. A Tiered Approach to Deterministic Models for Indoor Air Exposures. *Appl. Occup. Environ. Hyg.* **2000**, *15*, 145–151. [CrossRef] [PubMed]
59. Boelter, F.W.; Simmons, C.E.; Berman, L.; Scheff, P. Two-zone model application to breathing zone and area welding fume concentration data. *J. Occup. Environ. Hyg.* **2009**, *6*, 289–297. [CrossRef]
60. Jones, R.M.; Simmons, C.E.; Boelter, F.W. Comparing two-zone models of dust exposure. *J. Occup. Environ. Hyg.* **2011**, *8*, 513–519. [CrossRef]
61. Lopez, R.; Lacey, S.E.; Jones, R.M. Application of a Two-Zone Model to Estimate Medical Laser-Generated Particulate Matter Exposures. *J. Occup. Environ. Hyg.* **2015**, *12*, 309–313. [CrossRef] [PubMed]
62. Zhang, Y.; Banerjee, S.; Yang, R.; Lungu, C.; Ramachandran, G. Bayesian Modeling of Exposure and Airflow Using Two-Zone Models. *Ann. Occup. Hyg.* **2009**, *53*, 409–424. [PubMed]
63. Nicas, M. The near field/far field model with constant application of chemical mass and exponentially decreasing emission of the mass applied. *J. Occup. Environ. Hyg.* **2016**, *13*, 519–528. [CrossRef] [PubMed]

Discussion

Chapter 5

5. DISCUSSION

As presented in chapter 2, this Thesis sets out to address 5 objectives which are discussed in detail in this section by linking them to the key results and findings from this work. A summary of the objectives and how they were tackled is presented below and summarized in Figure 5.1. The specific results obtained, and their links to the objectives, are presented in the integrated discussion below.

1) To assess worker exposure in different real-world ceramic workplace scenarios in order to identify process parameters and material's characteristics influencing particle emissions:

The impact of particle emissions on workplace exposure was assessed 1) at a pilot plant scale during mechanical handling of 5 ceramic materials (+2 additional materials described in section "4.1.1 Additional results") with different particle characteristics and two energy levels (**Publication I**); and 2) at industrial scale during packing of a total of 8 materials and in 5 different packing lines (with different levels of enclosure and energy applied) (**Publications II and III**). Additionally, worker exposure was assessed in a thermal spraying industrial workshop where two spraying techniques were used (APS and HVOF) (**Publication IV**).

2) To evaluate decision making approaches (determination of statistically significant increases) and metrics to report worker exposure (mass, particle number concentrations and surface area):

The assessment of frequently used metrics to report worker exposure linking exposure to health effects was tackled in **Publication II**, a case study where a total of 7 materials were packed in 3 packing lines. Additionally, 4 decision-making approaches were evaluated and compared for particle number and mass concentrations, in the same case study.

3) To study materials dustiness as a tool for worker exposure prediction:

The potential of the dustiness index as a tool for exposure prediction was investigated by correlating dustiness indexes with exposure concentrations in two case scenarios: a pilot plant where 5 ceramic materials (+2 materials in section "4.1.1 Additional results") were handled (**Publication I**), and an industrial plant where 7 materials were processed in 3 packing lines (**Publication II**). In addition, the relevance of the dustiness index as an

input parameter for the one- and two-box mass-balance models (1 material in 2 packing lines) was also evaluated (**Publication III**).

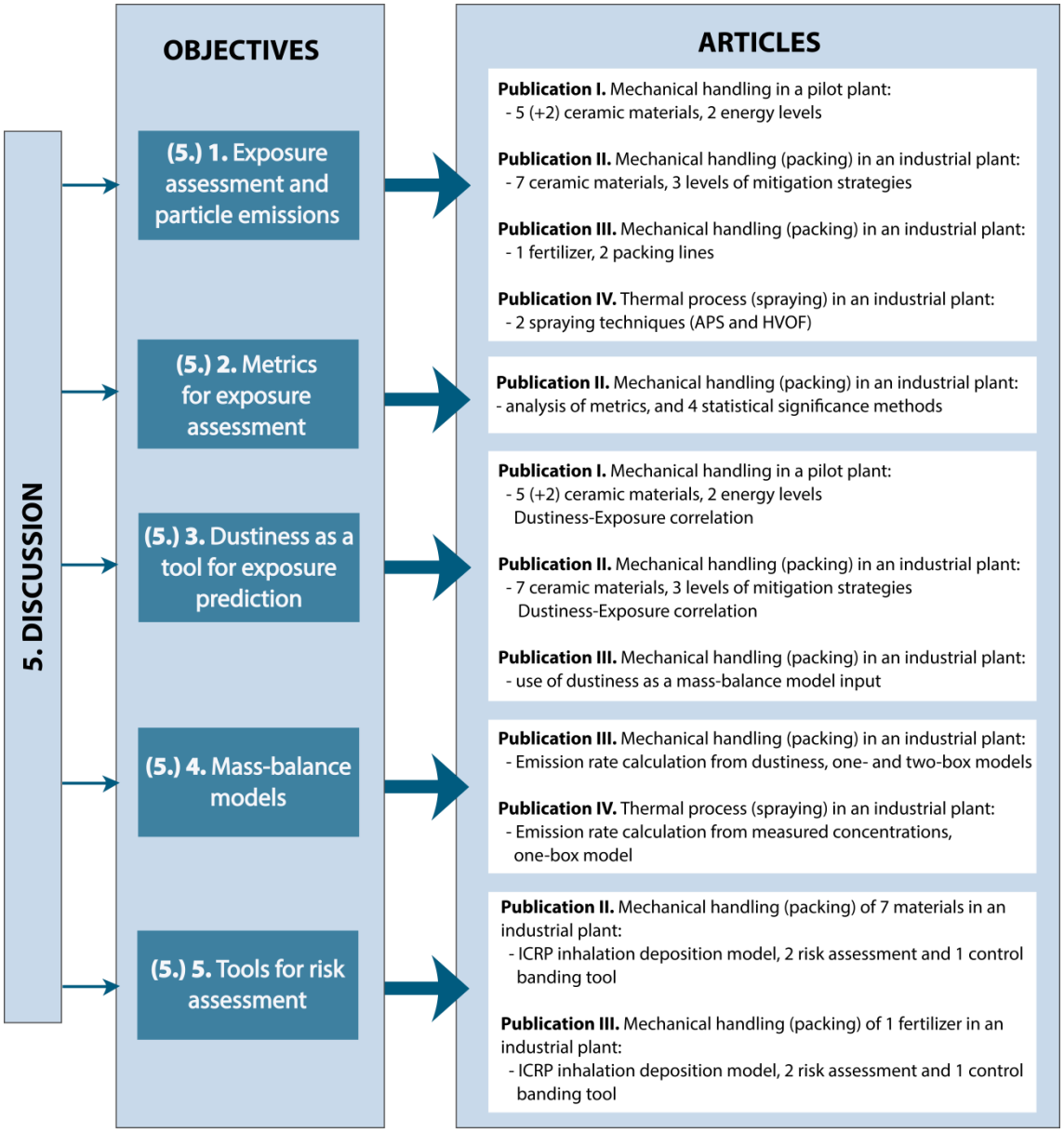

Figure 5.1 Links between the objectives of this Thesis and each of the research publications. ICRP: International Commission on Radiological Protection.

4) To evaluate mass-balance models (one- and two-box models) as worker exposure prediction tools under real-world settings:

One- and two-box mass-balance models were tested in two different scenarios, with low concentrations of coarse particles generated during mechanical handling of a granulated powder (**Publication III**), and with high NP concentrations emitted by a thermal spraying process (**Publication IV**).

5) To evaluate tools for health risk assessment such as the inhalation deposition dose ICRP model, and risk assessment and control banding tools:

Three risk assessment tools (ART, Stoffenmanager, NanoSafer), including one based on control banding (NanoSafer), were applied to two case studies where a total of 8 materials were packed in 5 different packing lines (**Publications II and III**). The models were also applied to the remaining case studies and the results are presented in sections 4.2.1 and 4.3.1 ("Additional results"). In addition, the ICRP inhalation deposition model was applied to the same case studies (**Publications II and III**).

5.1. Exposure assessment and particle emissions

Ceramic industry workplace exposure was assessed in a pilot plant and in 3 industrial settings, during handling or packing of 15 different types of powdered materials (Table 5.1; **Publications I, II and III**), and during a thermal process (thermal spraying).

Table 5.1 Summary of all materials subjected to mechanical handling, and their characteristics (particle shape, d_{50}, and dustiness index and classification). C.D: Continuous drop. R.D: Rotating drum.

Paper Nº	Material	Particle shape	Particle Size (d_{50}; µm)	Dustiness, Inhalable fraction (W_I)			
				Index (mg kg^{-1})		Classification	
				C.D	R.D	C.D	R.D
I	Si sand	Spherical	120	463	n/a	*Very low*	*n/a*
	Quartz 1.1	Spherical	12.1	4593	202	*Moderate*	*Very low*
	Quartz 1.2	Spherical	5.8	3855	164	*Low*	*Very low*
	Quartz 1.3	Spherical	3.4	3029	64	*Low*	*Very low*
	Kaolin 1.1	Plate-like	5.7	10012	410	*Moderate*	*Low*
	Clay 1.1	Plate-like	2.7	16811	968	*High*	*Moderate*
	Clay 1.2	Plate-like	5.0	20139	1097	*High*	*Moderate*
II	Clay 2.1	Plate-like	13	1733	96	*Low*	*Very low*
	Clay 2.2	Plate-like	10	5170	192	*Moderate*	*Very low*
	Kaolin 2.1	Plate-like	13	18886	353	*High*	*Low*
	Feldspar 2.1	Spherical	31-39	10246	455	*Moderate*	*Low*
	Quartz 2.1	Spherical	30-38	8891	480	*Moderate*	*Low*
	Feldspar 2.2	Spherical	22	9651	505	*Moderate*	*Low*
	Kaolin 2.2	Plate-like	8	12325	721	*Moderate*	*Moderate*
III	Fertilizer	Granulate	n/a	1026	76	*Low*	*Very low*

Results showed that handling of powdered materials (d_{50} 2.7-39 μm) increased inhalable and respirable particle mass concentrations significantly with regard to background concentrations, resulting in potential worker exposure risks (**Publications I, II and III**). In the same way, thermal spraying significantly increased respirable mass concentrations (**Publication IV**). OEL were, however, not exceeded. Conversely, concentrations in terms of particle number did in general not show statistically significant increases with regard to background concentrations, during the mechanical activities assessed in this Thesis (handling and packing of powders, ceramic materials and fertilizers) (**Publications I, II and III**). Statistically significant increases in particle number concentrations resulting in impacts on worker exposure were also detected in the mechanical activities assessed, but they were linked in most cases to NP emissions from parallel activities such as driving of diesel-powered forklifts or cleaning and vacuuming activities, as well as due to outdoor air infiltration (**Publication I, II and III**). Conversely, thermal spraying was seen to significantly impact particle number concentrations exceeding the nano-reference recommended limit value (40000 cm^{-3}) (**Publication IV**). As will be further discussed below, these results evidence the need to implement different particle monitoring strategies in workplace settings, given the variety of potential particle emission sources which results in a broad variety of particle characteristics and potential metrics (e.g., particle number and mass concentrations).

On average, mean inhalable particle mass concentrations monitored in the workplaces where mechanical handling was assessed ranged between 80 and 4000 μg m^{-3}, and were the highest for packing of ceramic materials in line where low mitigation strategies were applied (Table 5.2) (**Publication II**). Respirable mass concentrations showed similar tendency as inhalable mass concentrations, and ranged between 17 and 598 μg m^{-3} for mechanical handling (Figure 5.2 and Table 5.2). Conversely, particle number concentrations monitored were on average closer to urban background and traffic site concentrations in Europe (e.g., 1.5-3.0x10^4 cm^{-3}, Reche *et al*. 2011) than in the case of particle mass. As discussed above, this is linked to the smaller number of ultrafine particle or NP sources in the industrial scenarios assessed (with the exception of the thermal spraying plant). The highest mean particle number concentrations were recorded while handling of the inorganic fertilizer (7x10^4 cm^{-3}) and during thermal spraying with concentrations reaching averages of 10^6 and 10^5 cm^{-3} in booths and worker area, respectively (Figure 5.3 and Table 5.2) (**Publication III and IV**). For the thermal process, respirable mass concentrations ranged between 90-160 and 130-700 μg m^{-3} in

the worker area and inside the booths, respectively (**Publication IV**). Finally, mean particle diameters within the monitoring range of the portable SMPS NanoScan (20-420 nm) and MiniWras (10 nm-35 µm) ranged between 40 and 90 nm (Figure 5.4 and Table 5.2), while for most of the materials it was approximately 30-50 nm which was attributed to infiltration of ambient air urban ultrafine particles.

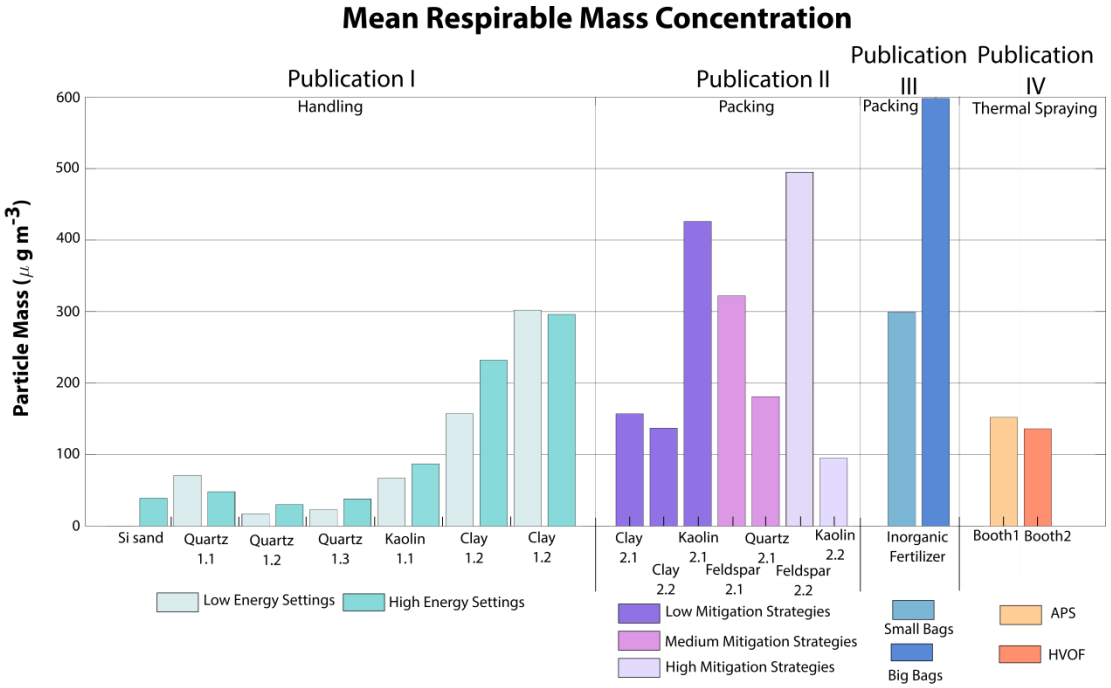

Figure 5.2 Bar plot for mean respirable mass concentrations measured for each case and material. Respirable mass concentrations were monitored with the Grimm mini-LAS.

Particle mass concentration was therefore identified as the most relevant metric for the scenarios assessed in this Thesis. At a fine temporal resolution, mass concentrations showed a cyclic behaviour, with major increases, which exceeded the 8h occupational exposure limits during short periods of time coinciding with each repetition of the specific activity under study. Major particle releases were also detected during accidents (**Publication I and II**). Particle mass concentrations usually showed relatively fast decreases to background levels after cessation of the activity, as opposed to particle number concentrations which progressively accumulated over time (**Publication I**). The impact of such short-term high particle mass concentrations would be undetected if only 8h TWAs were monitored and potentially significant impacts on worker's health would be under-reported. Therefore, this work highlights that time-resolved monitoring of particle metrics, at least particle mass and number concentrations, is essential. In addition, these results also support the conclusions by Koponen *et al.* (2015), who pointed out the need to consider the number of repetitions as a critical issue in worker

exposure assessment given that cycles are usually marked by a peak concentration at the beginning. Similar cyclic patterns were observed in the scenarios assessed in this Thesis.

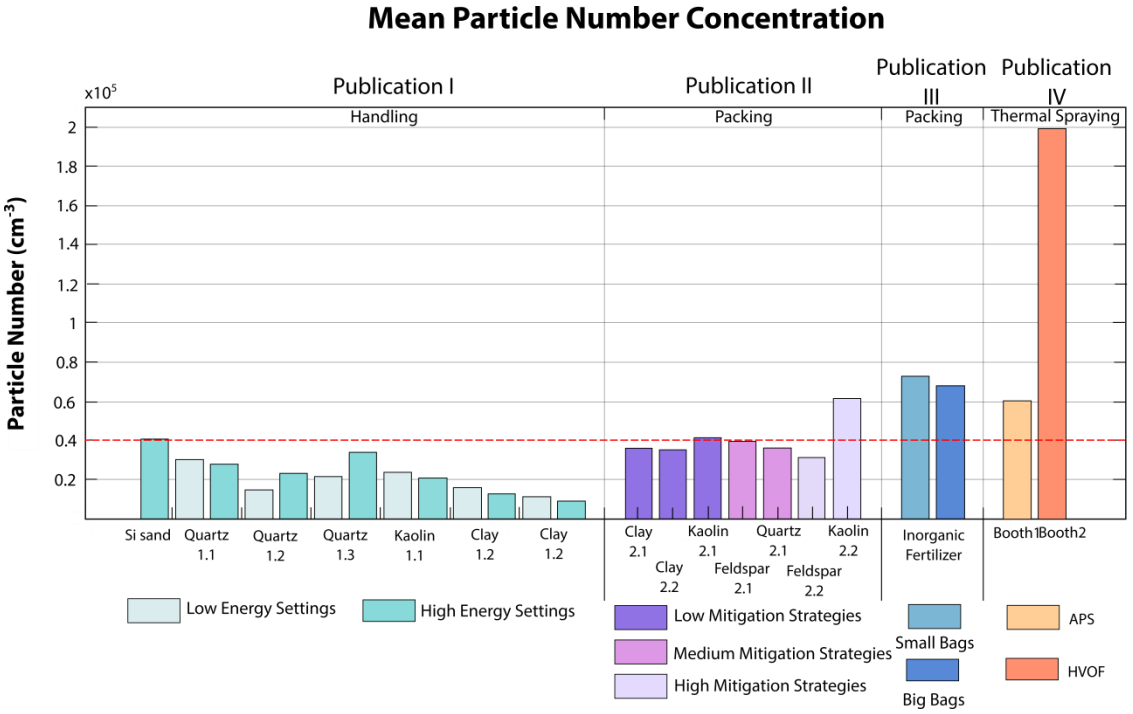

Figure 5.3 Bar plot for mean particle number concentrations measured for each material and case. Particle number concentration was monitored with the CPC except for publication III where NanoScan SMPS was used. Dashed line indicates the nano-reference value for particle number.

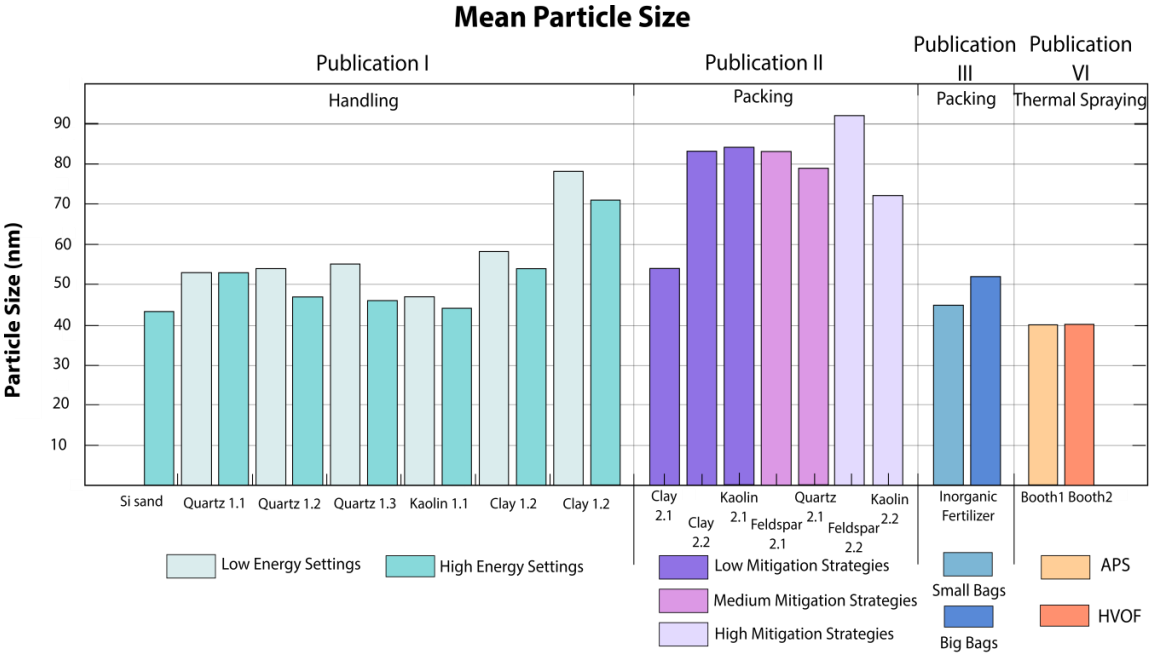

Figure 5.4 Bar plot for mean particle size measured for each case and material. Particle size was monitored with the NanoScan SMPS except for publication II where MiniWras was used.

Table 5.2 Summary of measured airborne particle concentrations. "Case": for Publication I, this refers to low and high energy settings; for Publication II, this refers to low, medium and high mitigation strategies applied along the packing line. *: device with asterisk was used (NanoScan, MiniWras). Concentrations given are for worker area measurements.

Paper N°	Material /Process	Case	Particle number (cm^{-3})	Particle size (nm)	Particle mass (Grimm mini-LAS) ($\mu g\ m^{-3}$)	
			CPC *NanoScan	NanoScan *MiniWras	Respirable	Inhalable
I	Si sand	Low	n/a	n/a	n/a	n/a
		High	40498	43.4	39.1	187.2
	Quartz 1.1	Low	30310	53.4	70.7	189.5
		High	28059	53.4	48.0	373.0
	Quartz 1.2	Low	15033	54.2	16.9	80.8
		High	23091	47.2	29.3	243.6
	Quartz 1.3	Low	21756	55.0	22.9	106.8
		High	34214	46.4	37.9	456.0
	Kaolin 1.1	Low	24002	47.0	66.8	319.1
		High	20880	44.1	87.4	429.6
	Clay 1.1	Low	16156	57.7	156.8	477.5
		High	12944	53.9	232.2	653.9
	Clay 1.2	Low	11374	78.2	301.7	1318.6
		High	9163	71.2	295.8	1122.5
II	Clay 2.1	Low	36216	*53.5	157.3	1638.0
	Clay 2.2	Low	35530	*82.5	137.0	1761.0
	Kaolin 2.1	Low	41448	*83.5	425.5	3676.0
	Feldspar 2.1	Medium	39464	*82.7	322.0	2336.0
	Quartz 2.1	Medium	35713	*78.5	181.0	1432.0
	Feldspar 2.2	High	31263	*92.0	495.0	2918.5
	Kaolin 2.2	High	61250	*71.5	95.0	556.5
III	Fertilizer	Small bags	*72123	45.1	298.5	1650.5
		Big bags	*68120	52.0	598.0	1455.5
IV	APS	Booth #1	60000	40.0	152.0	n/a
	HVOF	Booth #3	200000	39.6	135.5	n/a

On the other hand, the relevance of monitoring particle metrics in the worker breathing zone was identified. This is not only necessary to accurately determine worker exposure,

but also to obtain key information about the activity, materials and particle emissions generated. For example, in the packing line with low mitigation strategies (**Publication II**), where low dustiness materials were usually packed, the gravimetrically-determined respirable mass concentrations monitored were similar in the breathing zone and in the worker area (monitored 1.5-2 m away from the worker). Conversely, in the packing line with medium mitigation strategies, where materials being packed had higher dustiness levels, the respirable mass concentrations (also gravimetrically determined) in the breathing zone were higher than in the worker area, pointing out that workers were highly exposed specifically while closing the bag, when the extraction system was switched off. This piece of information, key in the design of measures to effectively reduce worker exposure, could only be obtained by simultaneously monitoring exposure concentrations in the breathing zone and in the worker area. Once again, this result evidences the value of carrying out experimental measurements of a wide variety of particle metrics, simultaneously in different locations, to achieve detailed and effective workplace exposure assessments which can in turn be used for efficient risk management as well as for model calibration and validation.

On the topic of exposure mitigation measures, several strategies were identified in the industrial environments assessed:

1) Source enclosure was evidenced to be an effective mitigation strategy in the workplaces and for the activities assessed, given that a clear inverse relationship was observed between exposure concentrations and degree of enclosure during packing of ceramic materials (**Publication II**). This was also observed in **Publication IV**, where particle number concentrations in the worker area during thermal spraying were significantly lower when the door connecting the booth and worker area was closed, compared to when it was partially open. This result is especially relevant due to the fact that it refers to particle number (not mass) concentrations. The results from this work show that, for the scenarios assessed, physical enclosures such as sliding doors or degree of isolation of the source are effective tools to reduce exposures to both particle number and mass concentrations, at a relatively low cost.

2) Modifying energy settings was seen to constitute another potentially effective mitigation strategy, for the mechanical activities assessed (handling and packing of powders and ceramic materials). For example, during handling of materials at high energy in a pilot plant (**Publication I**) particle emissions were from 26% up to 37%

higher than when handling was carried out with low energy. The subsequent reduction in particle exposures was thus significant. However, the feasibility of operating at lower energy and/or the increased industrial cost resulting from the longer time required for processing of the materials at lower energy should be considered and quantified.

3) Finally, results evidenced that particle morphology may significantly influence the resulting particle emissions during handling of raw materials (**Publication I**). When considering materials with similar primary particle dimeter (e.g., Kaolin 1.1, 5.7 µm; Clay 1, 2.7 µm; Quartz 1.2, 5.8 µm; and Quartz 1.3, 3.4 µm), handling of plate-like materials (e.g., Clays) resulted in significantly higher workplace exposure concentrations in terms of particle mass when compared to mostly spherical particles materials (e.g., Quartz) (Figure 5.5) (**Publication I**). In addition, plate-like materials dustiness was also generally higher than for spherical materials (Table 5.1). Thus, particle shape was pointed out as a factor to be considered when planning effective measures to reduce worker exposure. In this regard, when plate-like materials are handled, high effective measures should be implemented to adequately protect workers from exposure. As a limitation, it must be noted that particle monitoring instruments are calibrated based on spherical particles, and thus their performance when challenged with plate-like particles may decrease and this may have influenced the data collected and the conclusions extracted in this work.

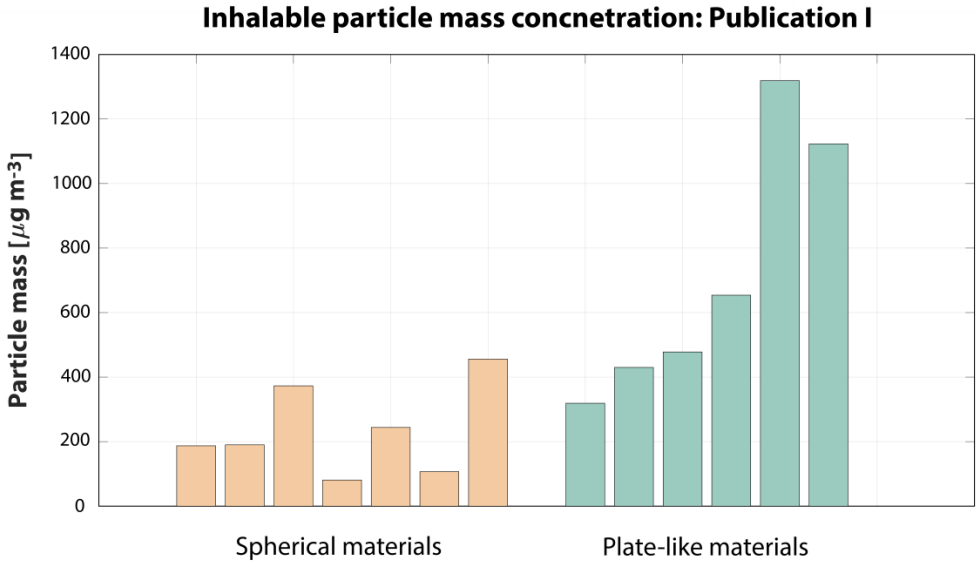

Figure 5.5 Bar plot for mean inhalable mass concentrations measured for spherical (ca. spherical) and plate-like shaped materials in Publications I. Inhalable mass concentrations were monitored with the Grimm mini-LAS.

5.2. Metrics and tools for exposure assessment

5.2.1. Metrics for exposure assessment

One major topic of discussion in exposure monitoring is the selection of the most adequate metrics to report exposure concentrations. In this PhD Thesis, particle number and mass (respirable and inhalable fractions) concentrations were monitored in different scenarios where micro- and NPs were emitted. When monitoring exposures to micron-sized particles due to mechanical handling, usually no significant increases in particle number concentration were detected due to the activity under study. However, monitoring particle number concentrations together with electron microscope (TEM and SEM) coupled with EDX helps to identify, through particle size and chemical composition analysis, the influence of other emission sources (e.g. parallel activities, or outdoor infiltration) which affected particle number concentrations (**Publications I, II and III**). Conversely, when monitoring high NP concentrations such as in the thermal spraying scenario, particle emissions were seen to affect both particle number and mass concentrations, specifically the respirable mass fraction (**Publication IV**). One key result was the observation by using electron microscope imagery that NPs may form aggregates, which can potentially affect particle mass concentrations, and as a result particle mass may also be an efficient metric even in scenarios where NPs are the dominant particle type (**Publication I, II and III**). Thus, considering the results obtained, simultaneous monitoring of particle number and mass concentrations should be encouraged for exposure assessment together with the use of microscope images and EDX technic, which were seen to be key to correctly identify sources, processes and external outdoor influence.

5.2.2. Statistical significance of particle impacts on exposure

Once particle emission impacts on exposure concentrations are detected, it is necessary to quantify their statistical significance to assess their relevance with regard to worker exposure and health risk. The nanoGEM approach (Asbach *et al*. 2012) has been widely used in research projects and industrial settings due to its simplicity and reliability, and it focuses on particle number concentrations. The need for a comparable approach to be applied to particle mass was identified in this work, and therefore a number of methods was tested for particle emissions in 7 packing cases (**Publication II**): 1) nanoGEM (Asbach *et al*. 2012); 2) the ARIMA models (proposed as "golden standard" by EN

17058:2018); and 3) traditional statistical tests which were used as reference. The nanoGEM approach proved useful for particle mass concentrations, although it was seen to underestimate the statistical significance in some of the cases when compared to traditional statistical tests results. Thus, the use of the nanoGEM approach for particle mass concentrations could be encouraged considering its limitations. The nanoGEM approach usefulness for particle number concentrations was confirmed. The ARIMA model was seen to be the least conservative when compared to the traditional statistical tests and the nanoGEM approach, and it was the most complex to apply as it requires specific expert statistical knowledge. Thus, the design of a user-friendly and specific approach tailored to particle mass concentrations would be advisable, possibly based on the nanoGEM strategy.

5.3. Dustiness as an exposure prediction tool

Discussions regarding the use of the dustiness index as a tool for exposure prediction are ongoing (Evans *et al.* 2013, Levin *et al.* 2014, Dubey *et al.* 2017), given that some authors found correlations with exposure (Heitbrink *et al.* 1989, Breum *et al.* 2003, Brouwer *et al.* 2006) whereas others did not (Heitbrink *et al.* 1990, Class *et al.* 2001, Fonseca *et al.* 2018). Therefore, studying which parameters affect this correlation is paramount in order to establish the potential of dustiness as an exposure prediction tool. In this PhD Thesis the correlation between dustiness and exposure during mechanical handling processes was studied at pilot plant (**Publication I)** and industrial scale (**Publication II**).

High degrees of correlation were found between dustiness and exposure concentrations during mechanical handling in a pilot plant (R^2 = 0.77-0.97; **Publication I)** and during packing at industrial scale (R^2 = 0.27-0.80; **Publication II)**. Thus, the results from this work point out dustiness as a useful tool for exposure prediction. However, certain limitations were brought to light:

1) **Dustiness-exposure correlations were seen to be stronger when the characteristics of the materials dominated over process characteristics**. This refers, for example, to the influence of mitigation strategies: at industrial scale, a high correlation dustiness-exposure was found for a packing line with low mitigation strategies (R^2 = 0.80), whereas no correlation was identified for packing lines with

medium and high levels of mitigation (R^2 = 0.27) (**Publication II**). This may explain the apparent contradictory results reported in the literature regarding dustiness correlation with exposure. Thus, for industrial activities where the main driver of exposure was the material being handled/packed, high correlations between dustiness and exposure concentrations were obtained and therefore, in these scenarios the dustiness index may be considered a useful tool for exposure prediction. In addition, dustiness can be used as a preliminary assessment tool to estimate whether mitigation strategies will be needed or not.

2) **Particle morphology plays a role in modifying dustiness**. The analysis of the different types of materials tested evidenced that Clays (plate-like shaped primary particles) were outliers in the correlation plots between dustiness and exposure concentrations, when compared with relatively spherical particles (**Publication I**). In addition, it was found that the highest exposure concentrations and dustiness indexes were measured for materials with very different specific surface area (SSA) values [e.g. Kaolin (K1) and Quartz (Q1), 9.6 and 1.4 $m^2 g^{-1}$, respectively] and different particle shapes (e.g. platy Kaolin and spherical Quartz) (**Publication I**), although when comparing different Quartzes and Kaolin samples separately, good correlations between dustiness and SSA were found (López-Lilao *et al.* 2015, 2016). This confirms the difficulty to establish a general relationship between dustiness and the physical-chemical properties of materials, as well as the need to assess the links between dustiness and exposure differentiating by material characteristics or groups. Instrumental limitations should also be considered (i.e., instrument performance when challenged with non-spherical particles). Further research is necessary in this direction.

3) **The selection of the dustiness method was found to be essential for material characterization, especially if dustiness is to be used as input parameter in models**. The highest correlation between dustiness and exposure concentrations during mechanical handling in a pilot plant (where material suffered rotation) was obtained for the R.D method, with the high energy setting (R^2 = 0.99) (**Publication I**, Additional results "section 4.1.1"). Conversely, when the C.D method was used for the same purpose, the correlation was slightly weaker (**Publication I**). This indicates that dustiness is a better predictor of exposure when using the dustiness method which mimics the actual activity being assessed better. This may also be an explanation to the apparent contradictory results reported in literature regarding the ability of dustiness to predict

worker exposure. In addition, although a strong correlation between the two available methods (C.D and R.D) was found when considering the inhalable fraction (R^2 = 0.78), which was previously reported in Evans *et al.* (2017) for the R.D and the venturi test, dustiness classifications in categories when using one or another method are not always comparable (Table 5.1). Specifically, materials are usually categorized as having a lower level of dustiness when using the R.D compared to the C.D.

Considering the results obtained, it may be concluded that dustiness could be considered a promising tool for worker exposure prediction in industrial settings such as the ones assessed in this work, as long as certain factors are taken into consideration: the selection of the dustiness method, the physical characteristics of the materials tested, and influence of process characteristics (e.g., enclosure) which might prevail over material properties as determinants of exposure in workplace settings.

Finally, the use of dustiness as input for mass-balance models was assessed in **Publication III**. The results obtained are presented and discussed in the following section.

5.4. Mass-balance models performance

One- and two-box mass-balance models were applied to two real-world scenarios with the aim to test their efficacy for different industrial environments. The two scenarios under study were 1) a mechanical process (packing of a fertilizer in small and big bags) where low concentrations of mainly coarse particles were emitted (**Publication III**); and 2) a thermal spraying process (APS and HVOF) where high concentrations of unintentionally-released NP were monitored (**Publication IV**).

For the mechanical process, the one- and the two-box models predicted mass concentrations within a ratio modelled/measured between 0.82 and 1.22 for all four study cases. Typically, a benchmark of 0.5-2.0 is considered for this kind of models (Jayjock *et al.* 2011). While both models provided relatively accurate results, the two-box model showed a slightly better performance when the layout of the industrial scenario resembled more closely a two-box model (**Publication III**). For the thermal spraying scenario, where only the one-box approach was tested, the model underestimated the particle number concentrations monitored (ratios ranging 0.2-0.7, and RMSLE ratios

0.4-1.7; **Publication IV**). Even though these ratios fall within the 0.5-2.0 benchmark in 13/14 of the cases, it may be concluded that the performance of the one-box model was poorer for the high particle concentration (**Publication IV**) than for the low particle concentration (**Publication III**) scenario. The causes for these differences are various and linked not only to the concentrations monitored, but also to the input particle data and the characterization of the airflows inside each of the industrial plants. This evidences the difficulties of particle modelling in real-world industrial scenarios, and the need for experimental measurements to validate modelling approaches.

The addition of outdoor and background concentrations to the models increased modelling precision and overall performance, which is a step-forward in mass-balance model application in real-scenarios (**Publication III** and **Publication IV**). Therefore, correctly monitoring and assessing outdoor and background concentrations is essential, as they can have an impact on worker exposure which needs to be contemplated during the application and evaluation of models.

After assessing the performance of the mass-balance models under high and low concentrations, and in terms of particle number and mass concentrations, it may be concluded that both the one- (even with its simplifications) and the two-box models may be useful tools for exposure assessment in industrial settings. However, modelling results are highly dependent on the parametrization, which is still sometimes not fully understood and for which experimental data are frequently lacking. Thus, a discussion on two of the most relevant parameters (particle emission rates and air flow characterization), as well as their implications regarding model performance, was developed in **Publication III** and **IV,** and is summarized below.

5.4.1. Dustiness and measurement-based particle emission rates

Three different methods were evaluated to quantify particle emission rates: dustiness-based, measurement-based convolution theorem, and measurement based cyclic steady state equation.

For mechanical processes in which powdered materials are handled, emission rates can be calculated by using the material's dustiness index as input parameter. While Koivisto *et al.* (2015) showed that this method has certain weaknesses, in this PhD Thesis good modelling predictions were obtained when using dustiness to calculate emission rate (**Publication III**). One limitation (see 5.3) was the need to include an energy factor (H)

to transpose the energy applied during the dustiness test to the energy applied during the process under study. This H parameter is not yet parametrized and gives rise to different interpretations which will also depend on the dustiness method used. Therefore, for a correct and standardized application of dustiness in mass-balance models, the most urgent need regarding calculation dustiness-based emission rates identified in **Publication III** is to establish guidelines which specify 1) which dustiness test should be used for each type of industrial activity; and 2) H values depending on the energy applied in the process, which could be calculated by using calibration dustiness-exposure curves for specific types of processes and groups of materials, according to what was discussed in section 5.3.

When emissions cannot be estimated based on the dustiness index (e.g. process-generated or unintentionally-released NP) emission rates must be estimated based on experimentally-monitored particle concentrations. Here, two methods with different degrees of complexity were assessed: the convolution theorem and the cyclic steady state equation (**Publication IV**). Although emission rates obtained with both methods were comparable, using the convolution theorem improved modelling results on a case by case basis, providing more case-sensitive modelling results. Therefore, although both provided acceptable modelling results, using the cyclic steady state equation would be advisable for preliminary exposure assessment whereas for more precise and case-specific results the convolution theorem would be better option. In sum, even though the calculation of emission rates using dustiness (**Publication III**) and particle monitoring (with convolution theorem or cyclic steady state, **Publication IV**) present some limitations and their parametrization still needs improvements, they provided acceptable modelling results which justify their use.

5.4.2. Air flow parametrization

Air flow characterization (general air exchange rate, AER, and NF-FF air flow (β)) was paramount to obtain accurate modelling results. In the setting assessed in **Publication III** the NF-FF β values were unknown, and thus literature values were used with the support of a sensitivity analysis. The selection of the NF-FF β values impacted modelling results strongly for the small bags scenario, with ratios (modelled/measured) varying broadly from 0.68 using the lowest β and up to 1.89 using the highest β. In **Publication IV,** ratios (modelled/measured) presented a narrower range 0.18-0.67 when using experimentally measured air speeds. These results evidenced that, to achieve good

model performance, air flows (incoming and internal flows) should be calculated or estimated as precisely as possible, given that small variations can lead to significant under- or overestimations of particle concentrations (**Publication III and IV**) and thus to impaired decision-making limiting the effectiveness of mass-balance models as exposure and risk assessment tools.

As a final conclusion regarding parametrization, literature data for particle emission rates and air flows were proved useful for modelling. Thus, reporting experimental data from exposure studies to publicly-accessible databases or libraries would be highly beneficial for modelling usability and expansion.

5.5. Risk assessment tools performance

Exposure assessment is at times not sufficient for decision making, and health risk assessment is required. However, there are yet not enough studies assessing the toxicology, exposure and health impacts of particles or of aerosol mixtures of micron-sized particles and NPs. As a result, several relatively user-friendly tools have been developed. In this PhD Thesis two types of tools were tested: an inhalation deposition model (ICRP model), and three risk assessment and control banding based tools (ART, Stoffenmanager and NanoSafer).

5.5.1. ICRP Inhalation deposition model

The ICRP deposition model, which requires as input experimentally-monitored particle size distributions, provides information regarding the regions in the respiratory tract where inhaled particles would deposit, irrespective of their chemical composition. As a result, an evaluation of the potential respiratory health risk can be conducted depending on how deep particles reach in the respiratory tract. In this Thesis, the ICRP model was applied for exposures monitored during packing of 7 ceramic materials (**Publication II**) and 1 inorganic fertilizer (**Publication III**) (Table 5.3). Particles emitted during packing of ceramic materials (packing lines with low, medium and high mitigation strategies; **Publication II**), deposited mainly in the head-airways 27-41%, with deposition increases when compared with background regional surface area deposition of 2-23%. Surface area deposition on tracheobronchial and alveolar regions were 7-10% and 51-64%, respectively, suffering decreases during packing when compared to background

deposition in the same regions of 1-5% and 1-18%, respectively. Similarly, during big bags packing of the inorganic fertilizer (**Publication III**), even though main deposition was again the alveolar region 52-62% due to forklifts activity influence, particles deposition increased in the head airways by 8% and decreased in the alveolar region by 7%. Thus, reduced effects on health due to packing emitted particles may be expected when comparing with case studies dominated by alveolar deposition, as in the case of the small bags packing of the inorganic fertilizer, where deposited particles during packing increased when compared to background deposition in the alveolar region by up to a 3% and decreased in head airways and trachea bronchial regions by up to 2% and 5%, respectively. Similarly, during thermal spraying, emitted particles were seen to deposit mainly in the alveolar region with 54-70% considering surface area (Salmatonidis *et al.* 2019) with an increased tracheobronchial deposition when compared to the other types of particles assessed (7-15%, Table 5.3). However, it should be noted that such models do not consider particle morphology or chemistry which can have an impact on health-respiratory disease.

Table 5.3 Calculated dose rates in surface area, and regional deposition in percentages on head airways, trachea bronchi and alveolar for cases in Publication II, III and in Salmatonidis *et al.* 2019.* values not published.

Paper N°	Material	Case	Deposited Surface Area			
			Total [$\mu m^2\ min^{-1}$]	Head Airways %	Trachea bronchi %	Alveolar %
II	Clay 2.1	Low	$9.7x10^5$	41	8	51
	Clay 2.2	Low	$6.7x10^5$	34	8	58
	Kaolin 2.1	Low	$1.2x10^6$	35	8	57
	Feldspar 2.1	Medium	$1.1x10^6$	33	9	59
	Quartz 2.1	Medium	$5.4x10^5$	33	9	59
	Feldspar 2.2	High	$8.6x10^5$	41	7	51
	Kaolin 2.2	High	$9.0x10^5$	27	10	64
III	Fertilizer	Small bags	$4.3\text{-}6.0x10^6$	26	14	60
		Big bags	$3.3\text{-}7.6\ x10^6$	25-36	13-14	52-62
Salmatonidis., Ribalta., *et al.* 2019	APS*	Booth #1	$3.9x10^6$	15-17	13-15	69-70
	HVOF	Booth #3	$3\text{-}6.3x10^6$	32-39	7-10	54-60

Particle deposition in the respiratory tract was studied in terms of particle number, mass and surface area. Absolute values and percentages were different for each metric, but results regarding the region in which emitted particles deposited were similar regardless of the metric used. Particle surface area was the metric which represented particle deposition in the respiratory tract in a more balanced and consistent way. The use of such models, which are relatively easy to use and only require knowledge on particle size distribution, is encouraged during exposure assessment as their outcomes provide risk information useful for decision making.

5.5.2. Risk assessment and control banding tools

Risk assessment and control banding based tools are designed to help users to estimate health risks due to exposure to airborne particles (Tielemans *et al.* 2008a, Kristensen *et al*. 2010, Fransman *et al.* 2011, ECHA 2016). They are mainly used in the framework of risk assessment of chemical hazards under the REACH regulation by private-sector industries. In this Thesis, two risk assessment tools (ART, Stoffenmanager) and one risk assessment tool based on control banding (NanoSafer) were applied to test their performance and usability on case studies of industrial packing of 7 ceramic materials (**Publication II**) and 1 inorganic fertilizer (**Publication III**). As discussed in previous sections, it should be noted that the NanoSafer tool was originally designed to assess risks from NP exposures, not from micron-sized particles, and therefore the cases presented in this work are not the ideal target for this tool, which is still under testing and calibration processes.

The two risk assessment tools (ART and Stoffenmanager) generally overestimated (ratio modelled/measured > 1) the experimentally-measured exposures (ART Bayesian, by 82% and Stoffenmanager, by 64%) although in some occasions underestimations (ratio modelled/measured < 1) were also detected (Stoffenmanager, 36%, and ART Mechanistic model, 73%). No clear pattern was detected. When compared with the 0.5-2.0 benchmark, the results from the ART Mechanistic and Bayesian models were within the benchmark in 27% of the cases, while the results from Stoffenmanager matched the benchmark in 64% of the cases assessed. The control banding tool NanoSafer (designed for nanomaterials assessment) overestimated monitored exposure respirable mass concentration for all the ceramic materials within a factor 13-120 and 1.1-38 when NF and FF modelled concentrations were considered, respectively (**Publication II**). Conversely, for the fertilizer packing NanoSafer NF concentrations overestimated monitored

concentrations by a factor 1.1 up to 6.8. In sum, results evidenced a better performance of Stoffenmanager for the cases assessed (mechanical handling of powders; packing) (Table 5.4), even though a pattern to understand the causes of the under or overestimations of the model was not identified.

Table 5.4 Ratio of modelled/measured concentrations considering ART (C.D based), Stoffenmanager and NanoSafer model outputs, and 8h TWA values. Acceptable ratio limits (0.5-2.0; benchmark by Jayjock *et al*. 2011). Bold and green: within the limits. Red: overestimation. Yellow: underestimation. Calculations were made by considering C.D dustiness index.

Paper Nº	Material	Ratio modelled/measured			
		ART Mechanistic	ART Bayesian	Stoffenmanager	NanoSafer NF-FF
II	*Clay 2.1*	0.2	**1.5**	**1.9**	13-**1.1**
	Clay 2.2	4.2	6.0	2.9	42-3.5
	Kaolin 2.1	**1.2**	2.7	**1.9**	75-6.3
	Feldspar 2.1	0.9	2.4	2.6	74-6.2
	Quartz 2.1	0.7	2.6	**1.6**	97-8.1
	Feldspar 2.2	**0.6**	**1.5**	0.3	120-38
	Kaolin 2.2	**1.7**	5.2	**0.8**	64-20
III	*Small Bags 1*	< 0.01	0.1	0.5	**1.2**-0.02
	Small Bags 2	< 0.01	0.1	**0.5**	**1.8**-0.03
	Big Bags 1	0.3	**1.8**	**1.2**	6.8-**1.1**
	Big Bags 2	0.4	2.1	**1.4**	6.7-**1.1**

The results from Stoffenmanager were relatively more stable for the same industrial process but different material, whereas the ART and NanoSafer models provided different results. For example, for Clay 2.1, Clay 2.2 and Kaolin 2.1, which are materials packed in the same line, ART and NanoSafer results ranged from an acceptable range, to over- and underestimations. Conversely, ART and NanoSafer are more versatile as they provide the user with the option to introduce a dustiness index value or level, as opposed to Stoffenmanager, which only has the option to introduce the type of material. In NanoSafer, health and safety and nano-specifications have high influence in the resulting scores, which are later transposed to estimated concentrations (section 3.6.2). In ART, what seems to have more importance were material-related inputs. The models usually

require a dustiness index or level, but it is not possible to differentiate between the different dustiness methods used. As shown in section 5.3, dustiness classification and correlation with exposure is different when using one or another dustiness test. This has implications regarding the energy factor needed to translate dustiness to exposure (section 5.4), which is also dependent on the dustiness method used.

In order to assess the relevance of the selection of the method to quantify dustiness (C.D or R.D), the ART models (mechanistic and Bayesian) were applied using both types of dustiness calculations, with the results shown in Table 5.5. R.D based ART Bayesian estimated concentrations were within the 0.5-2.0 benchmark by 46% whereas C.D based ART Bayesian only by 27%. However, C.D based ART Bayesian overestimated monitored exposures by 82%, from which overestimations with a ratio > 3 represent a 64%, while R.D ART Bayesian underestimated exposures with the same percentage (82%), which is considered detrimental for modelling. Thus, highly different estimated exposure concentrations results were obtained when using C.D or R.D dustiness indexes, pointing out the need to use the dustiness test which best represents the activity object of study.

Table 5.5 Ratio of modelled/measured concentrations considering ART (C.D based) and ART (R.D based) model outputs, and 8h TWA values. Acceptable ratio limits (0.5-2.0; benchmark by Jayjock *et al*. 2011). Bold and green: within the limits. Red: overestimation. Yellow: underestimation.

Paper Nº	Material	Ratio modelled/measured	
		ART Bayesian (C.D dustiness)	ART Bayesian (R.D dustiness)
II	*Clay 2.1*	**1.5**	0.3
	Clay 2.2	6.0	**1.2**
	Kaolin 2.1	2.7	0.4
	Feldspar 2.1	2.4	0.2
	Quartz 2.1	2.6	0.3
	Feldspar 2.2	**1.5**	**0.5**
	Kaolin 2.2	5.2	**1.7**
III	*Small Bags 1*	0.1	0.03
	Small Bags 2	0.1	0.04
	Big Bags 1	**1.8**	**0.56**
	Big Bags 2	2.1	**0.65**

In general, a lack of harmonization between risk assessment tools was evidenced through this work, regarding input parameters (e.g., dustiness method) and types of outputs (exposure concentrations vs. scores). This is in agreement with other authors who pointed out a lack of comparability between tools (Liguori *et al.* 2016, Sánchez Jiménez *et al.* 2016), as well as transparency in some cases (Koivisto *et al.* 2018), which limit a more wider-spread application of these tools. For example, NanoSafer is the only tool which considers cyclic processes, while room volume and air exchange values cannot be entered as specific measured values (only default drop down values) in ART or Stoffenmanager. As discussed above, these parameters were experimentally seen to be major determinants of worker exposure. In addition, even though tools were designed to be used by non-experts possibly in private-sector industries, expert criteria are required during the selection of certain of the options, and slight differences between processes are difficult to introduce in the models. As a result, and based on this work, it may be concluded that there is a clear need for evaluation, calibration and harmonization of risk assessment tools, especially when they are applied to real-world industrial settings.

Conclusions

Chapter 6

6. CONCLUSIONS

This PhD Thesis addresses worker exposure to airborne particles emitted during industrial and semi-industrial (pilot plant) activities (mechanical handling and thermal processes) in the ceramic sector. It aims to contribute to the harmonization of exposure assessment (in terms of metrics and decision making), the evaluation of dustiness as an exposure prediction tool, and the performance understanding of mass-balance models and risk assessment tools. The main conclusions extracted from this work are presented following the same structure as the Objectives and Discussion chapters.

Exposure assessment and particle emissions

- Mechanical handling of ceramic materials at pilot-plant and industrial-scale significantly impacted worker exposure in terms of particle mass; therefore these activities should always be performed under control to minimise particle emissions and avoid exceeding current occupational limits, set out for mass concentrations.
- Thermal processes (thermal spraying and diesel engines) significantly increased particle exposures in terms of particle number and mass concentrations and in some cases exceeded the nano-reference values.
- Modifying the degree of source enclosure (engineering control measure) and the energy applied to the process (process modification) were identified as effective strategies to reduce worker exposure. Nevertheless, in existing industrial scenarios the application of process modifications is usually limited or not feasible due to technical reasons, and thus they should be implemented during the process design phase.
- Packing of ceramic materials using low mitigation strategies was identified as the process assessed in this Thesis with the highest impact on worker exposure in terms of mass. However, monitored mass concentrations did not exceed the established Spanish OEL values, and were even lower than 50% of the OEL. Thus, the need for a revision of current OELs was identified as they do not promote the application of mitigation strategies when workers are exposed to high particle mass concentrations.

Metrics and tools for exposure assessment

- Simultaneously monitoring of particle number and mass concentrations when assessing worker exposure should be encouraged regardless of the case study and the type and size of particles expected (nano/coarse), since in scenarios where only micron-sized particles where expected, significant nano-sized particle concentrations in terms of number were also monitored, and vice versa. This highlights the fact that, in industrial settings, the main process is frequently not the only emission source, and the influence of external or secondary sources may have major implications on exposure.
- For regulatory purposes, exposure to particle mass concentrations is currently evaluated by comparison with OEL values. In this work, OEL values were not exceeded in any case even though high particle mass increases were detected. For these increases (e.g., exposure impacts not exceeding OELs, or having shorter duration) the need for a specific mass-tailored and user-friendly approach to identify statistically significant increases was identified. Such an approach would be comparable to the one already available for particle number concentrations.

Dustiness as a predictor tool

High correlation was found between the dustiness index and exposure concentrations in several exposure scenarios, indicating that dustiness could be a promising tool for worker exposure prediction and even for mass-balance models and risk assessment tools application. However, this correlation is not straightforward and several limitations were identified:

- The correlation was stronger when considering only materials with similar characteristics (e.g., primary particle shape). Other particle parameters such as surface area (SSA) or primary particle size (d_{50}) were not seen to have a clear influence on the correlation between dustiness and exposure.
- The correlation between dustiness and exposure was stronger when materials characteristics dominated over process characteristics. It has been observed that, in industrial scenarios, engineering controls (e.g., enclosure, or local exhaust ventilation) are stronger determinants of exposure than the material's dustiness, hence their parametrization is paramount to wider the application of the dustiness index.

- Each dustiness method selected provides different classification levels for the same materials. In addition, better correlation dustiness-exposure was obtained when the dustiness method applied was similar to actual process under study. Therefore, the method used to calculate the dustiness index should always be reported and adequately selected.

Mass-balance models

The one- and two-box models tested showed good performance for low mass concentrations and high particle number concentrations. Therefore, for scenarios comparable to those assessed in this PhD Thesis, box models could be recommended as tools for exposure assessment. The two-box model showed higher accuracy than one-box model when the layout of the modelled area was similar to that of a standard two-box model.

- The performance of the one- and two-box models resulted in higher accuracy when including outdoor and background concentrations in the model domain, especially when clear impacts of outdoor infiltration and parallel processes were detected.
- When estimating emission rates based on the dustiness index, an urgent need to establish and harmonize guidelines to select the appropriate dustiness method and to estimate the handling energy factor (H) was identified.
- Emission rates estimated from measurements (using the convolution theorem and the cyclic steady state equation) provided good modelling results. Using convolution theorem-based emission rates showed higher case-sensitive modelling results, and thus this option should be preferred when higher precision modelling is required, especially in time-variable emission sources. Conversely, cyclic steady state-based rates would be better option for preliminary exposure assessments and for modelling constant continuous or constant discontinuous emission sources, due to the lower computational efforts required.
- The application of the mass-balance models requires accurate air flowrate data. In this regard the experimental determination of air flowrates should be preferred to the application of theoretical values, despite the great experimental difficulties encountered in some real-world industrial scenarios to its experimental determination.

- The usefulness of libraries reporting values regarding dustiness indexes, energy factors, emission rates and local control efficacy among others, for modelling, was highlighted, due to the complexity of measuring many of these parameters in real-world scenarios.

Risk assessment

- The ICRP inhalation deposition model was a useful and user-friendly tool to provide information regarding health risk assessment, as it provided particle regional deposition values which can be transposed to respiratory health risks and requires only particle size distribution as input.
- From all the tools tested (ART, Stoffenmanager and NanoSafer), Stoffenmanager provided the most precise prediction of airborne concentrations emitted during mechanical handling (industrial packing) of ceramic materials and fertilizers. However, ART and NanoSafer were more versatile tools with more options to customise the assessments. The results from NanoSafer were not directly comparable as this model was developed for nanoparticle risk assessment. In spite of providing useful information for implementing mitigation measures, the results obtained in this work show that these risk assessment tools should currently be considered as semiquantitative models in term of exposure prediction.
- The dustiness index seems to be the parameter with the largest impact on concentrations modelled with ART. Nevertheless, the method used to determine the dustiness index should be clearly specified in risk assessment analyses, as very different results are obtained as a function of the method (rotating drum or continuous drop).
- A lack of harmonization between tools, and therefore limitations in comparability, were detected. Inputs and outputs are different between tools, which limits comparability. In addition, different tools which are recommended by the ECHA provide, for the same case study, very different results and conclusions regarding exposure risks. Therefore, these tools should be carefully used, and their parametrization reported, to ensure the adequate interpretation of their output results. Another potential use would be to assess expected risk reductions derived from introducing mitigation strategies and work guidelines in workplaces.

Limitations and Future Research

Chapter 7

7. Limitations and future research

From the results obtained in this PhD Thesis, several open questions and gaps have been identified which require further research:

- A general limitation encountered in exposure assessment studies is that the calibration of monitoring instruments is based on spherical particles, and thus their performance when challenged with non-spherical particles may vary, ultimately influencing the results and conclusions extracted. Additional tests at laboratory-scale and industrial facilities should be carried out to further the understanding of instruments performance when monitoring non-spherical or even fibrous particles.

- Even though some light was provided in this PhD Thesis regarding the use of dustiness as an exposure prediction tool, still difficulties remain regarding the relationship between dustiness and the physic-chemical properties of materials, as well as regarding the links between dustiness and exposure differentiating by material characteristics or groups. Therefore, dustiness still needs to be further studied and understood to be widely used for exposure assessment purposes. The extension of this work to nano-powders, currently underway, will make a very relevant contribution to this field of research.

- The energy factor (H), needed to transpose dustiness energy to the activity under study, requires definition and standardization in order to be widely used for exposure modelling.

- One- and two-box mass-balance models proved to be useful for exposure modelling. However, experimental data (particle monitoring in real-world scenarios) is still necessary for model validation. Furthermore, models are not yet at a stage where they can be widely applied in industrial settings, as they require detailed expert knowledge and experimentally determined particle concentrations for model calibration.

- The performance of mass-balance models and risk assessment tools was evaluated in this PhD Thesis using the benchmark proposed by Jayjock *et al.* (2011). The accuracy for these tools should be further assessed, and harmonised if the tools are meant to be used in industrial settings for comparable exposure and risk assessment. This would need to be carried out for different particle metrics, at least particle number and mass concentrations.

- Specifically for the case of risk assessment and control banding tools, a clear need for evaluation, calibration and harmonization of tools was identified, as different tools, which are proposed by the ECHA, provided different outcomes for the same case scenarios, leading to different conclusions, especially if they are not properly used.

- The need for a user-friendly decision making approach to statistically significant impacts on exposure in terms of particle mass was identified.

- Certain of the potential mitigation strategies identified in this PhD Thesis involve process modifications, and thus their application in industrial scenarios is limited. Implementation of mitigation strategies to reduce worker exposure should preferably be introduced during the process design phase, in order to include exposure considerations in the design. This is currently not the case in some European regions, in contrast to environmental considerations, which must be included as per current regulations. For example, modifying process energy was identified as a potential mitigation strategy. However, the increased industrial cost resulting from the longer time required for processing of the materials at lower energy should be evaluated and quantified. Therefore, the use of modelling tools to simulate worker exposure to micron- and nano-sized particles in industrial processes design should be fostered.

References

Chapter 8

REFERENCES

Agarwal, J.K. and Sem, G.J., 1980. Continuous flow, single-particle-counting condensation nucleus counter. *Journal of Aerosol Science*, 11 (4), 343–357.

Aitken, R.J., Creely, K.S., and Tran, C.L., 2004. *Nanoparticles: An Occupational Hygiene Review*. Health & Safety Executive. Research Report 274.

Alim, M.A., Biswas, M.K., Biswas, G., Hossain, M.A., and Ahmad, S.A., 2015. Respiratory health problems among the ceramic workers in Dhaka. *Faridpur Medical College Journal*, 9 (1), 19.

Amoros Albaro, J. L., 1987. *Pastas cerámicas para pavimentos de monococción. Influencia de las variables del proceso sobre las propiedades de la pieza en crudo y sobre su comportamiento durante el prensado y la cocción*. Thesis (PhD). University of Valencia.

Arnold, S.F., Shao, Y., and Ramachandran, G., 2017. Evaluating well-mixed room and near-field–far-field model performance under highly controlled conditions. *Journal of Occupational and Environmental Hygiene*, 14 (6), 427–437.

Asbach, C., Kuhlbusch, T., Kaminski, H., Stahlmecke, B., Plitzko, S., Götz, U., Voetz, M., Kiesling, H.-J., and Dahmann, D., 2012. *Standard Operation Procedures for assessing exposure to nanomaterials, following a tiered approach*.

Bailey, M.R. and Roy, M., 1994. Annexe E. Clearance of particles from the respiratory tract. *Annals of the ICRP*, 24 (1–3), 301–413.

Baldwin, P.E.J. and Maynard, A.D., 1998. A Survey of Wind Speeds in Indoor workplaces. *Annals of Occupational Hygiene*, 42 (5), 303–313.

Barba, A., Beltrán, V., Feliu, C., García, J., Gines, F., Sánchez, E., and Sanz, Vi., 2000. *Materias primas para la fabricación de soportes de baldosas cerámicas*. Thesis (PhD). Instituto de Tecnología Cerámica.

Baron, P.A., and Willeke, K., 2011. *Aerosol measurement: principles, techniques, and applications*. Wiley.

Behrens, I., Pena, A.I.V., Alonso, M.J., and Kissel, T., 2002. Comparative uptake studies of bioadhesive and non-bioadhesive nanoparticles in human intestinal cell lines and rats: the effect of mucus on particle adsorption and transport. *Pharmaceutical research*, 19 (8), 1185–93.

Bekker, C., Voogd, E., Fransman, W., and Vermeulen, R., 2016. The validity and applicability of using a generic exposure assessment model for occupational exposure to nano-objects and their aggregates and agglomerates. *Annals of Occupational Hygiene*, 60 (9), 1039–1048.

Bello, D., Wardle, B.L., Yamamoto, N., Guzman DeVilloria, R., Garcia, E.J., Hart, A.J., Ahn, K., Ellenbecker, M.J., and Hallock, M., 2009. Exposure to nanoscale particles and fibers during machining of hybrid advanced composites containing carbon nanotubes. *Journal of Nanoparticle Research*, 11 (1), 231–249.

Boelter, F.W., Simmons, C.E., Berman, L., and Scheff, P., 2009. Two-zone model

application to breathing zone and area welding fume concentration data. *Journal of Occupational and Environmental Hygiene*, 6 (5), 289–297.

Boverhof, D.R., Bramante, C.M., Butala, J.H., Clancy, S.F., Lafranconi, M., West, J., and Gordon, S.C., 2015. Comparative assessment of nanomaterial definitions and safety evaluation considerations. *Regulatory Toxicology and Pharmacology*, 73 (1), 137–150.

Breum, N.O., 1999. The rotating drum dustiness tester: Variability in dustiness in relation to sample mass, testing time, and surface adhesion. *Annals of Occupational Hygiene*, 43 (8), 557–566.

Breum, N.O., Schneider, T., Jørgensen, O., Valdbjørn Rasmussen, T., and Skibstrup Eriksen, S., 2003. Cellulosic Building Insulation versus Mineral Wool, Fiberglass or Perlite: Installer's Exposure by Inhalation of Fibers, Dust, Endotoxin and Fire-retardant Additives. *The Annals of Occupational Hygiene*, 47 (8), 653–669.

British Standards Institute, 2009. Particle size analysis — Laser diffraction methods, BS ISO 13320-1:1999.

British Standards Institution, 2018. BS 17058:2018. *Workplace exposure - Assessment of exposure by inhalation of nano-objects and their aggregates and agglomerates*.

Brouwer, D.H., Gijsbers, J.H.J., and Lurvink, M.W.M., 2004. Personal Exposure to Ultrafine Particles in the Workplace: Exploring Sampling Techniques and Strategies. *Annals of Occupational Hygiene*, 48 (5), 439–453.

Brouwer, D.H., Links, I.H.M., De Vreede, S.A.F., and Christopher, Y., 2006. Size selective dustiness and exposure; simulated workplace comparisons. *Annals of Occupational Hygiene*, 50 (5), 445–452.

Brouwer, D., Van Duuren-Stuurman, B., Berges, M., Jankowska, E., Bard, D., and Mark, D., 2009. From workplace air measurement results toward estimates of exposure? Development of a strategy to assess exposure to manufactured nano-objects. *Journal of Nanoparticle Research*, 11 (8), 1867–1881.

Brouwer, D., 2010. Exposure to manufactured nanoparticles in different workplaces. *Toxicology*, 269 (2–3), 120–127.

Brouwer, D., Berges, M., Virji, M.A., Fransman, W., Bello, D., Hodson, L., Gabriel, S., and Tielemans, E., 2012. Harmonization of measurement strategies for exposure to manufactured nano-objects; Report of a workshop. *Annals of Occupational Hygiene*, 56 (1), 1–9.

Brouwer, R., 2006. Do stated preference methods stand the test of time? A test of the stability of contingent values and models for health risks when facing an extreme event. *Ecological Economics*, 60 (2), 399–406.

Brunauer, S., Emmert, P.H., and Teller, E., 1928. Adsorption of gases in multimolecular layers. *Journal of the American Chemical Society*, 60, 309–319.

Cambra-López, M., Aarnink, A.J.A., Zhao, Y., Calvet, S., and Torres, A.G., 2010. Airborne particulate matter from livestock production systems: A review of an air pollution problem. *Environmental Pollution*, 158 (1), 1–17.

Canadian Centre for Occupational Health and Safety, 2017. OSH Answers Fact Sheets:

Risk Assessment [online]. Available from: https://www.ccohs.ca/oshanswers/hsprograms/risk_assessment.html [Accessed 25 Feb 2019].

Capstick, T.G. and Clifton, I.J., 2014. Expert Review of Respiratory Medicine Inhaler technique and training in people with chronic obstructive pulmonary disease and asthma. *Expert Review of Respiratory Medicine*, 6 (1), 91-103.

Carvalho, T.C., Peters, J.I., and Williams III, R.O., 2011. Influence of particle size on regional lung deposition – What evidence is there? *International Journal of Pharmaceutics*, 406 (1–2), 1–10.

Cena, L.G. and Peters, T.M., 2011. Characterization and Control of Airborne Particles Emitted During Production of Epoxy/Carbon Nanotube Nanocomposites. *Journal of Occupational and Environmental Hygiene*, 8 (2), 86–92.

Charron, A. and Harrison, R.M., 2003. Primary particle formation from vehicle emissions during exhaust dilution in the roadside atmosphere. *Atmospheric Environment*, 37 (29), 4109–4119.

Chen, D.R., Pui, D.Y.H., Hummes, D., Fissan, H., Quant, F.R., and Sem, G.J., 1998. Design and evaluation of a nanometer aerosol differential mobility analyzer (Nano-DMA). *Journal of Aerosol Science*, 29 (5–6), 497–509.

Chen, C. and Zhao, B., 2011. Review of relationship between indoor and outdoor particles: I/O ratio, infiltration factor and penetration factor. *Atmospheric Environment*, 45 (2), 275–288.

Cherrie, J.W. and Schneider, T., 1999. Validation of a New Method for Structured Subjective Assessment of Past Concentrations. *Annals of Occupational Hygiene*, 43 (4), 235–245.

Cherrie, J.W., MacCalman, L., Fransman, W., Tielemans, E., Tischer, M., and Van Tongeren, M., 2011. Revisiting the effect of room size and general ventilation on the relationship between near- and far-field air concentrations. *Annals of Occupational Hygiene*, 55 (9), 1006–1015.

Chiu Leung, C., Tak Sun Yu, I., and Chen, W., 2012. Silicosis. *The Lancet*, 379, 2008–2018.

Class, P., Deghilage, P., and Brown, R.C., 2001. Dustiness of different high-temperature insulation wools and refractory ceramic fibres. *Annals of occupational hygiene*, 45 (5), 381–4.

Colvin, V.L., 2003. The potential environmental impact of engineered nanomaterials. *Nature Biotechnology*, 21 (10), 1166–1170.

Cornelissen, R., Jongeneelen, F., van Broekhuizen, P., and van Broekhuizen, F., 2011. Guidance working safely with nanomaterials and nanoproducts. The guide for employers and employees. 1–17.

Council Directive 98/24/EC of 7 April 1998 on the protection of the health and safety of workers from the risks related to chemical agents at work (fourteenth individual Directive within the meaning of Article 16(1) of Directive 89/391/EEC). Official Journal of the European Union.

Council Directive 2008/50/EC of 21 of May 2008 on ambient air quality and cleaner air for Europe. Official Journal of the European Union.

Council Directive 2017/164/EU of 31 January 2017 establishing a fourth list of indicative occupational exposure limit values pursuant to Council Directive 98/24/EC, and amending Commission Directives 91/322/EEC, 2000/39/EC and 2009/161/EU. Official Journal of the European Union.

Council regulation (EC) No. 1907/2006 of 18 December 2006 concerning the Registration, Evaluation, Authorisation and Restriction of Chemicals (REACH), establishing a European Chemicals Agency. Official Journal of the European Union.

Council Regulation (EC) No. 1223/2009 of 30 November 2009 on cosmetic products. Official Journal of the European Union.

Council Regulation (EC) No. 528/2012 of 22 May 2012 concerning the making available on the market and use of biocidal products. Official Journal of the European Union.

Council Regulation (EU) 2015/2283 of 25 November 2015 on novel foods, amending Regulation (EU) No 1169/2011 of the European Parliament and of the Council and repealing Regulation (EC) No 258/97 of the European Parliament and of the Council and Commission Regulation (EC) No 1852/2001. Official Journal of the European Union.

Council Regulation (EU) 2017/745 of 5 April 2017 on medical devices, amending Directive 2001/83/EC, Regulation (EC) No 178/2002 and Regulation (EC) No 1223/2009 and repealing Council Directives 90/385/EEC and 93/42/EEC. Official Journal of the European Union.

Cousins, C., Boice Jr, J., Cooper, U.J., Lee, U.J., and Lochard, K.J., 2011. Annals of the ICRP Published on behalf of the International Commission on Radiological Protection International Commission on Radiological Protection Members of the 2010–2013 Main Commission of ICRP.

Dahmann, D., Taeger, D., Kappler, M., Büchte, S., Morfeld, P., Brüning, T., and Pesch, B., 2008. Assessment of exposure in epidemiological studies: The example of silica dust. *Journal of Exposure Science and Environmental Epidemiology*. 18 (5), 452–461.

Dazon, C., Witschger, O., Bau, S., Payet, R., Beugnon, K., Petit, G., Garin, T., and Martinon, L., 2017. Dustiness of 14 carbon nanotubes using the vortex shaker method. *Journal of Physics: Conf. Series*, 838.

Dehghan, F., Mohammadi, S., Sadeghi, Z., and Attarchi, M., 2009. Respiratory Complaints and Spirometric Parameters in Tile and Ceramic Factory Workers. *Tanaffos*, 8 (4), 19–25.

Demou, E., Peter, P., and Hellweg, S., 2008. Exposure to manufactured nanostructured particles in an industrial pilot plant. *Annals of Occupational Hygiene*, 52 (8), 695–706.

Demou, E., Stark, W.J., and Hellweg, S., 2009. Particle emission and exposure during nanoparticle synthesis in research laboratories. *Annals of Occupational Hygiene*, 53 (8), 829–838.

Determinación de sílice libre cristalina (cuarzo, cristobalita, tridimita) en aire -Método

del filtro de membrana / Difracción de rayos X MTA/MA -056/A06.

Dewangan, K.N. and Patil, M.R., 2014. Evaluation of Dust Exposure among the Workers in Agricultural Industries in North-East India. *Annals of Occupational Hygiene*, 59 (9), 1091–1105.

Ding, Y., Kuhlbusch, T.A.J., Van Tongeren, M., Jiménez, A.S., Tuinman, I., Chen, R., Alvarez, I.L., Mikolajczyk, U., Nickel, C., Meyer, J., Kaminski, H., Wohlleben, W., Stahlmecke, B., Clavaguera, S., and Riediker, M., 2017. Airborne engineered nanomaterials in the workplace—a review of release and worker exposure during nanomaterial production and handling processes. *Journal of Hazardous Materials*, 322, 17–28.

Dolovich, M.A., 2000. Influence of inspiratory flow rate, particle size, and airway caliber on aerosolized drug delivery to the lung. *Respiratory care*, 45 (6), 597–608.

Donaldson, K., Brown, D., Clouter, A., Duffin, R., MacNee, W., Renwick, L., Tran, L., and Stone, V., 2002. The Pulmonary Toxicology of Ultrafine Particles. *Journal of Aerosol Medicine*, 15 (2), 213–220.

Donaldson, K., Tran, L., Jimenez, L.A., Duffin, R., Newby, D.E., Mills, N., MacNee, W., and Stone, V., 2005. Combustion-derived nanoparticles: A review of their toxicology following inhalation exposure. *Particle and Fibre Toxicology*, 2 (10), 1–14.

Douwes, J., Cheung, K., Prezant, B., Sharp, M., Corbin, M., McLean, D., 't Mannetje, A., Schlunssen, V., Sigsgaard, T., Kromhout, H., LaMontagne, A.D., Pearce, N., and McGlothlin, J.D., 2017. Wood Dust in Joineries and Furniture Manufacturing: An Exposure Determinant and Intervention Study. *Annals of Work Exposures and Health*, 61 (4), 416–428.

Dubey, B., Pal, A.K., and Singh, G., 2012. Trace metal composition of airborne particulate matter in the coal mining and non–mining areas of Dhanbad Region, Jharkhand, India. *Atmospheric Pollution Research*, 3 (2), 238–246.

Dubey, P., Ghia, U., and Turkevich, L.A., 2017. Computational fluid dynamics analysis of the Venturi Dustiness Tester. *Powder Technology*, 312, 310–320.

Dubsky, S. and Fouras, A., 2015. Imaging regional lung function: A critical tool for developing inhaled antimicrobial therapies. *Advanced Drug Delivery Reviews*, 85, 100–109.

Dybdahl, M., Risom, L., Bornholdt, J., Autrup, H., Loft, S., and Wallin, H., 2004. Inflammatory and genotoxic effects of diesel particles in vitro and in vivo. *Mutation Research - Genetic Toxicology and Environmental Mutagenesis*, 562 (1–2), 119–131.

ECHA, 2015. Topical scientific workshop. Regulatory challenges in the risk assessment of nanomaterials. *Topical Scientific Workshop Regulatory Challenges in the Risk Assessment of Nanomaterials*. 61. Reference: ECHA-15-R-11-EN. Helsinki, Finland: European Chemicals Agency.

ECHA, 2016a. Guidance on Information Requirements and Chemical Safety Assessment. Part E: Risk Characterisation. *European Chemicals Agency*, 2.1 (November), 496.

ECHA, 2016b. *G*uidance on information requirements and chemical safety assessment. Chapter R. 14: Occupational exposure assessment. *European Chemicals Agency*, Version 3.0, 1-178.

Elihn, K. and Berg, P., 2009. Ultrafine Particle Characteristics in Seven Industrial Plants. *Annals of Occupational Hygiene*, 53 (5), 475–484.

European Committee for Standardization (CEN), 2013. *Workplace exposure: Measurement of the dustiness of bulk materials; Part1: Requirements and choice of test methods; Part 2: Rotating drum method; Part 3: Continuous drop method (EN 15051). [Stantdard] Brussels, Belgium, 2013*.

European Environment Agengy, 2018. *Air quality in Europe - 2018 report*. EEA Report No 12/2018.

Evans, D.E., Ku, B.K., Birch, M.E., and Dunn, K.H., 2010. Aerosol Monitoring during Carbon Nanofiber Production: Mobile Direct-Reading Sampling. *Annals of Occupational Hygiene*, 54 (5), 514–531.

Evans, D.E., Turkevich, L.A., Roettgers, C.T., Deye, G.J., and Baron, P.A., 2013. Dustiness of fine and nanoscale powders. *Annals of Occupational Hygiene*, 57 (2), 261–277.

Evans, D.E., Leonid, A.T., Gregory, J.D., 2017. Comparing the Venturi and rotating drum dustiness testing methods. *The 8th International Symposium on Nanotechnology, Occupational and Environmental Health. Helsingør, Denmark.*

Fang, S.C., Cassidy, A., and David, C.C., 2010. A systematic review of occupational exposure to particulate matter and cardiovascular disease. *International Journal of Environmental Research and Public Health*. 7 (4), 1773–1806.

Fernández Tena, A. and Casan Clarà, P., 2012. Deposition of inhaled particles in lungs. *Archivos de bronconeumologia*, 48 (7), 240–246.

Fierz, M., Burtscher, H., Steigmeier, P., and Kasper, M., 2010. Field Measurement of Particle Size and Number Concentration with the Diffusion Size Classifier (Disc). *In*: *SAE Technical Paper Series*.

Fierz, M., Houle, C., Steigmeier, P., and Burtscher, H., 2011. Design, calibration, and field performance of a miniature diffusion size classifier. *Aerosol Science and Technology*, 45 (1), 1–10.

Finlayson-Pitts, B.J. and Pitts, J.N., 2013. Chemistry of the upper and lower atmosphere. *Choice Reviews Online*, 37 (10), 37–5725.

Fonseca, A.S., Viana, M., Querol, X., Moreno, N., de Francisco, I., Estepa, C., and de la Fuente, G.F., 2015. Ultrafine and nanoparticle formation and emission mechanisms during laser processing of ceramic materials. *Journal of Aerosol Science*, 88, 48–57.

Fonseca, A.S., Maragkidou, A., Viana, M., Querol, X., Hämeri, K., de Francisco, I., Estepa, C., Borrell, C., Lennikov, V., and de la Fuente, G.F., 2016. Process-generated nanoparticles from ceramic tile sintering: Emissions, exposure and environmental

release. *Science of The Total Environment*, 565, 922–932.

Fonseca, 2016. *Exposure characterisation and sources of nanoparticles in workplace environments*. Thesis (PhD). University of Barcelona.

Fonseca, A. S., Koivisto, A. J., Koponen, I. K., Jensen, A. C. Ø., Kling, K. I., Levin, M., ... Jensen, K.A., 2017. Goodness of dustiness index for predicting human exposure to airborne nanomaterials. *In New tools and approaches for nanomaterial safety assessment - book of abstracts [#1552] Malaga, Spain*.

Fonseca, A.S., Kuijpers, E., Kling, K.I., Levin, M., Koivisto, A.J., Nielsen, S.H., Fransman, W., Fedutik, Y., Jensen, K.A., and Koponen, I.K., 2018. Particle release and control of worker exposure during laboratory-scale synthesis, handling and simulated spills of manufactured nanomaterials in fume hoods. *Journal of Nanoparticle Research*, 20 (2), 48.

Fransman, W., Schinkel, J., Meijster, T., Van Hemmen, J., Tielemans, E., and Goede, H., 2008. Development and evaluation of an Exposure Control Efficacy Library (ECEL). *Annals of Occupational Hygiene*, 52 (7), 567–575.

Fransman, W., Van Tongeren, M., Cherrie, J.W., Tischer, M., Schneider, T., Schinkel, J., Kromhout, H., Warren, N., Goede, H., and Tielemans, E., 2011. Advanced Reach Tool (ART): Development of the Mechanistic Model. *Annals of Occupational Hygiene*, 55 (9), 957–79.

Fröhlich, E. and Salar-Behzadi, S., 2014. Toxicological Assessment of Inhaled Nanoparticles: Role of in Vivo, ex Vivo, in Vitro, and in Silico Studies. *International Journal of Molecular Sciences*, 15 (3), 4795–4822.

Fujitani, Y., Kobayashi, T., Arashidani, K., Kunugita, N., and Suemura, K., 2008. Measurement of the Physical Properties of Aerosols in a Fullerene Factory for Inhalation Exposure Assessment. *Journal of Occupational and Environmental Hygiene*, 5 (6), 380–389.

Fukushima, S., Kasai, T., Umeda, Y., Ohnishi, M., Sasaki, T., and Matsumoto, M., 2018. Carcinogenicity of multi-walled carbon nanotubes: challenging issue on hazard assessment. *Journal of Occupational Health*, 60 (1), 10–30.

Gakidou, E., Afshin, A., Abajobir, A.A., and Al., A. et, 2017. Global, regional, and national comparative risk assessment of 84 behavioural, environmental and occupational, and metabolic risks or clusters of risks, 1990–2016: a systematic analysis for the Global Burden of Disease Study 2016. *The Lancet*, 390 (10100), 1345–1422.

Ganser, G.H. and Hewett, P., 2017. Models for nearly every occasion: Part II - Two box models. *Journal of Occupational and Environmental Hygiene*, 14 (1), 58–71.

Gilmour, P.S., Ziesenis, A., Morrison, E.R., Vickers, M.A., Drost, E.M., Ford, I., Karg, E., Mossa, C., Schroeppel, A., Ferron, G.A., Heyder, J., Greaves, M., MacNee, W., and Donaldson, K., 2004. Pulmonary and systemic effects of short-term inhalation exposure to ultrafine carbon black particles. *Toxicology and Applied Pharmacology*, 195 (1), 35–44.

Goede, H., Christopher-de Vries, Y., Kuijpers, E., and Fransman, W., 2018. A Review of Workplace Risk Management Measures for Nanomaterials to Mitigate Inhalation

and Dermal Exposure. *Annals of Work Exposures and Health*, 62 (8), 907–922.

Görner, P., Wrobel, R., and Simon, X., 2009. High efficiency CIP 10-I personal inhalable aerosol sampler. *Journal of Physics: Conference Series*, 151, 012061.

Görner, P., Görner, G., Simon, X., Wrobel, R., Kauffer, E., and Witschger, O., 2010. Laboratory Study of Selected Personal Inhalable Aerosol Samplers. *Annals of Occupational Hygiene*, 54 (2), 165–187.

Hamelmann, F. and Schmidt, E., 2003. Methods of Estimating the Dustiness of Industrial Powders – A Review. *KONA Powder and Particle Journal*, 21 (March), 7–18.

Hämeri, K., Lähde, T., Hussein, T., Koivisto, J., and Savolainen, K., 2009. Facing the key workplace challenge: Assessing and preventing exposure to nanoparticles at source. *Inhalation Toxicology*, 21 (sup1), 17–24.

Harrison, R.M., Shi, J.P., Xi, S., Khan, A., Mark, D., Kinnersley, R., and Yin, J., 2000. Measurement of number, mass and size distribution of particles in the atmosphere. *Philosophical Transactions of the Royal Society of London. Series A: Mathematical, Physical and Engineering Sciences*, 358 (1775), 2567–2580.

Hedmer, M., Isaxon, C., Nilsson, P.T., Ludvigsson, L., Messing, M.E., Genberg, J., Skaug, V., Tinnerberg, H., and Pagels, J.H., 2014. Exposure and Emission Measurements During Production, Purification, and Functionalization of Arc-Discharge-Produced Multi-walled Carbon Nanotubes A bstr Act. *Annals of Occupational Hygiene*, 58 (3), 355–379.

Heitbrink, W.A., Todd, W.F., and Fischbach, T.J., 1989. Correlation of tests for material dustiness with worker exposure from the bagging of powders. *Applied Industrial Hygiene*, 4 (1), 12–16.

Heitbrink, W.A., Tood, W.F., Cooper, T.C., and O'Brien, D.M., 1990. The Application of Dustiness Tests to the Prediction of Worker Dust Exposure. *American Industrial Hygiene Association Journal*, 51 (4), 217–223.

Heitbrink, W.A., Evans, D.E., Ku, B.K., Maynard, A.D., Slavin, T.J., and Peters, T.M., 2009. Relationships among particle number, surface area, and respirable mass concentrations in automotive engine manufacturing. *Journal of Occupational and Environmental Hygiene*, 6 (1), 19–31.

Hewett, P. and Ganser, G.H., 2017. Models for nearly every occasion: Part I - One box models. *Journal of Occupational and Environmental Hygiene*, 14 (1), 49–57.

Heyder, J. Gebhart, G. Rudolf, C. F. Schiller, W.S., 1986. Deposition of Particles in the Human Respiratory. *Journal of Aerosol Science*, 17 (5), 811–825.

Hinds, W.C., 1999. *Aerosol technology: Properties, Behavior, and Measurement of Airborne Particles.* Wiley-Interscience Publication. Wiley.

Höck, J., Epprecht, T., Furrer, E., Gautschi, M., Hofmann, H., Höhener, K., Knauer, K., Krug, H., Limbach, L., Gehr, P., Nowack, B., Riediker, M., Schirmer, K., Schmid, K., Som, C., Stark, W., Studer, C., Ulrich, A., von Götz, N., Weber, A., Wengert, S., and Wick, P., 2013. Guidelines on the Precautionary Matrix for Synthetic Nanomaterials. Version 3.0, (September), 1–38.

Hougaard, K.S., Jackson, P., Jensen, K.A., Sloth, J.J., Löschner, K., Larsen, E.H., Birkedal, R.K., Vibenholt, A., Boisen, A.-M.Z., Wallin, H., and Vogel, U., 2010. Effects of prenatal exposure to surface-coated nanosized titanium dioxide (UV-Titan). A study in mice. *Particle and Fibre Toxicology*, 7 (1), 16.

Hristozov, D., Gottardo, S., Semenzin, E., Oomen, A., Bos, P., Peijnenburg, W., van Tongeren, M., Nowack, B., Hunt, N., Brunelli, A., Scott-Fordsmand, J.J., Tran, L., and Marcomini, A., 2016a. Frameworks and tools for risk assessment of manufactured nanomaterials. *Environment International*, 95, 36–53.

Huang, C.H., Tai, C.Y., Huang, C.Y.U., Tsai, C.J., Chen, C.W., Chang, C.P., and Shih, T.S., 2010. Measurements of respirable dust and nanoparticle concentrations in a titanium dioxide pigment production factory. *Journal of Environmental Science and Health - Part A Toxic/Hazardous Substances and Environmental Engineering*, 45 (10), 1227–1233.

Huang, H., Li, H., and Li, X., 2016. Physicochemical Characteristics of Dust Particles in HVOF Spraying and Occupational Hazards: Case Study in a Chinese Company. *Journal of Thermal Spray Technology*, 25 (5), 971–981.

Hussain, M., Madl, P., and Khan, A., 2011. Lung deposition predictions of airborne particles and the emergence of contemporary diseases Part-I. *the Health*, 2 (2), 51–59.

Hussein, T., Korhonen, H., Herrmann, E., Hämeri, K., Lehtinen, K.E.J., and Kulmala, M., 2005. Emission rates due to indoor activities: Indoor aerosol model development, evaluation, and applications. *Aerosol Science and Technology*, 39 (11), 1111–1127.

Hussein, T., Glytsos, T., Ondráček, J., Dohányosová, P., Ždímal, V., Hämeri, K., Lazaridis, M., Smolík, J., and Kulmala, M., 2006. Particle size characterization and emission rates during indoor activities in a house. *Atmospheric Environment*, 40 (23), 4285–4307.

Hussein, T. and Kulmala, M., 2008. Indoor Aerosol Modeling: Basic Principles and Practical Applications. *Water, Air, & Soil Pollution: Focus*, 8 (1), 23–34.

Hussein, T., Wierzbicka, A., Löndahl, J., Lazaridis, M., and Hänninen, O., 2015. Indoor aerosol modeling for assessment of exposure and respiratory tract deposited dose. *Atmospheric Environment*, 106, 402–411.

Ibfelt, E., Bonde, J.P., and Hansen, J., 2010. Exposure to metal welding fume particles and risk for cardiovascular disease in Denmark: a prospective cohort study. *Occupational and environmental medicine*, 67 (11), 772–7.

IFA, 2013. Technical information: Ultrafine aerosols and nanoparticles at the workplace - Criteria for assessment of the effectiveness of protective measures [online]. Available from: https://www.dguv.de/ifa/fachinfos/nanopartikel-am-arbeitsplatz/index-2.jsp [Accessed 9 May 2019].

International Agency for Research on Cancer, 1997. *IARC Working Group on the Evaluation of Carcinogenic Risks to Humans, IARC monographs on the evaluation of carcinogenic risks to humans, Wood Dust and Formaldehyde, Volume 62*.

Isaxon, C., Gudmundsson, A., Nordin, E.Z., Lönnblad, L., Dahl, A., Wieslander, G.,

Bohgard, M., and Wierzbicka, A., 2015. Contribution of indoor-generated particles to residential exposure. *Atmospheric Environment*, 106, 458–466.

ISO, 1995. *ISO 7708:1995 - Air quality -- Particle size fraction definitions for health-related sampling*.

ISO, 1995. ISO 9277:1995. Determination of the Specific Surface Area of Solids by Gas Adsorption using the BET Method, German Institute of Normalization (DIN), 1-19.

Jayjock, M.A., Armstrong, T., and Taylor, M., 2011. The daubert standard as applied to exposure assessment modeling using the two-zone (NF/FF) model estimation of indoor air breathing zone concentration as an example. *Journal of Occupational and Environmental Hygiene*.

Jennings, B.R. and Parslow, K., 2006. Particle Size Measurement: The Equivalent Spherical Diameter. *Proceedings of the Royal Society A: Mathematical, Physical and Engineering Sciences*, 419 (1856), 137–149.

Jensen, A.C.Ø., Levin, M., Koivisto, A.J., Kling, K.I., Saber, A.T., and Koponen, I.K., 2015. Exposure Assessment of Particulate Matter from Abrasive Treatment of Carbon and Glass Fibre-Reinforced Epoxy-Composites – Two Case Studies. *Aerosol and Air Quality Research*, 15 (5), 1906–1916.

Jensen, A. C.Ø., Dal Maso, M., Koivisto, A., Belut, E., Meyer-Plath, A., Van Tongeren, M., Sánchez Jiménez, A., Tuinman, I., Domat, M., Toftum, J., and Koponen, I., 2018. Comparison of Geometrical Layouts for a Multi-Box Aerosol Model from a Single-Chamber Dispersion Study. *Environments*, 5 (5), 52.

Jensen, A.C.Ø., Poikkimäki, M., Brostrøm, A., Dal Maso, M., Nielsen, O.J., Rosenørn, T., Butcher, A., Koponen, I.K., and Koivisto, A.J., 2019. The Effect of Sampling Inlet Direction and Distance on Particle Source Measurements for Dispersion Modelling. *Aerosol and Air Quality Research*, (January).

Jensen, A.C.Ø., 2019. *Investigation of parameters influencing dispersion modelling in the occupational environment*. Thesis (PhD). University of Copenhagen.

Jensen, K., Saber, A., Kristensen, H., Koponen, I., Ligouri, B., and Wallin, H., 2014. NanoSafer vs 1.1 - Nanomaterial risk assessment using first order modeling. *6th International Symposium on Nanotechnology, Occupational and Environmental Health*, 22–23.

Johnson, M., Lam, N., Brant, S., Gray, C., and Pennise, D., 2011. Modeling indoor air pollution from cookstove emissions in developing countries using a Monte Carlo single-box model. *Atmospheric Environment*, 45 (19), 3237–3243.

Jones, R.M., Simmons, C.E., and Boelter, F.W., 2011. Comparing two-zone models of dust exposure. *Journal of Occupational and Environmental Hygiene*, 8 (9), 513–519.

Kaluza, S; Balderhaar, J.K; Orthen, B; Honnert, B; Jankowska, E; Pietrowski, P; Rosell, M.G; Tanarro, C; tejedor, J; Zugasti, A., 2013. *Workplace exposure to nanoparticles*.

Kaminski, H., Beyer, M., Fissan, H., Asbach, C., and Kuhlbusch, T.A.J., 2015. Measurements of Nanoscale TiO2 and Al2O3 in Industrial Workplace Environments – Methodology and Results. *Aerosol and Air Quality Research*, 15 (1), 129–141.

Kasai, T., Umeda, Y., Ohnishi, M., Mine, T., Kondo, H., Takeuchi, T., Matsumoto, M., and Fukushima, S., 2015. Lung carcinogenicity of inhaled multi-walled carbon nanotube in rats. *Particle and Fibre Toxicology*, 13 (1), 53.

Keil, C.B., 2000. A Tiered Approach to Deterministic Models for Indoor Air Exposures. *Applied Occupational and Environmental Hygiene*, 15 (1), 145–151.

Keil, C.B., 2015. Experimental measurements of near-source exposure modeling parameters. *Journal of Occupational and Environmental Hygiene*, 12 (10), 692–698.

Keil, C. and Zhao, Y., 2017. Interzonal airflow rates for use in near-field far-field workplace concentration modeling. *Journal of Occupational and Environmental Hygiene*, 14 (10), 793–800.

Klein Entink, R.H., Fransman, W., and Brouwer, D.H., 2011. How to statistically analyze nano exposure measurement results: using an ARIMA time series approach. *Journal of Nanoparticle Research*, 13 (12), 6991–7004.

Klepeis, N.E., Nelson, W.C., Ott, W.R., Robinson, J.P., Tsang, A.M., Switzer, P., Behar, J. V, Hern, S.C., and Engelmann, W.H., 2001. The National Human Activity Pattern Survey (NHAPS): a resource for assessing exposure to environmental pollutants. *Journal of Exposure Science & Environmental Epidemiology*, 11 (3), 231–252.

Klepeis, N.E., Bellettiere, J., Hughes, S.C., Nguyen, B., Berardi, V., Liles, S., Obayashi, S., Hofstetter, C.R., Blumberg, E., and Hovell, M.F., 2017. Fine particles in homes of predominantly low-income families with children and smokers: Key physical and behavioral determinants to inform indoor-air-quality interventions. *PLOS ONE*, 12 (5), e0177718.

Knol, A.B., de Hartog, J.J., Boogaard, H., Slottje, P., van der Sluijs, J.P., Lebret, E., Cassee, F.R., Wardekker, J.A., Ayres, J.G., Borm, P.J., Brunekreef, B., Donaldson, K., Forastiere, F., Holgate, S.T., Kreyling, W.G., Nemery, B., Pekkanen, J., Stone, V., Wichmann, H.-E., and Hoek, G., 2009. Expert elicitation on ultrafine particles: likelihood of health effects and causal pathways. *Particle and Fibre Toxicology*, 6 (1), 19.

Knutson, E.O. and Whitby, K.T., 1975a. Aerosol classification by electric mobility: apparatus, theory, and applications. *Journal of Aerosol Science*, 6 (6), 443–451.

Knutson, E.O. and Whitby, K.T., 1975b. Accurate measurement of aerosol electric mobility moments. *Journal of Aerosol Science*, 6 (6), 453–460.

Koivisto, A.J., Hussein, T., Niemelä, R., Tuomi, T., and Hämeri, K., 2010. Impact of particle emissions of new laser printers on modeled office room. *Atmospheric Environment*, 44 (17), 2140–2146.

Koivisto, A.J., Lyyränen, J., Auvinen, A., Vanhala, E., Hämeri, K., Tuomi, T., and Jokiniemi, J., 2012a. Industrial worker exposure to airborne particles during the packing of pigment and nanoscale titanium dioxide. *Inhalation Toxicology*, 24 (12), 839–849.

Koivisto, A.J., Aromaa, M., Mäkelä, J.M., Pasanen, P., Hussein, T., and Hämeri, K., 2012b. Concept To Estimate Regional Inhalation Dose of Industrially Synthesized Nanoparticles. *ACSNano*, 6, 1195–1203.

Koivisto, A.J., 2013. *Source Specific Risk Assessment of Indoor Aerosol Particles*. Thesis (PhD).University of Helsinki.

Koivisto, A.J., Jensen, A.C.Ø., Levin, M., Kling, K.I., Maso, M.D., Nielsen, S.H., Jensen, K.A., and Koponen, I.K., 2015. Testing the near field/far field model performance for prediction of particulate matter emissions in a paint factory. *Environmental Science: Processes Impacts*, 17 (1), 62–73.

Koivisto, A.J., Jensen, A.C.Ø., Kling, K.I., Nørgaard, A., Brinch, A., Christensen, F., and Jensen, K.A., 2017. Quantitative material releases from products and articles containing manufactured nanomaterials: Towards a release library. *NanoImpact*, 5, 119–132.

Koivisto, A.J., Jensen, A.C.Ø., Kling, K.I., Kling, J., Budtz, H.C., Koponen, I.K., Tuinman, I., Hussein, T., Jensen, K.A., Nørgaard, A., and Levin, M., 2018a. Particle emission rates during electrostatic spray deposition of TiO2 nanoparticle-based photoactive coating. *Journal of Hazardous Materials*, 341, 218–227.

Koivisto, A.J., Kling, K.I., Fonseca, A.S., Bluhme, A.B., Moreman, M., Yu, M., Costa, A.L., Giovanni, B., Ortelli, S., Fransman, W., Vogel, U., and Jensen, K.A., 2018b. Dip coating of air purifier ceramic honeycombs with photocatalytic TiO2 nanoparticles: A case study for occupational exposure. *Science of The Total Environment*, 630, 1283–1291.

Koivisto, A.J., Jensen, A.C.Ø., and Koponen, I.K., 2018c. The general ventilation multipliers calculated by using a standard Near-Field/Far-Field model. *Journal of Occupational and Environmental Hygiene*, 15 (5), D38–D43.

Koivisto, A.J., Kling, K.I., Hänninen, O., Jayjock, M., Löndahl, J., Wierzbicka, A., Fonseca, A.S., Uhrbrand, K., Boor, B.E., Jiménez, A.S., Hämeri, K., Maso, M.D., Arnold, S.F., Jensen, K.A., Viana, M., Morawska, L., and Hussein, T., 2019. Source specific exposure and risk assessment for indoor aerosols. *Science of The Total Environment*, 668, 13–24.

Koponen, I.K., Asmi, A., Keronen, P., Puhto, K., and Kulmala, M., 2001. Indoor air measurement campaign in Helsinki, Finland 1999 - The effect of outdoor air pollution on indoor air. *Atmospheric Environment*, 35 (8), 1465–1477.

Koponen, I.K., Koivisto, A.J., and Jensen, K.A., 2015. Worker exposure and high time-resolution analyses of process-related submicrometre particle concentrations at mixing stations in two paint factories. *Annals of Occupational Hygiene*, 59 (6), 749–763.

Kreatsoulas, C. and Anand, S.S., 2010. The impact of social determinants on cardiovascular disease. *Canadian Journal of Cardiology*, 26 (SUPPL. C), 8C–13C.

Kristensen, H.V., Hansen, S.V., Holm, G.R., 2010. *Nanopartikler i arbejdsmiljøet: Viden og inspiration om håndtering af nanomaterialer*. [Internet] Available from: http://nanosafer.i-bar.dk/media/Nanopartikler_i_arbejdsmiljoet_samlet.pdf.

Kuempel, E.D., Attfield, M.D., Vallyathan, V., Lapp, N.L., Hale, J.M., Smith, R.J., and Castranova, V., 2003. Pulmonary inflammation and crystalline silica in respirable coal mine dust: Dose response. *Journal of Biosciences*, 28 (1), 61–69.

Kuhlbusch, T.A.J., Neumann, S., and Fissan, H., 2004. Number Size Distribution, Mass Concentration, and Particle Composition of PM_{1}, $PM_{2.5}$, and PM_{10} in Bag Filling Areas of Carbon Black Production. *Journal of Occupational and Environmental Hygiene*, 1 (10), 660–671.

Kuhlbusch, T.A. J.; Krug, Harald F.; Nau, K., 2009. *NanoCare - Health related aspects of nanomaterials : final scientific report*. Frankfurt am Main.

Kuhlbusch, T.A., Asbach, C., Fissan, H., Göhler, D., and Stintz, M., 2011. Nanoparticle exposure at nanotechnology workplaces: A review. *Particle and Fibre Toxicology*, 8 (1), 22.

Kulmala, M., Vehkamäki, H., Petäjä, T., Dal Maso, M., Lauri, A., Kerminen, V.M., Birmili, W., and McMurry, P.H., 2004. Formation and growth rates of ultrafine atmospheric particles: a review of observations. *Journal of Aerosol Science*, 35 (2), 143–176.

Kumar, P., Robins, A., Vardoulakis, S., and Britter, R., 2010. A review of the characteristics of nanoparticles in the urban atmosphere and the prospects for developing regulatory controls. *Atmospheric Environment*, 44 (39), 5035–5052.

Landberg, H.E., Berg, P., Andersson, L., Bergendorf, U., Karlsson, J.E., Westberg, H., and Tinnerberg, H., 2015. Comparison and Evaluation of Multiple Users' Usage of the Exposure and Risk Tool: Stoffenmanager 5.1. *Annals of Occupational Hygiene*, 59 (7), 821–835.

Landberg, H.E., Axmon, A., Westberg, H., and Tinnerberg, H., 2017. A Study of the Validity of Two Exposure Assessment Tools: Stoffenmanager and the Advanced REACH Tool. *Annals of Work Exposures and Health*, 61 (5), 575–588.

Landrigan, P.J., Fuller, R., Acosta, N.J.R., Adeyi, O., Arnold, R., Basu, N. (Nil), Baldé, A.B., Bertollini, R., Bose-O'Reilly, S., Boufford, J.I., Breysse, P.N., Chiles, T., Mahidol, C., Coll-Seck, A.M., Cropper, M.L., Fobil, J., Fuster, V., Greenstone, M., Haines, A., Hanrahan, D., Hunter, D., Khare, M., Krupnick, A., Lanphear, B., Lohani, B., Martin, K., Mathiasen, K. V, McTeer, M.A., Murray, C.J.L., Ndahimananjara, J.D., Perera, F., Potočnik, J., Preker, A.S., Ramesh, J., Rockström, J., Salinas, C., Samson, L.D., Sandilya, K., Sly, P.D., Smith, K.R., Steiner, A., Stewart, R.B., Suk, W.A., van Schayck, O.C.P., Yadama, G.N., Yumkella, K., and Zhong, M., 2018. The Lancet Commission on pollution and health. *The Lancet*, 391 (10119), 462–512.

Levin, M., Koponen, I.K., and Jensen, K.A., 2014. Exposure Assessment of Four Pharmaceutical Powders Based on Dustiness and Evaluation of Damaged HEPA Filters. *Journal of Occupational and Environmental Hygiene*, 11 (3), 165–177.

Lidén, G., 2006. Dustiness Testing of Materials Handled at Workplaces. *Annals of Occupational Hygiene*, 50 (5), 437–439.

Liguori, B., Hansen, S.F., Baun, A., and Jensen, K.A., 2016. Control banding tools for occupational exposure assessment of nanomaterials — Ready for use in a regulatory context? *NanoImpact*, 2, 1–17.

Liu, B.Y.H., 1976. *Fine Particles: Aerosol Generation, Measurement, Sampling and Analysis*. Journal of Aerosol Science. Academic Press.

López-Lilao, A., Bruzi, M., Sanfélix, V., Gozalbo, A., Mallol, G., and Monfort, E., 2015.

Evaluation of the Dustiness of Different Kaolin Samples. *Journal of Occupational and Environmental Hygiene*, 12 (8), 547–554.

López-Lilao, A., Escrig, A., Orts, M.J., Mallol, G., and Monfort, E., 2016. Quartz dustiness: A key factor in controlling exposure to crystalline silica in the workplace. *Journal of Occupational and Environmental Hygiene*, 13 (11), 817–828.

López-Lilao, A., 2017. *Análisis de la influencia de las características de los materiales pulverulentos sobre su poder de emisión de polvo*. Thesis (PhD). University Jaume I.

Lopez, R., Lacey, S.E., and Jones, R.M., 2015. Application of a Two-Zone Model to Estimate Medical Laser-Generated Particulate Matter Exposures. *Journal of Occupational and Environmental Hygiene*, 12 (5), 309–313.

Madanchi, N., Leiden, A., Winter, M., Asbach, C., Lindermann, J., Herrmann, C., and Thiede, S., 2018. Cutting fluid emissions in grinding processes: influence of process parameters on particle size and mass concentration. *International Journal of Advanced Manufacturing Technology*.

Mallol, G., Amorós, J.L., Orts, M.J., and Llorens, D., 2008. Densification of monomodal quartz particle beds by tapping. *Chemical Engineering Science*, 63 (22), 5447–5456.

Marquart, H., Heussen, H., Le Feber, M., Noy, D., Tielemans, E., Schinkel, J., West, J., and Van Der Schaaf, D., 2008. 'Stoffenmanager', a web-based control banding tool using an exposure process model. *Annals of Occupational Hygiene*.

Martins, V., Moreno, T., Mendes, L., Eleftheriadis, K., Diapouli, E., Alves, C.A., Duarte, M., de Miguel, E., Capdevila, M., Querol, X., and Minguillón, M.C., 2016. Factors controlling air quality in different European subway systems. *Environmental Research*, 146, 35–46.

Maynard, A.D., Baron, P.A., Foley, M., Shvedova, A.A., Kisin, E.R., and Castranova, V., 2004. Exposure to Carbon Nanotube Material: Aerosol Release During the Handling of Unrefined Single-Walled Carbon Nanotube Material. *Journal of Toxicology and Environmental Health, Part A*, 67 (1), 87–107.

Mazaheri, M., Clifford, S., Jayaratne, R., Megat Mokhtar, M.A., Fuoco, F., Buonanno, G., and Morawska, L., 2014. School Children's Personal Exposure to Ultrafine Particles in the Urban Environment. *Environmental Science & Technology*, 48 (1), 113–120.

McMurry, P., 2000. A review of atmospheric aerosol measurements. *Atmospheric Environment*, 34 (12–14), 1959–1999.

Medved, A., Dorman, F., Kaufman, S.L., and Pöcher, A., 2000. A new corona-based charger for aerosol particles. *Journal of Aerosol Science*, 31, 616–617.

Mészáros, E., 1999. *Fundamentals of atmospheric aerosol chemistry*. Budapest: Akadémiai Kiadó.

Methner, M., Hodson, L., Dames, A., and Geraci, C., 2010. Nanoparticle emission assessment technique (NEAT) for the identification and measurement of potential inhalation exposure to engineered nanomaterials—part b: Results from 12 field studies. *Journal of Occupational and Environmental Hygiene*, 7 (3), 163–176.

Minguillón, M.C., Reche, C., Martins, V., Amato, F., de Miguel, E., Capdevila, M.,

Centelles, S., Querol, X., and Moreno, T., 2018. Aerosol sources in subway environments. *Environmental Research*, 167, 314–328.

Mølgaard, B., Ondráček, J., Šťávová, P., Džumbová, L., Barták, M., Hussein, T., and Smolík, J., 2014. Migration of aerosol particles inside a two-zone apartment with natural ventilation: A multi-zone validation of the multi-compartment and size-resolved indoor aerosol model. *Indoor and Built Environment*, 23 (5), 742–756.

Mølgaard, B., Viitanen, A.-K., Kangas, A., Huhtiniemi, M., Larsen, S.T., Vanhala, E., Hussein, T., Boor, B.E., Hämeri, K., Koivisto, A.J., Adamkiewicz, G., and Fabian, M.P., 2015. Exposure to Airborne Particles and Volatile Organic Compounds from Polyurethane Molding, Spray Painting, Lacquering, and Gluing in a Workshop. *International Journal of Environmental Research and Public Health*, 12 (4), 3756–3773.

Møller, K.L., Thygesen, L.C., Schipperijn, J., Loft, S., Bonde, J.P., Mikkelsen, S., and Brauer, C., 2014. Occupational exposure to ultrafine particles among airport employees-combining personal monitoring and global positioning system. *PLoS ONE*, 9 (9).

Monn, C., 2001. Exposure assessment of air pollutants: a review on spatial heterogeneity and indoor/outdoor/personal exposure to suspended particulate matter, nitrogen dioxide and ozone. *Atmospheric Environment*, 35, 1–32.

Monsé, C., Hagemeyer, O., Raulf, M., Jettkant, B., van Kampen, V., Kendzia, B., Gering, V., Kappert, G., Weiss, T., Ulrich, N., Marek, E.-M., Bünger, J., Brüning, T., and Merget, R., 2018. Concentration-dependent systemic response after inhalation of nano-sized zinc oxide particles in human volunteers. *Particle and Fibre Toxicology*, 15 (1), 8.

Morawska, L., He, C., Hitchins, J., Mengersen, K., and Gilbert, D., 2003. Characteristics of particle number and mass concentrations in residential houses in Brisbane, Australia. *Atmospheric Environment*, 37 (30), 4195–4203.

Morawska, L., Ayoko, G.A., Bae, G.N., Buonanno, G., Chao, C.Y.H., Clifford, S., Fu, S.C., Hänninen, O., He, C., Isaxon, C., Mazaheri, M., Salthammer, T., Waring, M.S., and Wierzbicka, A., 2017. Airborne particles in indoor environment of homes, schools, offices and aged care facilities: The main routes of exposure. *Environment International*, 108, 75–83.

Nazarenko, Y., Han, T.W., Lioy, P.J., and Mainelis, G., 2011. Potential for exposure to engineered nanoparticles from nanotechnology-based consumer spray products. *Journal of Exposure Science and Environmental Epidemiology*, 21 (5), 515–528.

Nazaroff, W.W. and Cass, G.R., 1989. Mathematical modeling of indoor aerosol dynamics. *Environmental Science and Technology*, 23 (2), 157–166.

Nazaroff, W.W., 2004. Indoor particle dynamics. *Indoor Air*, 14 (s7), 175–183.

Neghab, M., Zadeh, J.H., and Fakoorziba, M.R., 2009. Respiratory toxicity of raw materials used in ceramic production. *Industrial health*, 47 (1), 64–9.

Nicas, M., 2016. The near field/far field model with constant application of chemical mass and exponentially decreasing emission of the mass applied. *Journal of*

Occupational and Environmental Hygiene, 13 (7), 519–528.

NIOSH, 2002. Health Effects of Occupational Exposure to Respirable Crystalline Silica. *NIOSH Hazard Review*, (April), 145.

NIOSH, 2011. Occupational Exposure to Titanium Dioxide, Current Intellingence Bulletin 63, April 2011.

NIOSH, 2013. Occupational exposure to carbon nanotubes and nanofibers, Current Intelligence Bulletin 65, Publication No. 2013-145 (pp. 1-184). Cincinnati: National Institute for Occupational Safety and Health, Department of Health and Human Services.

Notø, H., Nordby, K.-C., Skare, Ø., and Eduard, W., 2018. Job Tasks as Determinants of Thoracic Aerosol Exposure in the Cement Production Industry. *Annals of Work Exposures and Health*, 62 (1), 88–100.

O'Shaughnessy, P.T., 2013. Occupational health risk to nanoparticulate exposure. *Environmental Science: Processes Impacts*, 15 (1), 49–62.

Oberdorster, G., Ferin, J., and Lehnert, B.E., 1994. Correlation between particle size, in vivo particle persistence, and lung injury. *Environmental Health Perspectives*. 173–179.

Oberdörster, G., 2001. Pulmonary effects of inhaled ultrafine particles. *International archives of occupational and environmental health*, 74 (1), 1–8.

Oberdörster, G., Sharp, Z., Atudorei, V., Elder, A., Gelein, R., Kreyling, W., and Cox, C., 2004. Translocation of Inhaled Ultrafine Particles to the Brain. *Inhalation Toxicology*, 16 (6–7), 437–445.

Oberdörster, G. and Kuhlbusch, T.A.J., 2018. In vivo effects: Methodologies and biokinetics of inhaled nanomaterials. *NanoImpact*. 10, 38–60.

OECD, 2015. *Harmonized Tiered Approach to Measure and Assess the Potential Exposure to Airborne Emissions of Engineered Nano-Objects and their Agglomerates and Aggregates at Workplaces*. Series on the Safety of Manufactured Nanomaterials No.55.

Onat, B. and Stakeeva, B., 2014. Assessment of fine particulate matters in the subway system of Istanbul. *Indoor and Built Environment*, 23 (4), 574–583.

Ostiguy, C., Roberge, B., Woods, C., and Soucy, B., 2010. *Engineered nanoparticles: Current knowledge about OHS risks and prevention measures*. IRSST Studies and research projects. 656.

Otterstedt, J.E. and Brandreth, D.A., 1998. Clays and Colloidal Silicas. *Small Particles Technology*. Boston, MA: Springer US, 525–525.

Paik, S.Y., Zalk, D.M., and Swuste, P., 2008. Application of a Pilot Control Banding Tool for Risk Level Assessment and Control of Nanoparticle Exposures. *Annals of Occupational Hygiene*, 52 (6), 419–428.

Park, J.Y., Ramachandran, G., Raynor, P.C., Eberly, L.E., and Olson, G., 2010. Comparing exposure zones by different exposure metrics using statistical parameters: Contrast

and precision. *Annals of Occupational Hygiene*, 54 (7), 799–812.

Persons, T.M., Droitcour, J.A., Larson, E.M., and Armes, M.W., 2014. Nanomanufacturing: Emergence and Implications for US Competitiveness, the Environment, and Human Health. *United States Government Accountability Office* (GAO-14-181SP).

Petavratzi, E., Kingman, S.W., and Lowndes, I.S., 2007. Assessment of the dustiness and the dust liberation mechanisms of limestone quarry operations. *Chemical Engineering and Processing: Process Intensification*, 46 (12), 1412–1423.

Peters, T.M., Elzey, S., Johnson, R., Park, H., Grassian, V.H., Maher, T., and O'Shaughnessy, P., 2008. Airborne Monitoring to Distinguish Engineered Nanomaterials from Incidental Particles for Environmental Health and Safety. *Journal of Occupational and Environmental Hygiene*, 6 (2), 73–81.

Plinke, M.A.E., Maus, R., and Leith, D., 1992. Experimental examination of factors that affect dust generation by using Heubach and MRI testers. *American Industrial Hygiene Association Journal*, 53 (5), 325–330.

Plinke, M.A.E., Leith, D., Boundy, M.G., and Löffler, F., 1995. Dust Generation from Handling Powders in Industry. *American Industrial Hygiene Association Journal*, 56 (3), 251–257.

Poulsen, S.S., Jackson, P., Kling, K., Knudsen, K.B., Skaug, V., Kyjovska, Z.O., Thomsen, B.L., Clausen, P.A., Atluri, R., Berthing, T., Bengtson, S., Wolff, H., Jensen, K.A., Wallin, H., and Vogel, U., 2016. Multi-walled carbon nanotube physicochemical properties predict pulmonary inflammation and genotoxicity. *Nanotoxicology*, 10 (9), 1263–1275.

Radnoff, D.L. and Kutz, M.K., 2014. Exposure to crystalline silica in abrasive blasting operations where silica and non-silica abrasives are used. *Annals of Occupational Hygiene*, 58 (1), 19–27.

Raes, F., Dingenen, R. Van, Vignati, E., Wilson, J., Putaud, J.-P., Seinfeld, J.H., and Adams, P., 2000. Formation and cycling of aerosols in the global troposphere. *Atmospheric Environment*, 34 (25), 4215–4240.

Ramachandran, G., 2005. *Occupational Exposure Assessment for Air Contaminants*. Taylor & Francis Group, LLC

Ramachandran, G., Ostraat, M., Evans, D.E., Methner, M.M., O'Shaughnessy, P., D'Arcy, J., Geraci, C.L., Stevenson, E., Maynard, A., and Rickabaugh, K., 2011. A Strategy for Assessing Workplace Exposures to Nanomaterials. *Journal of Occupational and Environmental Hygiene*, 8 (11), 673–685.

Raul, A.C. and D.J.Z., 2003. Regulatory Daubert: a proposal to enhance judicial review of agency science by incorporating Daubert principles into administrative law. *Law and Contemporary Problems*. 66 (7), 7–44.

Reche, C., Querol, X., Alastuey, A., Viana, M., Pey, J., Moreno, T., Rodríguez, S., González, Y., Fernández-Camacho, R., Sánchez De La Campa, A.M., De La Rosa, J., Dall'osto, M., Prévôt, A.S.H., Hueglin, C., Harrison, R.M., and Quincey, P., 2011. Atmospheric Chemistry and Physics New considerations for PM, Black Carbon and

particle number concentration for air quality monitoring across different European cities. *Atmospheric Chemistry and Physics*, 11, 6207–6227.

Reche, C., Viana, M., Rivas, I., Bouso, L., Àlvarez-Pedrerol, M., Alastuey, A., Sunyer, J., and Querol, X., 2014. Outdoor and indoor UFP in primary schools across Barcelona. *Science of the Total Environment*, 493, 943–953.

Ribalta, C., Koivisto, A.J., López-Lilao, A., Estupiñá, S., Minguillón, M.C., Monfort, E., and Viana, M., 2019a. Testing the performance of one and two box models as tools for risk assessment of particle exposure during packing of inorganic fertilizer. *Science of The Total Environment*, 650, 2423–2436.

Ribalta, C., López-Lilao, A., Estupiñá, S., Fonseca, A.S., Tobías, A., García-Cobos, A., Minguillón, M.C., Monfort, E., and Viana, M., 2019b. Health risk assessment from exposure to particles during packing in working environments. *Science of The Total Environment*, 671, 474–487.

Ribalta, C., Viana, M., López-Lilao, A., Estupiñá, S., Minguillón, M.C., Mendoza, J., Díaz, J., Dahmann, D., and Monfort, E., 2019c. On the Relationship between Exposure to Particles and Dustiness during Handling of Powders in Industrial Settings. *Annals of Work Exposures and Health*, 63 (1), 107–123.

Ribalta, C., Koivisto, A.J., Salmatonidis, A., López-Lilao, A., Monfort, E., and Viana, M., 2019d. Modeling of High Nanoparticle Exposure in an Indoor Industrial Scenario with a One-Box Model. *International Journal of Environmental Research and Public Health*, 16 (10), 1695.

Riedmann, R.A., Gasic, B., and Vernez, D., 2015. Sensitivity Analysis, Dominant Factors, and Robustness of the ECETOC TRA v3, Stoffenmanager 4.5, and ART 1.5 Occupational Exposure Models. *Risk Analysis*, 35 (2), 211–225.

Rodríguez, S., Van Dingenen, R., Putaud, J.-P., Martins-Dos Santos, S., and Roselli, D., 2005. Nucleation and growth of new particles in the rural atmosphere of Northern Italy—relationship to air quality monitoring. *Atmospheric Environment*, 39 (36), 6734–6746.

Rodríguez, S., Van Dingenen, R., Putaud, J.-P., Dell'Acqua, A., Pey, J., Querol, X., Alastuey, A., Chenery, S., Ho, K.-F., Harrison, R., Tardivo, R., Scarnato, B., and Gemelli, V., 2007. A study on the relationship between mass concentrations, chemistry and number size distribution of urban fine aerosols in Milan, Barcelona and London. *Atmospheric Chemistry and Physics*, 7 (9), 2217–2232.

Rufo, J.C., Madureira, J., Paciência, I., Slezakova, K., Pereira, M. do C., Pereira, C., Teixeira, J.P., Pinto, M., Moreira, A., and Fernandes, E. de O., 2015. Exposure of Children to Ultrafine Particles in Primary Schools in Portugal. *Journal of Toxicology and Environmental Health, Part A*, 78 (13–14), 904–914.

Saber, A.T., Jacobsen, N.R., Jackson, P., Poulsen, S.S., Kyjovska, Z.O., Halappanavar, S., Yauk, C.L., Wallin, H., and Vogel, U., 2014. Particle-induced pulmonary acute phase response may be the causal link between particle inhalation and cardiovascular disease. *Wiley Interdisciplinary Reviews: Nanomedicine and Nanobiotechnology*, 6 (6), 517–531.

Sachse, S., Silva, F., Irfan, A., Zhu, H., Pielichowski, K., Leszczynska, A., Blazquez, M.,

Kazmina, O., Kuzmenko, O., and Njuguna, J., 2012. Physical characteristics of nanoparticles emitted during drilling of silica based polyamide 6 nanocomposites. *IOP Conference Series: Materials Science and Engineering*, 40, 012012.

Sahmel, J., Unice, K., Scott, P., Cowan, D., and Paustenbach, D., 2009. The use of multizone models to estimate an airborne chemical contaminant generation and decay profile: Occupational exposures of hairdressers to vinyl chloride in hairspray during the 1960s and 1970s. *Risk Analysis*, 29 (12), 1699–1725.

Salmatonidis, A., Viana, M., Pérez, N., Alastuey, A., de la Fuente, G.F., Angurel, L.A., Sanfélix, V., and Monfort, E., 2018. Nanoparticle formation and emission during laser ablation of ceramic tiles. *Journal of Aerosol Science*, 126, 152–168.

Salmatonidis, A., Ribalta, C., Sanfélix, V., Bezantakos, S., Biskos, G., Vulpoi, A., Simion, S., Monfort, E., and Viana, M., 2019. Workplace Exposure to Nanoparticles during Thermal Spraying of Ceramic Coatings. *Annals of Work Exposures and Health*, 63 (1), 91–106.

Salmatonidis, A., Sanfélix, V., Carpio-Cobo, P., Pawłowski, L., Viana, M., and Monfort, E., 2019. Effectiveness of technological measures to mitigate nanoparticle exposures in thermal processes – industrial case studies. *International Journal of Hygine and Environmental Health*, under review.

Sánchez Jiménez, A.S., Tongeren, M. Van, and Cherrie, J.W., 2011. *A review of monitoring methods for inhalable hardwood dust* (May). IOM Research Report P937/1A.

Sánchez Jiménez, A., Varet, J., Poland, C., Fern, G.J., Hankin, S.M., and van Tongeren, M., 2016. A comparison of control banding tools for nanomaterials. *Journal of Occupational and Environmental Hygiene*, 13 (12), 936–949.

Savic, N., Gasic, B., Schinkel, J., and Vernez, D., 2017. Comparing the Advanced REACH Tool's (ART) Estimates With Switzerland's Occupational Exposure Data. *Annals of Work Exposures and Health*, 61 (8), 954–964.

Savic, N., Gasic, B., and Vernez, D., 2018. ART, Stoffenmanager, and TRA: A Systematic Comparison of Exposure Estimates Using the TREXMO Translation System. *Annals of Work Exposures and Health*, 62 (1), 72–87.

Savolainen, K., Backman, U., Brouwer, D., Fadeel, B., and Fernandes, T., 2013. *Nanosafety in Europe 2015-2025: Towards Safe and Sustainable Nanomaterials and Nanotechnology Innovations*. Finish Institute of Occupational Health.

Schenker, M.B., Pinkerton, K.E., Mitchell, D., Vallyathan, V., Elvine-Kreis, B., and Green, F.H.Y., 2009. Pneumoconiosis from agricultural dust exposure among young California farmworkers. *Environmental Health Perspectives*. 117 (6), 988-994.

Schinkel, J., Warren, N., Fransman, W., van Tongeren, M., McDonnell, P., Voogd, E., Cherrie, J.W., Tischer, M., Kromhout, H., and Tielemans, E., 2011. Advanced REACH Tool (ART): Calibration of the mechanistic model. *Journal of Environmental Monitoring*, 13 (5), 1374.

Schneider, T. and Jensen, K.A., 2007. Combined Single-Drop and Rotating Drum Dustiness Test of Fine to Nanosize Powders Using a Small Drum. *The Annals of Occupational Hygiene*, 52 (1), 23–34.

Schripp, T., Wensing, M., Uhde, E., Salthammer, T., He, C., and Morawska, L., 2008. Evaluation of Ultrafine Particle Emissions from Laser Printers Using Emission Test Chambers. *Environmental Science & Technology*, 42 (12), 4338–4343.

SER, 2012. Provisional nano reference values for engineered nanomaterials, Advisory Report 12/01, Sociaal Economische Raad, Den Haag.

Shepard, M.N. and Brenner, S., 2014. An occupational exposure assessment for engineered nanoparticles used in semiconductor fabrication. *Annals of Occupational Hygiene*, 58 (2), 251–265.

Spencer, J.W. and Plisko, M.J., 2007. A comparison study using a mathematical model and actual exposure monitoring for estimating solvent exposures during the disassembly of metal parts. *Journal of Occupational and Environmental Hygiene*, 4 (4), 253–259.

Spinazzè, A., Lunghini, F., Campagnolo, D., Rovelli, S., Locatelli, M., Cattaneo, A., and Cavallo, D.M., 2017. Accuracy evaluation of three modelling tools for occupational exposure assessment. *Annals of Work Exposures and Health*, 61 (3), 284–298.

Stahlmecke, B., Wagener, S., Asbach, C., Kaminski, H., Fissan, H., and Kuhlbusch, T.A.J., 2009. Investigation of airborne nanopowder agglomerate stability in an orifice under various differential pressure conditions. *Journal of Nanoparticle Research*, 11 (7), 1625–1635.

Stanislawska, M., Halatek, T., Cieslak, M., Kaminska, I., Kuras, R., Janasik, B., and Wasowicz, W., 2017. Coarse, fine and ultrafine particles arising during welding - Analysis of occupational exposure. *Microchemical Journal*, 135, 1–9.

Stefaniak, A.B., Virji, M.A., and Day, G.A., 2009. Characterization of exposures among cemented tungsten carbide workers. Part I: Size-fractionated exposures to airborne cobalt and tungsten particles. *Journal of Exposure Science and Environmental Epidemiology*, 19 (5), 475–491.

Steinfeld, J.I. and Pandis, S.N., 2006. Atmospheric Chemistry and Physics: From Air Pollution to Climate Change. *Environment: Science and Policy for Sustainable Development*, 40 (7), 26–26.

Stolzenburg, M.R. and McMurry, P.H., 1991. An Ultrafine Aerosol Condensation Nucleus Counter. *Aerosol Science and Technology*, 14 (1), 48–65.

Strasser, G., Hiebaum, S., and Neuberger, M., 2018. Commuter exposure to fine and ultrafine particulate matter in Vienna. *Wiener klinische Wochenschrift*, 130 (1–2), 62–69.

Thompson, J.C., Wilson, P.G., Shridas, P., Ji, A., de Beer, M., de Beer, F.C., Webb, N.R., and Tannock, L.R., 2018. Serum amyloid A3 is pro-atherogenic. *Atherosclerosis*, 268, 32–35.

Tielemans, E., Schneider, T., Goede, H., Tischer, M., Warren, N., Kromhout, H., Van Tongeren, M., Van Hemmen, J., and Cherrie, J.W., 2008a. Conceptual model for assessment of inhalation exposure: Defining modifying factors. *Annals of Occupational Hygiene*, 52 (7), 577–586.

Tielemans, E., Noy, D., Schinkel, J., Heussen, H., Van Der Schaaf, D., West, J., and

Fransman, W., 2008b. Stoffenmanager exposure model: Development of a quantitative algorithm. *Annals of Occupational Hygiene*, 52 (6), 443–454.

Tielemans, E., Warren, N., Fransman, W., Van Tongeren, M., McNally, K., Tischer, M., Ritchie, P., Kromhout, H., Schinkel, J., Schneider, T., and Cherrie, J.W., 2011. Advanced REACH Tool (ART): Overview of version 1.0 and research needs. *Annals of Occupational Hygiene*. 55 (9), 949–956

Tsai, S.J., Ada, E., Isaacs, J.A., and Ellenbecker, M.J., 2009. Airborne nanoparticle exposures associated with the manual handling of nanoalumina and nanosilver in fume hoods. *Journal of Nanoparticle Research*, 11 (1), 147–161.

Tsai, S.J., Ashter, A., Ada, E., Mead, J.L., Barry, C.F., and Ellenbecker, M.J., 2008. Airborne nanoparticle release associated with the compounding of nanocomposites using nanoalumina as fillers. *Aerosol and Air Quality Research*, 8 (2), 160–177.

UNE-EN 481:1995. *Workplace atmospheres. Size fraction definitions for measurementof airborne particles*.

UNE-EN 689:2019. *Workplace exposure - Measurement of exposure by inhalation to chemical agents - Strategy for testing compliance with occupational exposure limit values.*

Van Broekhuizen, P., Van Veelen, W., Streekstra, W.H., Schulte, P., and Reijnders, L., 2012. Exposure Limits for Nanoparticles: Report of an International Workshop on Nano Reference Values. *The Annals of Occupational Hygiene*, 56 (5), 515–524.

Van Tongeren, M., Fransman, W., Spankie, S., Tischer, M., Brouwer, D., Schinkel, J., Cherrie, J.W., and Tielemans, E., 2011. Advanced REACH Tool: Development and application of the substance emission potential modifying factor. *Annals of Occupational Hygiene*, 55 (9), 980–988.

Van Tongeren, M., Lamb, J., Cherrie, J.W., MacCalman, L., Basinas, I., and Hesse, S., 2017. Validation of Lower Tier Exposure Tools Used for REACH: Comparison of Tools Estimates With Available Exposure Measurements. *Annals of Work Exposures and Health*, 61 (8), 921–938.

Van Duuren-Stuurman, B., Vink, S.R., Verbist, K.J.M., Heussen, H.G.A., Brouwer, D.H., Kroese, D.E.D., Van Niftrik, M.F.J., Tielemans, E., and Fransman, W., 2012. Stoffenmanager Nano Version 1.0: A Web-Based Tool for Risk Prioritization of Airborne Manufactured Nano Objects. *Annals of Occupational Hygiene*, 56 (5), 525–541.

Vernez, D.S., Droz, P.-O., Lazor-Blanchet, C., and Jaques, S., 2004. Characterizing Emission and Breathing-Zone Concentrations Following Exposure Cases to Fluororesin-Based Waterproofing Spray Mists. *Journal of Occupational and Environmental Hygiene*, 1 (9), 582–592.

Viana, M., Díez, S., and Reche, C., 2011. Indoor and outdoor sources and infiltration processes of PM1 and black carbon in an urban environment. *Atmospheric Environment*, 45 (35), 6359–6367.

Viana, M., Fonseca, A.S., Querol, X., López-Lilao, A., Carpio, P., Salmatonidis, A., and Monfort, E., 2017. Workplace exposure and release of ultrafine particles during

atmospheric plasma spraying in the ceramic industry. *Science of the Total Environment*, 599–600, 2065–2073.

Viegas, S., Mateus, V., Almeida-Silva, M., Carolino, E., and Viegas, C., 2013. Occupational exposure to particulate matter and respiratory symptoms in portuguese swine barn workers. *Journal of Toxicology and Environmental Health - Part A: Current Issues*, 76 (17), 1007–1014.

Viitanen, A.-K., Uuksulainen, S., Koivisto, A.J., Hämeri, K., and Kauppinen, T., 2017. Workplace Measurements of Ultrafine Particles—A Literature Review. *Annals of Work Exposures and Health*, 61 (7), 749–758.

Vogel, U. and Cassee, F.R., 2018. Editorial: dose-dependent ZnO particle-induced acute phase response in humans warrants re-evaluation of occupational exposure limits for metal oxides. *Particle and Fibre Toxicology*, 15 (1), 7.

Vogel, U., Poulsen, S.S., Knudsen, K.B., Anne, T., Jacobsen, N.R., and Wallin, H., 2018. Cardiovascular disease as a occupational disease. *NanoSafe 2018*. Grenoble, France

Voliotis, A., Bezantakos, S., Giamarelou, M., Valenti, M., Kumar, P., and Biskos, G., 2014. Nanoparticle emissions from traditional pottery manufacturing. *Environmental Science: Processes & Impacts*, 16 (6), 1489.

Watson, J.G. and Chow, J.C., 2007. *Receptor models for source apportionment of suspended particles*. Introduction to environment forensics.

Wehner, B. and Wiedensohler, A., 2003. Long term measurements of submicrometer urban aerosols: statistical analysis for correlations with meteorological conditions and trace gases. *Atmospheric Chemistry and Physics*, 3 (3), 867–879.

Weschler, C.J., 2011. Chemistry in indoor environments: 20 years of research. *Indoor Air*, 21 (3), 205–218.

WHO, 1999. *Dust Control and Good Management*. Hazard Prevention and Control In The Work Environment : Airbone Dust.

WHO, 2016. Ambient Air Pollution: A global assessment of exposure and burden of disease. *World Health Organization*, 1–131.

WHO, 2017. *WHO guidelines on protecting workers: from potential risks of manufactured nanomaterials*.

Worrall, W.E., 1982. *Ceramic raw materials*. Great Britain: Pergamon Press.

Yan, C., Zheng, M., Yang, Q., Zhang, Q., Qiu, X., Zhang, Y., Fu, H., Li, X., Zhu, T., and Zhu, Y., 2015. Commuter exposure to particulate matter and particle-bound PAHs in three transportation modes in Beijing, China. *Environmental Pollution*, 204, 199–206.

Yeganeh, B., Kull, C.M., Hull, M.S., and Marr, L.C., 2008a. Characterization of airborne particles during production of carbonaceous nanomaterials. *Environmental Science and Technology*, 42 (12), 4600–4606.

Zalk, D.M. and Heussen, H., 2011. Banding the World Together ; The Global Growth of Control Banding and Qualitative Occupational Risk Management. *Safety And*

Health at work, 2 (December), 375–379.

Zhang, L., Guo, C., Jia, X., Xu, H., Pan, M., Xu, D., Shen, X., Zhang, J., Tan, J., Qian, H., Dong, C., Shi, Y., Zhou, X., and Wu, C., 2018. Personal exposure measurements of school-children to fine particulate matter (PM2.5) in winter of 2013, Shanghai, China. *PLOS ONE*, 13 (4), e0193586.

Zhang, S.H., Akutsu, Y., Russell, L.M., Flagan, R.C., and Seinfeld, J.H., 1995. Radial differential mobility analyzer. *Aerosol Science and Technology*, 23 (3), 357–372.

Zhang, Y., Banerjee, S., Yang, R., Lungu, C., and Ramachandran, G., 2009. Bayesian Modeling of Exposure and Airflow Using Two-Zone Models. *The Annals of Occupational Hygiene*, 53 (4), 409–424.

Zhao, J., Weinhold, K., Merkel, M., Kecorius, S., Schmidt, A., Schlecht, S., Tuch, T., Wehner, B., Birmili, W., and Wiedensohler, A., 2018. Concept of high quality simultaneous measurements of the indoor and outdoor aerosol to determine the exposure to fine and ultrafine particles in private homes. *Gefahrstoffe - Reinhaltung der Luft*, 78 (3), 73–78.

Ziemann, C., Escrig, A., Bonvicini, G., Ibanez, M.J., Monfort, E., Salomoni, A., and Creutzenberg, O., 2017. Organosilane-Based Coating of Quartz Species from the Traditional Ceramics Industry: Evidence of Hazard Reduction Using In Vitro and In Vivo Tests. *Annals of work exposures and health*, 61 (4), 468–480.

Glossary

Annex

ANNEX A. GLOSSARY, ACRONYMS AND SYMBOLS

Glossary

Background (BG) and pre-activity: it refers to temporal background concentrations usually measured before and/or after the process of study.

Breathing zone (BZ): measurements next to worker at height of the nose and mouth of the worker.

Coarse particles: particles > 2.5 µm.

Control banding: approach based on "computational" hazard and exposure for the control of workplace exposure.

Dustiness: measure of the tendency of a powdered material to release particles in response to a mechanical or aerodynamic stimulus.

d_{50}: median diameter (50th percentile).

dlaser: diameter of a sphere of same diameter as the cross-sectional area of the particle µm.

dstockes: diameter of a sphere of same diameter as the cross-sectional projection area of the particle µm.

Emission rate: amount of particles (mass or particle number) released by a process per unit of time.

Fine particles: particles between 0.1 and 2.5 µm.

Indoor: refers to spatial background concentrations measured during the process at a point where process particles do not affect measurements but at the same times representative of the space where the process is taking place.

Inhalable: mass fraction of total airborne particles which is inhaled through the nose and mouth It has 100% penetration for small particles (< 10 µm), dropping to 50% for 100 µm particles and has no median cut-off aerodynamic diameter.

Alveolar macrophages: specialized cells of the immune system (located in the lung alveoli) involved in detection, phagocytosis and destruction of anything that does not have the type of proteins specific to healthy body cells on its surface (e.g. cellular debris, small particles, bacteria or cancer cells). They initiate inflammation by releasing cytokines (molecules that activate other cells).

Mass-balance models: models based on a set of mass balance equations including information of the source (contaminant generation), particle transport, deposition and coagulation.

nanoGEM approach:
Mean concentration $> BG \pm 3 \cdot (\sigma BG)$; described in Asbach et al., 2012.

Nanomaterial: natural, incidental or manufactured material containing particles, in an unbound state or as an aggregate or agglomerate and where, for 50 % or more of the particles in the number size distribution, one or more external dimensions is in the size range 1 nm-100 nm.

Nanoparticles (NP): particles < 100 nm according to nanotechnology field classification.

Nucleation: particle formation from gaseous precursors.

Outdoor: refers to measurements conducted outdoors next to the industrial unit entrance through which outdoor infiltration occur.

PM_{10}: describes inhalable particles, with diameters that are generally 10 µm and smaller.

$PM_{2.5}$: particulate matter with diameters generally 2.5 μm and smaller.

Respirable: mass fraction of inhaled particles penetrating to the unciliated airways with a median aerodynamic diameter of 4.25 μm and 1.5 GSD.

Risk assessment tools: empirical models, based on dimensionless exposure modifying factors to calculate an exposure score which is further converted to an exposure value by using calibration factors.

Silicosis: occupational illness which is a form of pneumoconiosis (fibrogenic lung disease) caused by inhalation of crystalline silica dust, and is marked by inflammation and scarring in forms of nodular lesions in the upper lobes of the lungs.

Thoracic: mass fraction of inhaled particles penetrating beyond the larynx. The curve has a median diameter of 11.64 μm and geometric standard deviation (GSD) of 1.5.

Tiered approach: assessment strategy for the determination of exposure to nanoparticles in workplaces which consists of several hierarchical tiers.

UFP: Ultrafine particles; particles < 100 nm according to aerosol research field classification.

Worker Area (WA): measurements on a similar distance and position similar to where the worker is standing. The location can be considered representative of worker exposure but not be considered strictly breathing zone.

Acronyms

ACGIH: American Conference of Governmental Industrial Hygienists

ACH: Air Changes per Hour

AER: Air Exchange Ratio

Ag: Silver

Al_2O_3: Aluminium oxide

APS: Atmospheric Plasma Spraying

AR: Aspect Ratio

ARIMA: Autoregressive Integrated Moving Average

ART: the Advanced Reach Tool

Au: Gold

BAuA: Bundesanstalt für Arbeitsschutz und Arbeitsmedizin "Federal Institute for Occupational Safety and Health"

BET: Brunauer–Emmett–Teller theory

BG: Background

BZ: Breathing zone

CCOHS: Canadian Centre for Occupational Health and Safety

C.D: Continuous Drop dustiness

CEN: European Committee for Standardization

CPC: Condensation Particle Counter

CNT: Carbon nanotubes

DiSCmini: Diffusion Size Classifier miniature

DNEL: Derived No-Effect Level

DMA: Differential Mobility Analyser

ECHA: European Chemical Agency

EDX: Energy Dispersive X-ray

EEA: European Environmental Agency

EN: European Norm

ENP: Engineered Nanoparticles

ER: Emission Rate

FF: Far-Field

GSD: Geometrical Standard Deviation

Grimm mini-LAS: Grimm mini Laser Aerosol Spectrometer

H: Energy factor

HEPA: High Efficiency Particulate Filter

HR: Hausner Ratio

H_2SO_4: Sulfuric acid

HVOF: High Velocity Oxy-Fuel coating spraying

ICRP: International Commission on Radiological Protection

IFA: Institut für Arbeitsschutz der Deutschen Gesetzlichen Unfallversicherung "Institute for Occupational Safety and Health of the German Social Accident Insurance"

IGF: Institut für Gefahrstoff-Forschung "Institute for the Research on Hazardous Substances"

INSHT: Instituto Nacional de Seguridad e Higiene en el Trabajo

ISO: International Organization for Standardization

ITC: Instituto de Tecnología Cerámica "Institute of Ceramic Technology"

LC: Local Controls

LDSA: Lung Deposited Surface Area

LEV: Local Exhaust Ventilation

MAK: Maximum workplace concentrations

MNs: Manufactured Nanomaterials

NF: Near-Field

NH_3: Ammonia

NIOSH: National Institute for Occupational Safety and Health

NOx: Nitrogen Oxides

NP: Nanoparticles

NRCWE: National Research Center for the Working Environment

NRV: Nano-Reference Values

OECD: Organisation for Economic Co-operation and Development

OEL: Occupational Exposure Limits

OPC: Optical Particle Counter

OPS: Optical particle Sizer

PEL: Permissible Exposure Limits

PGNP: process-generated nanoparticles

PM: Particulate Matter

PPE: Personal Protection Equipment

PSD: Particle Size Distribution

PVC: Polyvinyl chloride

RCS: Respirable Crystalline Silica

R.D: Rotating Drum dustiness

REACH: Registration, Evaluation, Authorization and Restriction of Chemicals

REL: Recommended Exposure Limit

RMSLE: Root Mean Squared Logarithmic Error

SEM: Scanning Electron Microscopy

SER: Social Economic Council of the Netherland

SiO_2: Silicon dioxide

SMPS: Scanning Mobility Particle Sizer

SSA: Specific Surface Area

TEM: Transmission Electron Microscopy

TiO_2: Titanium dioxide

TLV: Threshold Limit Values

TNO: Nederlandse Organisatie voor Toegepast Natuurwetenschappelijk Onderzoek "Netherlands Organisation for Applied Scientific Research"

TSP: Total Suspended Particles

UFP: Ultrafine particles

UNE: Una Norma Española

US-OSHA: United States - Occupational Safety and Health Administration

VOCs: Volatile Organic Compounds

WA: Worker Area

WHO: World Health Organization

W_I: Dustiness inhalable fraction

W_R: Dustiness respirable fraction

8h TWA: 8-hours' time weighted average

Symbols in equations

ACH: Air changes per hour (h^{-1})

C_n: concentration during a specific operation

C_o: initial and incoming concentration (N: cm^{-3} or M: $\mu g\ m^3$)

C_{NF}: near field concentrations (N: cm^{-3} or M: $\mu g\ m^3$)

C_{FF}: far field concentrations (N: cm^{-3} or M: $\mu g\ m^3$)

$\bar{C}$: mean concentration (cm^{-3})

Cc: slip correction factor

Db: mobility diameter

D_I: respirable or inhalable dustiness index of a material (mg kg^{-1} or particles kg^{-1})

dM/dt: mass flow of the process (kg min^{-1})

H: handling energy factor (-)

LC: protection factor of localized controls (-)

M: mass concentration ($\mu g\ m^{-3}$).

N: number concentration (cm^{-3}).

N_{BG}: background particle concentration

Q: flow ($m^3\ h^{-1}$)

Q_{LC}: local control flow ($m^3\ h^{-1}$)

S and S_N: Emission source or emission rate in particle concentration per time unit (mg or particles min^{-1})

s: air speed ($m\ s^{-1}$)

SSA: specific surface area of the nanomaterial ($m^2\ g^{-1}$)

t_n: time (usually min)

V: volume (m^3)

V_{NF}: near-field volume (m^3)

V_{FF}: far-field volume (m^3)

Ø: diameter

β: flow rate between near-field and far-field ($m^3\ min^{-1}$)

γ: total particle decay rate (min^{-1})

δ: scattering parameter for air (0.905)

δ_{nano}: specific density of the nanomaterial (g cm^{-3})

ε_C: protection factor due to enclosure (-)

λ: ventilation rate (min^{-1})

λ_{air}: mean free path for air (0.066 μm)

ρ_{eff} : effective density (g cm^{-3})

σ: standard deviation

Supplementary Materials

Annex B

ANNEX B. Supplementary materials

1. Supporting Information Publication I: On the relationship between exposure to particles and dustiness during handling of powders in industrial settings

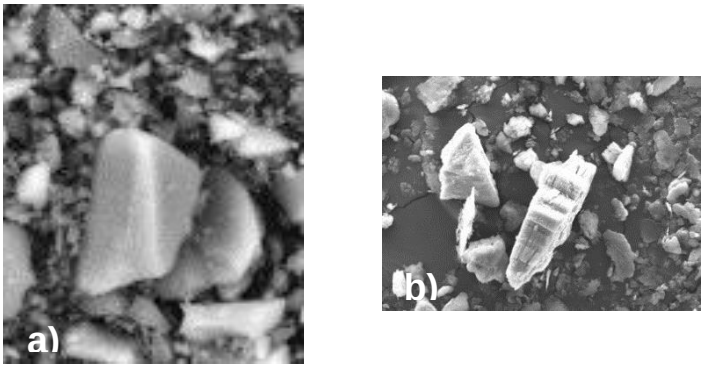

Figure S1 Micrographs of the original materials. (a) Q2 and (b) K1.

Method

Rotating drum

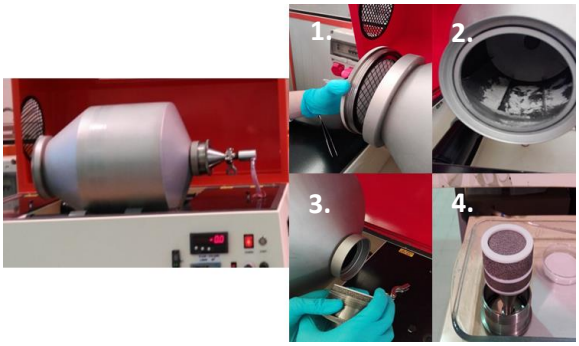

1. Inlet
2. Dust generation section (drum)
3. Dust collection
4. Foams and filter

Continuous drop

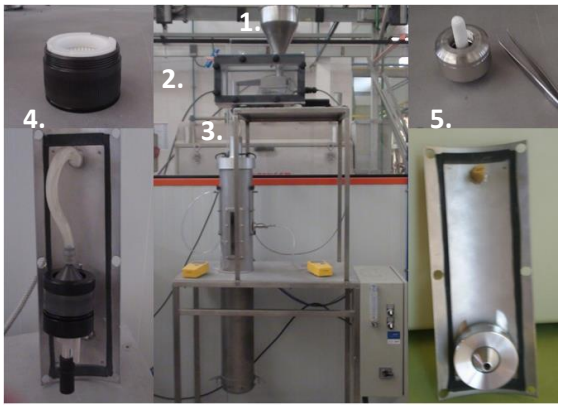

1. Sample tank
2. Metering device
3. Drop pipe
4. Sampling head for the respirable aerosol fraction
5. Sampling head the inhalable aerosol fraction

Figure S2 Pictures and description of the dustiness methods used, rotating drum and continuous drop.

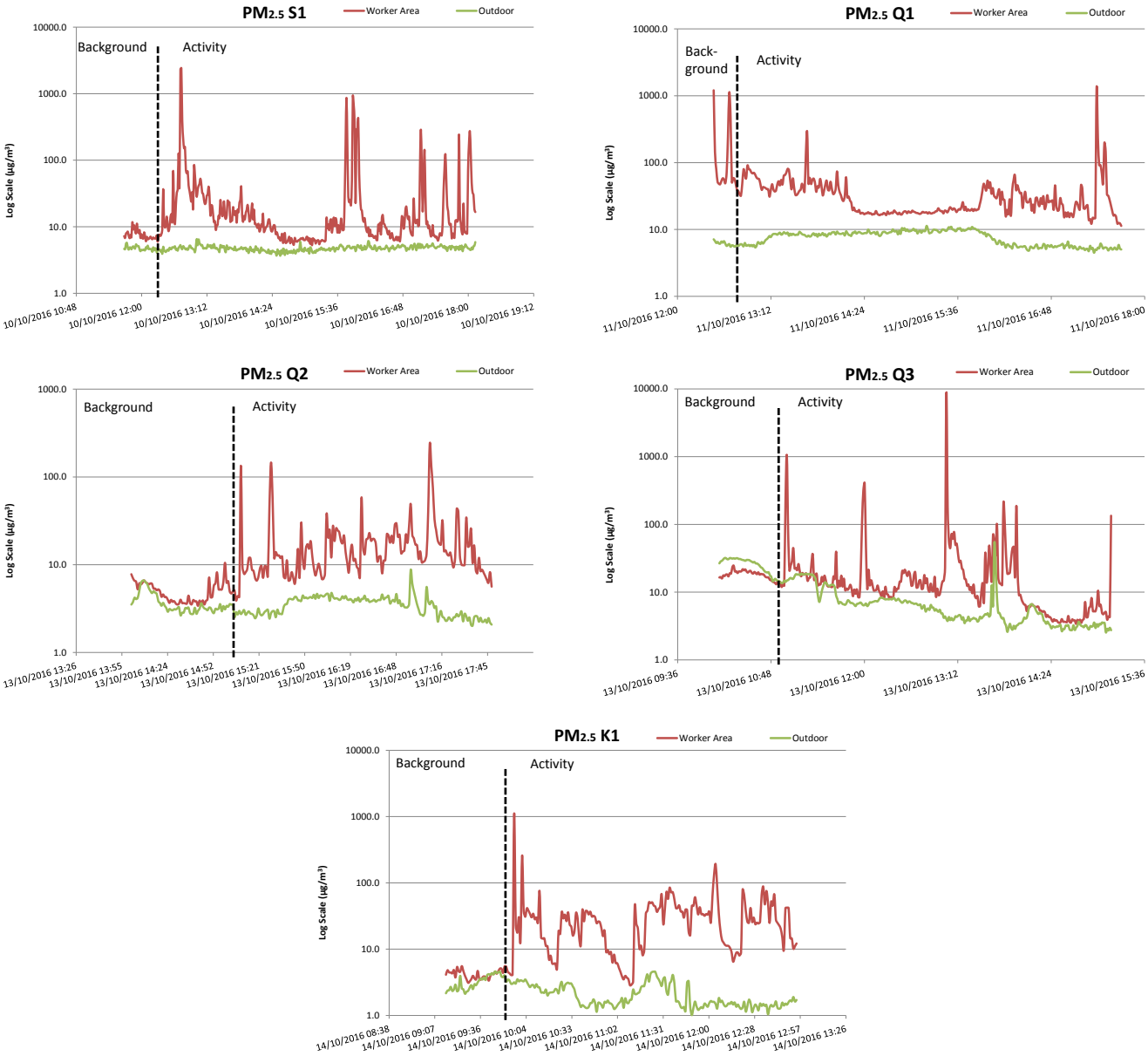

Figure S3 Time series of $PM_{2.5}$ in terms of µg/m^3 monitored with Grimm on the worker area and the outdoor measurement points for the materials S1, Q1, Q2, Q3 and K1. Note that the Y axis is in log scale. Worker Area is represented in red and outdoor in green. Background and activity periods are divided with a dotted black line.

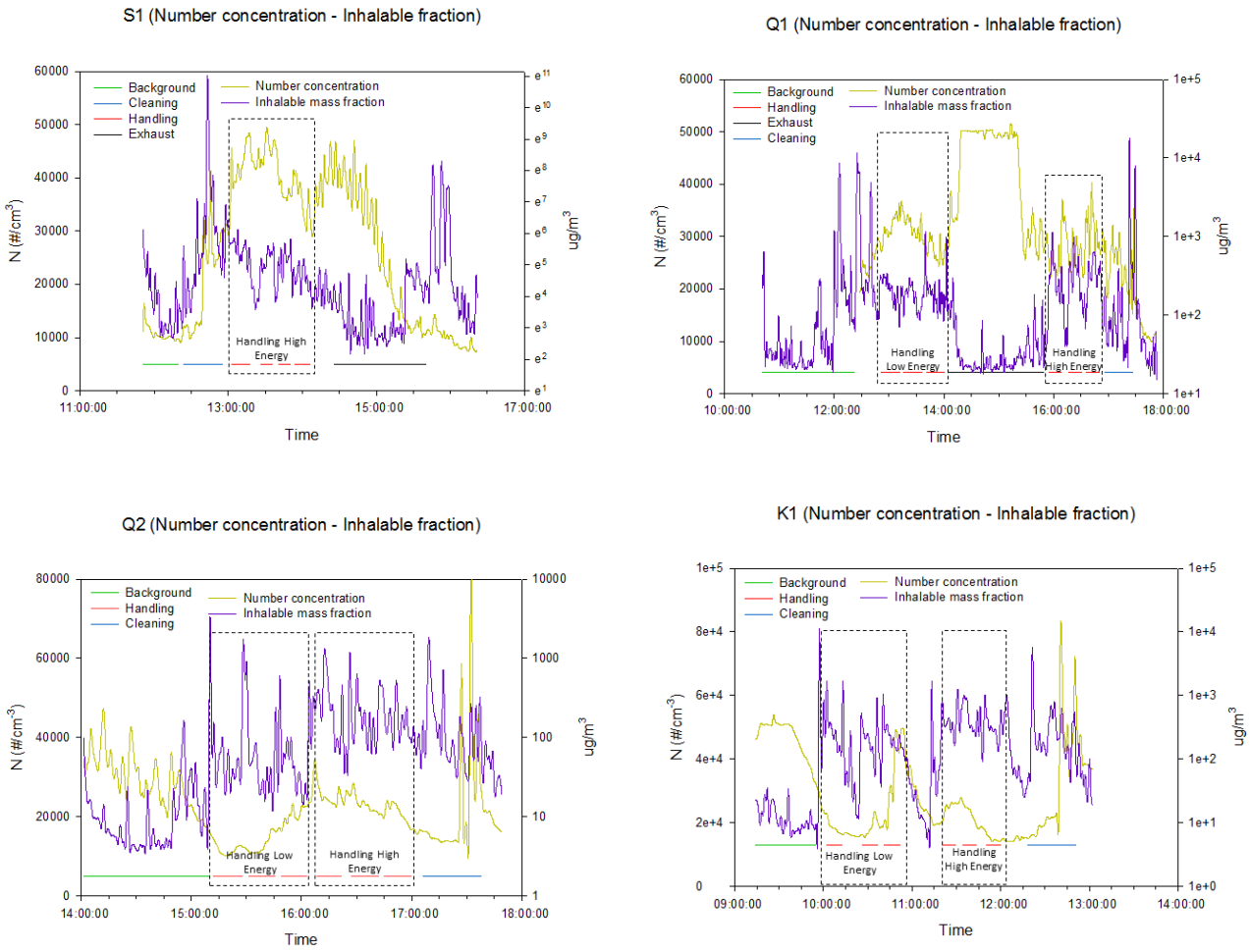

Figure S4 Time series of particle number concentration (monitored with CPC) and inhalable mass fraction in log scale (monitored with Grimm) for S1, Q1, Q2 and K1 materials. Background, exhaust, cleaning and handling repetitions for low and high energy settings are marked with colour bars at the bottom of the each graph (green, black, blue and red respectively). The three first red lines correspond to low energy settings and the last three ones to the high energy settings.

Potential mitigation strategies – Case study

The general room air extraction system was tested as a potential mitigation measure. Particle number and mass concentrations were then monitored. The extraction system was used three of the four days of the sampling campaign during approximately one hour during midday, when no other processes were ongoing. Figures 2 and S3 show that during when the air extraction system of the room was ON there was reduction of the inhalable mass fraction (coarse particles) as well as the respirable fraction. Other studies such as Cena and Peters, (2011); Douwes et al. (2017) and Jensen et al. (2015) also pointed out the relevance of the exhaust ventilation system on the removal of particles, although they used a local exhaust system. Contrarily, ultrafine particle concentrations during the time when the room air extraction system was ON did not decrease, and they even

increased during one day (when Q1 material was assessed, Figure 2 and Figure S1). Mean and maximum particle number concentrations during the time when room extraction system was ON were 42686 and 51461 #/cm^3, respectively. Figure S1 shows the particle size distribution in the worker area for materials S1 and Q1. In both cases the highest concentrations for particles in the range 20 – 50 nm were reached during the time when the air extraction system was ON. For the first day (10/10/2016 – S1 material) the increasing trend in nanoparticles concentration started minutes before the extraction system was switched ON, while for the second day (11/10/2016 – Q1) the increase in nanoparticles concentration was produced during the air extraction system period. The particle size range monitored, from 20 to 50 nm, points to outdoor road traffic emissions as the source of these particles, as this is the typical size range of these emissions (Brines et al., 2015) and the main door of the plant was open all the time during the tests. Therefore, the air extraction system showed a clear decrease in coarse particle concentrations, but did not favour ultrafine particle reduction.

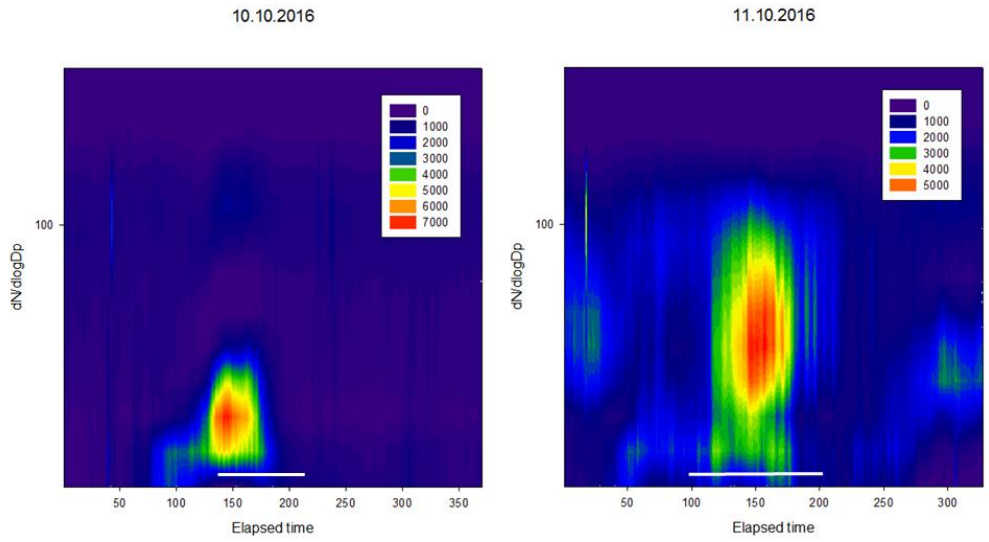

Figure S5 Particle size distribution (particle range from 10 to 420 nm) measured with the NanoScan for two of the sampling days 10/10/2016 and 11/10/2016, corresponding to materials S1 and Q1 respectively. Extraction system periods are marked with a white line under. Note that the particle number concentration colour scale is different for each graph.

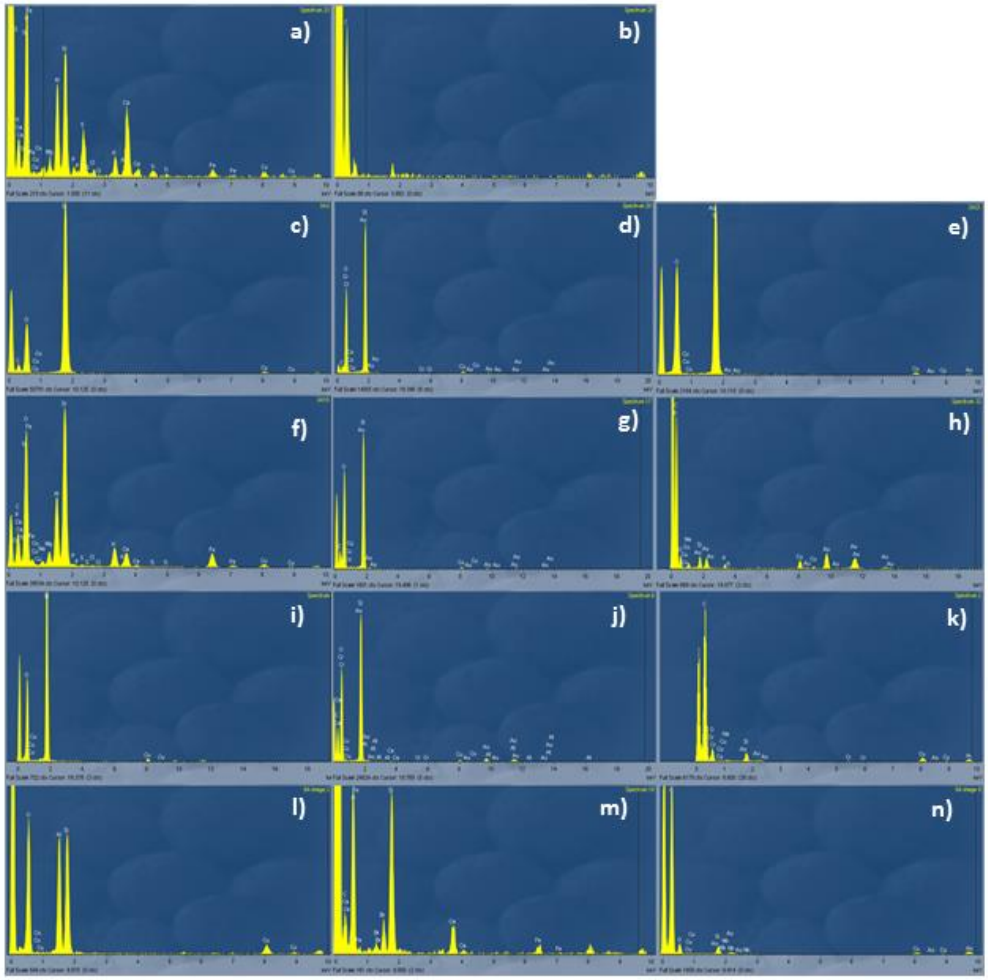

Figure S6 EDX spectrum analysis for TEM images presented in figure 7. EDX images correspond a) to 7a; b) to 7b and 7c; c) to 7d; d) to 7e; e) to 7f; f) to 7g; g) to 7h; h) to 7i; i) to 7j; j) to 7k; k) to 7l; l) to 7m; m) to 7n; n) to 7o.

Table S1 Materials chemical composition. Note: sand chemical composition was proportioned by the supplier.

Material	S1	Q1	Q2	Q3	K1
LOI 1050°C	NDA	0.3	0.63	0.40	12.8
SiO_2	32	99	98.4	99.6	49.1
Al_2O_3	NDA	0.60	0.80	0.02	36.7
TiO_2	NDA	0.03	0.06	0.01	0.11
Fe_2O_3	NDA	0.03	0.04	0.01	0.42
CaO	NDA	0.08	0.09	0.01	0.11
MgO	NDA	0.01	0.02	< 0.01	0.09
K_2O	NDA	0.1	0.07	0.01	0.59
Na_2O	NDA	0.01	< 0.01	< 0.01	0.03
ZrO_2	65	-			-

Table S2 TWA results for all materials and for inhalable and respirable mass fractions. For each material, temporal background concentrations, handling under low energy settings and handling under high energy settings are used for the calculation. TWA xh (µg/m^3): worker exposure during all the measurements period including temporal background, handling under low energy and under high energy settings. Note there are different sampling periods for each material. TWA 8h (µg/m^3): worker exposure using the temporal background concentrations to complete the 8h TWA. Limit values: inhalable 10000 µg/m^3 and respirable 3000 µg/m^3. Equation used:

$$TWA = \frac{t_1.c_1 + t_2.c_2 + \cdots t_n.c_n}{t_1 + t_2 + \cdots t_n}$$

where: c_n is the mean concentration during a specific operation and t_n is the time of the specific operation.

Material	**S1**		**Q1**		**Q2**		**Q3**		**K1**	
TWA_{xh} / TWA_{8h}	**$TWA_{2.5h}$** (µg/m^3)	**TWA_{8h}** (µg/m^3)	**$TWA_{4.1h}$** (µg/m^3)	**TWA_{8h}** (µg/m^3)	**$TWA_{3.5h}$** (µg/m^3)	**TWA_{8h}** (µg/m^3)	**$TWA_{3.6h}$** (µg/m^3)	**TWA_{8h}** (µg/m^3)	**TWA_{3h}** (µg/m^3)	**TWA_{8h}** (µg/m^3)
Inhalable fraction	591.4	256.5	242.2	152.8	134.4	67.4	626.2	295.6	267.9	107.5
Respirable fraction	106.9	42.6	56.9	39.4	24.3	14.0	139.7	72.8	51.6	22.6

Table S3 Mean particle number and mass concentration (inhalable and respirable fraction) in the worker area during cleaning operations for each material and their respective background concentrations. Statistically significant differences found after applying the exposure > 3σ+BG are marked in bold.

Material	Number concentration		Inhalable mass		Respirable mass	
	Background	Cleaning	Background	Cleaning	Background	Cleaning
S1	10620 (9179-16431)	9869 (7615-12995)	92.1 (14.6-1168.3)	33.2 (15.2-74.8)	11.0 (7.7-20.1)	12.5 (8.5-20.6)
Q1	42686 (25420-51461)	24176 (17865-35288)	39.6 (19.0-300.0	**624.1 (26.4-13824.2)**	22.2 (17.3-91.1)	**123.8 (15.0-2384.3)**
Q2	29226 (16645-47210)	22153 (13591-81248)	15.2 (3.8-135.1)	**205.3 (31.8-1672.8)**	5.9 (3.6-15.7)	**52.7 (14.2-427.7)**
Q3	33064 (24959-43430)	42131 (30647-64444)	34.1 (15.0-343.6)	**662.1 (43.5-8008.8)**	19.9 (13.1-32.7)	**83.0 (20.4-315.3)**
K1	46421 (30470-53894)	31131 (15048-77386)	13.0 (5.8-34.7)	**419.0 (40.9-5192.5)**	5.5 (4.0-8.0)	**76.4 (13.7-365.4)**

2. Supplementary material Publication II: Health risk assessment from exposure to particles during packing in working environments

Figure S1 Packing lines images.

Method

Continuous drop

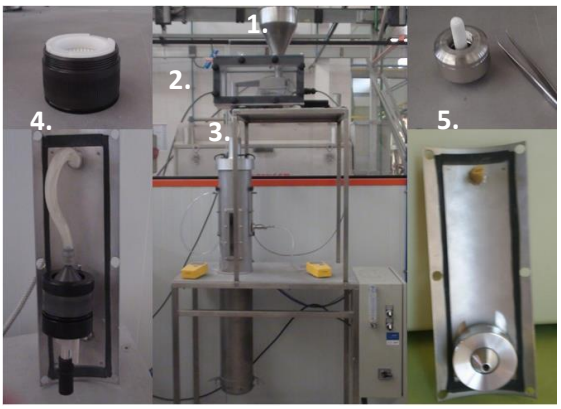

1. Sample tank
2. Metering device
3. Drop pipe
4. Sampling head for the respirable aerosol fraction
5. Sampling head the inhalable aerosol fraction

Figure S2 Pictures and description of the continuous drop dustiness method used for dustiness determination.

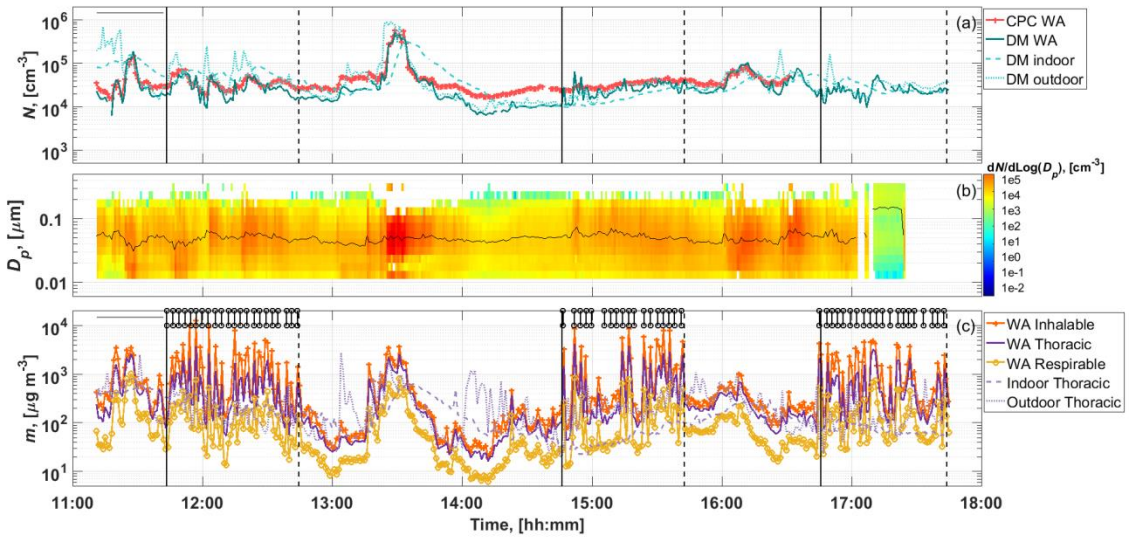

Figure S3 Particle concentration at the (WA) during packing of Clay 1: (a) particle number concentration time series (CPC and DM; DiSCmini); (b) particle size distribution time series measured with the NanoScan, solid black line shows NanoScan d_{50}; (c) mass concentration time series measured by Grimm mini-LAS. Black vertical lines indicate start (solid line) and stop (dashed line) of the each batch.

During packing of Clay 1, total particle number concentration measured with the CPC (34535-37898 cm^{-3}) was similar to pre-activity concentrations (42410±32660 cm^{-3}). The same was true for the respirable mass fraction (144-166 μg m^{-3} during packing vs. 212±260 μg m^{-3} during background). Contrarily, the inhalable mass fraction was higher (1370-1847 μg m^{-3}) than pre-activity concentrations (986±1000 μg m^{-3}) with increases between 384 and 861 μg m^{-3} although they were not statistically significant. Clear peaks can be identified for each bag being packed which coincide approximately with the start of the pouring process. Breathing zone and worker area respirable dust concentrations were 101 μg m^{-3} and 182 μg m^{-3} respectively. Particle mean dimeter (NanoScan) during packing was 50.8-55.9 nm.

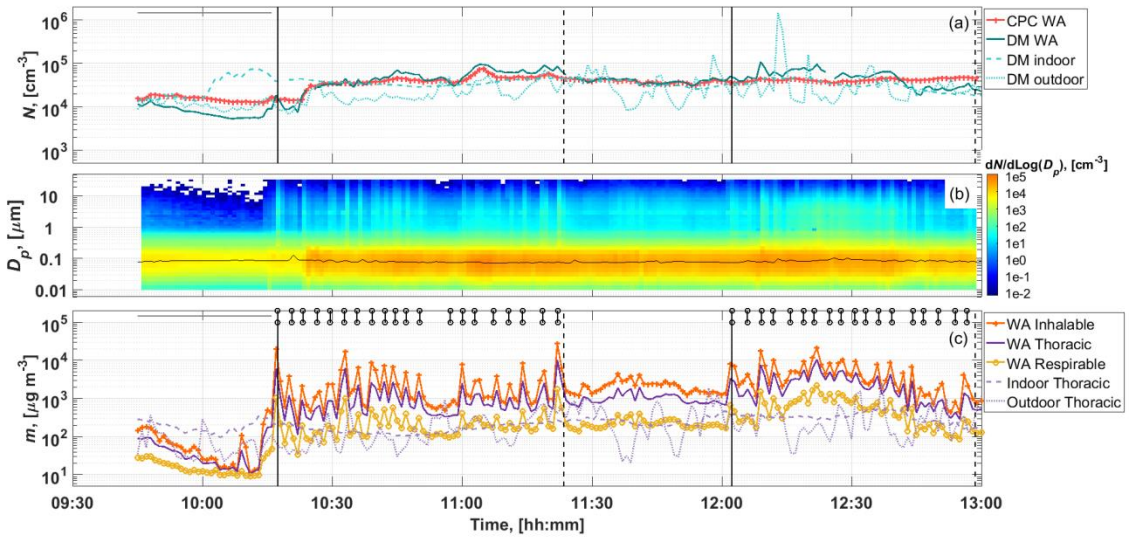

Figure S4 Particle concentration at the WA during packing of Kaolin 1: (a) particle number concentration time series (CPC and DM; DiSCmini); (b) particle size distribution time series measured with the MiniWras, solid black line shows MiniWras d_{50}; (c) mass concentration time series measured by Grimm mini-LAS. Black vertical lines indicate start (solid line) and stop (dashed line) of the each batch.

During packing of Kaolin 1, total particle number concentration measured with the CPC (40565-42331 cm^{-3}) was significantly higher than pre-activity concentrations (15721±2185 cm^{-3}). Inhalable (2647-4705 μg m^{-3}) and respirable (242-609 μg m^{-3}) mass fractions were also significantly higher than pre-activity concentrations (92±114 and 18±9 μg m^{-3} for inhalable and respirable mass fractions) with increases of 2554-4613 and 224-591 μg m^{-3} for the inhalable and respirable fractions. Peaks of particles around 5 μm at the start of each bag being pack are easily recognizable which coincide with the action of manually place the pallet in the packing area. Breathing zone and worker area respirable dust concentrations were 36 μg m^{-3} and 321 μg m^{-3} respectively. Mean particle dimeter (MiniWras) during packing was 79.7-86.5 nm.

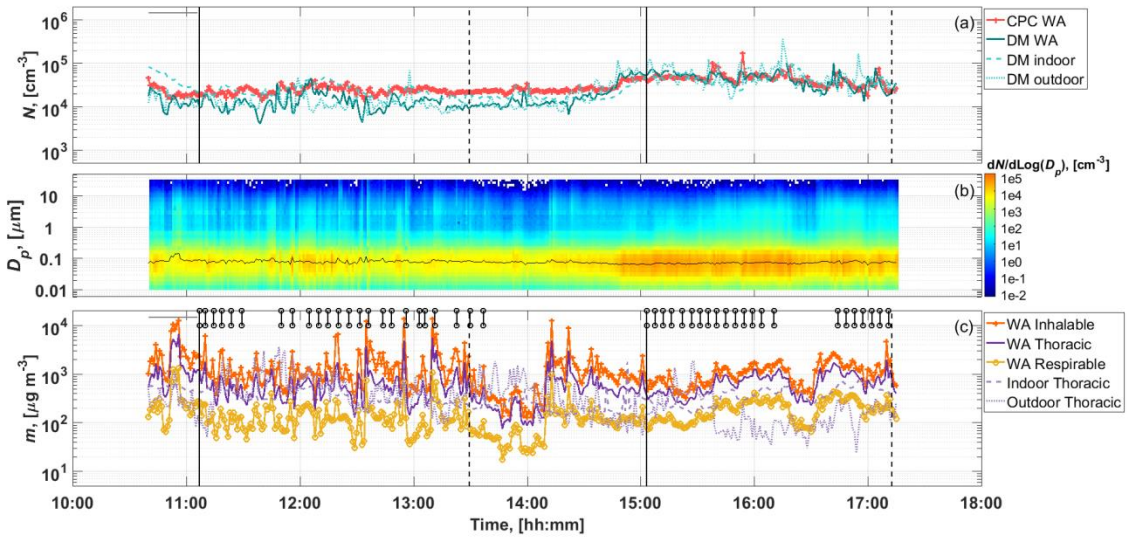

Figure S5 Particle concentration at the WA during packing of Quartz 1: (a) particle number concentration time series (CPC and DM; DiSCmini); (b) particle size distribution time series measured with the MiniWras, solid black line shows MiniWras d_{50}; (c) mass concentration time series measured by Grimm mini-LAS. Black vertical lines indicate start (solid line) and stop (dashed line) of the each batch.

During packing of Quartz 1, total particle number concentration measured with the CPC suffered a statistically significant increase during packing of batch 2 (46670±17666 cm^{-3}) compared to pre-activity (23291±6988 cm^{-3}) contrarily to what happened during batch 3 in which particle number concentrations remained the same (24755±4862 cm^{-3}). No increases of respirable (153-209 μg m^{-3}) and inhalable (1150-1714 μg m^{-3}) particle mass were observed during packing compared to pre-activity concentrations (353±351 μg m^{-3} for respirable and 3529±3324 μg m^{-3} for inhalable) although peaks can be identified at the beginning of some bags being packed. The fact that not significant increases were detected is mostly because before the packing process, maintenance processes were carried out, and even though a period between maintenance processes and packing was left, was not enough for concentrations to stabilize. If we compare inhalable mass fraction in the WA and indoor, 1432 μg m^{-3} in the WA vs. 851 μg m^{-3} indoor clear influence in mass concentrations in the WA due to packing are detected.

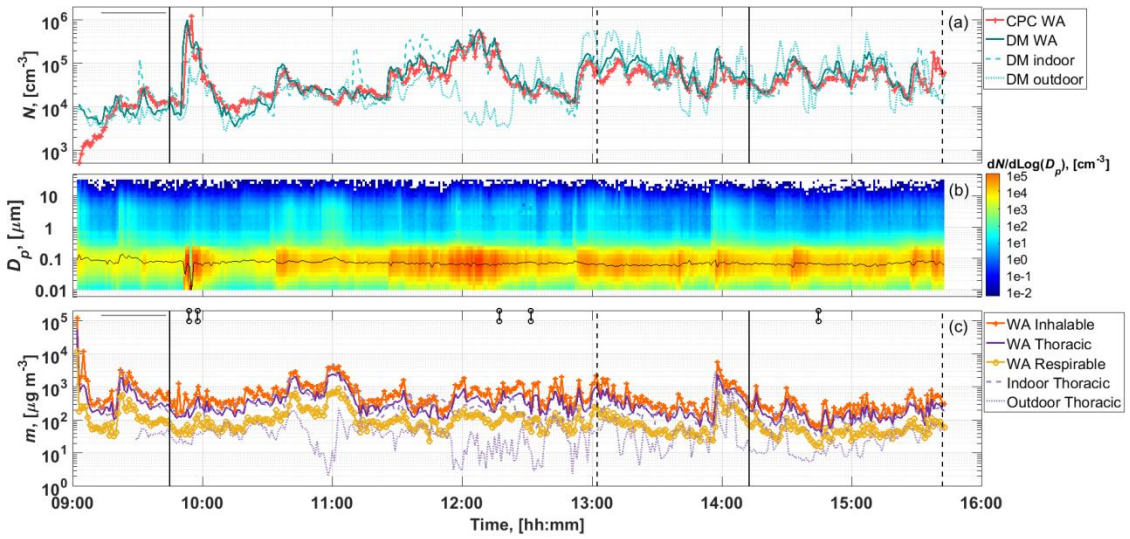

Figure S6 Particle concentration at the WA during packing of Kaolin 2: (a) particle number concentration time series (CPC and DM; DiSCmini); (b) particle size distribution time series measured with the MiniWras, solid black line shows MiniWras d_{50}; (c) mass concentration time series measured by Grimm mini-LAS. Black vertical lines indicate start (solid line) and stop (dashed line) of the each batch.

During packing of Kaolin 2 statistically significant increases of particle number concentration were monitored (54292-71996 cm-3) when comparing with pre-activity concentrations (9567±7230 cm^{-3}). However, this increase was due to outdoor and indoor influences (diesel forklifts activity). No increases on particle mass concentrations were also observed.

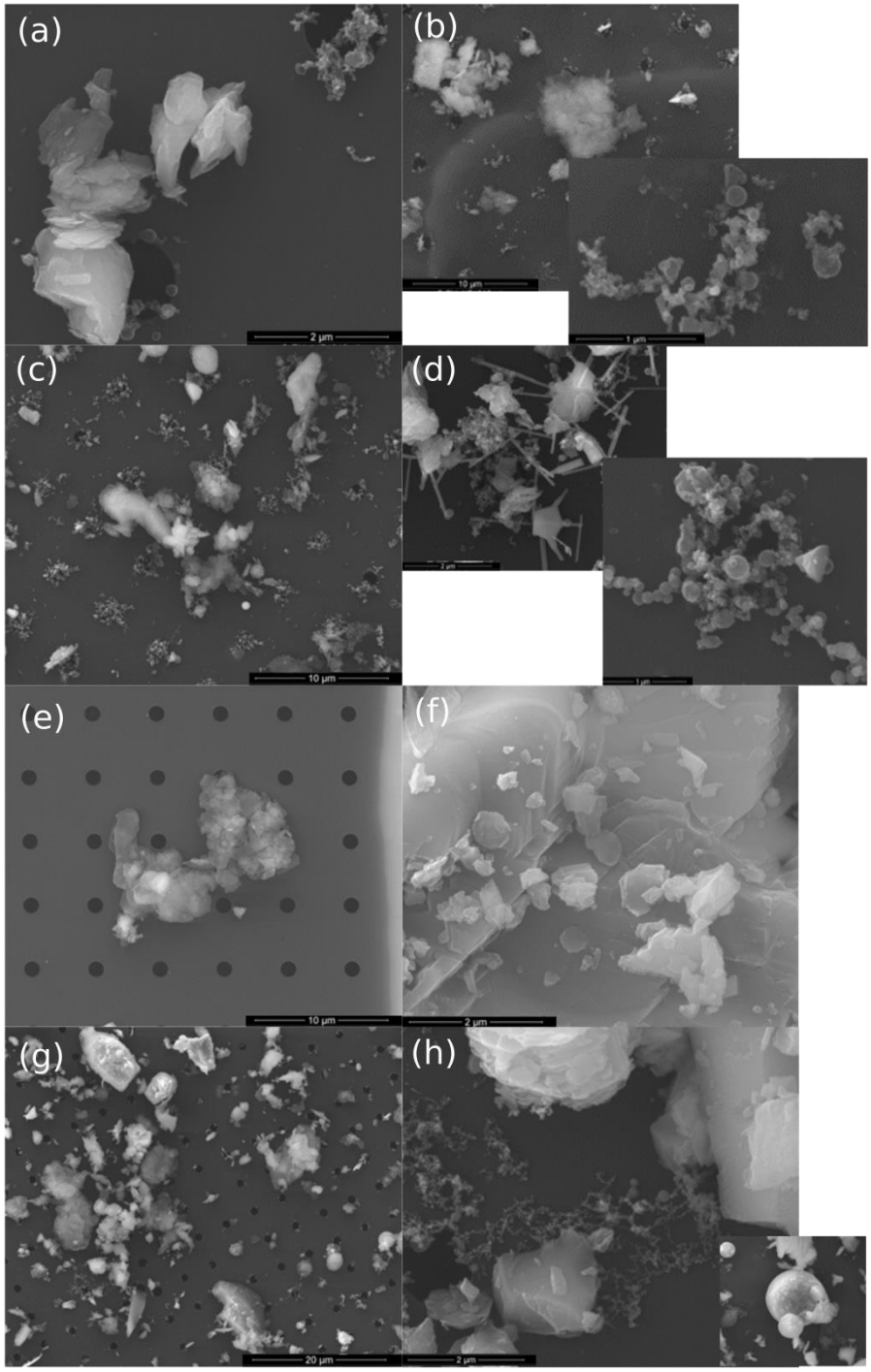

Figure S7 SEM images from particles collected in the worker area during materials packing.

Table S1 Materials particle size distribution and chemical composition. PSD: particle size distribution. L.O.I: loss of ignition.

Material	PSD			Chemical analysis (%)									
	d_{10} (µm)	d_{50} (µm)	d_{90} (µm)	SiO_2	Al_2O_3	Fe_2O_3	TiO_2	K_2O	MgO	Na_2O	CaO	Li_2O	L.O.I
Clay 1	3	13	56	64	26	0.8	0.75	1.4	0.2	0.15	0.2	-	7
Feldspar 1	4-5	31-39	101-117	69	17-18	0.1-0.2	0.02	10-11	0.04	2.2-2.4	0.4	-	0.4
Quartz 1	4-5	30-38	100-116	99	0.8-0.9	0.04-0.08	0.05-0.07	0.1	0.02	0.02	0.1	-	0.3
Clay 2	2	10	43	57	31	0.9	0.8	1.3	0.2	0.3	0.2	-	9
Kaolin 1	3	13	46	51	35	0.7	0.3	0.6	0.2	0.05	0.1	-	12
Feldspar 2	4	22	65	73	17	≤0.2	≤0.1	3	0.1	4	0.4	≥0.7	0.9
Kaolin 2	3	8	26	51	35	<0.7	<0.5	0.5	<0.2	<0.2	<0.3	-	13

Table S2 Intercomparison results.*Low degree of agreements between CPC and MW is due to differences in the measurement ranges and technics.

Number (CPC as Reference)		Mass Concentration (MiniWras as Reference)	
Instrument	2d-R^2	Instrument	1d-Thoracic R^2
MD1	0.78	Grimm 1	0.93
MD2	0.73	Grimm N	0.80
MD3	0.73	Grimm V	0.82
MD4	0.79	-	-
MW	0.41*	-	-

Table S3 Mean particle number concentrations (cm^{-3}), size (nm), lung deposited surface area (µm cm^{-2}) (DiSCmini) and mean inhalable, thoracic and respirable mass (µg m^3) in the worker area, indoor and outdoor locations for each day. Means were calculated considering the two/three batches. WA: worker area. LDSA: lung deposited surface area.

Sampling		DiSCmini			Mini-LAS (µg m^3)		
		N_{TOT} (cm^{-3})	Size (nm)	LDSA (µm cm^{-2})	Inhalable	Thoracic	Respirable
Clay 1_L Day 1	WA	27564	39	59	1638	709	157
	Indoor	34189	42	78	267	125	19
	Outdoor	40605	36	80	215	23	7
Feldspar 1_M Day 2	WA	40053	52.5	103.6	2447	1519	322
	Indoor	50546	45	123	1772	1400	382
	Outdoor	30776	41	70	1080	77	15
Quartz 1_M Day 3	WA	29746	37	58	1432	713	181
	Indoor	33934	40	70	851	391	52
	Outdoor	35961	40	61	431	55	10
Clay 2_L Day 4	WA	23558	43	56	1524	619	135
	Indoor	19113	46	49	285	239	96
	Outdoor	28643	37	57	301	36	16
Kaolin 1_L Day 5	WA	48424	41	108	3676	1838	425
	Indoor	35016	44	84	589	272	48
	Outdoor	47618	40	70	317	40	17
Feldspar 2_H Day 6	WA	21784	57	63	2919	1751	495
	Indoor	27615	48	63	1090	465	66
	Outdoor	25541	41	54	1090	465	66
Kaolin 2_H Day 7	WA	81257	32	124	567	323	96
	Indoor	68377	34	113	372	304	112
	Outdoor	57085	35	78	40	27	8

Table S4 Quartz 1 respirable crystalline silica results for the dustiness test

Sample	Mass (µg)		RCS (%)
	Total	Quartz	
Filter 1	940	915	97
Filter 2	470	475	100

Annex A: ARIMA models analysis

ARIMA models analysis and its results are presented here. Only two cases of the ARIMA analysis performed are shown due to space reasons. One example of an ARIMA disagreeing with the other tests used (nanoGEM, t test and MW "U" test) and one agreeing is shown.

Case 1) Feldspar 2 inhalable fraction concentration.

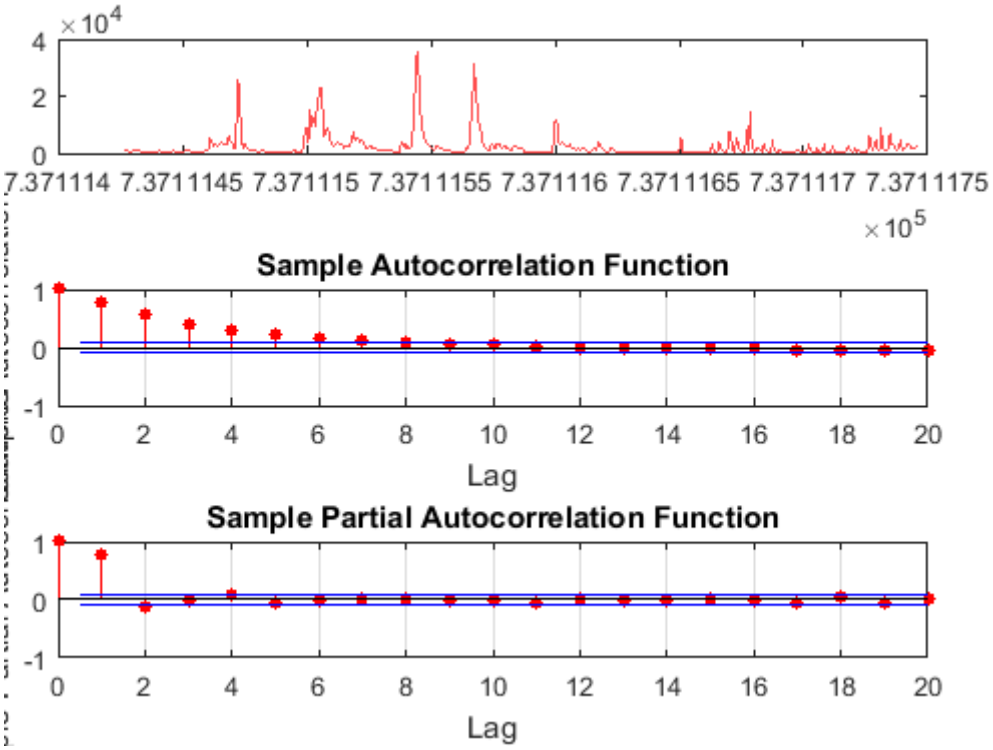

ARIMA model used was (1,0,0)

Parameter	Value	Standard Error	t Statistic
Intercept	642.86	4527.3	0.141996
AR{1}	0.773193	0.0155994	49.5654
Beta1	1881.05	4372.37	0.430214
Variance	7.47912e+06	192236	38.9059

Beta1 is < 1.95 therefore concentrations during process are not significantly higher than concentrations during pre-activity.

This result differ from the ones obtained by using the nanoGEM approach, the t test and the MW "U" test which conclude that concentrations during packing are significantly higher than pre-activity.

Case 2) Kaolin 1 inhalable fraction concentration.

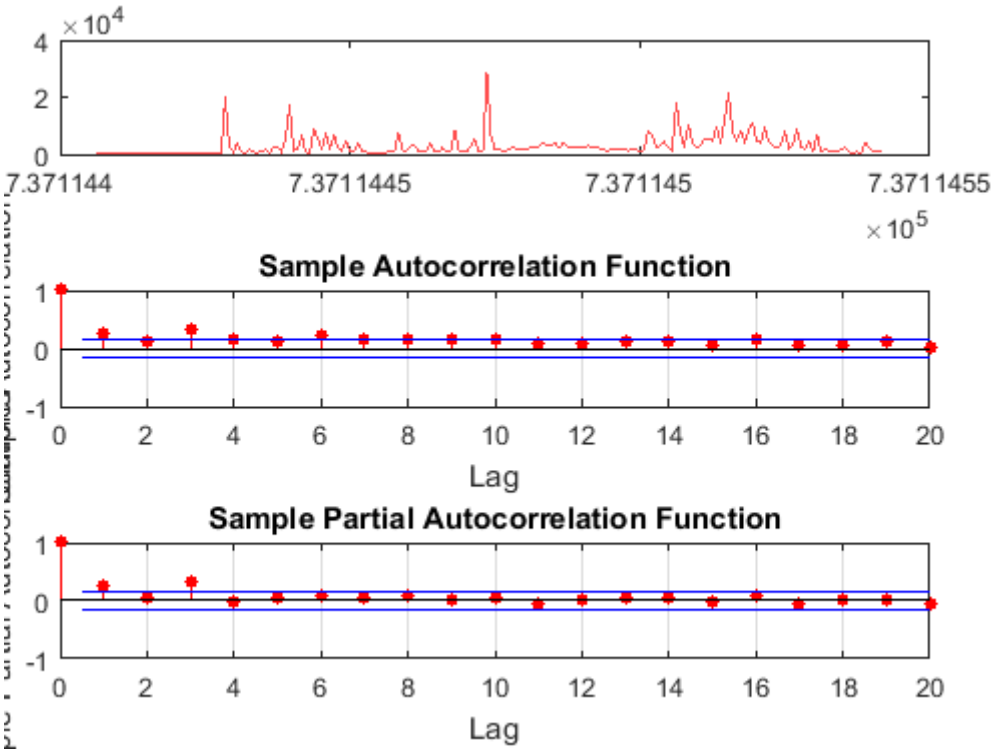

ARIMA model used was (1,0,1)

```
Regression with ARIMA(1,0,1) Error Model:
-----------------------------------------
Conditional Probability Distribution: Gaussian

                                Standard          t
 Parameter       Value          Error       Statistic
-----------   -----------   ------------   -----------
Intercept             -10        2016.28   -0.00495962
    AR{1}        0.899773       0.106432       8.45399
    MA{1}       -0.778286       0.156427      -4.97538
    Beta1         3528.06        1541.25       2.28909
 Variance    1.32595e+07         837807       15.8265
```

Beta1 is > 1.95 therefore concentrations during process are significantly higher than concentrations during pre-activity.

This result is in agreement with results obtained by using the nanoGEM approach, the t test and the MW "U" test which conclude that concentrations during packing are significantly higher than pre-activity.

Annex B: Web-based modelling tools output results

Web-based modelling tools reports are shown here. Only two cases for each tool are shown due to space reasons, one for packing line L and one for packing line M.

ART

a) Kaolin I, Packing line L

Details for Activity (untitled)

Emission sources: Near field — Duration (mins): 162

Far field ✓

Far-field exposure

Operational Conditions

Substance emission potential	
Substance product type	Powders, granules or pelletised material
Dustiness	18886 mg/kg for inhalable fraction
Moisture content	Dry product (< 5 % moisture content)
Powder weight fraction	0.9
Activity emission potential	
Activity class	Falling powders
Situation	Transferring 100 – 1000 kg/minute
Handling type	Routine transfer
Drop height	Drop height > 0.5 m
Containment level	Open process
Surface contamination	
Process fully enclosed?	No
Effective housekeeping practices in place?	Yes
Dispersion	
Work area	Indoors
Room size	Large workrooms only

Risk Management Measures

Localised controls	
Primary	Fixed capturing hood (90.00 % reduction)
Secondary	No localized controls (0.00 % reduction)
Segregation	No segregation (0.00 % reduction)
Personal enclosure	No personal enclosure (0.00 % reduction)
Dispersion	
Ventilation rate	10 air changes per hour (ACH)

Predicted exposure levels

ART predicts air concentrations in a worker's personal breathing zone outside of any Respiratory Protection Equipment (RPE). The use of RPE must be considered separately.

Mechanistic model results

The predicted 75th percentile full-shift exposure is 1.8 mg/m³.

The inter-quartile confidence interval is 0.98 mg/m³ to 3.5 mg/m³.

Bayesian model results

Data source	Proj. ref.		No. of sites	No. of workers	No. of records
Bagging fine powder with bagging machine with integrated LEV	V7607/02/01		1	2	9
		Totals	**1**	**2**	**9**

The predicted 75th percentile full-shift exposure is 4.1 mg/m³.

The inter-quartile confidence interval is 3 mg/m³ to 5.5 mg/m³.

b) Feldspar 1, Packing line M

Details for Activity Feldspar 1

Emission sources: Near field
Far field ✓

Duration (mins): 243

Far-field exposure

Operational Conditions

Substance emission potential	
Substance product type	Powders, granules or pelletised material
Dustiness	10246 mg/kg for inhalable fraction
Moisture content	Dry product (< 5 % moisture content)
Powder weight fraction	0.9
Activity emission potential	
Activity class	Falling powders
Situation	Transferring 100 – 1000 kg/minute
Handling type	Routine transfer
Drop height	Drop height > 0.5 m
Containment level	Handling that reduces contact between product and adjacent air. Note: This does not include processes that are fully contained by localised controls (see next questions).
Surface contamination	
Process fully enclosed?	No
Effective housekeeping practices in place?	Yes
Dispersion	
Work area	Indoors
Room size	Large workrooms only

Risk Management Measures

Localised controls	
Primary	Fixed capturing hood (90.00 % reduction)
Secondary	No localized controls (0.00 % reduction)
Segregation	No segregation (0.00 % reduction)
Personal enclosure	No personal enclosure (0.00 % reduction)
Dispersion	
Ventilation rate	10 air changes per hour (ACH)

Predicted exposure levels

ART predicts air concentrations in a worker's personal breathing zone outside of any Respiratory Protection Equipment (RPE). The use of RPE must be considered separately.

Mechanistic model results

The predicted 75th percentile full-shift exposure is 1.6 mg/m³.

The inter-quartile confidence interval is 0.86 mg/m³ to 3.1 mg/m³.

Bayesian model results

Data source	Proj. ref.		No. of sites	No. of workers	No. of records
Bagging fine powder with bagging machine with integrated LEV	V7607/02/01		1	2	9
		Totals	1	2	9

The predicted 75th percentile full-shift exposure is 4 mg/m³.

The inter-quartile confidence interval is 2.9 mg/m³ to 5.5 mg/m³.

Stoffenmanager

a) Kaolin I, Packing line L

Información básica	
Producto	Kaolin 1
Departamento	Stoffenmanager
Nombre de la evaluación de riesgos	A_K1
Resultados de la estimación de la exposición	
Componente	Polvo inhalable
Concentración de la tarea (mg/m3)	8,73
Concentración media diaria (mg/m3)	2,95
Resultados de las estimaciones de exposición	
Componente	Kaolin
Número CAS	1332-58-7
Concentración de la tarea (mg/m3)	7,86
Indice de Caracterización de Riesgo Tarea	2,62
Valor límite (mg/m3) + tipo	3 mg/m3 TWA-8 horas
Concentración media diaria (mg/m3)	2,65
Indice de Caracterización de Riesgo Día	0,88
Valor límite (mg/m3) + tipo	3 mg/m3 TWA-8 horas
Concentración en el producto inicial (%)	90
Características del producto	
Indicaciones de peligro H	
Pulverulencia del producto	Productos extremadamente pulverulentos
Proceso de trabajo o tarea	
Proceso de trabajo o tarea	Packing Euroarce (Hall 1-Packing line L and M)

Actividad	Manipulación de productos con una velocidad/fuerza relativamente alta que puede provocar cierta dispersión de polvo
PROC	PROC8b: Transferencia de sustancias o preparados (carga / descarga) en instalaciones específicas.
Duración (minutos)	162
Frecuencia de la tarea	2-3 días a la semana
Actividad en el área de respiración	No
Múltiples trabajadores	-
Evaporación, secado o curado después de la actividad	-
Protección respiratoria	Sin protección
Lugar de trabajo	
Lugar de trabajo	Euroarce packing hall 1
Volumen del recinto de trabajo	Volumen superior 1000 m³
Ventilación del recinto de trabajo	Ventilación general (ventanas y puertas abiertas)
Limpieza periódica del área de trabajo	Sí
Inspección y mantenimiento periódico	Sí
Medidas de control en la fuente	Sistema de extracción localizada
Separación del trabajador	El trabajador no trabaja en una cabina.

b) Feldspar 1, Packing line M

Información básica	
Producto	Feldspar 1
Departamento	Stoffenmanager
Nombre de la evaluación de riesgos	B_F1
Resultados de la estimación de la exposición	
Componente	Polvo inhalable
Concentración de la tarea (mg/m3)	8,73
Concentración media diaria (mg/m3)	4,42
Resultados de las estimaciones de exposición	
Componente	Feldspar
Número CAS	68476-25-5
Concentración de la tarea (mg/m3)	7,86
Indice de Caracterización de Riesgo Tarea	2,62
Valor límite (mg/m3) + tipo	3 mg/m3 TWA-8 horas
Concentración media diaria (mg/m3)	3,98
Indice de Caracterización de Riesgo Día	1,33
Valor límite (mg/m3) + tipo	3 mg/m3 TWA-8 horas
Concentración en el producto inicial (%)	90
Características del producto	
Indicaciones de peligro H	
Pulverulencia del producto	Productos extremadamente pulverulentos
Proceso de trabajo o tarea	
Proceso de trabajo o tarea	Packing Euroarce (Hall 1-Packing line L and M)

Actividad	Manipulación de productos con una velocidad/fuerza relativamente alta que puede provocar cierta dispersión de polvo
PROC	PROC8b: Transferencia de sustancias o preparados (carga / descarga) en instalaciones específicas.
Duración (minutos)	243
Frecuencia de la tarea	2-3 días a la semana
Actividad en el área de respiración	No
Múltiples trabajadores	-
Evaporación, secado o curado después de la actividad	-
Protección respiratoria	Sin protección
Lugar de trabajo	
Lugar de trabajo	Euroarce packing hall 1
Volumen del recinto de trabajo	Volumen superior 1000 m^3
Ventilación del recinto de trabajo	Ventilación general (ventanas y puertas abiertas)
Limpieza periódica del área de trabajo	Sí
Inspección y mantenimiento periódico	Sí
Medidas de control en la fuente	Sistema de extracción localizada
Separación del trabajador	El trabajador no trabaja en una cabina.

NanoSafer

a) Kaolin 1, Packing line L

NanoSafer Control Banding Report for Airborne Occupational Exposure Assessment

version 1.1

Assessment prepared by

Name: **Address:** **Phone:** **E-mail:** **Date:** Tuesday, Dec 4, 2018

Assessment of

Material assessed: Kaolin 1 **Producer:** SICA SL **Classified as nanomaterial consisting of:** Nanoobject	**Work situation assessed:** Packing Line L **Process type:** Powder Handling

Result of assessment

Estimated hazard level 0.2 **The hazard level is estimated based on** **High aspect ratio material:** No A high volume specific surface area of 41.60 m2/cm3 **OEL of analogue bulk material:** 3 mg/m3 **Solubility:** Insoluble (< 1 g/L) **Presence of surface coating:** No **Known hazards of analogue bulk material**	**Estimated time-resolved exposure index** 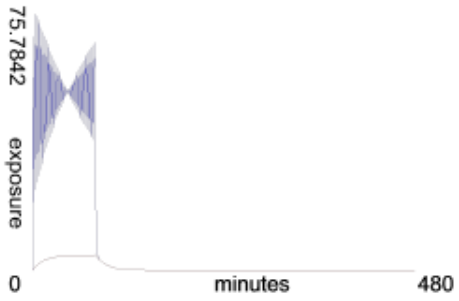

Near-field Acute	**Near-field Daily**	**Far-field Acute**	**Far-field Daily**
18.29 EB5: Very high exposure	4.151 EB5: Very high exposure	1.067 EB5: Very high exposure	0.3498 EB3: Moderate exposure potential

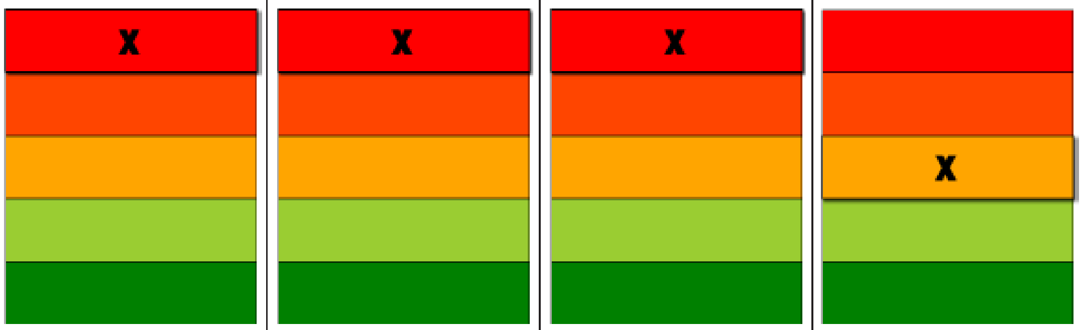

RL5: Very high toxicity suspected and/or moderate to very high exposure. The work should be conducted under strict dust release control, such as in a fume-hood, separate enclosure etc. Air-supplied respirators or highly efficient filter masks (PP3 or higher quality) may be used as a supplement and must be readily available in case of accidents. Expert advice is recommended.	RL5: Very high toxicity suspected and/or moderate to very high exposure. The work should be conducted under strict dust release control, such as in a fume-hood, separate enclosure etc. Air-supplied respirators or highly efficient filter masks (PP3 or higher quality) may be used as a supplement and must be readily available in case of accidents. Expert advice is recommended.	RL5: Very high toxicity suspected and/or moderate to very high exposure. The work should be conducted under strict dust release control, such as in a fume-hood, separate enclosure etc. Air-supplied respirators or highly efficient filter masks (PP3 or higher quality) may be used as a supplement and must be readily available in case of accidents. Expert advice is recommended.	RL3: Intermediate toxicity suspected and/or moderate exposure potential. The work should be conducted in a fume-hood or with highly efficient local exhaust ventilation in combination with use of respiratory protection equipment (PP3 or higher quality) depending on the work situation. Make sure to have the personal respiratory protection equipment available in case of accidents.

Based on the estimated hazard and exposure potential it is recommended to apply engineered protection equipment with a protection factor of 18.29
- corresponding to an efficacy of 94 %

Elaborated description of work situation assessed

Material, safety and contextual information used in the assessment

Material and safety data entered	**Exposure situation data entered**
Manufacturer: SICA SL **CAS:** 1332-58-7 **EINECS:** 310-191-1 **Relevance:** No **Coated:** No **Known shape:** No **Size is known:** Yes **Avererage size:** Yes **Size range known:** No **Average size:** 12700 nm **Surface area:** 16 m2/g **Relative density:** 2.6 g/cm3 **Solubility:** Insoluble (< 1 g/L) **Respirable dustiness:** 4.4 mg/kg	**Process type:** Powder handling **Energy level:** H4 (0.80) : High energy (eg. Pouring with > 30-100 cm drop height, big bags, packaging) **Amount used in cycle:** 1200 kg **Cyclus duration:** 1 min **Number of cycles per day:** 40 times **Pause between cycles:** 1 min **Mass handled per task in cycle:** 1200 kg **Time required per task in cycle:** 1 min **Length room:** 18 meters **Width room:** 9 meters **Height room:** 13 meters **Room air exchange rate:** 9 times per hour **Activity level room:** Moderate

Note: the local control (exhaust ventilation) was estimated to reduce particle emissions by 90%. A factor of 0.1 was applied to the respirable dustiness input parameter.

b) Feldspar 1, Packing line M

NanoSafer Control Banding Report for Airborne Occupational Exposure Assessment

version 1.1

Assessment prepared by

Name:
Address:
Phone:
E-mail:
Date: Tuesday, Dec 4, 2018

Assessment of

Material assessed: Feldspar1
Producer: SAMCA
Classified as nanomaterial consisting of: Nanoobject

Work situation assessed: Packing Line M
Process type: Powder Handling

Result of assessment

Estimated hazard level 0.8
The hazard level is estimated based on
High aspect ratio material: No
OEL of analogue bulk material: 3 mg/m3
Solubility: Insoluble (< 1 g/L)
Presence of surface coating: No
Known hazards of analogue bulk material
H373 May cause damage to organs through prolonged or repeated exposure

Estimated time-resolved exposure index

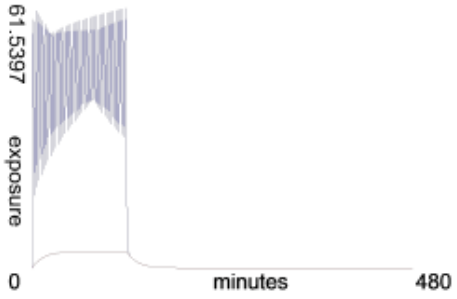

Near-field Acute	Near-field Daily	Far-field Acute	Far-field Daily
15.24	5.566	0.9588	0.4690
EB5: Very high exposure	EB5: Very high exposure	EB4: High exposure potential	EB3: Moderate exposure potential

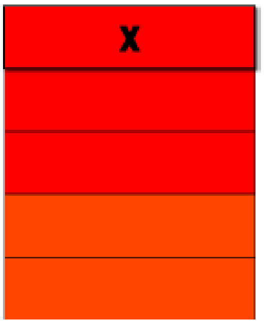	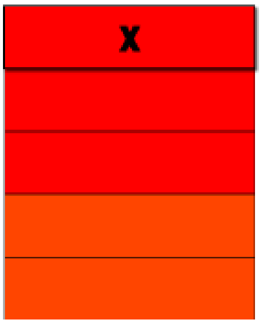	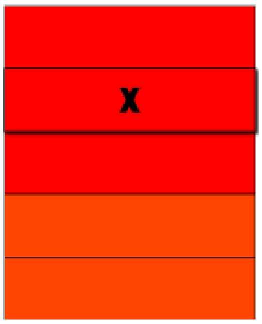	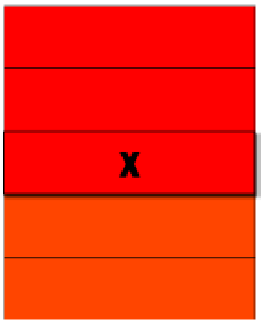
RL5: Very high toxicity suspected and/or moderate to very high exposure. The work should be conducted under strict dust release control, such as in a fume-hood, separate enclosure etc. Air-supplied respirators or highly efficient filter masks (PP3 or higher quality) may be used as a supplement and must be readily available in case of accidents. Expert advice is recommended.	RL5: Very high toxicity suspected and/or moderate to very high exposure. The work should be conducted under strict dust release control, such as in a fume-hood, separate enclosure etc. Air-supplied respirators or highly efficient filter masks (PP3 or higher quality) may be used as a supplement and must be readily available in case of accidents. Expert advice is recommended.	RL5: Very high toxicity suspected and/or moderate to very high exposure. The work should be conducted under strict dust release control, such as in a fume-hood, separate enclosure etc. Air-supplied respirators or highly efficient filter masks (PP3 or higher quality) may be used as a supplement and must be readily available in case of accidents. Expert advice is recommended.	RL5: Very high toxicity suspected and/or moderate to very high exposure. The work should be conducted under strict dust release control, such as in a fume-hood, separate enclosure etc. Air-supplied respirators or highly efficient filter masks (PP3 or higher quality) may be used as a supplement and must be readily available in case of accidents. Expert advice is recommended.

Based on the estimated hazard and exposure potential it is recommended to apply engineered protection equipment with a protection factor of 15.24
- corresponding to an efficacy of 93 %

Elaborated description of work situation assessed

Material, safety and contextual information used in the assessment

Material and safety data entered	Exposure situation data entered
Manufacturer: SAMCA **CAS:** 68476-25-5 **EINECS:** 270-666-7 **Relevance:** No **Coated:** No **Known shape:** No **Size is known:** Yes **Avererage size:** Yes **Size range known:** No **Average size:** 35000 nm **Surface area:** 1.13 m2/g **Relative density:** 2.6 g/cm3 **Solubility:** Insoluble (< 1 g/L) **Respirable dustiness:** 5.9 mg/kg	**Process type:** Powder handling **Energy level:** H4 (0.80) : High energy (eg. Pouring with > 30-100 cm drop height, big bags, packaging) **Amount used in cycle:** 1200 kg **Cyclus duration:** 2 min **Number of cycles per day:** 40 times **Pause between cycles:** 1 min **Mass handled per task in cycle:** 1200 kg **Time required per task in cycle:** 2 min **Length room:** 18 meters **Width room:** 9 meters **Height room:** 13 meters **Room air exchange rate:** 9 times per hour **Activity level room:** Moderate

Note: the local control (exhaust ventilation) was estimated to reduce particle emissions by 90%. A factor of 0.1 was applied to the respirable dustiness input parameter.

3. Supplementary material Publication III: Testing the performance of one and two box models as tools for risk assessment of particle exposure during packing of inorganic fertilizer

a) Small bags packing line

b) Small bags worker area instruments location

c) Big bags packing line and worker area instruments location

Figure S1 Images of the small and big bags packing lines plus instrument location.

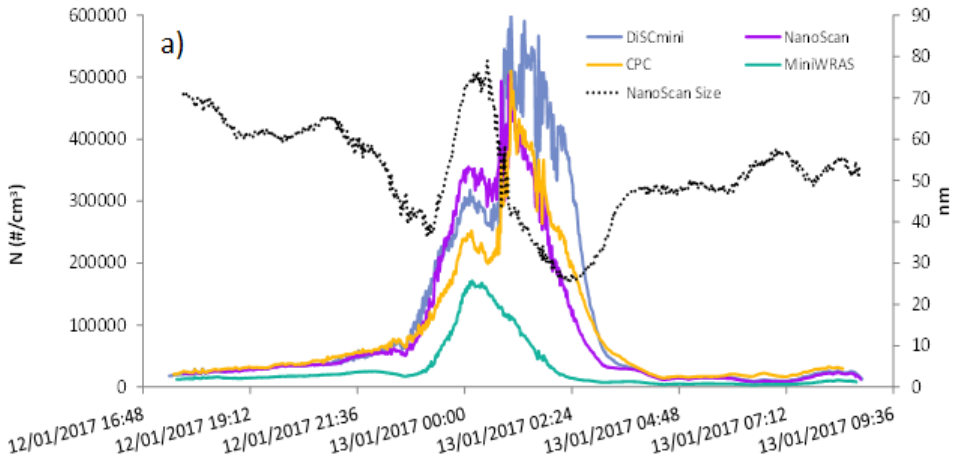

Figure S2 DiSCmini, NanoScan, MiniWras and CPC number concentration during an intercomparison previous to the packing measurements. We can observe that the MiniWras, unlike CPC, NanoScan and DiSCmini cannot detect an increase of particles under 45-50 nm of diameter.

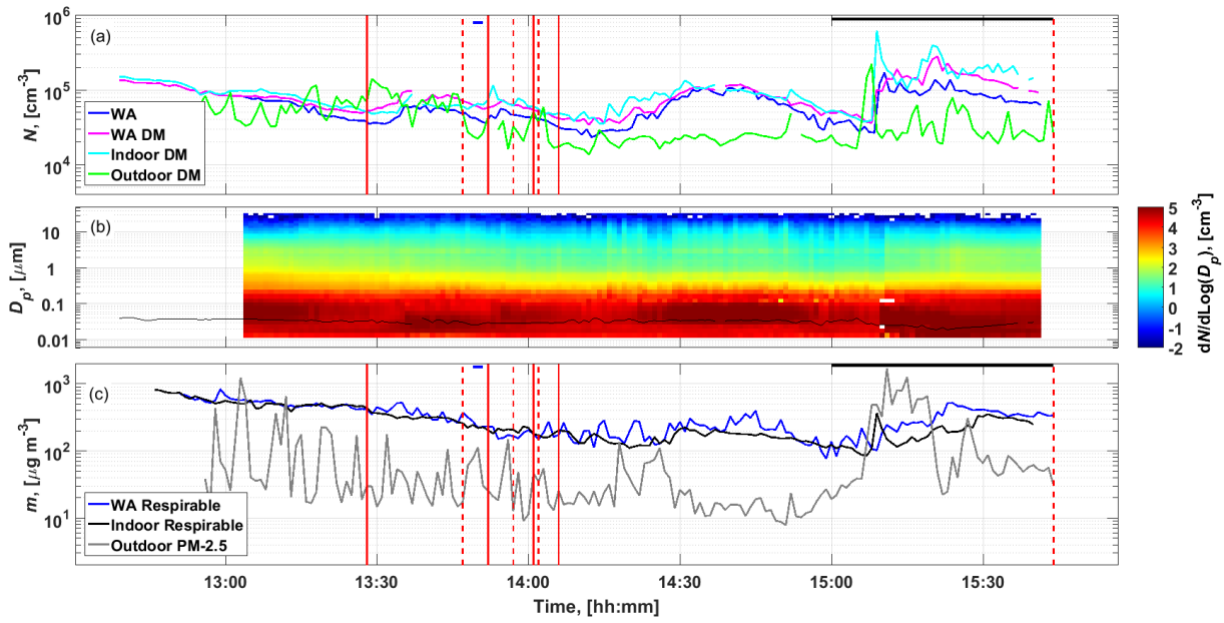

Figure S3 Particle concentration in the packing area (WA) during small bags day 1 (SB1): (a) particle number concentration time series; (b) particle size distribution time series measured with the MiniWras and the NanoScan, solid black line shows DiSCmini (DM) D_{50}; (c) mass concentration time series. Red vertical lines indicate start (solid line) and stop (dashed line) of the packing operation and horizontal black and blue lines on the top of the graphs indicate diesel and electric forklifts activity respectively.

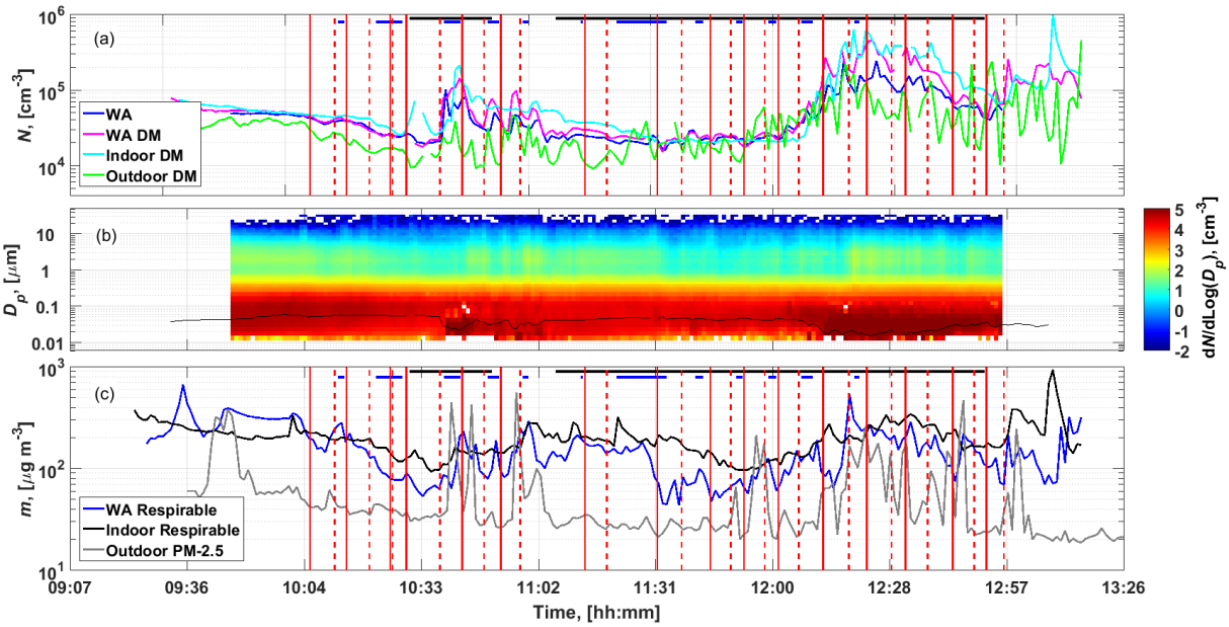

Figure S4 Particle concentration in the packing area (WA) during big bags day 2 (BB2): (a) particle number concentration time series; (b) particle size distribution time series measured with the MiniWras and the NanoScan, solid black line shows DiSCmini (DM) D_{50}; (c) mass concentration time series. Red vertical lines in (a) and (c) indicate start (solid line) and stop (dashed line) of the packing operation and horizontal black and blue lines on the top of the graphs indicate diesel and electric forklifts activity respectively.

Table S1 Mean number concentration and particle size for background (pre-activity) and packing process measured with the DiSCmini in the worker area, indoor and outdoor measurement locations. *NaN: information not available due to technical problems. Values in bold indicate a statistically significant differences compared with background concentrations.

Material	Process	Worker area (WA)		Indoor		Outdoor	
		Number (cm^{-3})	Size (nm)	Number (cm^{-3})	Size (nm)	Number (cm^{-3})	Size (nm)
SB1	Background	115845	38	126803	43	52681	23
	Packing	**72263**	32	81903	37	39514	20
SB2	Background	130834	28	*NaN	*NaN	83865	31
	Packing	78200	37	*NaN	*NaN	77566	31
BB1	Background	145232	33	117211	38	86871	29
	Packing	113087	37	102988	43	103404	32
BB2	Background	-	-	-	-	-	-
	Packing	41955	44	45277	57	30512	43

Table S2 Mean particle mass concentration for background (pre-activity) and packing processes measured with the Grimm – mini LAS laser spectrometer in the indoors and outdoors locations. Values are in μg m^{-3}. Values in bold indicate a statistically significant differences compared with background concentrations.

Material	Process	Indoor			Outdoor		
		Inhalable	Thoracic	Respirable	PM-10	PM-2.5	PM-1
SB1	Background	2063	1630	706	1570	212	25
	Packing	1142	**771**	**245**	694	105	16
SB2	Background	1232	878	281	1303	111	23
	Packing	1599	1144	349	1114	118	24
BB1	Background	1537	1120	350	974	82	19
	Packing	1514	1269	549	1538	**205**	33
BB2	Background	-	-	-	-	-	-
	Packing	1171	902	339	624	150	31

Table S3 Calculated dose rates in particle number, $\dot{n}$ and mass, $\dot{m}$ and regional deposition in percentages to head airways, trachea bronchi and alveolar regions.

Metric	Day 1 - Small Bags 1		Day 2 - Small Bags 2		Day 3 - Big Bags 1		Day 4 - Big Bags 2	
	BG	Packing	BG	Packing	BG	Packing	BG	Packing
$\dot{n}_{,\cdot 10^6}$ [min^{-1}]	770	857	834	1035	882	1122	-	682
$\dot{n}_{,}$.Head airways [%]	11.7	12.6	12.1	11.5	10.7	12.2	-	12.8
$\dot{n}_{,}$.Trachea bronchi [%]	19.1	20.4	20.0	19.4	18.0	20.0	-	20.7
$\dot{n}_{,}$.Alveolar [%]	69.2	67.0	68.0	69.1	71.3	67.8	-	66.6
$\dot{m}_{,\cdot 10^{-3}}$ [µg min^{-1}]	24.0	22.1	20.1	26.4	21.7	40.4	-	10.0
$\dot{m}_{,}$.Head airways [%]	90.8	93.5	92.0	92.4	89.0	91.0	-	91.6
$m_{,}$.Trachea bronchi [%]	3.6	2.6	3.3	3.1	4.3	3.6	-	3.3
$\dot{m}_{,}$.Alveolar [%]	5.7	3.9	4.8	4.5	6.7	5.4	-	5.1

Table S4 Stoffenmanager report for the small bags case scenario.

Basic information	
Product	YaraMila COMPLEX
Department	Stoffenmanager
Name risk assessment	BCL packing small bags
Results exposure estimation	
Component	Inhalable dust
Task concentration (mg/m³)	1,80
Daily average concentration (mg/m³)	0,90
Results exposure estimations	
Component	Ammonium nitrate
CAS-number	6484-52-2
Task concentration (mg/m³)	0,36
Risk Characterization Ratio Task	< 0,01
Limit value (mg/m³)	37,6 mg/m³ TWA-8 hours | European Chemicals Agency (ECHA)
Daily average concentration (mg/m³)	0,18
Risk Characterization Ratio Day	< 0,01
Limit value (mg/m³)	37,6 mg/m³ TWA-8 hours | European Chemicals Agency (ECHA)
Concentration in initial product (%)	20
Component	Potassium nitrate
CAS-number	7757-79-1
Task concentration (mg/m³)	0,27
Risk Characterization Ratio Task	< 0,01
Limit value (mg/m³)	36,7 mg/m³ TWA-8 hours | European Chemicals Agency (ECHA)
Daily average concentration (mg/m³)	0,14
Risk Characterization Ratio Day	< 0,01
Limit value (mg/m³)	36,7 mg/m³ TWA-8 hours | European Chemicals Agency (ECHA)

Concentration in initial product (%)	15
Component	Calcium fluoride
CAS-number	7789-75-5
Task concentration (mg/m³)	0,054
Risk Characterization Ratio Task	0,011
Limit value (mg/m³)	5 mg/m³ TWA-8 hours | European Chemicals Agency (ECHA)
Daily average concentration (mg/m³)	0,027
Risk Characterization Ratio Day	< 0,01
Limit value (mg/m³)	5 mg/m³ TWA-8 hours | European Chemicals Agency (ECHA)
Concentration in initial product (%)	3
Product characteristics	
H-statements	H272: May intensify fire; oxidiser H319: Causes serious eye irritation
Dustiness product	Granules/grains/flakes
Process	
Process	BCL packing small bags
Activity	Handling of products where due to high pressure, speed or force, large quantities of dust are generated and dispersed
PROC	PROC0: Other
Duration (minutes)	240
Frequency of the task	4-5 days a week
Activity in breathing zone	No
Multiple employees	-
Evaporation, drying or curing after activity	-
Respiratory protection	No protection
Workplace	
Workplace	BCL packing hall (Small Bags)
Volume of the working room	Volume over 1000 m³
Ventilation working room	General ventilation (open windows and doors)
Regular cleaning of work area	Yes
Regular inspection and maintenance	Yes
Control measures at the source	Containment of the source
Segregation of employee	The employee does not work in a cabin.
Conclusion	
Checked for substitution	▫ Yes ▫ No
Result of the substitution test / Reason for waiving a substitution	
Control measures	▫ Control measures sufficient ▫ Control measures not sufficient ▫ Further investigation required
Responsible person	
Date risk assessment	

Table S5 Stoffenmanager report for the big bags case scenario.

Basic information	
Product	YaraMila COMPLEX
Department	Stoffenmanager
Name risk assessment	BCL big bags
Results exposure estimation	
Component	Inhalable dust
Task concentration (mg/m³)	4,11
Daily average concentration (mg/m³)	2,06
Results exposure estimations	
Component	Ammonium nitrate
CAS-number	6484-52-2
Task concentration (mg/m³)	0,82
Risk Characterization Ratio Task	0,022
Limit value (mg/m³)	37,6 mg/m³ TWA-8 hours | European Chemicals Agency (ECHA)
Daily average concentration (mg/m³)	0,41
Risk Characterization Ratio Day	0,011
Limit value (mg/m³)	37,6 mg/m³ TWA-8 hours | European Chemicals Agency (ECHA)
Concentration in initial product (%)	20
Component	Potassium nitrate
CAS-number	7757-79-1
Task concentration (mg/m³)	0,62
Risk Characterization Ratio Task	0,017
Limit value (mg/m³)	36,7 mg/m³ TWA-8 hours | European Chemicals Agency (ECHA)
Daily average concentration (mg/m³)	0,31
Risk Characterization Ratio Day	< 0,01
Limit value (mg/m³)	36,7 mg/m³ TWA-8 hours | European Chemicals Agency (ECHA)
Concentration in initial product (%)	15
Component	Calcium fluoride
CAS-number	7789-75-5
Task concentration (mg/m³)	0,12
Risk Characterization Ratio Task	0,025
Limit value (mg/m³)	5 mg/m³ TWA-8 hours | European Chemicals Agency (ECHA)
Daily average concentration (mg/m³)	0,062
Risk Characterization Ratio Day	0,012
Limit value (mg/m³)	5 mg/m³ TWA-8 hours | European Chemicals Agency (ECHA)
Concentration in initial product (%)	3
Product characteristics	
H-statements	H272: May intensify fire; oxidiser H319: Causes serious eye irritation
Dustiness product	Granules/grains/flakes

Process	
Process	BCL packing big bags
Activity	Handling of products where due to high pressure, speed or force, large quantities of dust are generated and dispersed
PROC	PROC0: Other
Duration (minutes)	240
Frequency of the task	4-5 days a week
Activity in breathing zone	No
Multiple employees	-
Evaporation, drying or curing after activity	-
Respiratory protection	No protection
Workplace	
Workplace	BCL packing hall
Volume of the working room	Volume over 1000 m³
Ventilation working room	General ventilation (open windows and doors)
Regular cleaning of work area	Yes
Regular inspection and maintenance	Yes
Control measures at the source	No control measures at the source
Segregation of employee	The employee does not work in a cabin.
Conclusion	
Checked for substitution	▫ Yes ▫ No
Result of the substitution test / Reason for waiving a substitution	
Control measures	▫ Control measures sufficient ▫ Control measures not sufficient ▫ Further investigation required
Responsible person	
Date risk assessment	

4. Supplementary material Publication IV: Modeling of high nanoparticle exposure in an indoor industrial scenario with a one-box model

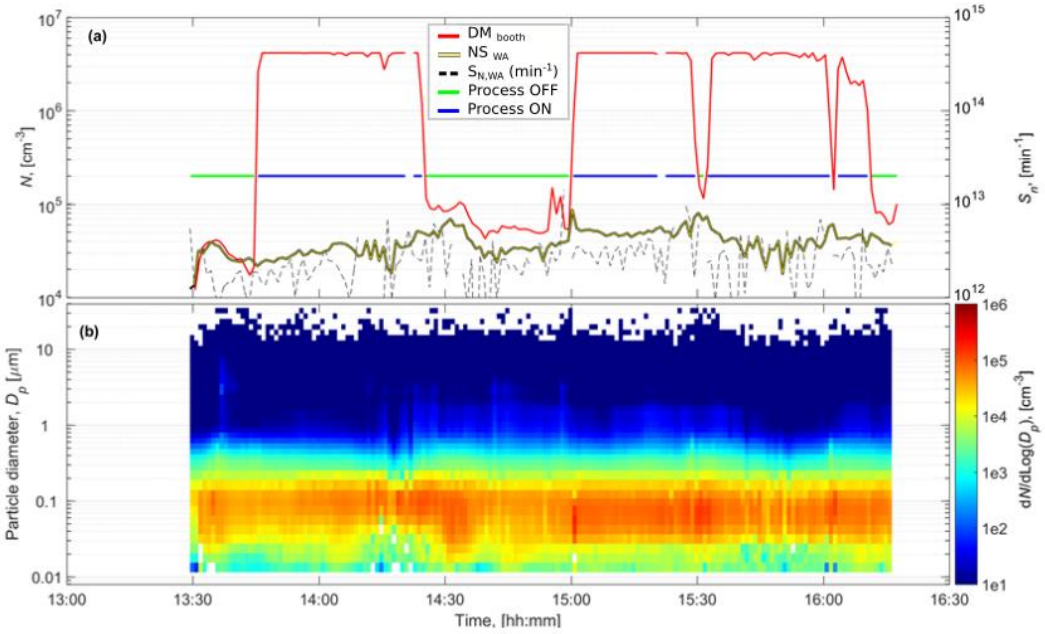

Figure S1 Booth #1, Day 1 a) shows particle number concentrations measured inside the booth by DiSCmini (DM), from worker area by NanoScan (WA) and particle emission rates solved by convolution from NanoScan WA concentrations. Blue line shows when the DM concentration was >10^5 cm^{-3} indicating that the plasma spray was ON and green line when the DM concentration was <10^5 cm^{-3} indicating that the plasma spray was OFF. Figure b) shows the particle size distributions measured by the NanoScan in the WA.

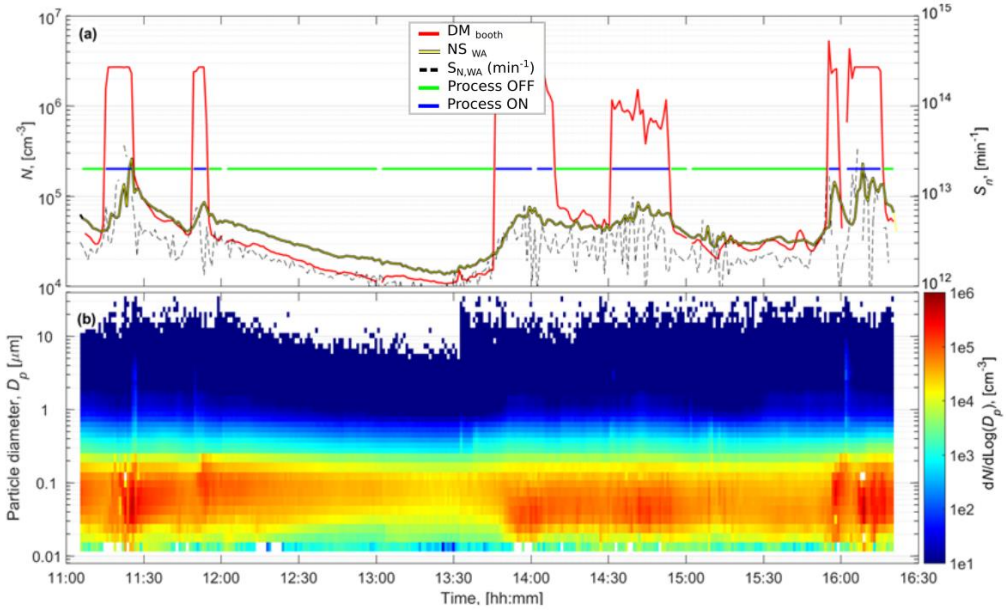

Figure S2. Booth #1, Day 2 a) shows particle number concentrations measured inside the booth by DiSCmini (DM), from worker area by NanoScan (WA) and particle emission rates solved by convolution from NanoScan WA concentrations. Blue line shows when the DM concentration was >105 cm-3 indicating that

the plasma spray was ON and green line when the DM concentration was <105 cm-3 indicating that the plasma spray was OFF. Figure b) shows the particle size distributions measured by the NanoScan in the WA.

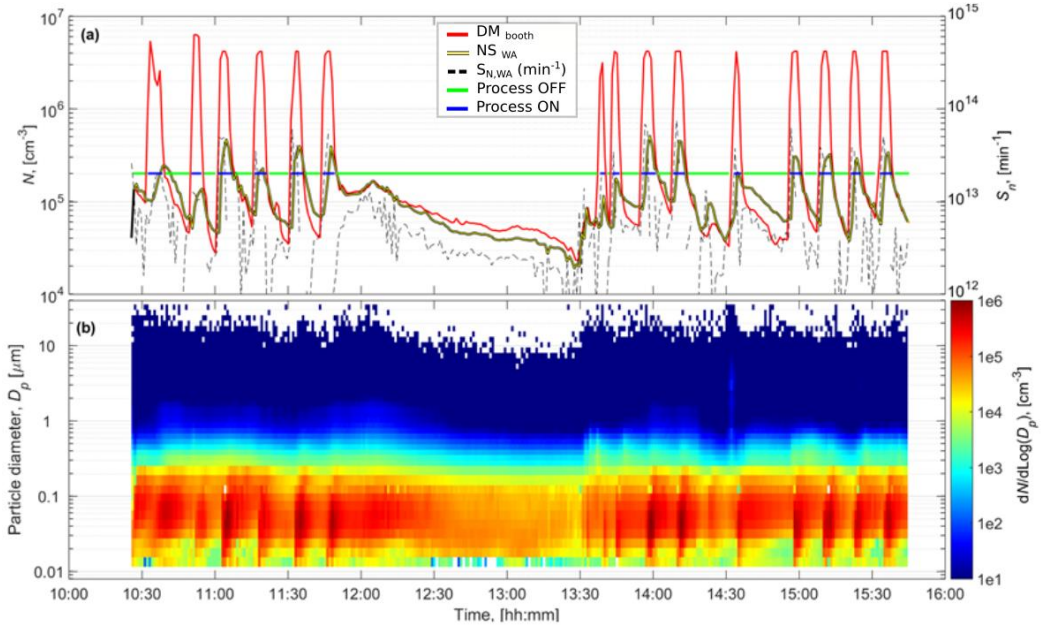

Figure S3 Booth #3, Day 4 a) shows particle number concentrations measured inside the booth by DiSCmini (DM), from worker area by NanoScan (WA) and particle emission rates solved by convolution from NanoScan WA concentrations. Blue line shows when the DM concentration was >10^5 cm^{-3} indicating that the plasma spray was ON and green line when the DM concentration was <10^5 cm^{-3} indicating that the plasma spray was OFF. Figure b) shows the particle size distributions measured by the NanoScan in the WA.

Table S1 Sampling day, booth, technic used (HVOF or APS), and feedstock materials summary. A: afternoon; M: morning. APS: atmospheric plasma spraying; HVOF: High Velocity Oxy-Fuel.

Day nº	Booth Model area	Spraying Technique	Shift	Feedstock Material	Composition
Day 1	#1	APS	A	Amdry 6228 & ANVAL 50/50	Al_2O_3 13TiO_2 & Cr/Ni
Day 2	#1	APS	M and A	Amdry 6228 & ANVAL 50/50	Al_2O_3 13TiO_2 & Cr/Ni
Day 3	#3	HVOF	M and A	WOKA 3702-1	WC 20Cr3C2 7Ni
Day 4	#3	HVOF	M and A	WOKA 3702-1	WC 20Cr3C2 7Ni

Table S2 Respirable mass concentration during the thermal spraying activity. Statistically significant increases are marked in bold.

Day	Period	Inside Booth	Worker Area (WA)	Inactivity (Background)
		Respirable ($\mu g\ m^{-3}$)	Respirable ($\mu g\ m^{-3}$)	Respirable ($\mu g\ m^{-3}$)
Booth #1 Model Area (Day 1)	Afternoon	n/a	**172**	53
Booth #1 Model Area (Day 2)	Morning	**130**	**161**	31
	Afternoon	**169**	**123**	
Booth #3 Model Area (Day 3)	Morning	**698**	**142**	26
	Afternoon	**709**	**93**	
Booth #3 Model Area (Day 4)	Morning	**522**	**171**	37
	Afternoon	**367**	**136**	

Table S3 Parameterization of the single box model considering booth door open: V (m^3) is volume used for modelling, Q ($m^3\ h^{-1}$) is ventilation air volume flow through the Worker Area and ACH (h^{-1}) is the air changes per hour calculated from measured air speeds.

Model Area	*V*, [m^3]	*Q*, [m^3h^{-1}]	ACH, [h^{-1}]
#1	465	32155	69
#3	250	12291	49

Table S4 One Box modelled concentrations considering booth door open, and using the convolution theorem and the cyclic steady state (Cyclic SS) approach to calculate emission rate (S_N) from NanoScan data.

Day	Calculated S_N in WA (min^{-1})		Shift	Modelled concentrations (cm^{-3})		WA measured (cm^{-3})	Ratio (modelled/measured)	
	Conv.	Cyclic SS		Conv.	Cyclic SS		Conv.	Cyclic SS
Booth #1 Model Area (Day 1)	$1.4x10^{11}$	$1.3x10^{12}$	A	$1.4x10^{4}$	$1.6x10^{4}$	$4.2x10^{4}$	0.33	0.38
Booth #1 Model Area (Day 2)	$3.4x10^{12}$	$3.0x10^{12}$	M	$1.9x10^{4}$	$1.9x10^{4}$	$7.8x10^{4}$	0.24	0.24
			A	$2.1x10^{4}$	$2.0x10^{4}$	$4.9x10^{4}$	0.43	0.41
Booth #3 Model Area (Day 3)	$1.2x10^{13}$	$7.9x10^{12}$	M	$3.9x10^{4}$	$3.3x10^{4}$	$2.5x10^{5}$	0.16	0.13
			A	$4.0x10^{4}$	$3.3x10^{4}$	$9.0x10^{4}$	0.44	0.37
Booth #3 Model Area (Day 4)	$7.9x10^{12}$	$1.4x10^{13}$	M	$4.7x10^{4}$	$5.5x10^{4}$	$1.5x10^{5}$	0.31	0.37
			A	$4.5x10^{4}$	$5.1x10^{4}$	$1.3x10^{5}$	0.35	0.39

Additional Scientific Contributions

Annex

ANNEX C. Additional scientific contributions

Peer-reviewed research publications

1. Salmatonidis, A., Ribalta, C., Sanfélix, V., Bezantakos, S., Biskos, G., Vulpoi, A., Simion, S., Monfort, E., Viana, M., 2019. Workplace Exposure to Nanoparticles during Thermal Spraying of Ceramic Coatings. Ann. Work Expo. Heal. 63, 91–106. https://doi.org/10.1093/annweh/wxy094

Conference attendance as oral presenter

1. Ribalta C., Koivisto A.J., Salmatonidis A., Lopéz-Lilao A., Estupiñá S., Minguillón M.C., Monfort E., Viana M (2018) Modelling nanoparticle emissions in industrial settings: testing box models performance under high and low concentration scenarios, NanoSafe conference, Grenoble, France 5-9 November 2018

2. Ribalta C., Viana M., Lopéz-Lilao A., Estupiñá S., García-Cobos A., Minguillón M.C., Monfort E., (2018) Parameters influencing worker exposure during handling of ceramic powder materials, (V Congreso Hipano-Luso de Carámic y Vidrio 2018), Barcelona, Spain 8 – 10 October 2018.

3. Ribalta C., Koivisto A.J., Lopéz-Lilao A., Estupiñá S., Minguillón M.C., Monfort E., Viana M (2018) Performance of one- and two-box models as tools for risk assessment: a case study of fertilizer, Aerosol Technology 2018 (AT2018), Bilbao, Spain 18 June - 20 June 2018.

4. Ribalta C., Viana M., Minguillón M.C., Lopéz-Lilao A., Estupiñá S., Monfort E. (2017) Prediction and quantification of emissions and workers exposure during ceramic industrial processes, European Aerosol Conference (EAC2017), Zurich, Switzerland 27 August-1 September 2017.

5. Ribalta C., Viana M., López-Lilao A., Minguillón M.C., Estupiñá S., Monfort E. (2017) Is dustiness a predictor of exposure to particles in the ceramic industry?, RICTA, 5th Iberian Meeting on Aerosol Science and Technology, Barcelona, Spain 4-5 July 2017.

6. Ribalta C., López-Lilao A., Estupiñá S., Viana M., Minguillón M.C, Monfort E. (2017). Exposición ocupacional a material particulado en la indústria cerámica: predicción y

cuantificación de emisiones y exposición, I Jornada de Jóvenes Investigadores en la UJI. (ITC-UJI) (ICV-CSIC).

7. Ribalta C., Salmatonidis A., Fonseca A.S., Viana M., Minguillón M.C., López-Lilao A., Estupiñá S, Ibáñez M.J, Monfort E. (2016) Prediction of emissions and exposure to micro- and nanoparticles in industrial environments: Case study in the ceramic industry, NanoSafe conference, Grenoble, France 7-10 November 2016.

ACKNOWLEDGEMENTS

This Thesis would not have been possible without the cooperation and help of many people to whom I would like to express my gratitude.

Primeramente quiero agradecer a la Dra. Mar Viana (IDAEA) y al Profesor Eliseo Monfort (ITC), los directores de esta tesis, por confiar en mí des de un inicio, aunque este tema fuera completamente nuevo para mí, y por ofrecerme la gran oportunidad de realizar esta tesis. Muchas gracias a los dos por vuestra apoyo, consejos y correcciones a lo largo de estos tres años. He de decir que no puedo estar más agradecida de haberos tenido a los dos como directores, no solo sois grandes profesionales de los cuales he podido aprendido muchísimo a nivel laboral, sino que además habéis estado a mi lado siendo mucho más que mis directores de tesis. Gracias a los dos por vuestra cercanía, humildad y comprensión en todo momento. En especial, quiero agradecer a Mar por el día a día y las charlas que nada tiene que ver con el trabajo, por haber resuelto dudas y problemas, y en definitiva por estar disponible siempre que lo he necesitado. Gracias por haber hecho este camino mucho más fácil. Agrair també al tutor de la Universitat de Barcelona, Dr. Alex Tarancón, per acceptar ser part d'aquest tesi i per el suport ofert durant aquest temps.

I would like to offer my special thanks to Dra. María Cruz Minguillón (IDAEA) and Dr. Joonas Koivisto, for given me valuable support and advice during this last years. Without them this Thesis would not have been possible. Muchas gracias MariCruz por tus exhaustivas correcciones y excelentes aportaciones que me han ayudado a realizar un trabajo mucho mejor. Gracias por haber estado cuando lo he necesitado y por revisar esta tesis. Agradecerte también por las visitas al despacho y tus charlas con ese toque teatral que nos han animado los días en el despacho. To Joonas, thank you for given me the opportunity to learn so much about exposure modelling, for sharing your knowledge on modelling and exposure assessment, for your support, and for solving all my doubts, that were not few!

Having reached this point, I would also like to thank all the people from the National Research Center for the Working Environment (NRCWE) as well as from the Instituto de Tecnologia Ceramica (ITC) with whom I had the pleasure to work, for the fruitful collaborations and for making me feel so welcomed.

Un especial agradecimiento se lo debo a la Dra. Ana López-Lilao (ITC) y a Sara Estupiñá (ITC), así como a la Dra. Ana Sofia Fonseca (NRCWE). A Ana y Sara, mis compañeras de campaña con las que hemos pasado largas pero estupendas horas de muestreos, gracias! Ha sido genial poder trabajar a vuestro lado y aprender tanto de vosotras. Muchas gracias a las dos por haber dedicado tantas horas a este proyecto, sin vosotras, vuestro esfuerzo y dedicación, esta tesis no habría sido posible. En especial, gracias Ana por haberme enseñado tanto sobre dustiness y por haber estado siempre dispuesta a ayudarme y escucharme. A Sara, gracias por todas las horas que has pasado en planta piloto haciendo ensayos de dustiness. A Sofia, muchas gracias tanto por tu ayuda profesional y tus aportaciones a esta tesis, como por haberme cuidado tantísimo en Copenhague, pase unos grandes días a vuestro lado.

I would also like to express my gratitude to Dr. Dirk Dahmann (IGF) and Dr. Aureli Tobias for their valuable advice and contributions to this Thesis.

Agrair també al grup de TEM del CCiTUB, en especial al Joan Mendoza per estar sempre disposat a ajudar-me amb les mostres.

Un especial agradecimiento se lo debo a todo el grupo del IDAEA-EGAR. Muchas gracias a todas y todos por crear este fantástico ambiente de trabajo. Ha sido genial poder compartir todo este tiempo con vosotros. Gracias! os deseo lo mejor. En especial, quiero agradecer a todas mis compañeras y compañeros de despacho por crear ese "cálido" ambiente tan característico del 1543. Gracias a los que estáis y a las que os habéis ido. Agradecer también a Diana, por sus visitas y charlas, a Garay y Elena por la ayuda con los papeles de viajes imposibles y a Xavi y Andrés por las revisiones finales de esta tesis.

A la meva família i amics, gràcies per estar sempre al meus costat, preocupar-vos per mi, i per donar-me tants bons moments. To Felix, thank you for helping me with the design of this thesis, but most importantly for your constant support and understanding. I am so grateful to have you in my life.

Finalment, agrair a la meva mare tot el que ha fet i fa per mi. Gràcies per haver confiat sempre en mi, per animar-me i consolar-me quan ha fet falta, i per ser la persona en la que sempre podré confiar. Gràcies per haver-me donat tant, no seria on sóc sense el teu esforç.

FUNDING SOURCES

The work presented in this Thesis was carried out with the financial support from the Spanish MINECO (CGL2015-66777-C2-1-R, 2-R), and through project PCIN-2015-173-C02-01, under the frame of SIINN, the ERA-NET for a Safe Implementation of Innovative Nanoscience and Nanotechnology, by SIINN-ERANET project CERASAFE (id.:16). Additional support was provided by Generalitat de Catalunya AGAUR 2017 SGR41, the Spanish Ministry of the Environment (13CAES006), FEDER (European Regional Development Fund) "Una manera de hacer Europa". Special thanks are due to the following companies: Bulk Cargo Logistics, S.A., Euroarce Samca, and TM COMAS for their committed cooperation.